

**Department of**

**College of Engineering  
The University of Iowa  
Iowa City, Iowa**

---

# **Loss of Prestress, Camber, and Deflection of Noncomposite and Composite Structures Using Different Weight Concretes**

**Final Report**

**by**

**D. E. Branson**

**B. L. Meyers**

**K. M. Kripanarayanan**

**Report No. 70-6**

**Prepared Under Iowa State Highway  
Commission Research Project HR-137**

**August 1970**

LOSS OF PRESTRESS, CAMBER, AND DEFLECTION  
OF NON-COMPOSITE AND COMPOSITE STRUCTURES  
USING DIFFERENT WEIGHT CONCRETES

Final Report

by

D. E. Branson  
Professor of Civil Engineering

B. L. Meyers  
Associate Professor of Civil Engineering

K. M. Kripanarayanan  
Research Associate in Civil Engineering

The opinions, findings, and conclusions expressed in  
this publication are those of the authors and not  
necessarily those of the Iowa State Highway Commission.

Report No. 70-6  
Prepared Under Iowa State Highway  
Commission Research Project HR-137

Department of Civil Engineering  
University of Iowa  
Iowa City

August 1970

## FOREWORD

This is a report of research conducted under the Iowa State Highway Commission Research Project No. HR-137. The project was initiated in February 1968. A progress report, No. 69-1, was submitted in February 1969.

This project is being coordinated with the Iowa State Highway Commission Research Project No. HR-136, "Creep and Shrinkage Properties of Lightweight Concrete Used in the State of Iowa" (see final report dated August 1970); and with the Iowa Highway Research Board Project No. HR-104, "Field Observation of Five Lightweight Aggregate Pretensioned Prestressed Concrete Bridge Beams" (see final report by J. A. Young).

Acknowledgment is made of the assistance of Messrs. S. E. Roberts, Research Engineer, C. Pestotnik, Bridge Engineer, Y. H. Gee, Assistant Bridge Engineer, and J. A. Young, Research Technician, of the Iowa Highway Commission; and Mr. J. H. Boehmler, Jr., President, Prestressed Concrete of Iowa, Inc.

The authors would also like to thank the Idealite Co., Denver, Colorado, and the Hydraulic Press Brick Co., Brooklyn, Indiana for donating materials used in the experimental program.

## ABSTRACT

Presented in this report are the results of an investigation of the use of lightweight concretes in prestressed and reinforced concrete structures. Both "sand-lightweight" and "all-lightweight" concretes are included in the study. The sand-lightweight concrete consists of 100% sand substitution for fines, along with Idealite coarse and medium lightweight aggregate and Type I cement. The all-lightweight concrete consists of Haydite coarse, medium, and fine aggregates along with Type I cement.

The study is divided into three parts: a materials study of the concretes themselves, a laboratory study of the behavior of both non-composite and composite beams that included prestressed (15 beams) and reinforced (3 beams) beams, and the field measurement of camber of prestressed girders (5 girders) used in the fabrication of a composite bridge in Iowa. The minimum test period for the laboratory beams is 6 months, although data is recorded for 1 year for 3 of the beams. The test period for the bridge girders is 560 days.

The laboratory prestressed concrete beams are designed in five groups (3 beams in each group) to investigate the loss of

prestress, initial and time-dependent camber, load-deflection behavior (under single and repeated load cycles) and the effect of different slab casting schedules. One group of 3 reinforced beams is used to investigate the initial and time-dependent deflection, load-deflection behavior after sustained loading, and the effect of different slab casting schedules.

The methods described for predicting material behavior and structural response are generalized to apply to prestressed and reinforced structures of normal weight, sand-lightweight, and all-lightweight concrete. Continuous time functions are provided for all needed parameters, so that the general equations readily lend themselves to computer solution. Approximate equations are also included.

Design procedures are presented for the following:

1. Calculation of strength and elastic properties, creep and shrinkage of the lightweight concretes of this project at any time, including ultimate values. An indication is also given of the calculation of these properties for other concretes in general.
2. Calculation of loss of prestress and camber at any time, including ultimate values, of non-composite and composite prestressed structures.
3. Calculation of deflections at any time, including ultimate values, of non-composite and composite reinforced structures.
4. Calculation of deflections of prestressed concrete members under single and repeated load cycles (with constant as well as increasing stress range). Calculation of deflections of reinforced concrete members under sustained loads in the non-linear range for short times (24 hours) is also included.

Results computed by these methods are shown to be in good agreement with the control specimen data, the laboratory beam data, and the bridge girder data.

Published experimental data concerning the time-dependent (prestress loss, camber, and deflection) effects and load deflection response of prestressed and reinforced beams are shown to be in reasonable agreement with the results computed by the design methods presented in this report. Ranges of variation are also shown. These data include normal weight, sand-lightweight and all-lightweight concrete, non-composite and composite members, and both laboratory specimens and actual structures.

This project is thought to be the first such comprehensive study of the initial plus time-dependent material behavior and related structural response of both non-composite and composite structures using different weight concretes. A new procedure is also developed for predicting the entire load-deflection curve of both reinforced and prestressed members under repeated load cycles into the cracking range.

Keywords: all-lightweight concrete; beams (structural); bridge girders; camber; composite construction (concrete to concrete); creep (materials); deflection; lightweight concrete; loss of prestress; modulus of elasticity; normal weight concrete; precast concrete; prestressed concrete, repeated cycle; sand-lightweight concrete; shrinkage; single cycle; steel relaxation; strain; stress; structural design; sustained; test beams; time-dependent.

## TABLE OF CONTENTS

Chapter		Page
	List of Tables	ix
	List of Figures	xi
	Notation	xvii
1.	INTRODUCTION	1
	1.1 Statement of the Problem	1
	1.2 Objectives and Scope	2
	1.3 Review of Literature	3
2.	DESCRIPTION OF EXPERIMENTAL INVESTIGATION	8
	2.1 Materials and Test Specimens	8
	2.2 Instrumentation and Test Data	10
3.	STRENGTH AND ELASTIC PROPERTIES, CREEP AND SHRINKAGE	12
	3.1 Strength and Elastic Properties	12
	3.2 Creep and Shrinkage	16
4.	LOSS OF PRESTRESS AND CAMBER	21
	4.1 Relaxation Tests	21
	4.2 Computed Loss of Prestress, Camber and Deflection	23
	4.3 Required Calculations and Summary of General Parameters	38

## TABLE OF CONTENTS (Cont'd)

Chapter		Page
4.4	Sample Calculations	41
4.5	Experimental Loss of Prestress, Camber and Deflection Results	44
4.6	Discussion of Experimental Results and Conclusions	62
4.7	Comparison of Computed and Measured Data Reported by Others	70
4.8	Summary of Results Reported by Others and Conclusions	89
5.	LOAD DEFLECTION STUDIES OF PRESTRESSED AND REINFORCED CONCRETE BEAMS	92
5.1	General	92
5.2	Single Cycle Load Tests of Prestressed Members	93
5.3	Repeated Load Tests of Prestressed Members	107
5.4	Increasing Load Plus 24-Hour Sustained Load Tests	127
5.5	Results Reported by Others	132
5.6	Summary and Conclusions	148
6.	SUMMARY AND CONCLUSIONS	155
	LIST OF REFERENCES	161
	APPENDIX A Specimen Details	Ap 1
	APPENDIX B Creep and Shrinkage Variables	Ap 12
	APPENDIX C Specimen Details for the Data in the Literature	Ap 20

TABLE OF CONTENTS (Cont'd)

Chapter	Page
APPENDIX D Camber Equations for Common Prestress Profiles	Ap 29
APPENDIX E Photographs of Laboratory Specimens	Ap 31
APPENDIX F Computer Flow Charts and Typical Outputs	Ap 37

## LIST OF TABLES

Table		Page
1	EXPERIMENTAL AND COMPUTED LOSS OF PRESTRESS FOR LABORATORY BEAMS AND COMPUTED LOSS OF PRESTRESS FOR BRIDGE GIRDERS	54
2	MEASURED AND COMPUTED MIDSPAN CAMBER & DEFLECTION FOR LABORATORY BEAMS & BRIDGE GIRDERS	56
3	COMPUTED ULTIMATE LOSS OF PRESTRESS AT MIDSPAN, BY TERMS, FOR THE LABORATORY BEAMS AND BRIDGE GIRDERS, USING THE GENERAL EQUATIONS (14) & (17) WITH EXPERIMENTAL PARAMETERS	58
4	COMPUTED ULTIMATE MIDSPAN CAMBER, BY TERMS, FOR THE LABORATORY BEAMS AND BRIDGE GIRDERS, USING THE GENERAL EQS. (15), (16), (18) & (20) WITH EXPERIMENTAL PARAMETERS	60
5	WORKING LOAD, COMPUTED AND OBSERVED VALUES OF ULTIMATE LOAD AS WELL AS VALUES OF WORST DISCREPANCY BETWEEN COMPUTED AND OBSERVED DEFLECTION CURVES	103
6	DETAILS OF REPEATED LOAD CYCLES AND DISCREPANCY IN THE OBSERVED AND COMPUTED VALUES OF MIDSPAN DEFLECTION FOR BEAMS OF GRPS C & E	124
7	DETAILS OF INCREASING LOAD PLUS 24-HR SUSTAINED LOAD TESTS WITH REGARD TO WORKING LOADS, ULTIMATE LOADS AND DEFLECTIONS UNDER THESE LOADS	131

LIST OF TABLES (Cont'd)

Table		Page
A1	DETAILS OF LABORATORY BEAMS (GRPS A, B, C) AND BRIDGE GIRDERS	Ap 2
A2	DETAILS OF LABORATORY BEAMS (GRPS D, E AND F)	Ap 4
A3	DETAILS OF CONCRETE MIXES AND MIXING PROCEDURE FOR LT-WT CONCRETES	Ap 6
A4	CONCRETE PROPERTIES (GRPS A, B, C AND BRIDGE GIRDERS), TEMPERATURE AND HUMIDITY DATA	Ap 7
A5	CONCRETE PROPERTIES (GRPS D, E, & F), TEMPERATURE AND HUMIDITY DATA	Ap 9
A6	CONCRETE PROPERTIES OF LAB BEAMS AT "LOAD-DEF" STUDIES	Ap 11
C1	PROPERTIES OF TEST BEAMS AT UNIVERSITY OF FLORIDA ( <u>23</u> )	Ap 21
C2	PROPERTIES OF TEST BEAMS AT UNIVERSITY OF ILLINOIS ( <u>24</u> )	Ap 22
C3	PROPERTIES OF TEST BEAMS AT TEXAS A & M UNIVERSITY ( <u>27</u> )	Ap 23
C4	PROPERTIES OF TEST BEAMS AT UNIVERSITY OF MISSOURI ( <u>31</u> )	Ap 24
C5	DETAILS OF BEAMS REPORTED BY ABELES ( <u>56</u> )	Ap 25
C6	DETAILS OF BEAMS REPORTED BY WARAWARUK, SOZEN & SIESS ( <u>41</u> )	Ap 26
C7	DETAILS OF BEAMS REPORTED BY SHAIKH AND BRANSON ( <u>49</u> )	Ap 27
C8	DETAILS OF BEAMS REPORTED BY BURNS & SIESS ( <u>54</u> )	Ap 28

## LIST OF FIGURES

Figure		Page
1	Laboratory beams and bridge girders	9
2	Concrete strength vs time curves for lab concretes (Gps B, C)	14
3	Creep coefficient vs time curves for lab concretes (Gps A, B, C)	14
4	Shrinkage vs time curves for lab concretes (Gps A, B, C)	14
5	Concrete strength vs time curves for lab concrete (Gps E, F)	15
6	Creep coefficient vs time curves for lab concrete (Gps D, E, F)	15
7	Shrinkage vs time curves for lab concretes (Gps D, E, F)	15
8	Results of steel relaxation tests	22
9	Determination of experimental loss of prestress	22
10	Computed and experimental loss of prestress of beams of Group A (three non-composite beams)	45
11	Computed and experimental loss of prestress of beams of Groups B and C (two non-composite and four composite beams)	46
12	Computed and experimental loss of prestress of beams of Groups D and E (two non-composite and four composite beams)	47

LIST OF FIGURES (Cont'd)

Figure		Page
13	Computed loss of prestress of five composite bridge girders	48
14	Computed and experimental midspan camber of beams of Group A (three non-composite beams)	49
15	Computed and experimental midspan camber of beams of Groups B and C (two non-composite and four composite beams)	50
16	Computed and experimental midspan camber of beams of Groups D and E (two non-composite and four composite beams)	51
17	Computed and experimental midspan deflection of beams of Group F (one non-composite and two composite beams)	52
18	Computed and experimental midspan camber of five composite bridge girders	53
19	Computed and experimental loss of prestress at end of beams reported in Reference (23)	72
20	Computed and experimental loss of prestress at center of beams reported in Reference (23)	73
21	Computed and experimental midspan camber of beams reported in Reference (23)	74
22	Computed and experimental loss of prestress at center of beams reported in Reference (24)	77
23	Computed and experimental midspan camber of beams reported in Reference (24)	78
24	Computed and experimental loss of prestress at end of beams reported in Reference (27)	81

## LIST OF FIGURES (Cont'd)

Figure		Page
25	Computed and experimental loss of prestress at center of beams reported in Reference (27)	82
26	Computed and experimental midspan camber of beams reported in Reference (27)	83
27	Computed and experimental loss of prestress at end of beam reported in Reference (31)	86
28	Computed and experimental loss of prestress at center of beam reported in Reference (31)	87
29	Computed and experimental midspan camber of beam reported in Reference (31)	88
30	Two point loading for 'load-deflection' studies of laboratory beams	94
31	Moment of inertia of cracked section ( $I_{cr}$ )	98
32	Observed and computed midspan deflection versus load curves for beams of Group A (three non-composite prestressed beams)	100
33	Observed and computed midspan deflection versus load curves for beams of Group B (one non-composite and two composite prestressed beams)	101
34	Observed and computed midspan deflection versus load curves for beams of Group D (three non-composite prestressed beams)	102
35	Details of deflections under repeated loadings	110
36	Sample calculations	114
37	Observed and computed midspan deflection vs load curve of beam C1 under 3 cycles of repeated loading (one non-composite prestressed beam)	118

LIST OF FIGURES (Cont'd)

Figure		Page
38	Observed and computed midspan deflection versus load curve of beam C2 under 3 cycles of repeated loading (one non-composite prestressed beam)	119
39	Observed and computed midspan deflection versus load curve of beam C3 under 3 cycles of repeated loading (one composite prestressed beam)	120
40	Observed and computed midspan deflection versus load curve of beam E1 under 3 cycles of repeated loading (one non-composite prestressed beam)	121
41	Observed and computed midspan deflection versus load curves for beams E2 and E3 under 3 cycles of repeated loading (two composite prestressed beams)	122
42	Effect of repeated loading (in the cracked range) on total deflections of laboratory beams of Groups C and E	123
43	Observed and computed values of midspan deflection for beams of Group F under 24-hr sustained loading (one non-composite and two composite reinforced beams)	130
44	Observed and computed midspan deflection (using Eqs. (38) and (41) for beams under static loading as in (A) (Data from Reference 56) and as in (B) (Data from Reference 41)	134
45	Observed and computed midspan deflection (using Eqs. (38), (40), and (41) for beams under static loading as in (A) (Data from Reference 49) and for beams under repeated loading as in (B) (Data from Reference 54)	138
46	Comparison of computed and observed values of midspan deflection of beams in Reference (54), under two cycles of repeated loading (three non-composite reinforced beams)	141

LIST OF FIGURES (Cont'd)

Figure		Page
47	Range of validity of Eqs. (38), (40) and (41) for rectangular beams with different steel percentages -- included in this dimensionless plot are also the results from studies made on rectangular prestressed beams from Reference (41), (49), (54) and (56) as well as the current study	143
48	Range of validity of Eqs. (38), (40), and (41) for T beams with different steel percentages -- included in this dimensionless plot are the results from the current study only	144
B1	Strain components	Ap 14
B2	Time-dependent strain variables	Ap 16
B3	Nominal creep and shrinkage correction factors for the parameters shown from Ref. 18	Ap 18
E1	View of laboratory showing beams in foreground and prestressing bed containing additional beams at right	Ap 32
E2	Forms for beams in prestressing bed	Ap 32
E3	Strain gage indicator and switching and balancing unit used with load cells to measure prestress force	Ap 33
E4	Prestressing bed, jacking equipment and beams stored in bed	Ap 33
E5	Close-up of jacking equipment, bulkheads, and grips	Ap 34
E6	Shrinkage specimens in foreground and 7 beams (1 beam crosswise in foreground). Two additional beams in prestressing bed	Ap 34
E7	Two of 4 composite beams. Strain gage points and dial gages can be seen. Strands used in relaxation tests are seen at right	Ap 35

LIST OF FIGURES (Cont'd)

Figure		Page
E8	Cylinders loaded in creep racks and Whittemore gage used to measure strains of beams and shrinkage and creep specimens	Ap 35
E9	View of beam C1 showing the crack pattern prior to failure	Ap 36
E10	View of beam C1 after failure	Ap 36

## NOTATION

- 1 = subscript denoting cast-in-place slab of composite beam or effect of slab
- 2 = subscript denoting precast beam
- A** = area of section
- $A_g$  = area of gross section, neglecting the steel
- $A_s$  = area of tension steel in reinforced members and area of prestressed steel in prestressed members
- $A'_s$  = area of compression steel in reinforced members and area of non-tensioned steel in prestressed members
- $A_t$  = area of transformed section
- a = distance from end of beam to the nearest of 2 symmetrical disphrams. Also used as the distance from end to harped pt. in 2-pt. harping. Also used as empirical constant--see Eq. (1). Also used as distance of load from the near support--see Eq. (41).
- b = empirical constant determined in the laboratory--see Eq. (1). Also used as distance between applied loads--see Eq. (41). Also used as compression flange width.
- $C_s$  = creep coefficient defined as ratio of creep strain to initial strain at slab casting.
- $C_t$  = creep coefficient at any time t
- $C_{t1}$  = creep coefficient of the composite beam under slab dead load
- $C_{t2}$  = creep coefficient of the precast beam concrete

- $C_u$  = ultimate creep coefficient defined as ratio of ultimate creep strain to initial strain
- C.F. = correction factor to account for conditions other than standard
- c = subscript denoting composite section. Also used to denote concrete, as  $E_c$
- cp = subscript denoting creep
- D = differential shrinkage strain. Also used as a subscript to denote dead load
- DS = subscript denoting differential shrinkage
- d = effective depth of section
- E = modulus of elasticity
- $E_c$  = modulus of elasticity of concrete such as at 28 days
- $E_{ci}$  = modulus of elasticity of concrete at the time of initial loading, such as at transfer of prestress, etc.
- $E_{cs}$  = modulus of elasticity of concrete at the time of slab casting
- $E_s$  = modulus of elasticity of steel
- e = eccentricity of steel
- $e_c$  = eccentricity of steel at center of beam. Also used, as indicated, to denote eccentricity of steel in composite section
- $e_o$  = eccentricity of steel at end of beam
- F = prestress force after losses
- $F_i$  = initial tensioning force
- $F_o$  = prestress force at transfer (after elastic loss)

- $\Delta F$  = loss of prestress due to time-dependent effects only (such as creep, shrinkage, steel relaxation). The elastic loss is deducted from the tensioning force,  $F_i$ , to obtain  $F_o$
- $\Delta F_s$  = total loss of prestress at slab casting minus the initial elastic loss that occurred at the time of prestressing
- $\Delta F_t$  = total loss of prestress at any time minus the initial elastic loss
- $\Delta F_u$  = total ultimate loss of prestress minus the initial elastic loss
- $f_c$  = concrete stress at steel c.g.s due to prestress and pre-cast beam dead load
- $f_{cd}$  = concrete stress at steel c.g.s due to differential shrinkage
- $f_{cs}$  = concrete stress at steel c.g.s due to slab dead load (plus diaphragm dead load where applicable)
- $f'_c$  = compressive strength of concrete
- $(f'_c)_t$  = compressive strength of concrete at time  $t$
- $(f'_c)_{28}$  = compressive strength of concrete at 28 days
- $(f'_c)_u$  = ultimate (in time) compressive strength of concrete
- $f'_{cb}$  = modulus of rupture of concrete
- $f'_t$  = tensile strength of concrete
- $f_o$  = stress in prestressing steel at transfer (after elastic loss)
- $f_{si}$  = initial or tensioning stress in prestressing steel
- $f_y$  = yield strength of steel (defined herein as 0.1% offset)
- $H$  = relative humidity in percent
- $I_1$  = moment of inertia of slab
- $I_2$  = moment of inertia of precast beam

- $I_c$  = moment of inertia of composite section with transformed slab. The slab is transformed into equivalent precast beam concrete by dividing the slab width by  $E_{c2}/E_{c1}$
- $I_{cr}$  = moment of inertia of cracked transformed section
- $I_{eff}$  = effective moment of inertia
- $I_g$  = moment of inertia of gross section, neglecting the steel
- $I_{rep}$  = effective moment of inertia under repeated loads
- $I_t$  = moment of inertia of transformed section, such as an uncracked prestressed concrete section
- $i$  = subscript denoting initial value
- $K$  = deflection coefficient. For example, for beams of uniform section and uniformly loaded:
 

		Also for
		<u>Shrinkage</u>
	cantilever beam, $K = 1/4$	, $K_w = 1/2$
	simple beam, $K = 5/48$	, $K_w = 1/8$
	hinged-fixed beam, $K = 8/185$	, $K_w = 11/128$
	(one end continuous)	
	fixed-fixed beam, $K = 1/32$	, $K_w = 1/16$
	(both ends continuous)	
- $K_1$  = deflection constant for the slab dead load
- $K_2$  = deflection constant for the precast beam dead load
- $K_w$  = deflection coefficient for warping due to shrinkage or temperature change -- see  $K$  for values of  $K_w$
- $k$  = distance of neutral axis from compression flange -- see Eq. (39), also  $k_r = 0.85 - 0.45(A_s'/A_s)$ .
- $k_r$  = reduction factor to take into account the effect of compression steel, movement of neutral axis, and progressive cracking in reinforced flexural members; and effect of non-tensioned steel in prestressed flexural members, see  $k$  for values of  $k_r$
- $k_s = 1 + e^2/r^2$ , where  $r^2 = I_g/A_g$

- L = span length in general and longer span for rectangular slabs. Also used as a subscript to denote live load
- LA = subscript denoting loading age
- M = bending moment. When used as the numerical maximum bending moment, for beams of uniform section and uniformly loaded:
- cantilever beam , (-)  $M = q L^2/2$
  - simple beam , (+)  $M = q L^2/8$
  - hinged-fixed beam (one end continuous), (-)  $M = q L^2/8$
  - fixed-fixed beam (both ends continuous), (-)  $M = q L^2/12$
- $M_1$  = maximum bending moment under slab dead load for composite beams
- $M_2$  = maximum bending moment under precast beam dead load
- $M_{1D}$  = bending moment between symmetrically placed diaphragms
- $M_{S, Di}$  = bending moment due to slab or slab plus diaphragm, etc., dead load
- $M_{cr}$  = cracking moment
- $M_{max}$  = maximum moment under service loads
- m = modular ratio of the precast beam concrete,  $E_s/E_{cs}$ , at the time of slab casting. Also used as subscript to indicate measured values
- n = modular ratio,  $E_s/E_{ci}$ , at the time of loading, such as at release of prestress for prestressed concrete members. Also usually used as  $E_s/E_c$  for reinforced members
- P = applied transverse load for load-deflection studies
- $P_{cr}$  = applied transverse load corresponding to the cracking moment,  $M_{cr}$
- $P_{rep}$  = maximum value of applied repeated transverse load in a cycle

- $P_{ult}$  = applied transverse load corresponding to the ultimate strength of the beam
- $PG$  = prestress gain in percent of initial tensioning stress or force
- $PG_{cp}$  = prestress gain due to creep under slab dead load at time  $t$
- $PG_{DS}$  = prestress gain due to differential shrinkage at time  $t$
- $PG_{el}$  = elastic prestress gain at slab casting
- $PL$  = total prestress loss in percent of initial tensioning stress or force
- $PL_{cp1}$  = prestress loss due to creep prior to slab casting at time  $t$
- $PL_{cp2}$  = prestress loss due to creep after slab casting at time  $t$
- $PL_{cp}$  = prestress loss due to creep at time  $t$
- $PL_{el}$  = prestress loss due to elastic shortening
- $PL_r$  = prestress loss due to steel relaxation at time  $t$
- $PL_{sh}$  = prestress loss due to shrinkage of concrete at time  $t$
- $PL_t$  = total prestress loss at any time  $t$
- $PL_u$  = ultimate prestress loss
- $p$  = steel percentage,  $A_s/bd$  for cracked members, and  $A_s/A_g$  for uncracked members. Also used in percent in shrinkage warping equations
- $p'$  = compressive steel percentage,  $A'_s/bd$  for cracked members, and  $A'_s/A_g$  for uncracked members. Also used in percent in shrinkage warping equations
- $Q$  = differential shrinkage force -  $D A_1 E_1/3$ . The factor 3 provides for the gradual increase in the shrinkage force from day 1, and also approximates the creep and varying stiffness effects.

- q = uniformly distributed load
- r = radius of gyration,  $r^2 = I_g/A_g$
- s = subscript denoting time of slab casting. Also used to denote steel. Also used as subscript to indicate sustained load
- sh = subscript denoting shrinkage
- t = total depth or thickness of section. Also subscript to denote time-dependent
- t = time in general, time in hours in the steel relaxation equation, and time in days in other equations herein
- $t_{LA}$  = age of concrete when loaded, in days
- u = subscript denoting ultimate value
- w = unit weight of concrete in pcf
- x = subscript to indicate distance as measured from the end of the beam -- see Eq. (35)
- $y_{cs}$  = distance from centroid of composite section to centroid of slab
- $y_t$  = distance from centroid of gross section to extreme fiber in tension
- $\alpha$  = ratio of creep coefficient at any time to ultimate creep coefficient,  $C_t/C_u$
- $\alpha_s$  = ratio of creep coefficient at the time of slab casting to  $C_u$
- $\beta$  = creep correction factor for the precast beam concrete age when loaded
- $\beta_s$  = creep correction factor for the precast beam concrete age when the slab is cast for composite beams
- $\gamma_s$  = ratio of shrinkage at slab casting to shrinkage at ultimate (referred to 7-day initial reading)

- $\gamma'_s$  = ratio of shrinkage after slab casting to shrinkage at ultimate (referred to 7-day initial reading)
- $\Delta$  = deflection or camber
- $\Delta_i$  = initial deflection, camber
- $(\Delta_i)_1$  = initial deflection under slab dead load
- $(\Delta_i)_{1D}$  = initial deflection due to diaphragm dead load
- $(\Delta_i)_2$  = initial deflection under precast beam dead load
- $(\Delta_i)_D$  = initial dead load deflection
- $(\Delta_i)_{F_0}$  = initial camber due to the initial prestress force,  $F_0$
- $\Delta_{DS}$  = differential shrinkage deflection
- $\Delta_L$  = live load deflection
- $\Delta_t$  = total camber, deflection, at any time
- $\Delta_u$  = ultimate camber, deflection
- $(\epsilon_{sh})_t$  = shrinkage strain in inches/inch or cm/cm, etc., at time  $t$
- $(\epsilon_{sh})_u$  = ultimate shrinkage strain in inches/inch or cm/cm, etc.
- $\phi$  = curvature
- $\phi_{sh}$  = curvature due to shrinkage warping -- see Eq. (16)
- $\phi_{ss_2}$  = curvature due to shrinkage warping of precast beam up to slab casting -- see Eq. (20)
- $\psi_1$  = load ratio for repeated load studies -- see Eq. (40)

## Chapter 1

## INTRODUCTION

1.1 Statement of the Problem

As a result of the increased use of structural lightweight concrete for precast bridge girders along with normal weight concrete deck slabs, a need exists for a better understanding of the factors, primarily time-dependent, that affect prestress loss and camber (in the case of prestressed girders) and deflection (in the case of reinforced girders) in composite beams of these materials. Of particular interest in this study is the behavior of sand-lightweight (100% sand substitution for fines along with lightweight coarse aggregate) and all-lightweight prestressed structures in relation to normal weight prestressed structures, and the effect of the composite slab on the ultimate loss of prestress and camber. The effect of composite slabs on the deflection of reinforced concrete members is also included in this study.

In order to complete a comprehensive study of the initial plus time-dependent deformational behavior of non-composite and composite structures, the load-deflection response of reinforced and prestressed members under single cycle and repeated cycle short-time load tests (with constant and increasing load levels) into the cracking range are

also included in this study. Twenty-four hour sustained load tests into the cracking range are also studied.

### 1.2 Objectives and Scope

The principal objective of this investigation is to evaluate experimentally the time-dependent behavior of sand-lightweight and all-lightweight concrete beams (prestressed and reinforced), including composite beams, in order to present practical design methods, and to give an indication of their accuracy for predicting loss of prestress and camber (in the case of prestressed beams) and deflections (in the case of reinforced beams).

The study is divided into three parts: a materials study of the concretes themselves, a laboratory study of the behavior of both non-composite and composite beams that included prestressed (15 beams) and reinforced (3 beams) beams, and the field measurement of camber of prestressed girders (5 girders) used in the fabrication of a composite bridge in Iowa. The minimum test period for the laboratory beams is 6 months, although data is recorded for 1 year for 3 of the beams. The test period for the bridge girders is 560 days.

The laboratory prestressed concrete beams are designed in five groups (3 beams in each group) to investigate the loss of prestress, initial and time-dependent camber, load-deflection behavior

(under single and repeated load cycles) and the effect of different slab casting schedules. One group of 3 reinforced beams is used to investigate the initial and time-dependent deflection, load-deflection behavior after sustained loading, and the effect of different slab casting schedules.

Results computed by the methods described for predicting material behavior and structural response are shown to be in good agreement with the control specimen data, the laboratory beam data, the bridge girder data, and other published experimental data. Continuous time functions are provided for all needed parameters, so that the general equations readily lend themselves to computer solution. Approximate equations are also included.

### 1.3 Review of Literature

Shrinkage of concrete is its contraction due to drying and chemical change. Various empirical equations are presented in the literature (1), (2), (3) for predicting shrinkage strains. ACI Committee 435 (4) has given a quantitative resume of available information on creep and shrinkage as applied to deflections of reinforced concrete beams.

Concrete undergoes time-dependent deformations under the action of sustained loads that are attributed to creep of the concrete. The contributions of Lorman (5), McHenry (6), Neville (7), Ross (8), and Troxell, et al (9) are noted. Lorman and Ross

suggested the use of hyperbolic expressions for predicting creep (used in this report in modified form). McHenry's concept of "superposition technique for creep" is used in this report; for example, in the case of creep under slab dead load. Neville's study of the physical nature of creep is noted.

A number of creep theories and mechanisms of creep have been reviewed by Neville (7), Ali and Kessler (10), and Meyers, et al (11). Meyers and Neville (12) and Pauw and Chai (13) have summarized the primary factors that influence creep. The influence of the size and shape of the member on creep and shrinkage was also reported by Hansen and Mattock (14).

The principal articles referred to in this report on the subject of creep and shrinkage of all-lightweight and sand-lightweight concrete are those of Jones, et al (15), ACI Committee 213 (16), Pfeifer (17), Christiason (18), Schumann (19), and this project (33).

Although the behavior of non-composite and composite prestressed beams of normal weight concrete has been studied in References (20) through (34), etc., (most of these referred to non-composite beams only), it appears that no such investigation has been made of composite prestressed members of lightweight concrete.

Lofroos and Ozell (21) were apparently the first to report experimental results of time-dependent camber of prestressed concrete beams. The specimens were two pairs of post-tensioned

normal weight non-composite beams under different prestress levels.

Branson and Ozell (23) examined experimentally the initial plus time-dependent camber of both composite and non-composite post-tensioned beams of normal weight concrete. Methods for calculating camber were developed using certain experimentally determined coefficients. The predicted results were in fair agreement with the measured values. It was also concluded that camber tends to reach an ultimate value relatively early compared to creep and shrinkage, because of the offsetting effects of loss of prestress and camber growth due to creep.

Corley, Sozen and Siess (24) discussed at great length the reduced modulus method, the rate of creep method, and the superposition method in a study of the time-dependent camber of prestressed concrete beams. The rate of creep method was deemed preferable on account of its relative simplicity. It was concluded that time-dependent camber could be objectionably high, if there was high stress gradient in the beam.

Sinno (27) in his study of lightweight non-composite prestressed bridge girders, concluded that hyperbolic functions can be used to predict loss of prestress and camber (used in modified form in this report). He also observed that camber tends to reach an ultimate value relatively early as compared to creep and shrinkage.

Yang (28) in a recent study of lightweight non-composite prestressed beams, concluded that creep under constant stress and variable stress was proportional to the applied stress within limits of about 40% of the ultimate strength.

Methods used in this study for predicting loss of prestress and camber were based in part on the papers of ACI Committee 435 (29) and Branson (23), (30).

With respect to short-time deflection of prestressed members under static and repeated loading, the works of Abeles (35) - (38), Burns (39), Hutton (40), and Warawaruk, Sozen, and Siess (41) are noted. Abeles' work primarily deals with partially prestressed members under static and fatigue loading. In general, it is concluded that maximum tensile stress of the order of the modulus of rupture of the concrete may be permitted under working loads without any detrimental effects on the serviceability and safety of the prestressed members.

Burns (39) has presented a detailed analytical method for obtaining the moment-curvature relationship for partially prestressed beams. The study was limited to prestressed concrete beams without non-tensioned steel.

Warawaruk, et al (41) in a comprehensive study of noncomposite prestressed beams presented methods for the prediction of deflections of prestressed members at the various loading stages.

This method, however, is too elaborate as a design procedure.

The procedure developed by Branson (50), (4), (30), (42) for predicting the deflection of reinforced beams under single-cycle loading and adopted for the 1971 ACI Code (51), and applied to prestressed beams by Shaikh and Branson (49), is extended in this study to the prediction of deflections of both reinforced and prestressed beams under repeated load cycles into the cracking range.

## Chapter 2

## DESCRIPTION OF EXPERIMENTAL INVESTIGATION

2.1 Materials and Test Specimens

The details of the laboratory beams and bridge girders are shown in Figure 1 and Tables A1 and A2. The laboratory beams were designed as follows:

Group A -- 3 non-composite beams with different prestress moments made of sand-lightweight concrete.

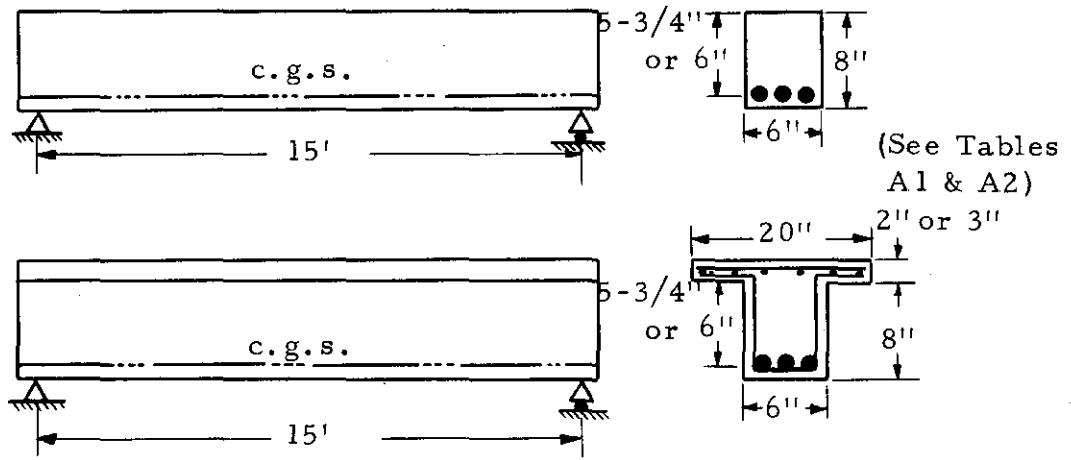
Group B -- 3 beams, two of which are composite beams. The beams are made of sand-lightweight concrete. The slabs (of normal weight concrete) were cast at 4 weeks and 10 weeks after the casting of the beams. The same prestress moment is used for the three beams.

Group C -- Same as Group B but with a different prestress moment.

Group D -- Same as Group A but made of all-lightweight concrete.

Group E -- Same as Group B but with a higher stress level.

Group F -- 3 reinforced (non-prestressed) beams, two of which are composite beams. The beams are made of sand-lightweight concrete. The slabs (of normal weight concrete) were cast at 4 weeks and 10 weeks after the casting of the reinforced beams. The same steel percentage is used for the three beams.



Laboratory non-composite and composite beams

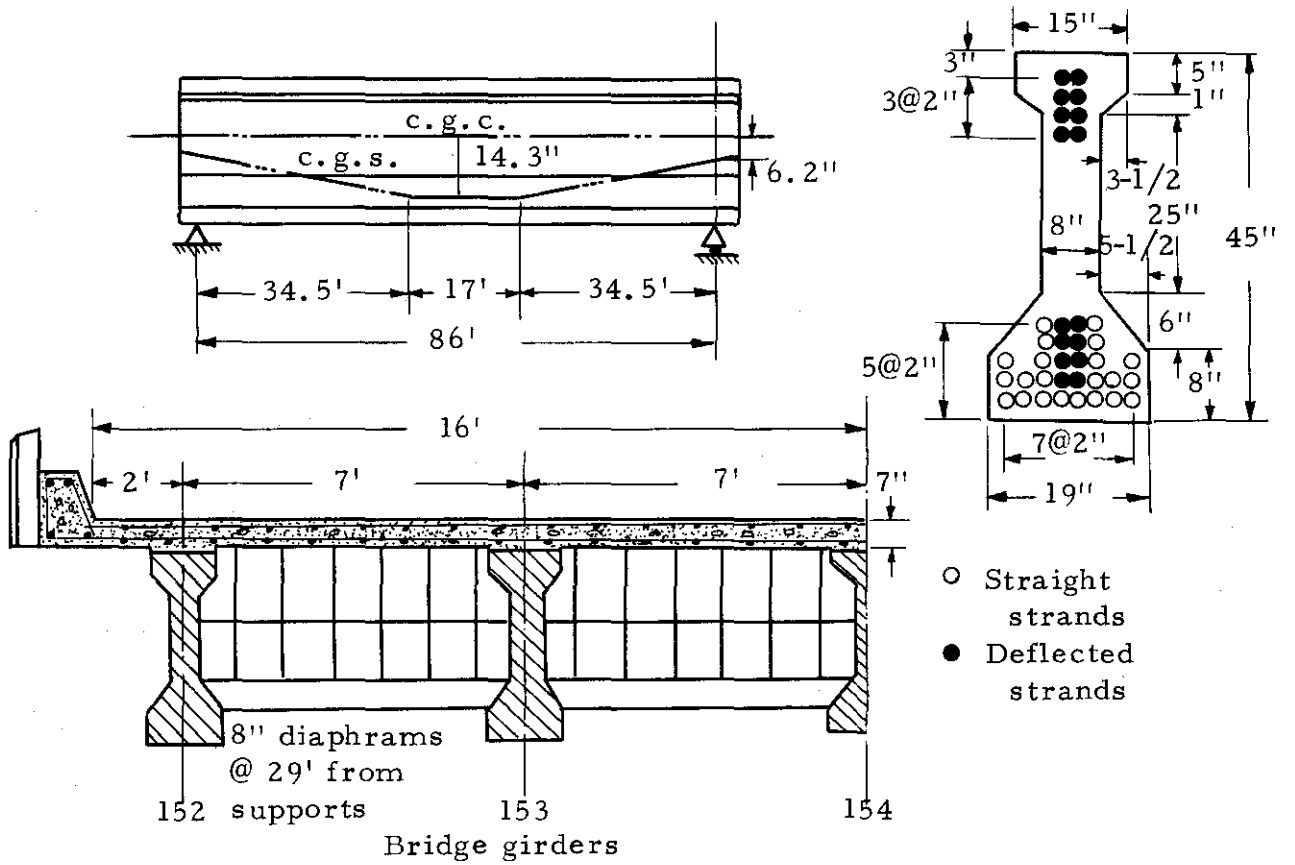


Figure 1 Laboratory beams and bridge girders

The beams for groups A, B, C, D, E, and F were moist cured for 3 days. Prestressing was done at age 7-9 days for the beams of groups A, B, C, D and E. The reinforced beams of group F were in position at age 21 days. The bridge girders (steam cured until prestressed at age 2-3 days) are sand-lightweight concrete (100% sand substitution for fines along with lightweight coarse aggregate), while the slabs are normal weight concrete. The composite bridge deck was cast 9 weeks after the bridge girders were cast.

The concrete mix ingredients and the mixing procedure for the different concretes are shown in Table A3. Two shrinkage specimens and 3 creep specimens (6" by 12" cylinders placed under a sustained uniform stress - see Tables A4 and A5) were cast for each lightweight concrete.

## 2.2 Instrumentation and Test Data

Steel collars with electrical strain gages (SR-4) mounted thereon were used as load cells for individual strands to measure the prestressing force applied to each laboratory beam.

Dial gages were used on both sides of each beam at midspan to measure both initial and time-dependent camber of the laboratory beams. A level rod and a precise level were used to obtain the camber measurements for the bridge girders.

A Whittemore mechanical strain gage (10" gage length) was used to measure the concrete strains of the creep and shrinkage specimens and the laboratory beams.

The experimental data for the laboratory specimens consists of the following:

1. Concrete strength properties, elastic properties, creep and shrinkage data from control specimens. Steel properties.
2. Temperature and humidity data.
3. Steel relaxation data.
4. Initial and time-dependent concrete beam strains. These are used in determining the experimental loss of prestress.
5. Initial and time-dependent camber.
6. Load-deflection, cracking, and ultimate strength data.

Camber data for the bridge girders is included in this report from Reference (32).

The concrete properties, temperature, and humidity data are shown in Tables A4 and A5.

## Chapter 3

## STRENGTH AND ELASTIC PROPERTIES, CREEP AND SHRINKAGE

3.1 Strength and Elastic Properties

A study of concrete strength versus time in this project and Reference (18) indicates an appropriate general equation in the form of Eq. (1) for predicting compressive strength at any time.

$$(f'_c)_t = \frac{t}{a + bt} (f'_c)_{28d} \quad (1)$$

where a and b are constants,  $(f'_c)_{28d}$  = 28-day strength, and t is time.

The following equations were developed in this study and Reference (18), and used in Reference (33), for normal weight, sand-lightweight, and all-lightweight concrete (using both moist and steam cured concrete, and types I and III cement). Eqs. (2) and (4) refer to the concrete (type I cement) of this project:

Moist cured concrete, type I cement

$$(f'_c)_t = \frac{t}{4.00 + 0.85t} (f'_c)_{28d}; \text{ or } (f'_c)_{7d} = 0.70(f'_c)_{28d}, \quad (2)$$

$$(f'_c)_u = 1.18(f'_c)_{28d}$$

Moist cured concrete, type III cement

$$(f'_c)_t = \frac{t}{2.30 + 0.92t} (f'_c)_{28d}; \text{ or } (f'_c)_{7d} = 0.80(f'_c)_{28d}, \quad (3)$$

$$(f'_c)_u = 1.09(f'_c)_{28d}$$

Steam cured concrete, type I cement

$$(f'_c)_t = \frac{t}{1.00 + 0.95t} (f'_c)_{28d}; \text{ or } (f'_c)_{2.5d} = 0.74(f'_c)_{28d}, \quad (4)$$

$$(f'_c)_u = 1.05(f'_c)_{28d}$$

Steam cured concrete, type III cement

$$(f'_c)_t = \frac{t}{0.70 + 0.98t} (f'_c)_{28d}; \text{ or } (f'_c)_{2.5d} = 0.80(f'_c)_{28d}, \quad (5)$$

$$(f'_c)_u = 1.02(f'_c)_{28d}$$

where  $t$  is age of concrete in days, and  $(f'_c)_u$  refers to an ultimate (in time) value. The results of Eqs. (2) and (4) agree with the experimental data of this project, as shown in Figures 2 and 5. As shown in References (18) and (42), Eqs. (2) - (5) refer to average values only. See these references for ranges of variation.

The secant, initial tangent, and computed (using Eq. 6) moduli of elasticity for the laboratory beams and bridge girder concretes are shown in Tables A4 and A5.

$$E_c = 33w^{1.5} \sqrt{f'_c}, \text{ psi; } w \text{ in pcf and } f'_c \text{ in psi} \quad (6)$$

The computed values for the limited number of tests were from 6%

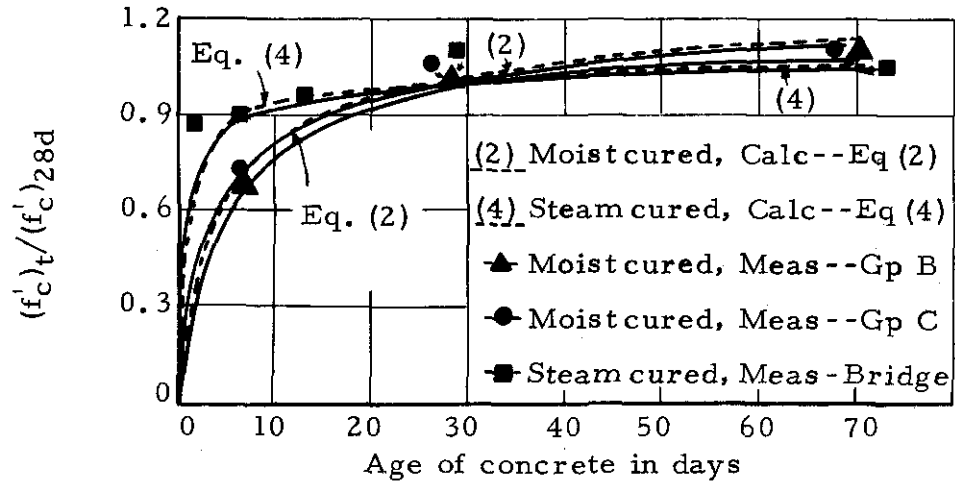


Figure 2. Concrete strength vs time curves for lab concretes (Gps B, C and bridge girder concrete)

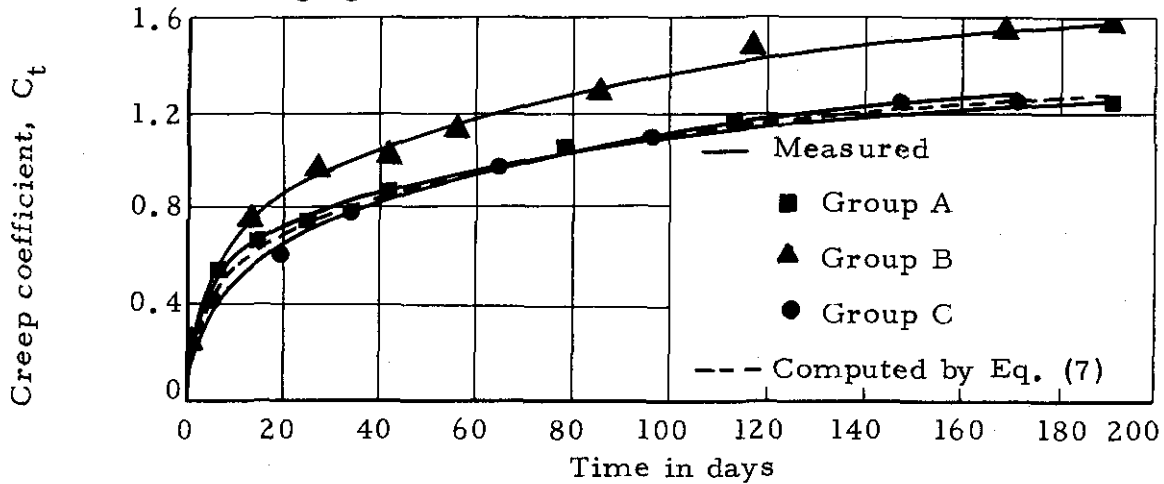


Figure 3. Creep coefficient vs time curves for lab concretes (Gps A, B, C)

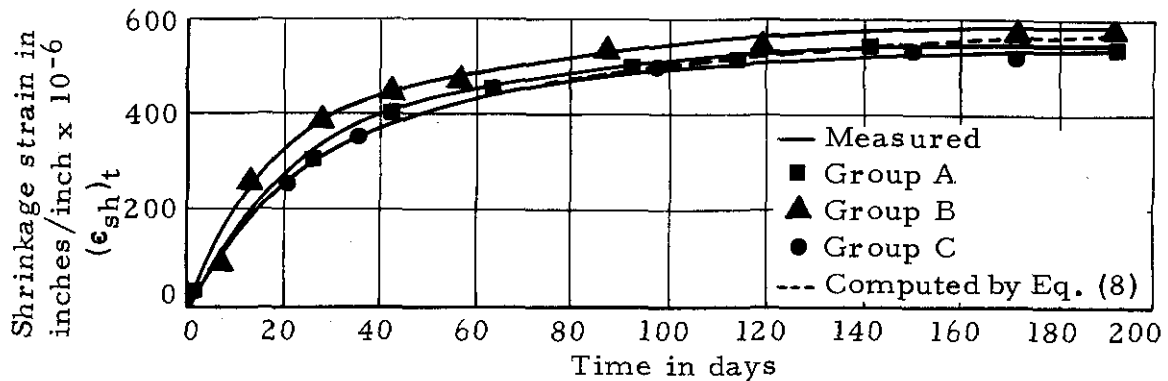


Figure 4. Shrinkage vs time curves for lab concretes (Gps A, B, C)

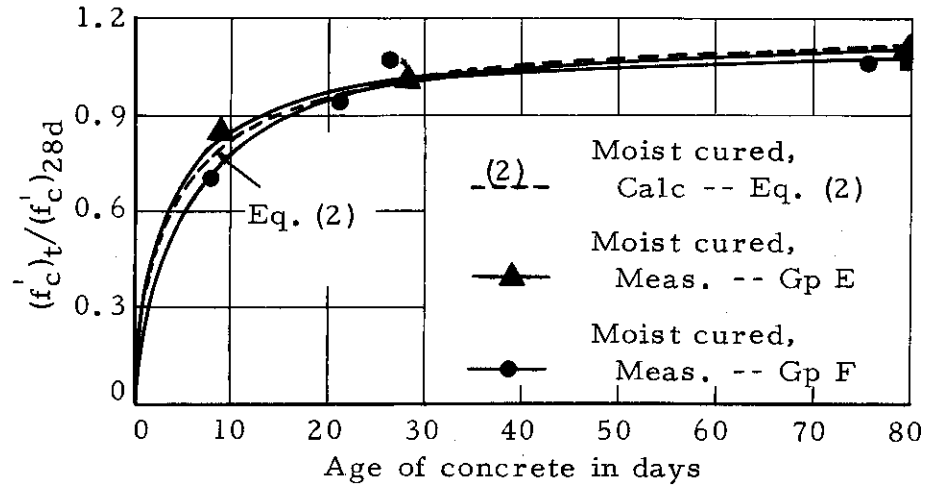


Fig. 5 Concrete strength vs time curves for lab concrete (Gps E, F)

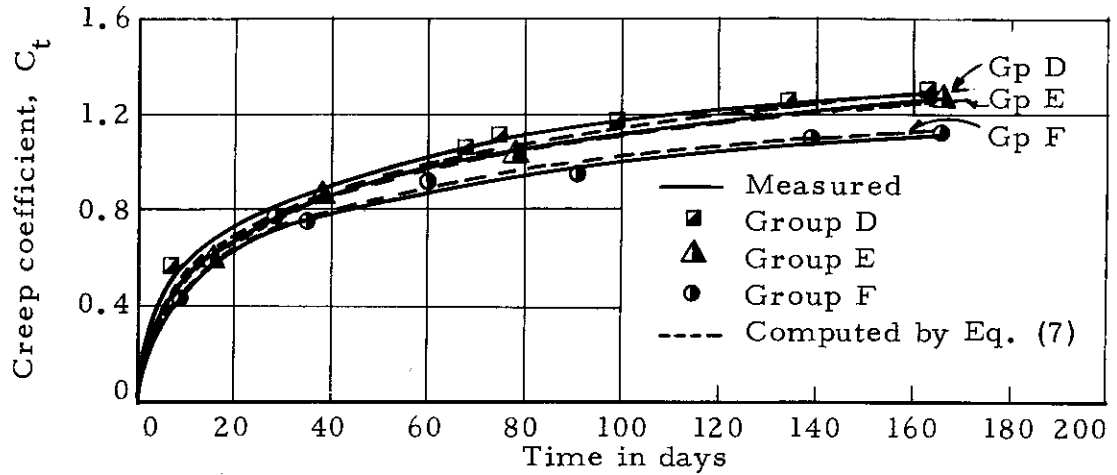


Fig. 6 Creep coefficient vs time curves for lab concrete (Gps D, E, F)

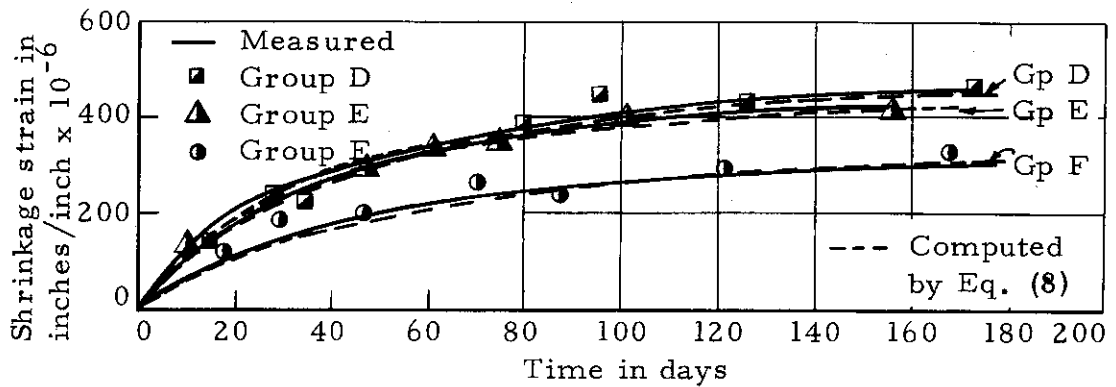


Fig. 7 Shrinkage vs time curves for lab concretes (Gps D, E, F)

to 15% higher than the initial tangent values. However, the computed initial camber of the laboratory beams and bridge girders was in agreement with the measured results (Table 4). Eq. 6, developed in Reference (18), is considered satisfactory for normal weight, sand-lightweight, and all-lightweight concrete.

### 3.2 Creep and Shrinkage

The principal variables that affect creep and shrinkage are outlined and discussed in Appendix B. The design approach presented herein for predicting creep and shrinkage refers to "standard conditions" and correction factors for other than standard conditions.

Based largely on the data and information from References and this project, the following design procedure (developed in this project and Reference (18), and used in Reference (42)), is recommended for predicting a creep coefficient and unrestrained shrinkage at any time, including ultimate values. The general values suggested for  $C_u$  and  $(\epsilon_{sh})_u$  should be used only in the absence of specific creep and shrinkage data for local aggregates and conditions. However, the "time-ratio" part (right-hand side except for  $C_u$  and  $(\epsilon_{sh})_u$ ) of Eqs. (7) - (9) have been found (18) to apply quite generally. As shown in References (18) and (42), these general values of  $C_u$  and  $(\epsilon_{sh})_u$  refer to average values only. See these references for ranges of variation.

Standard creep equation -- 3" or less slump, 40% ambient relative humidity, minimum thickness of member 6" or less, loading age 7 days for moist cured and 1-3 days for steam cured concretes

$$C_t = \frac{t^{0.60}}{10 + t^{0.60}} C_u \quad (7)$$

For the laboratory beam lightweight concretes (moist cured) of this project, the following values apply:

<u>Group</u>	<u>Load. Age</u>	<u>Rel. Hum.</u>	<u>C<sub>u</sub></u>
A, B, C	7 days	40%	1.75
D	7	50	1.87
E	9	50	1.80
F	21	50	1.63

For the bridge girder sand-lightweight concrete (steam cured) of this project -- C<sub>u</sub> = 2.15 for H = 40%. H was 70%. From Eq. (12) for H = 70%, C<sub>u</sub> = 0.80(2.15) = 1.72.

General value suggested for all weights of structural concrete (both moist and steam cured concrete, types I and III cement) -- C<sub>u</sub> = 2.35 for H = 40%. From Eq. (12) for H = 70%, C<sub>u</sub> = 0.80(2.35) = 1.88.

Standard shrinkage equations -- 3" or less slump, 40% ambient relative humidity, minimum thickness of member 6" or less

Shrinkage at any time after age 7 days for moist cured concrete

$$(\epsilon_{sh})_t = \frac{t}{35 + t} (\epsilon_{sh})_u \quad (8)$$

For the laboratory beams lightweight concretes (moist cured) of this project, the following values apply:

<u>Group</u>	<u>Ini. Read. Age</u>	<u>Rel. Hum.</u>	<u>(<math>\epsilon_{sh}</math>)<sub>u</sub></u>
A, B, C	7 days	40%	650 x 10 <sup>-6</sup> in/in.
D	7	50	540
E	9	50	510
F	21	50	385

General value suggested for all weights of structural concrete (both types I and III cement) --  $(\epsilon_{sh})_u = 800 \times 10^{-6}$  in/in for  $H = 40\%$ .  
From Eq. (13) for  $H = 70\%$ ,  $(\epsilon_{sh})_u = 0.70(800 \times 10^{-6}) = 560 \times 10^{-6}$  in/in.

Shrinkage at any time after age 1-3 days for steam cured concrete

$$(\epsilon_{sh})_t = \frac{t}{55 + t} (\epsilon_{sh})_u \quad (9)$$

For the bridge girder sand-lightweight concrete of this project --  $(\epsilon_{sh})_u = 560 \times 10^{-6}$  in/in for  $H = 40\%$ .  $H$  was  $70\%$ . From Eq. (13) for  $H = 70\%$ ,  $(\epsilon_{sh})_u = 0.70(560 \times 10^{-6}) = 392 \times 10^{-6}$  in/in.

General value suggested for all weights of structural concrete (both types I and III cement) --  $(\epsilon_{sh})_u = 730 \times 10^{-6}$  in/in for  $H = 40\%$ .  
From Eq. (13) for  $H = 70\%$ ,  $(\epsilon_{sh})_u = 0.70(730 \times 10^{-6}) = 510 \times 10^{-6}$  in/in.

In Eqs. (7), (8) and (9),  $t$  is time in days after loading for creep and time after initial shrinkage is considered.

Values from the Standard Eqs. (7) - (9) of  $C_t/C_u$  and

$(\epsilon_{sh})_t/(\epsilon_{sh})_u$  are:

	<u>1 mth</u>	<u>3 mths</u>	<u>6 mths</u>	<u>1 yr</u>	<u>5 yrs</u>
$C_t/C_u$ , Eq. (7) --	0.44	0.60	0.69	0.78	0.90
$(\epsilon_{sh})_t/(\epsilon_{sh})_u$ , Eq. (8) --	0.46	0.72	0.84	0.91	0.98
$(\epsilon_{sh})_t/(\epsilon_{sh})_u$ , Eq. (9) --	0.35	0.62	0.77	0.87	0.97

The lower creep and shrinkage for the concrete of this project, as compared to the average or general values, was probably due to the high concrete strengths attained. The computed (in Eqs. 7 and 8) and measured creep and shrinkage for the moist cured concrete of this project are shown in Figures 3, 4, 6 and 7.

Correction factors

All correction factors are applied to ultimate values. However, since creep and shrinkage for any period in Eqs. (7), (8), and (9) are linear functions of the ultimate values, the correction factors in this procedure may be applied to short-term creep and shrinkage as well.

For slumps greater than 3", see Figure B3.

For loading ages later than 7 days for moist cured concrete and later than 1-3 days for steam cured concrete, use Eqs. (10) and (11) for the creep correction factors (18).

$$\text{Creep (C.F.)}_{LA} = 1.25 t_{LA}^{-0.118} \quad \text{for moist cured concrete} \quad (10)$$

$$\text{Creep (C.F.)}_{LA} = 1.13 t_{LA}^{-0.095} \quad \text{for steam cured concrete} \quad (11)$$

where  $t_{LA}$  is the loading age in days. For example,

When $t_{LA} = 10$ days, mo. cu. (C.F.) <sub>LA</sub> = 0.95, st. cu. (C.F.) <sub>LA</sub> = 0.90.		
20	0.87	0.85
30	0.83	0.82
60	0.77	0.76
90	0.74	0.74

For shrinkage considered from other than 7 days for moist cured concrete and other than 1-3 days for steam cured concrete, determine the differential in Eqs. (8) and (9) for any period starting after this time. For shrinkage of moist cured concrete from 1 day (used to estimate differential shrinkage in composite beams, for example), use Shrinkage C.F. = 1.20.

For greater than 40% ambient relative humidity, use Eqs. (12) and (13) for the creep and shrinkage correction factors (18), (43), (44).

$$\text{Creep (C.F.)}_H = 1.27 - 0.0067 H, \quad H = 40\% \quad (12)$$

$$\begin{aligned} \text{Shrinkage (C.F.)}_H &= 1.40 - 0.010 H, \quad 40\% = H = 80\% \\ &= 3.00 - 0.030 H, \quad 80\% = H = 100\% \end{aligned} \quad (13)$$

where H is relative humidity in percent. For example,

When H = 40%,	Creep (C.F.) <sub>H</sub> = 1.00,	Shrinkage (C.F.) <sub>H</sub> = 1.00.
50	0.94	0.90
60	0.87	0.80
70	0.80	0.70
80	0.73	0.60
90	0.67	0.30
100	0.60	0.00

For minimum thickness of members greater than 6", see Figure B3 for the creep and shrinkage correction factors, as a function of length of drying and loading periods. For most design purposes, this effect (as shown in Appendix B) can be neglected for creep of members up to about 10" to 12" minimum thickness, and for shrinkage of members up to about 8" to 9" minimum thickness.

This method of treating the effect of member size was based on information from References (14), (18), (44), and this project. For large-thickness members, refer to the method of Reference (14), and others, for relating size and shape effects for creep and shrinkage to the volume/surface ratio of the members, etc.

Other correction factors for creep and shrinkage, which are usually not excessive and tend to offset each other, are described in Appendix B. For design purposes, these may normally be neglected.

## Chapter 4

## LOSS OF PRESTRESS AND CAMBER

4.1 Relaxation Tests

Relaxation measurements were made for three different diameter 7-wire prestressing strands. The results agreed well with the equation suggested in Reference (45), as can be seen in Figure 8.

It should be noted, however, that the relaxation of steel stress in a prestressed member takes place under decreasing steel strain (due to creep, shrinkage, etc.), rather than at constant length as in a relaxation test. The loss of prestress due to steel relaxation is also affected by slab casting (level of stress in steel is raised) in the case of composite beams. Due to these effects and the practice of over-tensioning to counteract the relaxation that takes place between the time of tensioning and effective bonding of concrete to steel (this practice was assimilated in the laboratory beam tests, where it is noted in Figure 8 that about 2% relaxation takes place in 24 hours, for example), it is felt that about 75% of the steel relaxation in a constant-length relaxation test should be used in prestressed concrete loss calculations.

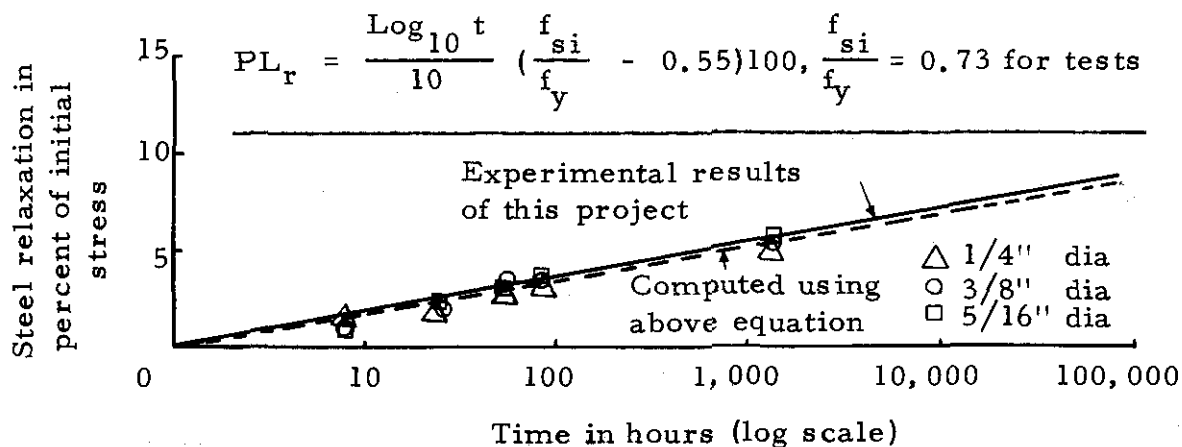
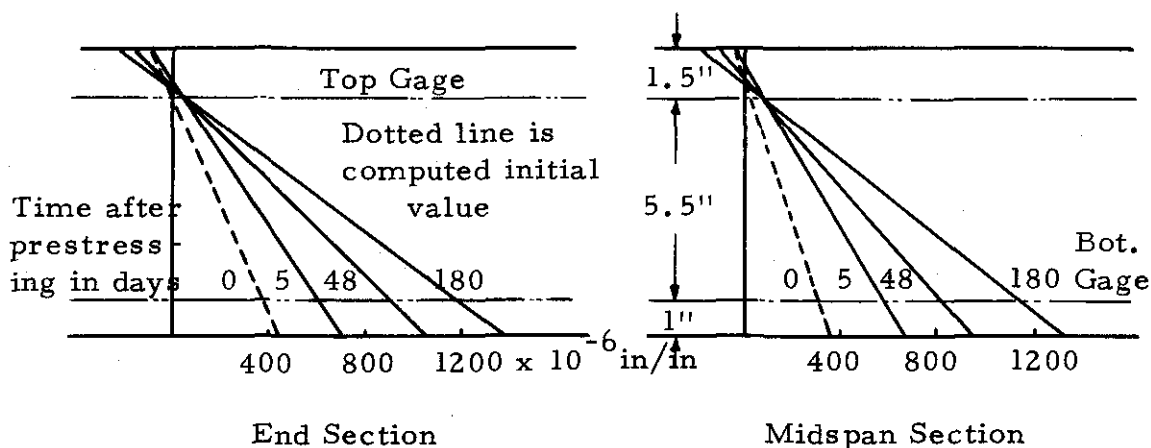


Figure 8. Results of steel relaxation tests



Initial plus time-dependent strain distribution diagrams from concrete strains measured on the sides of the beams

Typical experimental prestress loss determined for end section at 180 days

$f_{si} = 172$  ksi,  $E_s = 27 \times 10^3$  ksi, Observed conc. strain at cgs =

$1001 \times 10^{-6}$  in/in.

Loss from meas. strains =  $(1001 \times 10^{-6})(27 \times 10^3)(100)/172 = 15.7\%$

Inc. in meas. loss due to lateral distr. (det. as 2.5% of 15.7) = 0.4

Meas. loss due to steel relaxation (75% of value from Figure 8) = 5.5

Total experimental loss of prestress = 21.6%

Figure 9. Determination of experimental loss of prestress

It was concluded in Reference (46) that steel relaxation is probably insignificant beyond 100,000 hours (11.4 yrs), and that this ultimate value might be taken as twice the value at 1000 hours (1.4 mths). The relaxation equation recommended in this paper is the same time-function (Log t) as that of Reference (45), except reduced by 25% in magnitude and incorporating the idea of Reference (46) that the ultimate value be taken as twice the value at 1000 hours. This results in an ultimate steel relaxation for prestressed concrete of 7.5%, as shown in Term (4) of Eq. (14). Although Term (4) of Eq. (14) was suggested on the basis of relaxation studies of 7-wire prestressing strands used for pretensioned specimens, it is felt that this is valid even for post-tensioned specimens (see comparison of loss of prestress and camber of other published data in Sec. 4.7).

#### 4.2 Computed Loss of Prestress, Camber, and

Deflection (23), (24), (25), (29), (30), (33), (42), (45), (46), (47)

Non-composite beams at any time, including ultimate values

The loss of prestress, in percent of initial tensioning stress, is given by Eq. (14).

$$PL_t = \left[ \overbrace{(nf_c)}^{(1)} + \overbrace{(nf_c)C_t \left(1 - \frac{\Delta F_t}{2F_o}\right)}^{(2)} + \overbrace{(e_{sh})_t E_s / (1 + npk_s)}^{(3)} + \overbrace{\frac{f_{si}}{100} 1.5 \text{Log}_{10} t}^{(4)} \right] \frac{100}{f_{si}} \quad (14)$$

where:

Term (1) is the prestress loss due to elastic shortening =  $PL_{el} \cdot f_c = \frac{F_i}{A_t} + \frac{F_i e^2}{I_t} - \frac{M_{De}}{I_t}$ , and  $n$  is the modular ratio at the time of prestressing. Frequently  $F_o$ ,  $A_g$ , and  $I_g$  are used instead of  $F_i$ ,  $A_t$ , and  $I_t$ , where  $F_o = F_i(1 - n p)$ . Only the first two terms for  $f_c$  apply at beam ends.

Term (2) is the prestress loss due to concrete creep. The expression,  $C_t(1 - \frac{\Delta F_t}{2 F_o})$ , was used in References (23) and (30) to approximate the creep effect resulting from the variable stress history. See the section on Required Calculations and Summary of General Parameters for approximate values of  $\Delta F_t/F_o$  (in form of  $\Delta F_s/F_o$  and  $\Delta F_u/F_o$ ) for this secondary effect at various times.

Term (3) is the prestress loss due to shrinkage (47). The expression,  $(\epsilon_{sh})_t E_s$ , somewhat (approximately 1% loss differential for the bridge girder ultimate value in the example herein) overestimates (on safe side) Term (3).

Term (4) is the prestress loss due to steel relaxation. Assumes Max. value = 7.5% (at or above  $10^5$  hrs = 11.4 yrs). In this term,  $t$  is time after initial stressing in hours. This expression applies only when  $f_{si}/f_y$  is greater than or equal to 0.55, in which  $f_y$  is the 0.1%-offset yield strength.

The camber is given by Eq. (15). It is suggested that an average of the end and midspan loss be used for straight tendons (laboratory beams herein) and 1-pt. harping, and the midspan loss for 2-pt. harping (bridge girders herein).

$$\Delta_t = \underbrace{(\Delta_i)_{F_o}}_{(1)} - \underbrace{(\Delta_i)_D}_{(2)} + \underbrace{\left[ -\frac{\Delta F_t}{F_o} + \left(1 - \frac{\Delta F_t}{2 F_o}\right) C_t \right]}_{(3)} \underbrace{(\Delta_i)_{F_o}}_{(4)} - \underbrace{C_t (\Delta_i)_D}_{(4)} - \underbrace{\Delta_L}_{(5)} \quad (15)$$

where:

Term (1) is the initial camber due to the initial prestress force after elastic loss,  $F_o$ . See Appendix D for common cases of prestress moment diagrams with formulas for computing camber,  $(\Delta_i)_{F_o}$ . Here  $F_o = F_i (1 - n f_c / f_{s1})$ , where  $f_c$  is determined as in Term (1) of Eq. (14).

Term (2) is the initial dead load deflection of the beam.

$$(\Delta_i)_D = K M L^2 / E_{ci} I_g. \quad \text{See Notation for K and M formulas.}$$

Term (3) is the creep (time-dependent) camber of the beam due to the prestress force. This expression includes the effects of creep and loss of prestress; that is, the creep effect under variable stress.  $\Delta F_t$  refers to the total loss at any time minus the elastic loss. It is noted that the term,  $\Delta F_t / F_o$ , refers to the steel stress or force after elastic loss, and the prestress loss in percent, PL (as used herein), refers to the initial tensioning stress or force.

The two are related as:  $\frac{\Delta F_t}{F_o} = \frac{1}{100} (PL_t - PL_{el}) \frac{f_{si}}{f_o}$ , and can be closely approximated by  $\frac{\Delta F_t}{F_o} = \frac{1}{100} (PL_t - PL_{el}) \frac{1}{1 - n_p}$ .

Term (4) is the dead load creep deflection of the beam.

Term (5) is the live load deflection of the beam.

The deflection at any time for a non-prestressed reinforced beam is given by Eq. (16).

$$\Delta_t = \underbrace{-(\Delta_i)_D}_{(1)} - \underbrace{k_r C_t (\Delta_i)_D}_{(2)} - \underbrace{K_w \phi_{sh} L^2}_{(3)} - \underbrace{(\Delta_L)}_{(4)} \quad (16)$$

where:

Term (1) is the initial dead load deflection of the beam.

$(\Delta_i)_D = K M L^2 / E_{ci} I_g$ . See Notation for K and M formulas.

Term (2) is the dead load creep deflection of the beam.  $k_r$  takes into account the movement of the neutral axis. See Notation for values of  $k_r$ .

Term (3) is the deflection due to shrinkage warping.

$(\Delta_{sh})_t = K_w \phi_{sh} L^2$  See Notation for values of  $K_w$ ;  $\phi_{sh} = .7 (\epsilon_{sh})_t^{1/3} / t$

where p is the steel percentage and t is the thickness of the member.

Term (4) is the live load deflection of the beam.

Unshored and shored composite beams at any time, including ultimate values

Subscripts 1 and 2 are used to refer to the slab (or effect of

the slab such as under slab dead load) and precast beam, respectively.

The loss of prestress, in percent of initial tensioning stress, for unshored and shored composite beams is given by Eq. (17).

$$\begin{aligned}
 PL_t = & \left[ \overbrace{(nf_c)}^{(1)} + \overbrace{(nf_c)C_{s_2} \left(1 - \frac{\Delta F_s}{2 F_o}\right)}^{(2)} + \overbrace{(nf_c)(C_{t_2} - C_{s_2}) \left(1 - \frac{\Delta F_s + \Delta F_t}{2 F_o}\right) \frac{I_2}{I_c}}^{(3)} \right. \\
 & + \overbrace{(\epsilon_{sh})_t E_s / (1 + npk_s)}^{(4)} + \overbrace{\frac{f_{si}}{100} 1.5 \text{Log}_{10} t}^{(5)} - \overbrace{(mf_{cs})}^{(6)} - \overbrace{(mf_{cs})C_{t_1} \frac{I_2}{I_c}}^{(7)} \\
 & \left. - \overbrace{PG_{DS}}^{(8)} \right] \frac{100}{f_{si}} \tag{17}
 \end{aligned}$$

where:

Term (1) is the prestress loss due to elastic shortening.

See Term (1) of Eq. (14) for the calculation of  $f_c$ .

Term (2) is the prestress loss due to concrete creep up to the time of slab casting.  $C_{s_2}$  is the creep coefficient of the precast beam concrete at the time of slab casting. See Term (2) of Eq. (14) for comments concerning the reduction factor,  $\left(1 - \frac{\Delta F_s}{2 F_o}\right)$ .

Term (3) is the prestress loss due to concrete creep for any period following slab casting.  $C_{t_2}$  is the creep coefficient of the precast beam concrete at any time after slab casting. The reduction factor,  $\left(1 - \frac{\Delta F_s + \Delta F_t}{2 F_o}\right)$ , with the incremental creep coefficient,

$(C_{t_2} - C_{s_2})$ , estimates the effect of creep under the variable prestress force that occurs after slab casting. The reduction factor term was modified from previous references. The expression,  $I_2/I_c$ , modifies the initial value and accounts for the effect of the composite section in restraining additional creep curvature (strain) after slab casting.

Term (4) is the prestress loss due to shrinkage. See Term (3) of Eq. (14).

Term (5) is the prestress loss due to steel relaxation. In this term  $t$  is time after initial stressing in hours. See Term (4) of Eq. (14) for the maximum value and limitations.

Term (6) is the elastic prestress gain due to slab dead load, and  $m$  is the modular ratio at the time of slab casting.

$$f_{cs} = \frac{M_{S, Di} e}{I_g}, \quad M_{S, Di} \text{ refers to slab or slab plus diaphragm dead}$$

load, and  $e, I_g$  refer to the precast beam section properties for unshored construction and the composite beam section properties for shored construction.

Term (7) is the prestress gain due to creep under slab dead load.  $C_{t_1}$  is the creep coefficient for the slab loading, where the age of the precast beam concrete at the time of slab casting is considered.

Term (8) is the prestress gain due to differential shrinkage.

$PG_{DS} = mf_{cd}$ , where  $f_{cd} = \frac{Qy_{cs}e_c}{I_c}$ , and  $f_{cd}$  is the concrete stress at the steel c.g.s. See Notation for additional descriptions of terms. Since this effect results in a prestress gain, not loss, and is normally small (see Table 3), it may usually be neglected.

The camber of unshored and shored composite beams is given by Eqs. (18) and (19), respectively.

Unshored construction:

$$\begin{aligned}
 \Delta_t = & \underbrace{(\Delta_i)_{F_0}}_{(1)} - \underbrace{(\Delta_i)_2}_{(2)} + \underbrace{\left[ -\frac{\Delta F_s}{F_0} + \left(1 - \frac{\Delta F_s}{2F_0}\right)C_{s2} \right]}_{(3)} (\Delta_i)_{F_0} \\
 & + \underbrace{\left[ -\frac{\Delta F_t - \Delta F_s}{F_0} + \left(1 - \frac{\Delta F_s + \Delta F_t}{2F_0}\right)(C_{t2} - C_{s2}) \right]}_{(4)} (\Delta_i)_{F_0} \frac{I_2}{I_c} \\
 & - \underbrace{C_{s2}}_{(5)} (\Delta_i)_2 - \underbrace{(C_{t2} - C_{s2})}_{(6)} (\Delta_i)_2 \frac{I_2}{I_c} - \underbrace{(\Delta_i)_1}_{(7)} \\
 & - \underbrace{C_{t1}}_{(8)} (\Delta_i)_1 \frac{I_2}{I_c} - \underbrace{\Delta_{DS}}_{(9)} - \underbrace{\Delta_L}_{(10)} \tag{18}
 \end{aligned}$$

where:

Term (1) is the initial camber due to the initial prestress force after elastic loss,  $F_0$ . See Appendix D for common cases of

prestress moment diagrams with formulas for computing camber,

$(\Delta_i)_{F_0}$ . See Term (1) of Eq. (15) for determining  $F_0$ .

Term (2) is the initial dead load deflection of the precast beam.  $(\Delta_i)_2 = KM_2 L^2/E_{ci} I_g$ . See Notation for K and M formulas.

Term (3) is the creep (time-dependent) camber of the beam, due to the prestress force, up to the time of slab casting. See Term (3) of Eq. (15) and Terms (2) and (3) of Eq. (16) for further explanation.

Term (4) is the creep camber of the composite beam, due to the prestress force, for any period following slab casting. Again, see Term (3) of Eq. (15) and Terms (2) and (3) of Eq. (16) for further explanation.

Term (5) is the creep deflection of the precast beam up to the time of slab casting due to the precast beam dead load.

Term (6) is the creep deflection of the composite beam for any period following slab casting due to the precast beam dead load.

Term (7) is the initial deflection of the precast beam under slab dead load.  $(\Delta_i)_1 = KM_1 L^2/E_{cs} I_g$ . See Notation for K and M formulas. When diaphragms are used, add to  $(\Delta_i)_1$ :

$$(\Delta_i)_{1D} = \frac{M_{1D}}{E_{cs} I_g} \left( \frac{L^2}{8} - \frac{a^2}{6} \right), \text{ where } M_{1D} \text{ is the moment between dia-}$$

phrams, and  $a$  is  $L/4$ ,  $L/3$ , etc., for 2 symmetrical diaphragms at

the quarter points, third points, etc., respectively.

Term (8) is the creep deflection of the composite beam due to slab dead load.  $C_{t1}$  is the creep coefficient for the slab loading, where the age of the precast beam concrete at the time of slab casting is considered.

Term (9) is the deflection due to differential shrinkage. For simple spans,  $\Delta_{DS} = Q y_{cs} L^2 / 8 E_{cs} I_c$ , where  $Q = D A_1 E_1 / 3$ . See Notation for additional descriptions of terms. The factor 3 provides for the gradual increase in the shrinkage force from day 1, and also approximates the creep and varying stiffness effects (25). This factor 3 is also consistent with the data herein and elsewhere. See Table 4 for numerical values herein. In the case of continuous members, differential shrinkage produces secondary moments (similar to effect of prestressing but opposite in sign--normally) that should be included.

Term (10) is the live load deflection of the composite beam, in which the gross-section flexural rigidity,  $E_c I_c$ , is normally used.

Shored construction:

$\Delta_t =$  Eq. (18), with Terms (7) and (8) modified as follows: (19)

Term (7) is the initial deflection of the composite beam under slab dead load.  $(\Delta_i)_1 = K M_1 L^2 / E_{cs} I_c$ . See Notation for K and M formulas.

Term (8) is the creep deflection of the composite beam under slab dead load =  $C_{t1} (\Delta_i)_1$ . The composite-section effect is already included in Term (7).

The deflection of ordinary reinforced composite beams of unshored and shored construction is given by Eqs. (20) and (21).

Unshored construction:

$$\begin{aligned}
 \Delta_t = & \underbrace{- (\Delta_i)_D}_{(1)} - \underbrace{k_r C_{s2} (\Delta_i)_D}_{(2)} - \underbrace{k_r (C_{t2} - C_{s2}) (\Delta_i)_D}_{(3)} \frac{I_2}{I_c} \\
 & - \underbrace{K_w \phi_{ss2} L^2}_{(4)} - \underbrace{K_w (\phi_{sh2} - \phi_{ss2}) L^2}_{(5)} \frac{I_2}{I_c} - \underbrace{(\Delta_i)_1}_{(6)} \\
 & - \underbrace{k_r C_{t1} (\Delta_i)_1}_{(7)} \frac{I_2}{I_c} - \underbrace{\Delta_{DS}}_{(8)} - \underbrace{\Delta_L}_{(9)} \tag{20}
 \end{aligned}$$

Term (1) is the initial dead load deflection of the beam.

$$(\Delta_i)_D = K M L^2 / E_{ci} I_g. \text{ See Notation for K and M formulas.}$$

Term (2) is the dead load creep deflection up to the time of slab casting.  $k_r$  takes into account the movement of the neutral axis.

See Notation for values of  $k_r$ .

Term (3) is the creep deflection of the composite beam for any period following slab casting due to the precast beam dead load.

Term (4) is the deflection due to shrinkage warping up to the time of slab casting. See Term (3) of Eq. (16) for further explanation.

Term (5) is the deflection due to shrinkage warping for any period following slab casting due to the shrinkage of the precast beam. See Term (3) of Eq. (16) for further explanation.

Term (6) is the initial deflection of the precast beam under slab dead load.  $(\Delta_i)_1 = K M L^2 / E_{cs} I_g$ . See Notation for K and M formulas. When diaphragms are used, add to  $(\Delta_i)_1$ :

$(\Delta_i)_{1D} = \frac{M_{1D}}{E_{cs} I_g} \left( \frac{L^2}{8} - \frac{a^2}{6} \right)$ , where  $M_{1D}$  is the moment between diaphragms, and a is L/4, L/3, etc., for symmetrical diaphragms at quarter points, third points, etc., respectively.

Term (7) is the creep deflection of the composite beam due to slab dead load.  $C_{t_1}$  is the creep coefficient for slab loading, where the age of the precast beam concrete at the time of slab casting is considered.

Term (8) is the deflection due to differential shrinkage. See Term (9) of Eq. (18) for further explanation.

Term (9) is the live load deflection of the composite beam, in which the gross-section flexural rigidity,  $E_c I_c$ , is normally used.

Shored construction:

$$\Delta_t = \text{Eq. (20), with Terms (6) and (7) modified as follows:} \quad (21)$$

Term (6) is the initial deflection of the composite beam under slab dead load.  $(\Delta_i)_1 = K M L^2 / E_{cs} I_c$ . See Notation for K and M formulas.

Term (7) is the creep deflection of the composite beam under slab dead load  $= C_{t_1} (\Delta_i)_1$ . The composite-section effect is already included in Term (6).

It is suggested that the 28-day moduli of elasticity for both slab and precast beam concretes, and the gross I (neglecting the steel), be used in computing the composite moment of inertia,  $I_c$ , in Eqs. (17), (18), (19), (20), and (21).

Special case of "ultimate loss of prestress, camber, and deflection"

For computing ultimate values of loss of prestress and camber, Eqs. (22) - (29) correspond term by term to Eqs. (14) - (21), respectively.

Loss of prestress for non-composite beams, as per Eq. (14):

$$\begin{aligned}
 PL_u = & \left[ \overbrace{(n f_c)}^{(1)} + \overbrace{(n f_c) C_u \left(1 - \frac{\Delta F_u}{2 F_o}\right)}^{(2)} + \overbrace{(\epsilon_{sh})_u E_s / (1 + npk_s)}^{(3)} \right. \\
 & \left. + \overbrace{0.075 f_{si}}^{(4)} \right] \frac{100}{f_{si}} \quad (22)
 \end{aligned}$$

Camber of non-composite beams, as per Eq. (15):

$$\Delta_u = \underbrace{(\Delta_i)_{F_o}}_{(4)} - \underbrace{(\Delta_i)_D}_{(5)} + \underbrace{\left( -\frac{\Delta F_u}{F_o} + \left(1 - \frac{\Delta F_u}{2 F_o}\right) C_u \right)}_{(3)} (\Delta_i)_{F_o}$$

$$- \underbrace{C_u (\Delta_i)_D}_{(4)} - \underbrace{\Delta_L}_{(5)} \quad (23)$$

Deflection of non-composite non-prestressed reinforced beams, as per Eq. (16):

$$\Delta_u = \underbrace{-(\Delta_i)_D}_{(1)} - \underbrace{k_r C_u (\Delta_i)_D}_{(2)} - \underbrace{K_w \phi_u L^2}_{(3)} - \underbrace{\Delta_L}_{(4)} \quad (24)$$

Loss of prestress for unshored and shored composite beams, as per Eq. (17):

$$PL_u = \left[ \underbrace{(n f_c)}_{(4)} + \underbrace{(n f_c)(\alpha_s C_u)}_{(2)} \underbrace{\left(1 - \frac{\Delta F_s}{2 F_o}\right)}_{(5)} + \underbrace{(n f_c)(1 - \alpha_s) C_u}_{(3)} \underbrace{\left(1 - \frac{\Delta F_s + \Delta F_u}{2 F_o}\right)}_{(6)} \right] \frac{I_2}{I_c}$$

$$+ \underbrace{(\epsilon_{sh_u}) E_s / (1 + npk_s)}_{(7)} + \underbrace{0.075 f_{si}}_{(8)} - \underbrace{(m f_{cs})}_{(6)}$$

$$- \left[ \underbrace{(m f_{cs})(\beta_s C_u)}_{(4)} \frac{I_2}{I_c} - \underbrace{PG_{DS}}_{(5)} \right] \frac{100}{f_{si}} \quad (25)$$

Camber of unshored composite beams, as per Eq. (18):

$$\begin{aligned}
 \Delta_u = & \underbrace{(\Delta_i)_{F_o}}_{(1)} - \underbrace{(\Delta_i)_2}_{(2)} + \underbrace{\left( -\frac{\Delta F_s}{F_o} + \left(1 - \frac{\Delta F_s}{2 F_o}\right) \alpha_s C_u \right)}_{(3)} (\Delta_i)_{F_o} \\
 & + \underbrace{\left( -\frac{\Delta F_u - \Delta F_s}{F_o} + \left(1 - \frac{\Delta F_s + \Delta F_u}{2 F_o}\right) (1 - \alpha_s) C_u \right)}_{(4)} (\Delta_i)_{F_o} \frac{I_2}{I_c} \\
 & - \underbrace{\alpha_s C_u (\Delta_i)_2}_{(5)} - \underbrace{(1 - \alpha_s) C_u (\Delta_i)_2 \frac{I_2}{I_c}}_{(6)} - \underbrace{(\Delta_i)_1}_{(7)} - \underbrace{\beta_s C_u (\Delta_i)_1 \frac{I_2}{I_c}}_{(8)} \\
 & - \underbrace{\Delta_{DS}}_{(9)} - \underbrace{\Delta_L}_{(10)} \tag{26}
 \end{aligned}$$

Deflection of unshored composite non-prestressed reinforced beams, as per Eq. (20):

$$\begin{aligned}
 \Delta_u = & - \underbrace{(\Delta_i)_D}_{(1)} - \underbrace{k_r \alpha_s C_u (\Delta_i)_D}_{(2)} - \underbrace{k_r (1 - \alpha_s) C_u (\Delta_i)_D \frac{I_2}{I_c}}_{(3)} - \underbrace{K_w \gamma_s \phi_u L^2}_{(4)} \\
 & - \underbrace{K_w \gamma_{s1} \phi_u L^2 \frac{I_2}{I_c}}_{(5)} - \underbrace{(\Delta_i)_1}_{(6)} - \underbrace{k_r \beta_s C_u (\Delta_i)_1 \frac{I_2}{I_c}}_{(7)} - \underbrace{\Delta_{DS}}_{(8)} \\
 & - \underbrace{\Delta_L}_{(9)} \tag{27}
 \end{aligned}$$

Camber of shored composite beams, as per Eq. (19):

$\Delta_u$  = Eq. (26), except that the composite moment of inertia is used in Term (7) to compute  $(\Delta_i)_1$ , and the ratio  $I_2/I_c$ , is eliminated in Term (8). (28)

Deflection of shored composite non-prestressed reinforced beams, as per Eq. (21):

$\Delta_u$  = Eq. (27), except that the composite moment of inertia is used in Term (6) to compute  $(\Delta_i)_1$ , and the ratio  $I_2/I_c$ , is eliminated in Term (7). (29)

It is noted that Eqs. (14) - (29) could be greatly shortened by combining terms and substituting the approximate parameters given below, but are presented in the form of separate terms in order to show the separate effects or contributions to the behavior (such as due to prestress force, dead load, creep, shrinkage, etc., that occur both before and after slab casting.

Grossly approximate equations:

Non-composite beams (prestressed) --

$$\Delta_u = \Delta_i + \Delta_i C_u \left(1 - \frac{\Delta F_u}{2 F_o}\right), \Delta_i = (\Delta_i)_{F_o} - (\Delta_i)_D \quad (30)$$

Composite beams (prestressed) --

$$PL_u = \left[ n f_c \left(1 + \frac{C_u}{2}\right) - n f_{cs} + (\epsilon_{sh})_u E_s + 0.075 f_{si} \right] \frac{100}{f_{si}} \quad (31)$$

$$\Delta_u = \Delta_i + \Delta_i C_u \left(\frac{I_2}{I_c}\right), \quad \Delta_i = (\Delta_i)_{F_o} - (\Delta_i)_2 - (\Delta_i)_1 \quad (32)$$

Non-composite beams (non-prestressed) --

$$\Delta_u = -(\Delta_i)_D - C_u (\Delta_i)_D - K_w (\varphi_{sh})_u L^2, \quad \text{where} \quad (33)$$

$\varphi_{shu} = \gamma_s (\epsilon_{sh})_u / t$ , and  $K_w$  is defined in Notation.

Composite beams (non-prestressed) --

$$\Delta_u = \Delta_i + \Delta_i C_u \left(\frac{I_2}{I_c}\right) - K_w (\varphi_{sh})_u L^2, \quad \text{where} \quad (34)$$

$\Delta_i = -(\Delta_i)_2 - (\Delta_i)_1$ ,  $(\varphi_{sh})_u = \gamma_s (\epsilon_{sh})_u / t$ , and

$K_w$  is defined in Notation.

#### 4.3 Required Calculations and Summary of General Parameters

Continuous time functions are provided for all needed material parameters (and for different weight concretes, moist and steam cured), so that the equations herein readily lend themselves to computer solutions. Certain other read-in data (such as for the effect of behavior before and after slab casting --  $\alpha_s$ ,  $\beta_s$ ,  $m$ , and  $\Delta F_s / F_o$ ) are also included. The parameters related to material properties are summarized below, so that for composite beam hand calculations for example; in addition to the section properties, prestress force,  $F_o$ , and concrete stresses,  $f_c$ ,  $f_{cs}$ , the only calculations needed for computing prestress loss and camber are the initial camber, deflections --

---

\* The ratio  $I_2 / I_c$  is dropped out for the shrinkage term to account for the cumulative effects of shrinkage - i. e., before slab casting, after slab casting and due to differential shrinkage. For values of  $\gamma_s$ , see Section 4.3.

$(\Delta_i)_{F_0}$ ,  $(\Delta_i)_2$ ,  $(\Delta_i)_1$ , and  $\Delta_{DS}$ ,  $\Delta_L$ .

The following loss of prestress ratios at the time of slab casting and ultimate are suggested for most calculations:

$\Delta F_s / F_0$  for 3 wks to 1 mth between prestressing and slab casting = 0.11 for Nor. Wt., 0.13 for Sand-Lt. Wt., 0.15 for All-Lt. Wt.

$\Delta F_s / F_0$  for 2 to 3 mths between prestressing and slab casting = 0.15 for Nor. Wt., 0.18 for Sand-Lt. Wt., 0.21 for All-Lt. Wt.

$\Delta F_u / F_0 = 0.22$  for Nor. Wt., 0.25 for Sand-Lt. Wt., 0.31 for All-Lt. Wt.

Note that these are defined as the total loss (at slab casting and ultimate) minus the initial elastic loss divided by the prestress force after elastic loss. The different values for the different weight concretes are due primarily to different initial strains (because of different E's) for normal stress levels.

The following average modular ratios are based on  $f'_c = 4000$  to 4500 psi for both moist cured (M.C.) and steam cured (S.C.) concrete and type I cement; up to 3-mths  $f'_c = 6360$  to 7150 psi (using Eq. 2) for moist cured and 3-mths  $f'_c = 6050$  to 6800 psi (using Eq. 4) for steam cured, and for both 250 K and 270 K prestressing strands:

	Modular Ratio	Nor. Wt.		Sand- Lt. Wt.		All- Lt. Wt.	
		(w = 145)		(w = 120)		(w = 100)	
		M. C.	S. C.	M. C.	S. C.	M. C.	S. C.
At release of prestress	n =	7.3	7.3	9.8	9.8	12.9	12.9
For the time bet- ween prestressing and slab casting:	m =	6.1	6.3	8.1	8.3	10.7	10.9
1 month,		6.0	6.2	8.0	8.2	10.5	10.7
2 months,		5.9	6.1	7.9	8.2	10.3	10.6
3 months,		5.8	6.0	7.7	8.0	10.2	10.5

$E_s = 27 \times 10^6$  psi for 250 K strands,  $E_s = 28 \times 10^6$  psi for  
 270 K strands,  $\alpha_s$  refers to the part of the total creep that takes place  
 before slab casting ( $\alpha_s = \frac{t^{0.60}}{10 + t^{0.60}}$ , as per Eq. 7), and  $\beta_s$  (= the  
 avg. Creep (C.F.)<sub>LA</sub> from Eqs. 10 and 11) is the creep correction  
 factor for the precast beam concrete age when the slab is cast (under  
 slab dead load). See Eqs. (7), (8), (9), and the correction factors  
 herein, for suggested values for  $C_u$  and  $(\epsilon_{sh})_u$ .

The following may be substituted for normal weight, sand-  
 lightweight, and all-lightweight concrete (moist and steam cured,  
 and types I and III cement):

For the time bet- = 3 weeks,	$\alpha_s = 0.38,$	$\beta_s = 0.85$
ween prestressing 1 month,	0.44,	0.83
and slab casting: 2 months,	0.54,	0.78
3 months,	0.60,	0.75

The following may be substituted for normal weight, sand-  
 lightweight and all-lightweight concrete (moist cured) and Types I  
 and III cement for composite non-prestressed beams.

		(For 'beam in position' at 7 days)*	
For the time bet-	= 2 weeks,	$\gamma_s = 0.29,$	$\gamma_{s1} = 0.71$
ween 'beam in pos-	3 weeks,	0.38,	0.62
ition' and slab	1 month,	0.46,	0.54
casting	2 months,	0.63,	0.37
	3 months,	0.72,	0.29

#### 4.4 Sample Calculations

The following numerical substitutions for ultimate loss of prestress at midspan, using Eqs. (17), (25), and ultimate midspan camber, using Eqs. (18), (26), with the general parameters given herein, are made for the sand-lightweight, steam cured composite bridge girders (with slab moist cured) of this project:

Parameters and terms for interior girders

Span = 86 ft, girder spacing = 7 ft, 2-point harping at 0.4L-pt. from end,  $e$  (midspan) = 14.3 in,  $e$  (end) = 6.2 in,  $f_{si} = 190,000$  psi,  $F_i = 867$  kips,  $A_s = 4.56$  in<sup>2</sup>,  $A_g = 520$  in<sup>2</sup>,  $p = 0.00883$ ,  $I_g = 108,500$  in<sup>4</sup>,  $M_D$  (precast beam) = 410 ft-k,  $I_c = 334,100$  in<sup>4</sup> (using slab width divided by a factor of  $E_{stem}/E_{slab} = 3.42/3.41 = 1.00$ ),  $M_{S,Di}$  (slab plus diaphragm moment at midspan) = 630 ft-k.

Modulii of elasticity (using Eqs. 2, 4, and 6 for concrete):

$E_s = 28 \times 10^6$  psi, as suggested for 270 K grade strands herein.

\* The differentials are to be used when the beam is 'in position' at an age other than 7 days. Eg: For a slab cast at age of beam = 35 days with the beam in position at age = 28 days, the values of  $\gamma_s$  and  $\gamma_{s1}$  are (0.46 for 35 days - 7 days = 1 month minus 0.38 for 28 days - 7 days = 3 weeks) = 0.08, and (1.00 - 0.46) = 0.54, respectively.

Slab  $E_c = 3.41 \times 10^6$  psi, for  $f'_c = 3500$  psi,  $w = 145$  pcf (Table A4).

Precast beam -- (see description of  $m$  and  $n$  in general parameters section herein for concrete properties).

$$E_{ci} = E_s/n = 28 \times 10^6/9.8 = 2.86 \times 10^6 \text{ psi.}$$

$$E_{cs} = E_s/m = 28 \times 10^6/8.2 = 3.42 \times 10^6 \text{ psi.}$$

Using  $F_i$ ,  $A_t$ , and  $I_t$ , as per Term (1) of Eq. (14) or (17) or (25)  $f_c = 2467$  psi. As per Term (6) of Eq. (16) or (21),  $f_{cs} = 1006$  psi. These concrete stresses refer to the midspan section. As per Term (1) of Eq. (15) or (18) or (26), for camber,  $F_o = F_i (1 - n f_c / f_{si}) = 758$  kips, using  $f_c = 2467$  psi.

From the general parameters section:  $n = E_s/E_{ci} = 9.8$ ;  
for 2 months period between prestressing and slab casting --  
 $m = E_s/E_{cs} = 8.2$ ,  $\alpha_s = 0.54$ ,  $\beta_s = 0.78$ ,  $\Delta F_s/F_o = 0.18$ ;  $\Delta F_u/F_o = 0.25$ .

From Eqs. (7) and (9), for  $H = 70\%$ ,  $C_u = 1.88$ ,  $(\epsilon_{sh})_u = 510 \times 10^{-6}$  in/in.

Initial camber and deflection, and differential shrinkage deflection:

$$(\Delta_i)_{F_o} = 4.09 \text{ in, as per Term (1) of Eq. (15) or (18) or (26).}$$

$$(\Delta_i)_2 = 1.74 \text{ in, as per Term (2) of Eq. (15) or (18) or (26).}$$

$$(\Delta_i)_1 = 2.26 \text{ in, as per Term (7) of Eq. (18) or (26). This}$$

deflection is due to the slab and diaphragm dead load.

$$\Delta_{DS} = 0.49 \text{ in, as per Term (9) of Eq. (18) or (26).}$$

Solutions for interior girders

Ultimate loss of prestress at midspan using Eq. (25):

$$PL_u = \begin{matrix} (1) & (2) & (3) & (4) & (5) & (6) & (7) & (8) \\ 12.7 & + & 11.7 & + & 2.8 & + & 6.5 & + & 7.5 & - & 4.3 & - & 2.0 & - & 1.6 & = & 33.3\% \end{matrix}$$

Ultimate midspan camber using Eq. (26) minus  $\Delta_L$ :

$$\begin{aligned} \Delta_u &= \begin{matrix} (1) & (2) & (3) & (4) & (5) & (6) & (7) & (8) & (9) \\ 4.09 & - & 1.74 & + & 3.05 & + & 0.80 & - & 1.77 & - & 0.48 & - & 2.26 & - & 1.06 & - & 0.49 \end{matrix} \\ &= 0.14 \text{ in.} \end{aligned}$$

Ultimate loss of prestress at midspan using the approximate

Eq. (31):

$$PL_u = 24.6 - 5.2 + 7.5 + 7.5 = 34.4\%.$$

Ultimate midspan camber using the approximate Eq. (32):

$$\Delta_u = 0.09 + 0.05 = 0.14 \text{ in, where } \Delta_i = 4.09 - 1.74 - 2.26 = 0.09 \text{ in.}$$

Tabulated in Tables 1, 2, 3 and 4 are the prestress loss, camber, and deflection results by the more reliable Eqs. (14) - (18), (20) and (22) - (27), and the approximate Eqs. (30) - (34), for the laboratory beams and bridge girders. Although the agreement above is good (note the camber is near zero due to the slab effect for the bridge girders) by these methods, the approximate method may be suitable in many cases for rough calculations only (see Tables 1 - 2). Also, the calculations needed by the approximate methods are not significantly fewer than by other methods. The more reliable

equations should be preferable for computer use.

#### 4.5 Experimental Loss of Prestress, Camber, and Deflection

##### Results

The loss of prestress at the end and midspan for the laboratory beams was determined from the measured concrete strains. However, this measured loss does not include the steel relaxation loss, since steel relaxation is a "stress relaxation at constant length --or nearly so in the case of a prestressed concrete beam" phenomenon. Separate relaxation tests were made and the results shown in Figure 8. From these and other tests, the relaxation equation given in Term (4) of Eq. (14) was determined. An example of the experimental determination of prestress loss for a typical laboratory beam is shown in Figure 9.

Experimental and computed loss of prestress versus time curves for the laboratory beams are shown in Figures 10, 11 and 12, and the computed curves for the bridge girders in Figure 13. Measured and computed midspan camber versus time curves for the beams and girders are shown in Figures 14 - 18. The general Eqs. (14) - (18), (20) with experimental parameters were used in all comparisons with test results in Figures 14 - 18. These results are shown in Tables 1 - 4 at release of prestress (camber only), just before slab casting (3 and 9 weeks for the beams and 9 weeks for

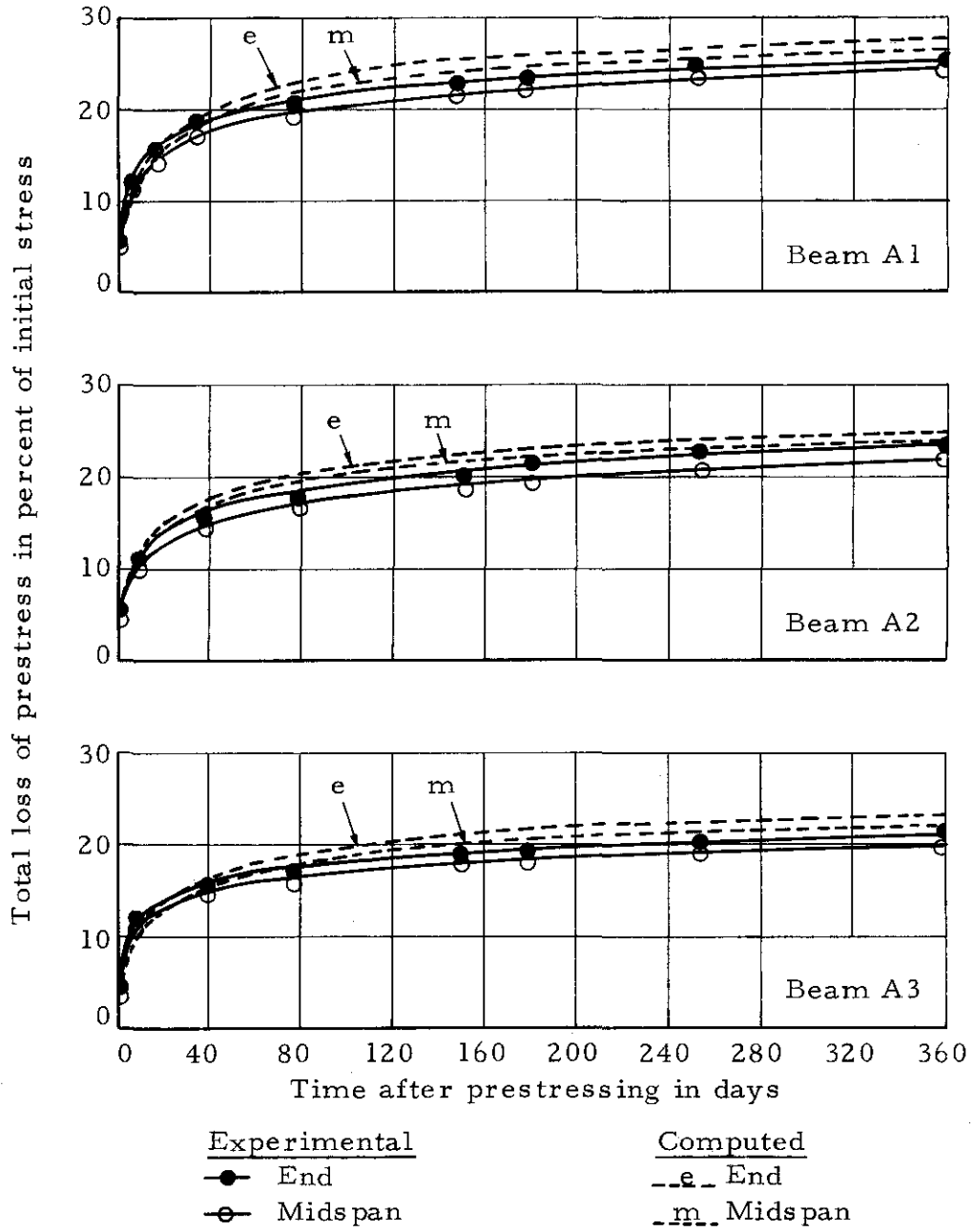


Figure 10 Computed and experimental loss of prestress of beams of Group A (three non-composite beams)

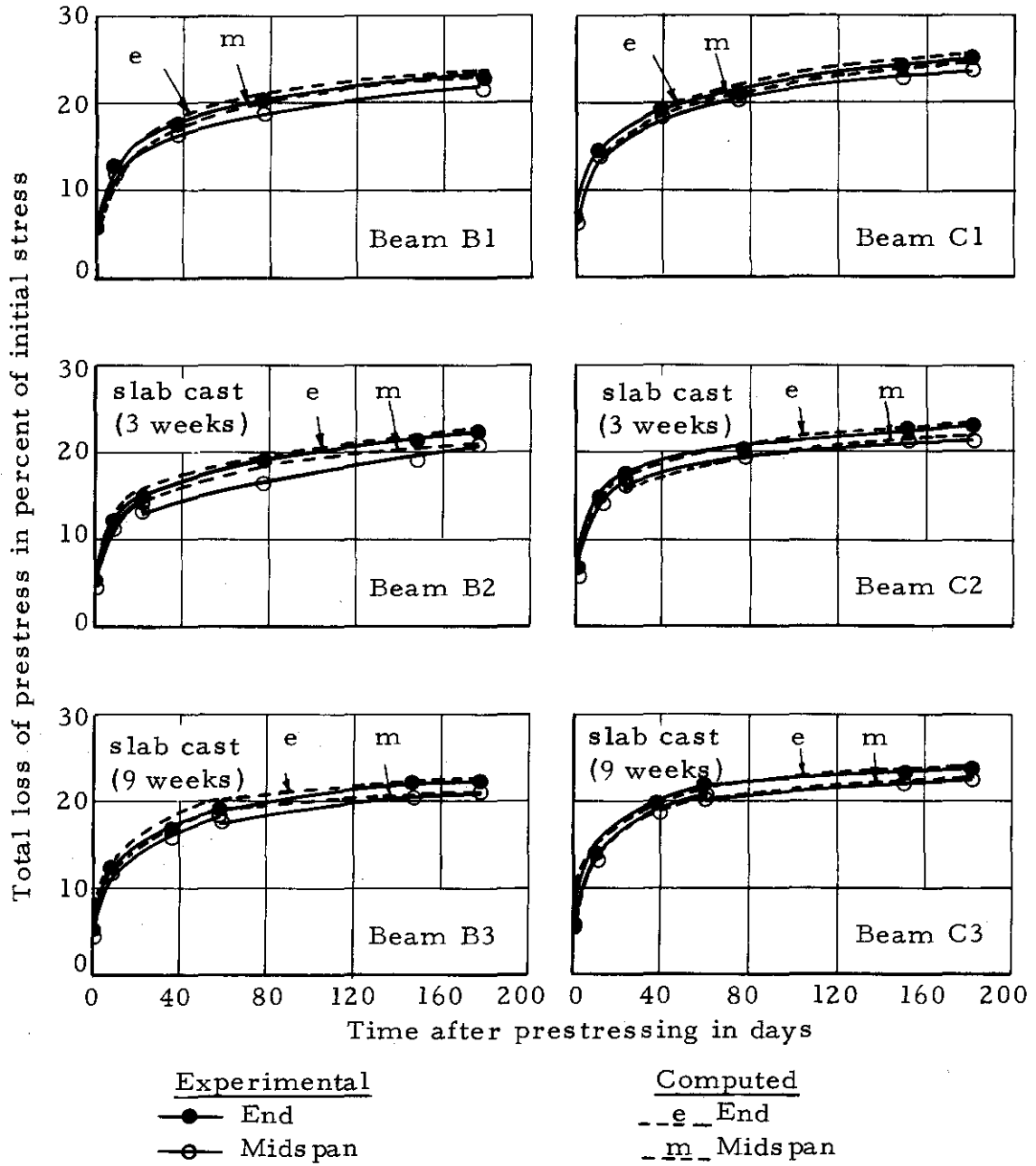


Figure 11 Computed and experimental loss of prestress of beams of Groups B and C (two non-composite and four composite beams)

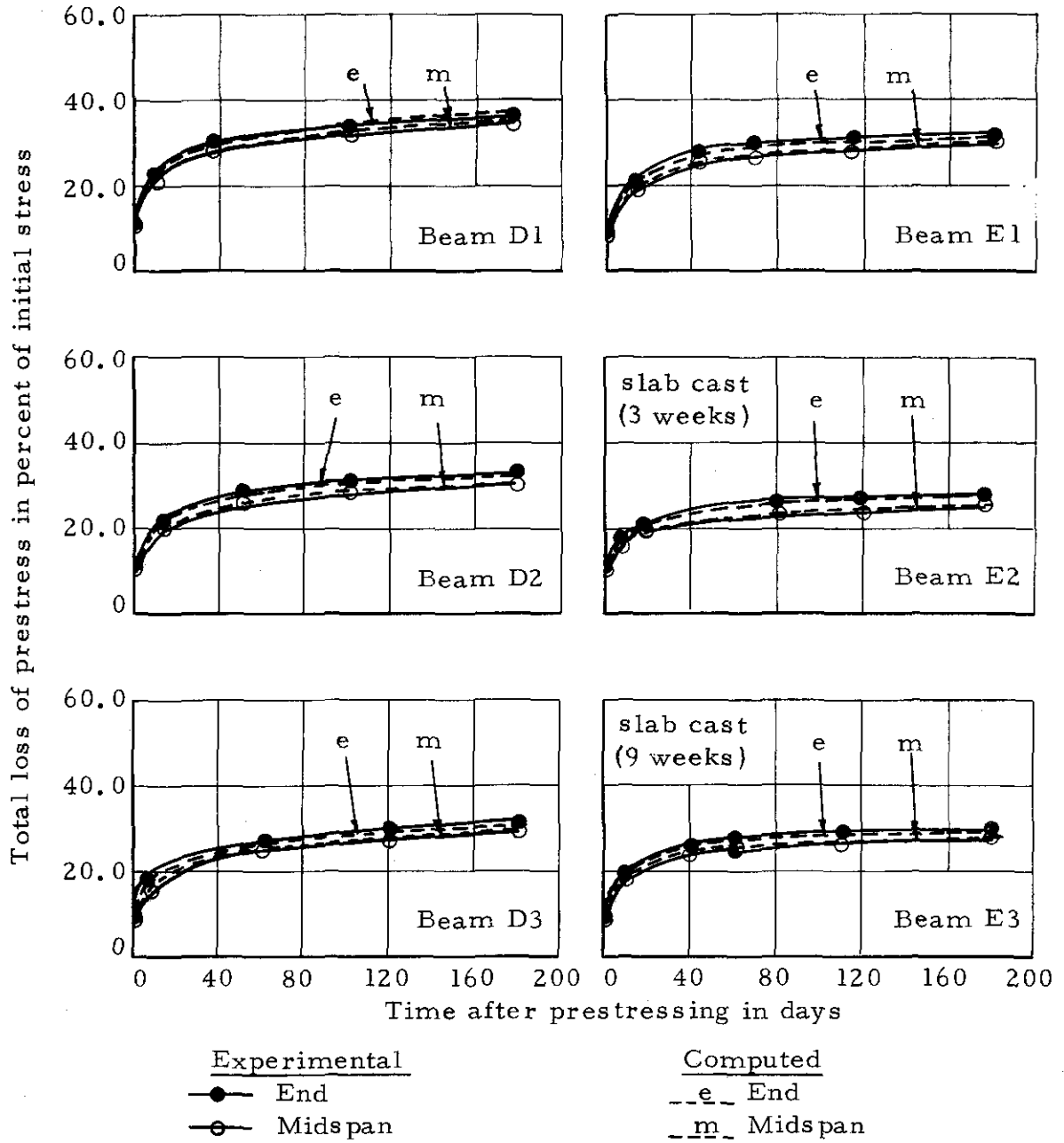


Figure 12 Computed and experimental loss of prestress of beams of Groups D and E (two non-composite and four composite beams)

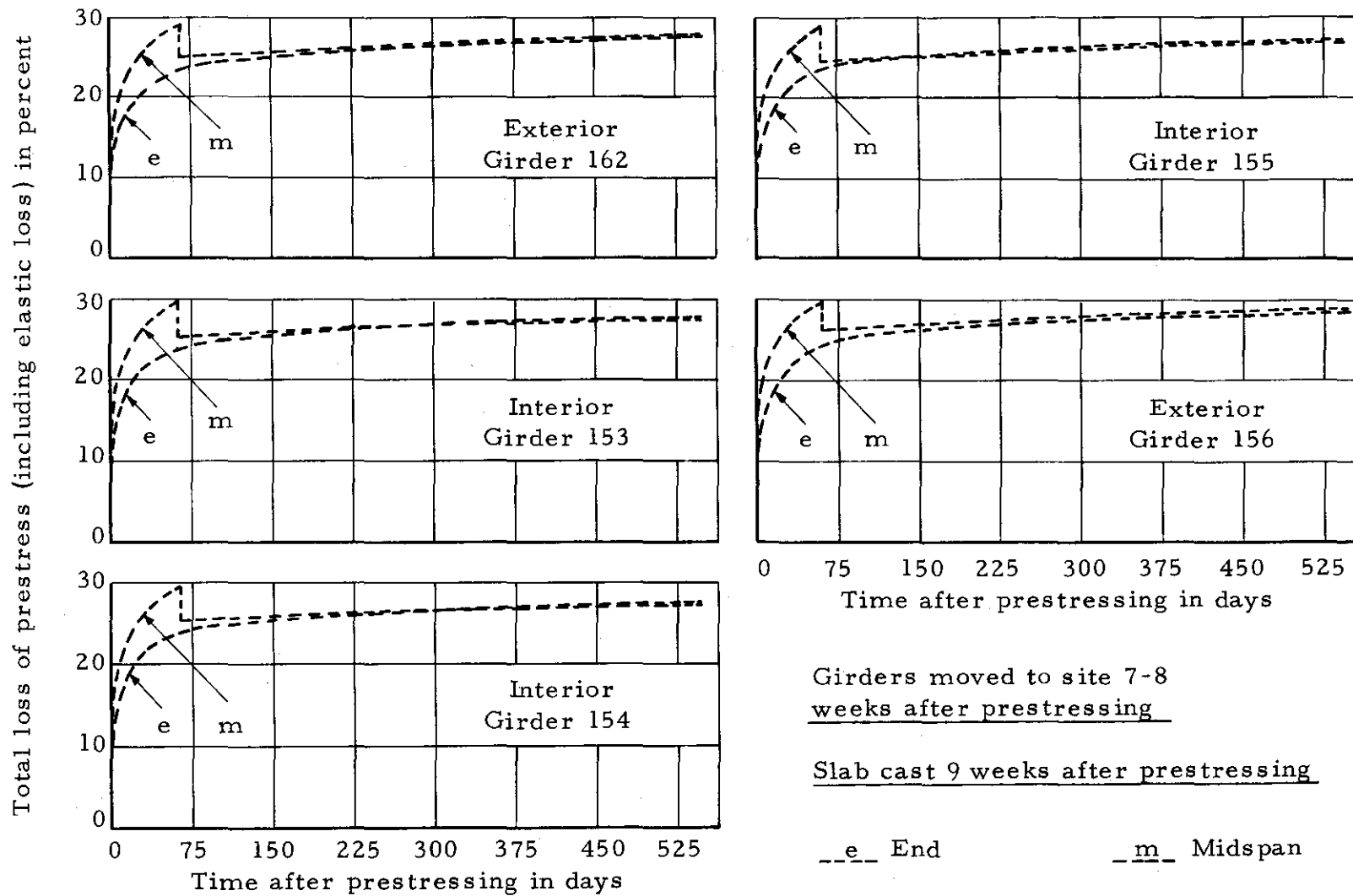


Figure 13 Computed loss of prestress of five composite bridge girders

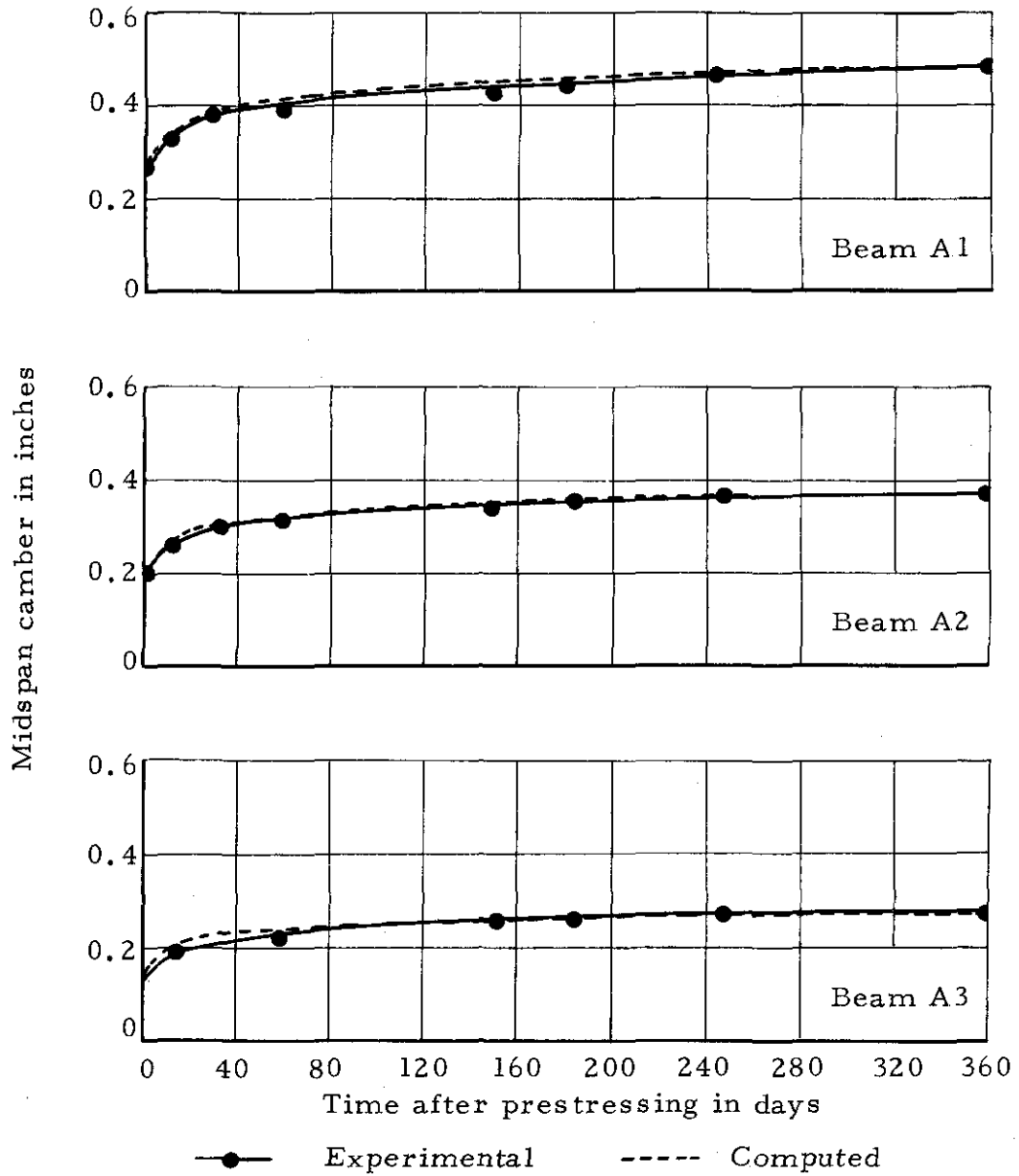


Figure 14 Computed and experimental midspan camber of beams of Group A (three non-composite beams)

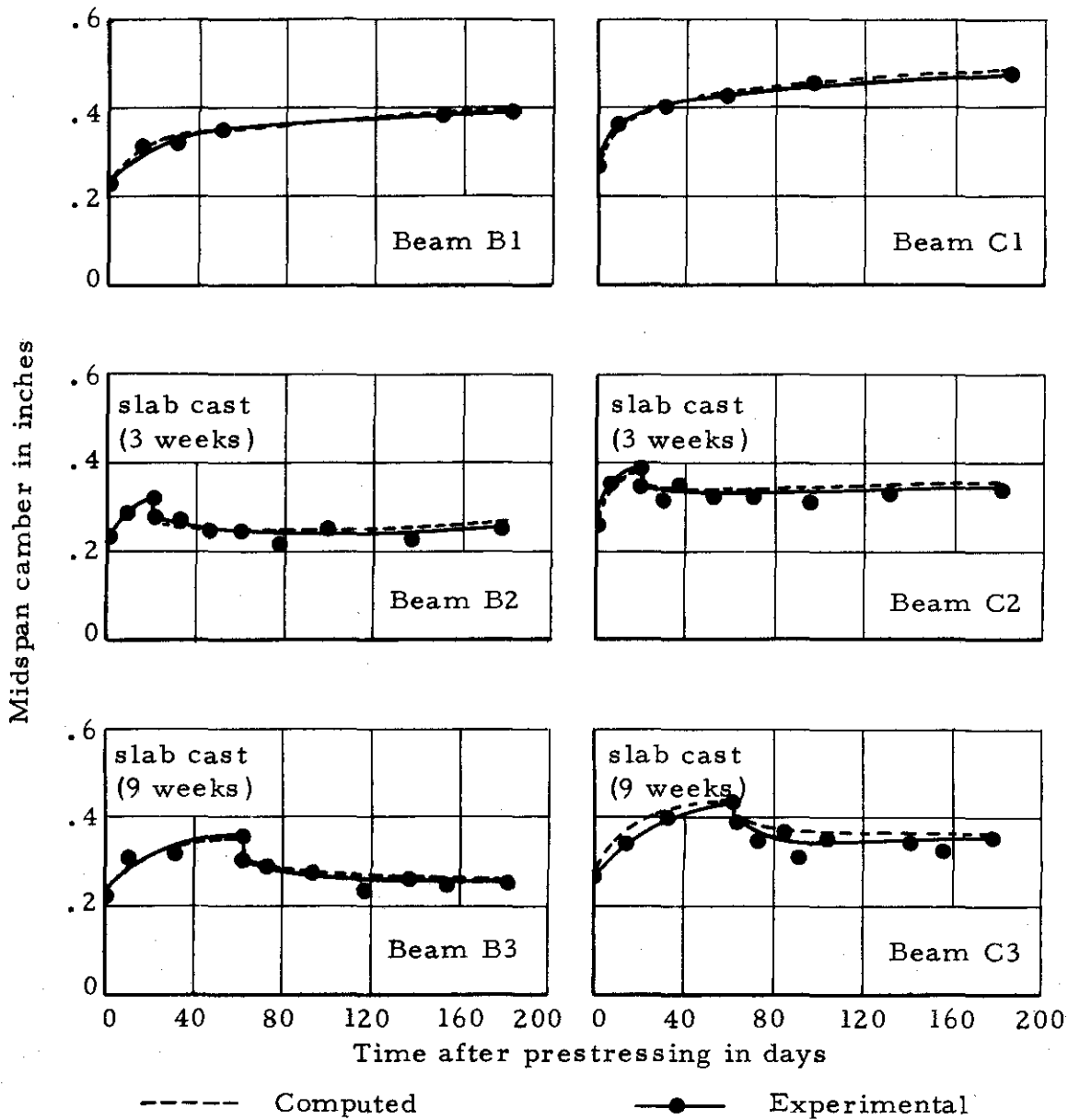


Figure 15 Computed and experimental midspan camber of beams of Groups B and C (two non-composite and four composite beams)

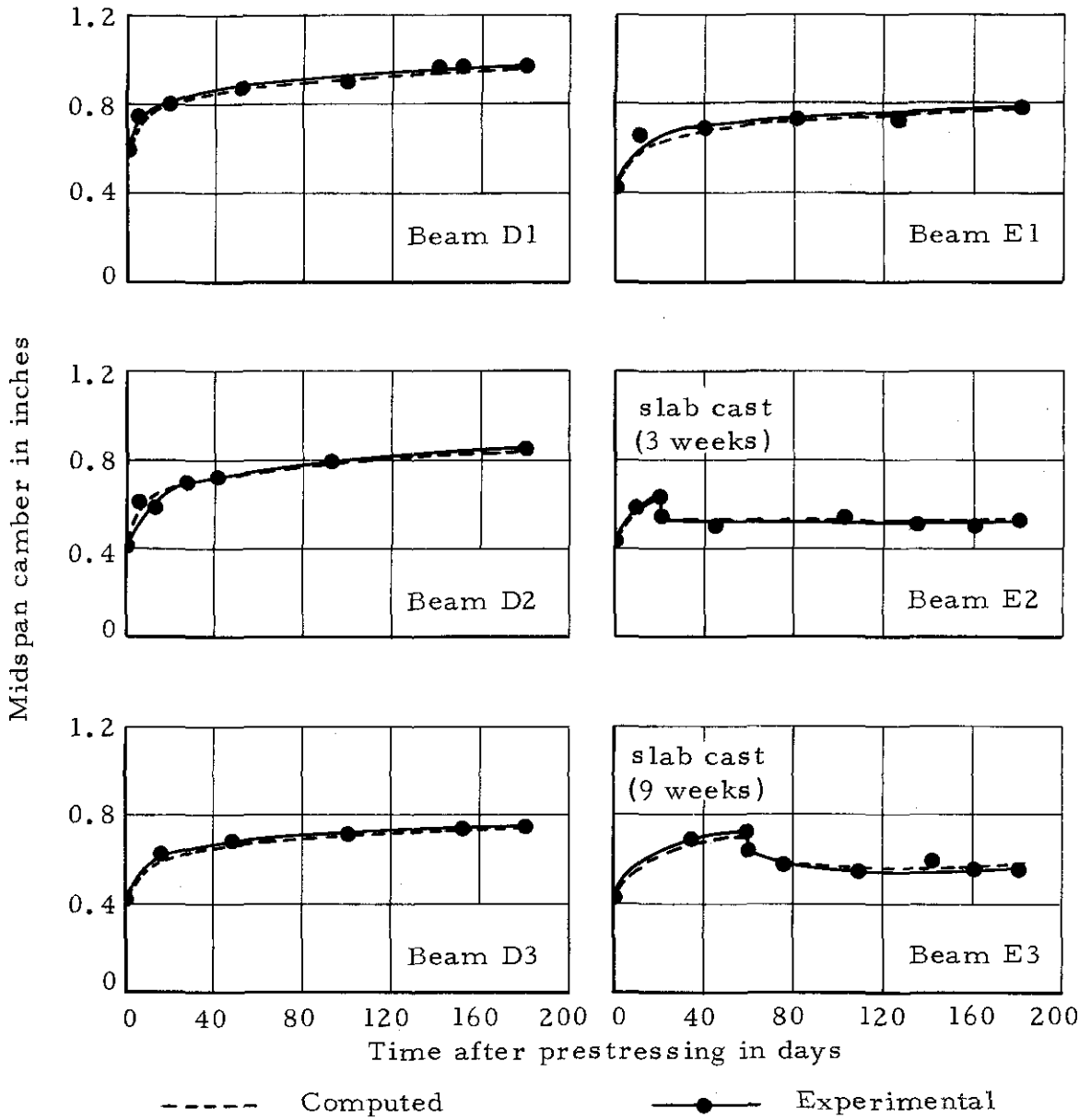


Figure 16 Computed and experimental midspan camber of beams of Groups D and E (two non-composite and four composite beams)

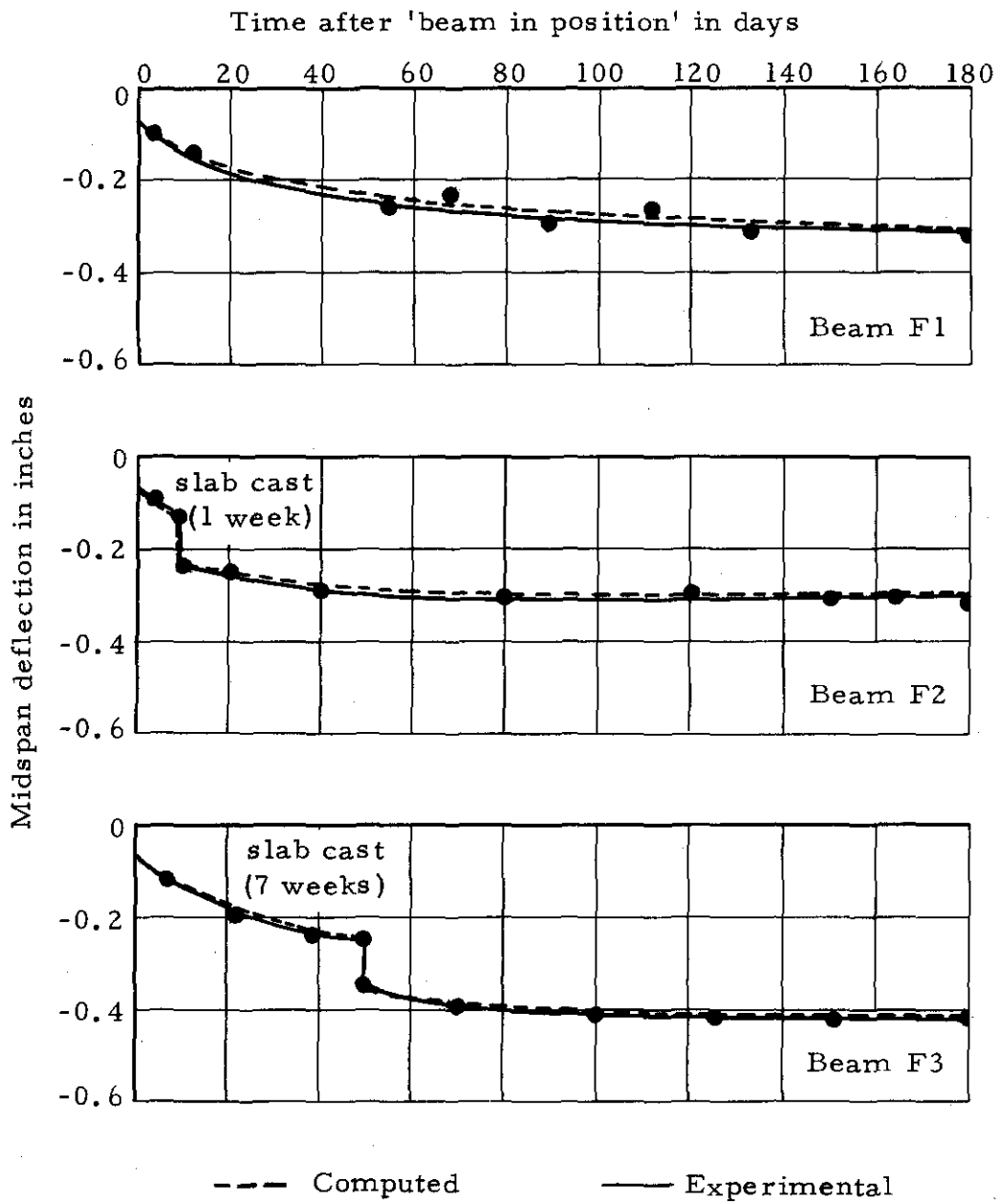


Figure 17 Computed and experimental midspan deflection of beams of Group F (one non-composite and two composite beams)

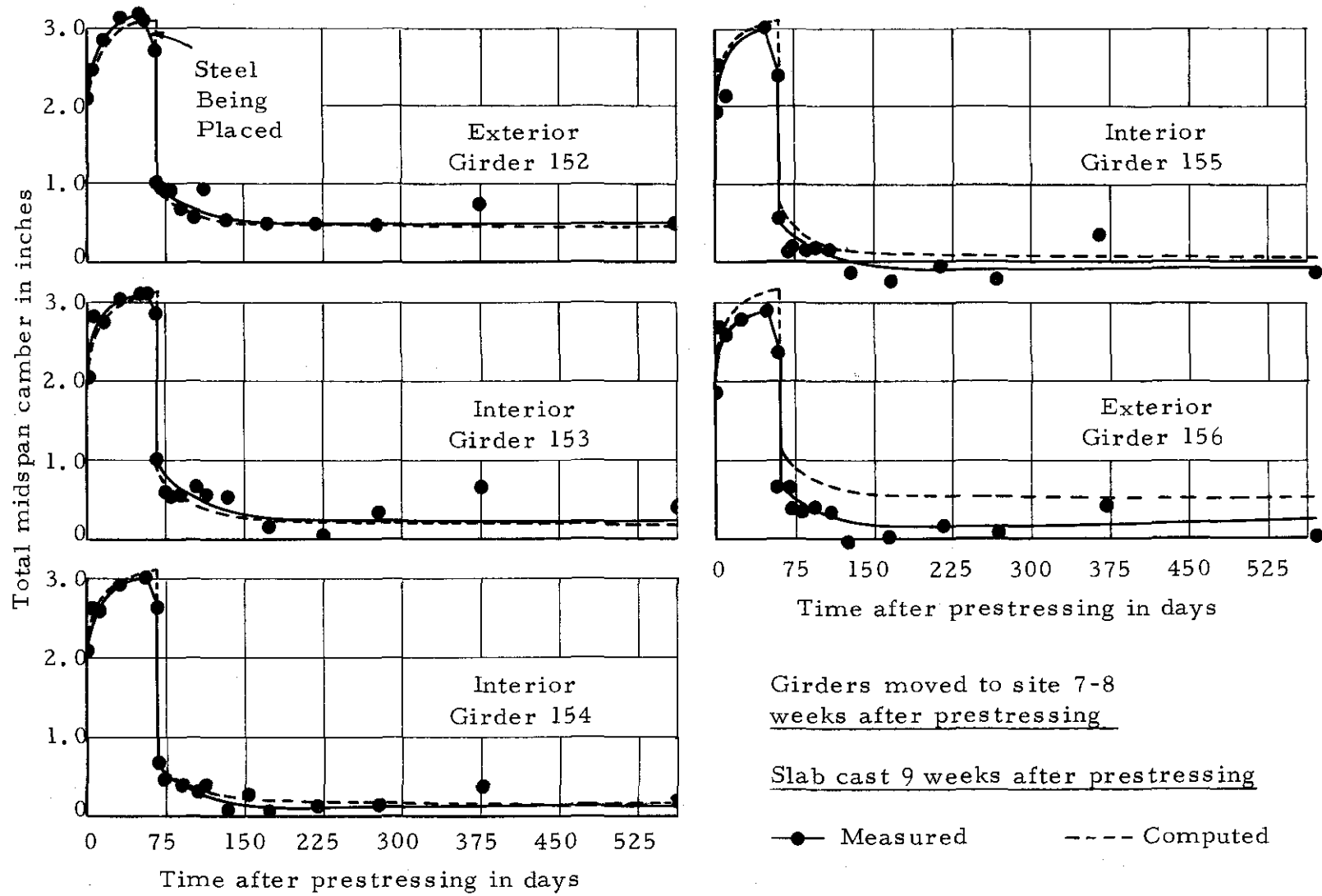


Figure 18 Computed and experimental midspan camber of five composite bridge girders

<sup>a</sup> TABLE 1

EXPERIMENTAL AND COMPUTED LOSS OF PRESTRESS FOR LABORATORY BEAMS AND COMPUTED LOSS OF PRESTRESS FOR BRIDGE GIRDERS

Beam No.	<sup>b</sup> Time Bet. Pres. & Slab Cast	Computed Loss Just Before Slab Cast		Experi- mental Loss at 180 days		Computed Loss by General Eqs. (14), (17) with exp. param. at 180d for Lab. B and 560d for bdg gird.				<sup>d</sup> Computed Ultimate Loss					
										Gen. Eqs. (14), (17) with exp. param.		Ult. Eqs. (22), (25) with gen. param.		Approx. Eq. (31) with gen. param.	
		Mid	Ratio	End	Mid	End	Ratio	Mid	Ratio	End	Mid	End	Mid	End	Mid
<u>Laboratory Beams</u>															
A1	-	-	-	23.5	22.0	25.5	1.09	24.6	1.12	31.7	30.5	36.9	35.4	-	-
A2	-	-	-	21.0	19.5	23.2	1.10	22.3	1.14	28.9	27.8	33.5	32.1	-	-
A3	-	-	-	19.0	18.5	21.4	1.13	20.4	1.10	26.7	25.5	32.0	30.6	-	-
B1	-	-	-	21.6	21.0	24.0	1.11	22.9	1.09	29.8	28.6	34.6	33.1	-	-
B2	21d	15.0	1.07	21.9	20.5	22.2	1.02	20.7	1.01	26.5	25.0	28.9	27.2	31.0	29.4
B3	63d	19.4	1.10	21.4	20.0	22.6	1.06	21.1	1.05	26.8	25.2	29.4	27.6	31.0	29.4
C1	-	-	-	25.0	24.0	25.7	1.03	24.7	1.03	31.9	30.8	37.2	35.7	-	-
C2	21d	16.4	0.97	23.0	21.4	23.7	1.03	22.4	1.05	28.2	26.7	30.9	29.3	33.1	31.6
C3	63d	21.1	1.01	23.6	22.3	24.4	1.03	23.0	1.03	28.7	27.2	31.7	30.0	33.1	31.6
D1	-	-	-	36.2	35.0	36.9	1.02	35.8	1.02	45.6	44.2	53.9	52.1	-	-
D2	-	-	-	33.0	31.0	32.3	0.98	31.0	1.00	40.0	38.5	46.9	44.9	-	-
D3	-	-	-	31.9	28.0	30.5	0.96	29.2	1.04	37.9	36.3	44.8	43.0	-	-
E1	-	-	-	32.0	29.0	31.2	0.98	30.2	1.04	38.7	37.5	46.2	44.8	-	-
E2	19d	20.9	1.02	28.0	25.0	27.0	0.96	25.3	1.01	31.1	29.4	35.4	33.4	37.8	36.0
E3	61d	26.1	1.00	30.0	28.0	28.7	0.96	27.0	0.96	32.7	30.9	36.8	34.8	37.8	36.0

TABLE 1 (Cont'd)

Beam No.	Time Bet. Pres. & Slab Cast	Computed Loss Just Before Slab Cast		Experimental Loss at 180 days		Computed Loss by General Eqs. (14), (17) with exp. param. at 180d for Lab. B and 560d for bdg gird.				Computed Ultimate Loss					
										Gen. Eqs. (14), (17) with exp. param.		Ult. Eqs. (22), (25) with gen. param.		Approx. Eq. (31) with gen. param.	
		Mid	Ratio	End	Mid	End	Ratio	Mid	Ratio	End	Mid	End	Mid	End	Mid
	<u>Bridge Girders</u>														
152	65d	28.4	-	-	-	27.3	-	27.6	-	29.5	29.9	30.4	34.0	30.5	35.0
153	65d	29.4	-	-	-	28.1	-	28.0	-	30.3	30.1	30.3	33.3	30.5	34.4
154	65d	29.4	-	-	-	28.0	-	28.0	-	30.2	30.1	30.3	33.3	30.5	34.4
155	60d	28.4	-	-	-	27.1	-	26.6	-	29.3	28.7	30.3	33.3	30.5	34.4
156	60d	29.8	-	-	-	28.3	-	28.9	-	30.5	31.0	30.4	34.0	30.5	35.0

<sup>a</sup> All losses are expressed in percent of initial stress. The ratios in the table are: Computed/Experimental. See Footnote b, Table 3, for a description of experimental parameters.

<sup>b</sup> The laboratory beams and bridge girders were prestressed at age 7-9 days and 2-3 days, respectively.

<sup>c</sup> See Figure 9 for an example of the experimental loss determination. The 180 day and 560 day times in the table refer to times after prestressing.

<sup>d</sup> The laboratory beam concrete strengths (for Gps. A-C) at release were well beyond the range specified for the general parameters; so the n and m values for these lab. beams were computed separately. However, for the lab. beams of Gps. D and E, the suggested n and m values are used. Where general parameters are used, a correction factor is applied for rel. hum. only.

<sup>e</sup> No approximate equation was given for non-composite beams for loss of prestress.

<sup>a</sup>TABLE 2

MEASURED AND COMPUTED MIDSPAN CAMBER & DEFLECTION  
FOR LABORATORY BEAMS & BRIDGE GIRDERS

Beam No.	Initial Camber			Time Bet. Prest. & Slab Cast	Camber just Before Slab Cast			Comp. camber by			<sup>d</sup> Computed Ult. Camber		
								Gen. Eqs. (15), (16) (18) & (20) with exp. param. @ 180d for lab. B & 560d-Br.G.			Gen. Eqs. (15), (16), (18), (20) with exp. param.	Ult. Eqs. (23), (24), (26), (27) with gen. param.	Approx. Eqs. (30) (32), (33) (34) with gen. par.
	Meas	Comp	Ratio		Meas	Comp	Ratio	Meas	Comp	Ratio			
	<u>Laboratory Beams</u>												
A1	0.27	0.25	0.93	-	-	-	-	0.44	0.46	1.04	0.54	0.68	0.77
A2	0.20	0.19	0.95	-	-	-	-	0.35	0.35	1.00	0.42	0.52	0.59
A3	Bad D	0.15	-	-	-	-	-	0.27	0.26	0.96	0.31	0.38	0.44
B1	0.22	0.22	1.00	-	-	-	-	0.39	0.39	1.00	0.46	0.58	0.66
B2	0.23	0.22	0.96	21d	0.32	0.32	1.00	0.25	0.27	1.08	0.28	0.26	0.29
B3	0.23	0.22	0.96	63d	0.36	0.35	0.97	0.26	0.27	1.04	0.28	0.28	0.30
C1	0.27	0.27	1.00	-	-	-	-	0.47	0.49	1.04	0.57	0.73	0.75
C2	0.27	0.27	1.00	21d	0.39	0.39	1.00	0.34	0.36	1.06	0.38	0.37	0.39
C3	0.27	0.27	1.00	63d	0.44	0.44	1.00	0.35	0.37	1.06	0.39	0.39	0.39
D1	0.56	0.54	0.96	-	-	-	-	0.98	0.95	0.97	1.10	1.44	1.67
D2	0.43	0.45	1.05	-	-	-	-	0.84	0.82	0.98	0.94	1.19	1.39
D3	0.41	0.40	0.98	-	-	-	-	0.75	0.73	0.97	0.86	1.05	1.24
E1	0.42	0.42	1.00	-	-	-	-	0.78	0.77	0.99	0.90	1.12	1.29
E2	0.42	0.43	1.02	19d	0.62	0.59	0.95	0.52	0.52	1.00	0.55	0.58	0.51
E3	0.42	0.43	1.02	61d	0.72	0.71	0.99	0.54	0.57	1.05	0.59	0.62	0.51
<sup>e</sup> F1	-	0.07	-	-	-	-	-	0.34	0.30	0.89	0.38	0.47	0.55
<sup>e</sup> F2	-	0.07	-	7d	0.13	0.14	1.08	0.32	0.28	0.88	0.30	0.45	0.58
<sup>e</sup> F3	-	0.07	-	51d	0.25	0.24	0.96	0.45	0.40	0.89	0.43	0.59	0.58

TABLE 2 (Cont'd)

Beam No.	Initial Camber			<sup>b</sup> Time Bet. Prest. & Slab Cast	Camber Just Before Slab Cast			Comp. camber by Gen. Eqs. (15), (16) (18) & (20) with exp. param, @ 180d for lab. B & 560d-Br. G.			<sup>d</sup> Computed Ult. Camber		
											Gen. Eqs. (15), (16), (18), (20) with exp. param	Ult. Eqs. (23), (24), (26), (27) with gen. param.	Approx. Eqs. (30), (32), (33) (34) with gen. par.
	Meas	Comp	Ratio		Meas	Comp	Ratio	Meas	Comp	Ratio			
	<u>Bridge Girders</u>												
152	2.05	2.14	1.04	65d	3.10	3.06	0.98	0.50	0.47	0.93	0.45	0.51	0.53
153	2.05	2.22	1.08	65d	3.10	3.13	1.02	0.25	0.21	0.84	0.17	0.14	0.14
154	2.10	2.22	1.06	65d	3.05	3.13	1.03	0.20	0.21	1.05	0.17	0.14	0.14
155	1.90	2.14	1.13	60d	2.95	3.04	1.03	-0.02	0.07	-	0.01	0.14	0.14
156	1.85	2.27	1.23	60d	2.92	3.16	1.08	0.30	0.54	<sup>c</sup> 1.80	0.50	0.51	0.53

<sup>a</sup> All camber values are in inches. Ratios are: Computed/Measured. See Footnote b, Table 3, for a description of experimental parameters. Also, see Sample Calculations for a description of general parameters.

<sup>b</sup> See Footnote b, Table 1. Beams F1-F3 were in position at beam age = 21 days.

<sup>c</sup> Camber has been reduced from about 3" before slab casting to less than 1/2" after 1 year (see Figure 18). This ratio is large for the near zero camber, even though the difference in camber is 0.22".

<sup>d</sup> See Footnote d, Table 1.

<sup>e</sup> The camber of beams F1, F2, and F3 being non-prestressed reinforced beams are negative in magnitude, i. e., the values in this table for the beams (F1, F2, F3) refer to deflections.

a, b  
TABLE 3

COMPUTED ULTIMATE LOSS OF PRESTRESS AT MIDSPAN,  
BY TERMS, FOR THE LABORATORY BEAMS AND BRIDGE GIRDERS,  
USING THE GENERAL EQUATIONS (14) & (17) WITH EXPERIMENTAL PARAMETERS

Beam No.	Elast. Loss	Creep Loss Before Slab Cast	Creep Loss After Slab Cast	Shrink Loss	Relax Loss	El. Gain Due to Slab	Creep Gain Due to Slab	Gain Due to Diff. Shrink	Total Loss, Eqs. (14), (17)
	<u>Laboratory Beams</u>								
A1	5.2	8.0	-	9.8	7.5	-	-	-	30.5
A2	4.1	6.3	-	9.9	7.5	-	-	-	27.8
A3	3.2	4.8	-	10.0	7.5	-	-	-	25.5
B1	4.5	6.9	-	9.7	7.5	-	-	-	28.6
B2	4.5	2.9	1.2	9.7	7.5	-0.4	-0.2	-0.2	25.0
B3	4.5	4.0	0.9	9.7	7.5	-0.4	-0.2	-0.8	25.2
C1	5.4	8.3	-	9.6	7.5	-	-	-	30.8
C2	5.4	3.5	1.5	9.6	7.5	-0.4	-0.2	-0.2	26.7
C3	5.4	4.8	1.1	9.6	7.5	-0.4	-0.2	-0.6	27.2
D1	11.2	18.2	-	7.3	7.5	-	-	-	44.2
D2	8.9	14.6	-	7.5	7.5	-	-	-	38.5
D3	8.0	13.2	-	7.6	7.5	-	-	-	36.3
E1	8.8	14.0	-	7.2	7.5	-	-	-	37.5
E2	8.9	5.6	1.5	7.2	7.5	-0.7	-0.2	-0.4	29.4
E3	8.9	8.2	1.1	7.1	7.5	-0.7	-0.2	-1.0	30.9

a, b TABLE 3 (Cont'd)

Beam No.	Elast. Loss	Creep Loss Before Slab Cast	Creep Loss After Slab Cast	Shrink Loss	Relax Loss	El. Gain Due to Slab	Creep Gain Due To Slab	Gain Due to Diff. Shrink	Total Loss, Eqs. (14), (17)
	<u>Bridge Girders</u>								
152	11.5	9.8	2.2	4.6	7.5	-3.7	-1.5	-0.5	29.9
153	12.0	10.3	2.3	4.5	7.5	-4.2	-1.7	-0.6	30.1
154	12.0	10.3	2.3	4.5	7.5	-4.2	-1.7	-0.6	30.1
155	11.5	9.6	2.2	4.5	7.5	-4.3	-1.7	-0.6	28.7
156	12.3	10.3	2.4	4.4	7.5	-3.8	-1.5	-0.6	31.0

<sup>a</sup> The table is arranged in order of terms in Eq. (17). All losses are expressed in percent of initial stress.

<sup>b</sup> The experimental parameters used in the calculations for this table are shown in Tables A4 and A5 and elsewhere herein for the lightweight concretes of this project. The slab shrinkage is shown here only. The correction factors given herein for age of loading, humidity, and member thickness (8" for Br. Gir.) are used where appropriate with the experimental parameters. The resulting creep and shrinkage factors used are:

		<u>Laboratory Beams</u>				<u>Bridge Girder</u>
		<u>Gp. A, B, C</u>	<u>Gp D</u>	<u>Gp E</u>	<u>Gp F</u>	<u>152-156</u>
Avg. Rel. Humidity		40%	50%	50%	50%	70%
Precast Beam Creep	$C_u =$	1.75	1.87	1.80	1.63	1.62
Precast Beam Shrink (x 10 <sup>-6</sup> in/in)	$(\epsilon_{sh})_u =$	650	540	510	385	352
Slab Shrink. (from day 1) used in comp. diff.str. (x 10 <sup>-6</sup> in/in)	$(\epsilon_{sh})_u =$	470*	-	440	440	330

Also see the Sample Calculations for a comparison with the general parameter results.

a, b TABLE 4

COMPUTED ULTIMATE MIDSPAN CAMBER, BY TERMS, FOR THE LABORATORY BEAMS AND BRIDGE GIRDERS, USING THE GENERAL EQS (15), (16), (18) & (20) WITH EXPERIMENTAL PARAMETERS

Bm No.	Initial Camber due to Prest.	Initial Defl. due to Bm. DL	<sup>c</sup> Creep camb. up to sl. cast or shk. warp up to sl. cast	<sup>c</sup> Creep camb. after sl. cast or shk. warp up to sl. cast	DL Crp defl. up to slab cast	Bm DL defl. after sl. cast	EI def due to slab DL	Crp def due to slab DL	Defl due to diff. shk.	Total Camber using Eqs. (15), (16), (18), (20)
<u>Laboratory Beams</u>										
A1	0.30	-0.05	0.37	-	-0.09	-	-	-	-	0.53
A2	0.24	-0.05	0.31	-	-0.09	-	-	-	-	0.41
A3	0.19	-0.05	0.25	-	-0.09	-	-	-	-	0.30
B1	0.27	-0.05	0.34	-	-0.10	-	-	-	-	0.46
B2	0.27	-0.05	0.14	0.07	-0.04	-0.02	-0.05	-0.02	-0.01	0.29
B3	0.27	-0.05	0.19	0.05	-0.05	-0.01	-0.04	-0.02	-0.04	0.30
C1	0.32	-0.05	0.40	-	-0.09	-	-	-	-	0.58
C2	0.32	-0.05	0.16	0.08	-0.03	-0.02	-0.04	-0.02	-0.01	0.39
C3	0.32	-0.05	0.22	0.06	-0.05	-0.01	-0.04	-0.02	-0.04	0.39
D1	0.61	-0.07	0.69	-	-0.13	-	-	-	-	1.10
D2	0.51	-0.07	0.63	-	-0.13	-	-	-	-	0.94
D3	0.47	-0.07	0.59	-	-0.13	-	-	-	-	0.86
E1	0.49	-0.06	0.58	-	-0.11	-	-	-	-	0.90
E2	0.49	-0.06	0.24	0.07	-0.04	-0.01	-0.09	-0.03	-0.02	0.55
E3	0.49	-0.06	0.34	0.05	-0.06	-0.01	-0.09	-0.02	-0.05	0.59
F1	-	-0.07	-0.22	-	-0.09	-	-	-	-	-0.38
F2	-	-0.07	-0.02	-0.04	-0.02	-0.01	-0.10	-0.02	-0.02	-0.30
F3	-	-0.07	-0.11	-0.02	-0.05	-0.01	-0.10	-0.10	-0.05	-0.43

a, b TABLE 4 (Cont'd)

Bm No.	Initial Camber due to Prest.	Initial Defl. due to Bm.DL	<sup>c</sup> Creep camb. up to sl. cast or shk. warp up to sl. cast	<sup>c</sup> Creep camb. after sl. cast or shk. warp up to sl. cast	DL Crp defl. up to slab cast	Bm DL defl. after sl. cast	El def due to slab DL	Crp def due to slab DL	Defl due to diff. shk.	Total Camber using Eqs. (15), (16) (18), (20)
	<u>Bridge Girders</u>									
152	3.71	-1.56	2.32	0.68	-1.42	-0.36	-1.96	-0.79	-0.17	0.45
153	3.87	-1.64	2.39	0.71	-1.49	-0.38	-2.21	-0.89	-0.19	0.17
154	3.87	-1.64	2.39	0.71	-1.49	-0.38	-2.21	-0.89	-0.19	0.17
155	3.72	-1.57	2.29	0.70	-1.40	-0.37	-2.26	-0.91	-0.19	0.01
156	3.96	-1.68	2.38	0.73	-1.50	-0.40	-2.01	-0.80	-0.18	0.50

<sup>a</sup>All values in the table are in inches.

<sup>b</sup>See Footnote b, Table 3, for a description of the experimental parameters.

<sup>c</sup>The shrinkage warping term and the total deflection term refers to beams with non-prestressed reinforcement only.

the girders, after prestressing), and at 180 days for the laboratory beams and 560 days for the bridge girders. The test period for the laboratory beams (except Group A) was terminated after 6 months in order to conduct load-deflection tests. The test period for Group A specimens was 1 year.

The computed ultimate values are also tabulated in Tables 1 - 2 using the general Eqs. (14) - (18) with experimental parameters determined for the sand-lightweight concrete of this project, and using the ultimate-value Eqs. (22) - (27) with general parameters given for normal weight, sand-lightweight, and all-lightweight concrete. For the general parameters, the same creep and shrinkage factors are suggested for all three concretes, with different modular ratios and prestress loss ratios ( $\Delta F_s/F_o$  and  $\Delta F_u/F_o$ ) for each. The computed ultimate values for loss of prestress and camber are shown term by term in Tables 3 and 4 using the general Eqs. (14) - (20) with experimental parameters.

#### 4.6 Discussion of Experimental Results and Conclusion

The experimental and computed loss of prestress and camber for the lightweight concrete structures of this project are shown in Figures 10 - 18 and Tables 1 - 4. Results by both general Eqs. (14) - (20) (for values at any time, including ultimate) with experimental parameters, and ultimate-value Eqs. (22) - (27) and (30) - (34) with

general parameters (given herein) are included. These results serve to substantiate the generalized procedure presented for predicting loss of prestress and camber of non-composite and composite prestressed structures. The approximate Eqs. (30) - (34) may be suitable for rough calculations only in some cases.

Results computed by the material parameter Eqs. (2), (4), (7) - (9) are compared with the data of this project in Figures 2 - 7. Eqs. (2) - (6), (7) - (8) are generalized for different weight concretes. The procedure for predicting creep and shrinkage is one of providing standard functions, with suggested ultimate values for different weight concretes, and correction factors for pertinent conditions other than "standard" (18). These conditions are briefly described in the text and Appendix B. The ultimate values suggested should be used only in the absence of specific information pertaining to local aggregates and conditions.

Continuous time functions are provided for all needed material parameters (and for different weight concretes, moist and steam cured), so that the prestress loss and camber equations readily lend themselves to computer solutions. Certain other read-in data (such as for the effect of behavior before and after slab casting--  $\alpha_s$ ,  $\beta_s$ ,  $m$ ,  $\gamma_s$ ,  $\gamma_{s_1}$ , and  $\Delta F_s/F_o$ ) is also included, along with a summary of parameters convenient for hand calculations. Using these parameters,

the calculations needed in the approximate Eqs. (30) - (34) are not significantly fewer than in the more reliable Eqs. (14) - (20).

It is noted that Eqs. (14) - (27) could be greatly shortened by combining terms, but are presented in the form of separate terms (see results in Tables 3 and 4 and the Sample Calculations) in order to show the separate effects or contributions to the behavior (such as due to the prestress force, dead load, creep, shrinkage, etc., that occur both before and after slab casting).

The following specific observations and conclusions are made relative to the results in Figures 8, 10 - 18, Tables 1 - 4 and other parts of the report:

1. The ultimate steel relaxation percentage recommended for regular 7-wire strand to be used in prestressed concrete structures is 7.5%. See the results and discussion of Figure 8, Term (4) of Eq. (14), and References (45) and (46).

2. The computed initial camber agreed well in most cases with the measured initial camber, as shown in Table 2.

3. The computed prestress loss for the laboratory non-composite beams was varied (from -1.4% to 2.8% prestress loss differential after 6 months) from the experimental results (see Figures 10 - 12 and Table 1). The direct application of laboratory creep data for uniformly loaded specimens to beams with non-uniform

stress distribution appears to slightly overestimate the creep effect. The same effect, however, was not noticed in the camber results. This is probably due to the fact that in the loss computations, the  $F/A$  stress component is a dominant factor while in the camber computations, there is no corresponding deformational component. Other prestress loss and camber results in Figures 13 - 18, and Tables 1 and 2 are considered to be in very good agreement. For these cases (non-composite beam camber and composite beam loss and camber), offsetting creep (and shrinkage in the case of composite beams) effects occur.

4. As shown in Figures 10 - 12 and Table 1 the difference in the end and midspan prestress loss was quite small for the laboratory beams, and relatively large for the bridge girders before slab casting. After slab casting, the prestress loss in the bridge girders was only slightly different at end and midspan.

5. The loss of prestress for the sand-lightweight concrete bridge girders was of the order of 27% to 29% at 560 days after prestressing and 29% to 31% ultimately (see Figure 13 and Table 1). It seems clear that loss percentages for bridges under similar conditions using normal weight concrete will normally be somewhat lower than these (of the order of 25%); and using all-lightweight concrete will normally be somewhat higher than these (of the order of 35% or higher).

6. Slab casting causes an elastic deflection (downward) and prestress gain, and a time-dependent deflection and prestress gain, due to creep and differential shrinkage. Loss of prestress due to creep and camber growth under the prestress force and precast beam dead load are also reduced by the effect of the hardened slab (as opposed to the case of no composite slab). These results can be seen in Tables 3 and 4 and the Sample Calculations. The composite slab reduces the ultimate loss of prestress at midspan of the bridge girders about 11% (as 41% - 30% = 11%). It can be seen in Figure 18 and Table 4 that the camber curves have nearly levelled off at about 3.0" just before slab casting. After slab casting and up to ultimate, the camber is reduced to near zero.

7. The effect of the 3-week and 9-week slab casting schedules for the laboratory beams had only a small effect on loss of prestress (Figures 11 and 12) and a more noticeable effect on camber (Figures 15 and 16). When considering a 3-week slab (slab cast 3 weeks after prestressing) for the bridge girders, as compared to the actual 9-week slab, the ultimate loss of prestress at midspan was about 2% less and the ultimate midspan camber about 0.10" less for the 3 week case. These results serve to point out the relatively small beneficial effect of casting the deck slab as early as possible (also indicated in Reference (24)). It is noted that there are also

offsetting effects in the case of the effect of slab casting schedules. An earlier slab tends to reduce total creep deformation (causing upward camber) by forming an earlier composite section, but also reduces differential shrinkage deformation (causing downward deflection).

8. The different individual contributions to prestress loss and camber, as illustrated by the different terms in Eqs. (14) - (29), are sensitive to the stiffness, creep, and shrinkage concrete properties. However, the net results of these equations tend toward more correct solutions than the individual terms because of offsetting effects. This is especially true in the case of composite beams, and is less the case for non-composite beams. See Tables 1 and 2 and the comparison of ultimate-value results with experimental parameters and general parameters.

9. The inclusion of all terms in Eqs. (14) - (29) appears to incorporate all significant effects in the reliable prediction of prestress loss and camber. These effects can be seen in the term-by-term tabulations in Tables 3 and 4, and the Sample Calculations. In the sample calculations for the bridge girders using the general parameters, for example, the 7 terms (omitting differential shrinkage--Term 8) for loss of prestress varied from 1.6% to 12.7%, and the 9 terms for camber varied from 0.48" to 4.09". The results by

the approximate Eqs. (30) - (34) and the more reliable equations were in reasonably good agreement (see Tables 1 and 2 and the Sample Calculations) for most of the structures of this project.

10. All of the bridge girder data in Figure 18 showed an increase in camber of about 0.4" between 300 to 370 days (starting in April). This appears to be due to higher temperatures and is consistent with the observations of Delarue (34).

11. The systematic procedures described in this paper for predicting time-dependent behavior are deterministic in nature. Probabilistic methods are also needed for estimating variability of behavior.

12. Sand-lightweight concretes using Haydite (as the coarse aggregate) show slightly higher creep ( $C_u = 2.00$ ) than sand-lightweight concretes using Idealite (as the coarse aggregate) ( $C_u = 1.75$ ) under identical loading and environmental conditions, (Figures 3 and 6).

13. There does not seem to be any fundamental difference between all-lightweight Haydite concrete and sand-lightweight Haydite concrete as far as the creep properties are concerned. (Figure 6). The loss of prestress for beams made of all-lightweight Haydite concrete is substantially greater than for beams made of sand-lightweight Haydite concrete (Figure 12 and Tables 1 and 3). This is

due to the high elastic deformation of all-lightweight concrete (due to its low elasticity modulus) and not due to the difference in creep behavior of the two concretes.

14. The effect of the 4-week and 10-week slab casting schedule for the laboratory reinforced beams had a very noticeable effect on deflection (Figure 17). An earlier slab tends to reduce total creep deformation (causing downward deflection) by forming an earlier composite section, and also reduces differential shrinkage deformation (also downward deflection). When considering a 4-week slab (slab cast at beam age = 4 weeks) for the laboratory beams (reinforced), as compared to the 10-week slab (slab cast at beam age = 10 weeks), the ultimate deflection was about 0.13" less for the 4-week case. These results serve to point out the relatively large beneficial effect of casting the deck slab as early as possible for reinforced beams.

15. In comparing non-composite reinforced beams with composite reinforced beams, it is noticed that the ultimate deflection of the non-composite beam was about 0.08" greater than the 4-week case, but about 0.05" lesser than the 10-week case. The earlier composite section (4-week slab) reduces the total deformation by its composite action, while the later composite section (10-week slab) increases the total deformation due to the various shrinkage effects

(Table 4). This effect, however, may become very small in regions of high humidity.

#### 4.7 Comparison of Computed and Measured Data Reported by Others (23), (24), (27), (31)

Simultaneously measured deflections and strains of prestressed concrete beams reported in the literature are scarce. The strains and deflections reported by Branson (23) were taken from post-tensioned beams. Both composite and non-composite beams were included in the study. Unit creep curves of the concrete were not reported. The total strains of the beams were measured and reported. A reciprocal approach can be used from these strains to arrive at a value of the ultimate creep and shrinkage coefficients. The report of Corley, Sozen, and Siess (24) and Sinno (27) included all the relevant information required to perform the predictions by methods presented in this paper. Pauw and Breen (31) have reported the strains and camber measurements of two post-tensioned composite bridge girders. Separate creep tests are not included in this report. The experimental loss of prestress is determined from the measured concrete strains in a manner similar to that described in Figure 9. The loss due to steel relaxation is as given by Term (4) of Eq. (14).

Prediction of loss of prestress and camber for the beams in

References (23), (24), (27) and (31) are obtained using the general Eqs. (14) - (20) and experimental parameters (where available) and the general parameters mentioned in this report, and each is compared with the measured results.

#### Results of Tests at the University of Florida (23)

##### Description of Specimens :

Ten post-tensioned normal weight concrete beams of spans 19'-6" were cast and studied for a period of about 5 months for both camber and loss of prestress. Eight of these were stored in the laboratory and the other two were stored in the field. Cast-in-place slabs were cast on five of the beams at ages varying from 37 to 101 days. The properties of the test specimens are shown in Table C1. Shrinkage specimens were also cast.

##### Discussion of measured and computed results:

The results for the loss of prestress (at end and midspan) as well as for the midspan camber are shown in Figures 19 - 21, using both the general parameters (suggested in this report) and the experimental parameters (estimated from reported strains). From this comparison (Figures 19 - 21), the following observations are made:

1. The general parameters being slightly smaller than the experimental parameters tends to underestimate the loss of

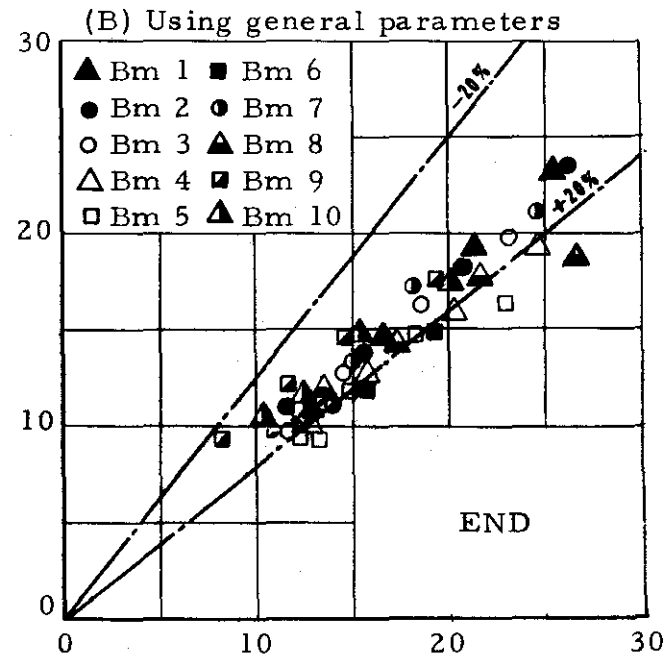
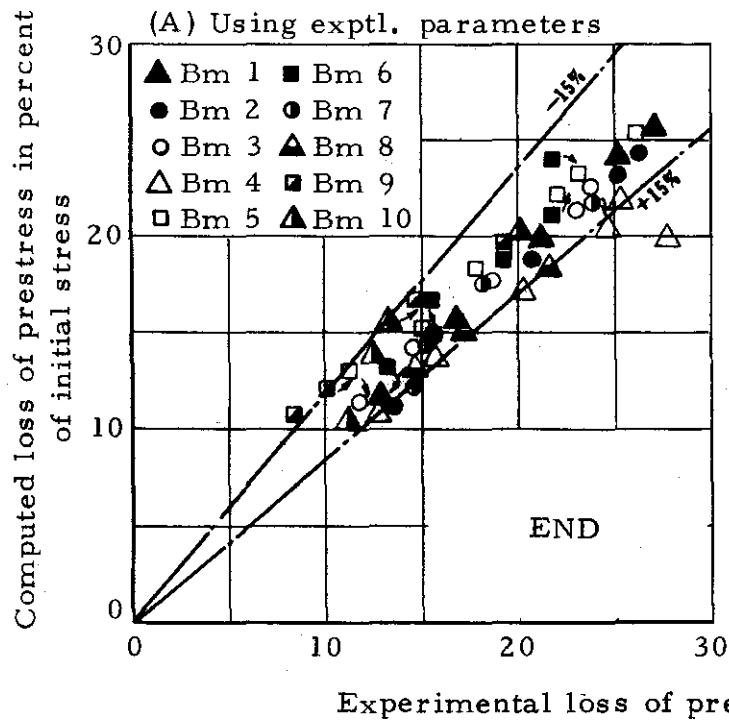


Figure 19 Computed and experimental loss of prestress at end of beams reported in Reference (23)

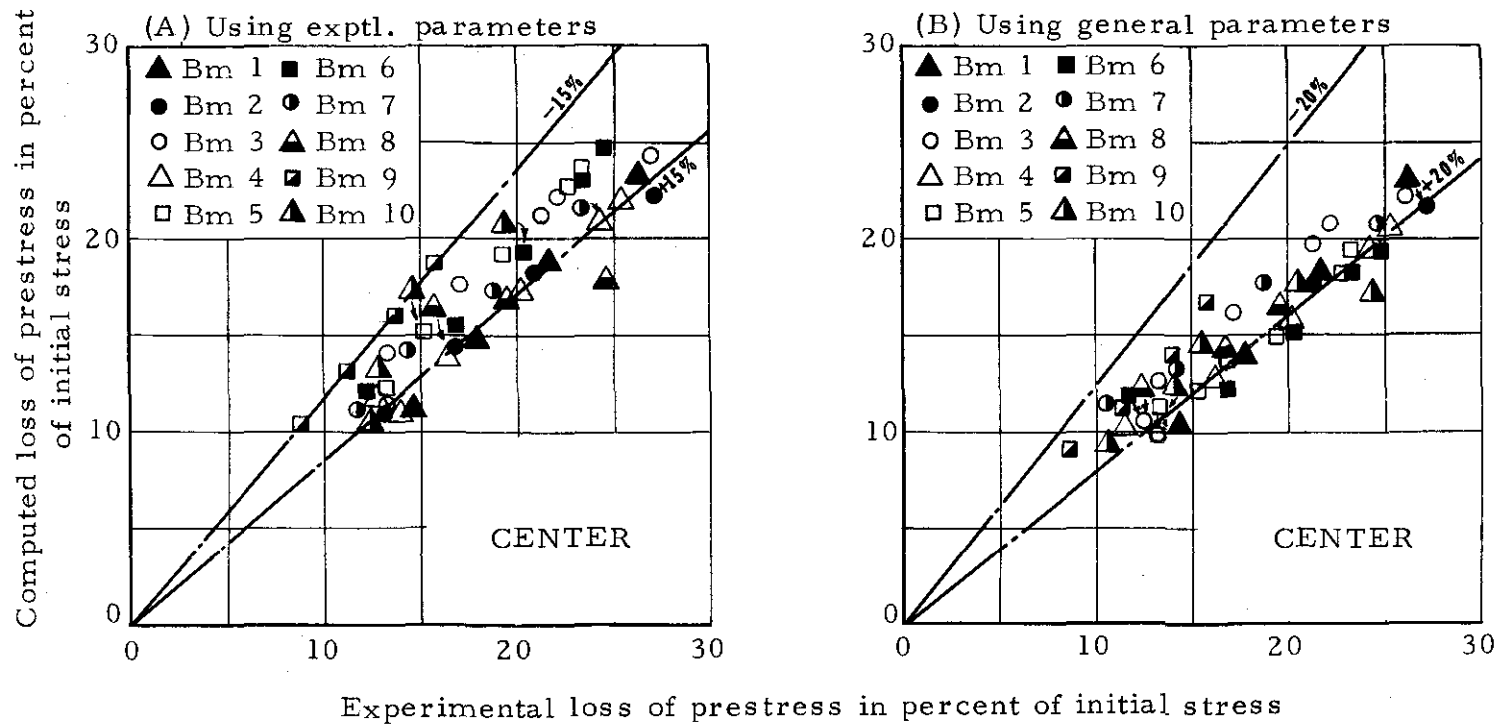


Figure 20 Computed and experimental loss of prestress at center of beams reported in Reference (23)

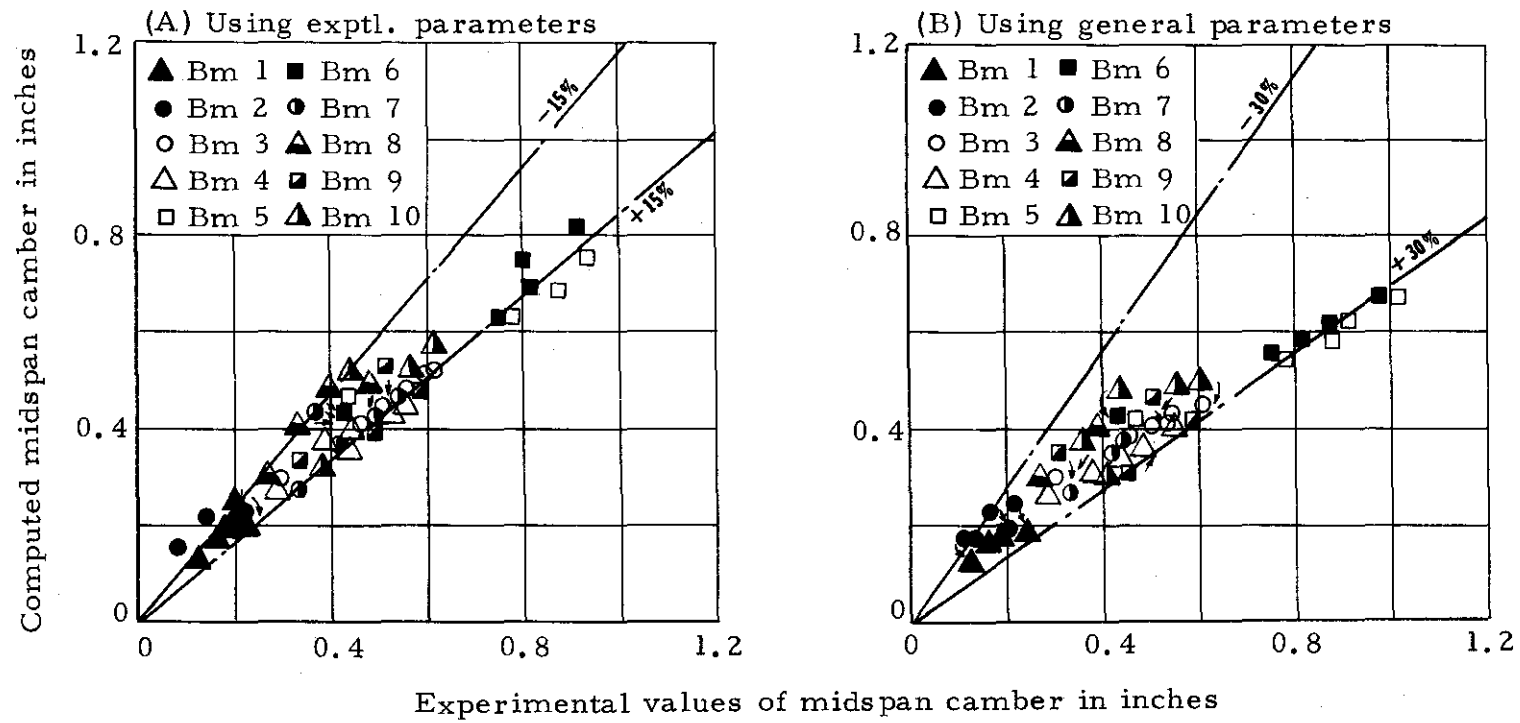


Figure 21 Computed and experimental midspan camber of beams reported in Reference (23)

prestress and camber. The scatter between the measured and computed loss of prestress, using experimental parameters, is  $\pm 15\%$ , while the same, using general parameters is  $\pm 20\%$ .

2. The scatter between the measured and computed values of camber, using experimental parameters, is  $\pm 15\%$ , while the same, using general parameters is  $\pm 30\%$ . The increase in scatter of  $\pm 15\%$  for camber and only  $\pm 5\%$  for loss of prestress (using general parameters) suggests that camber is more sensitive to changes in parameters than loss of prestress.

3. The computed initial values of camber agrees very well with the measured values for all of the beams.

#### Results of Tests at the University of Illinois (24)

##### Description of Specimens:

Two pretensioned non-composite rectangular beams of normal weight concrete and 6' spans were observed over a period of two years under laboratory conditions. Midspan camber and strains were recorded periodically. The properties of the test beams are shown in Table C2.

This paper includes all the relevant information pertaining to elastic properties, creep, and shrinkage characteristics, that are needed to perform the predictions presented in this study for the loss of prestress and camber.

### Discussion of Measured and Computed Results:

The results for the two beams for loss of prestress (at center only) and midspan camber are shown in Figures 22 - 23. From these comparisons, the following observations are made:

1. The general parameters (suggested in this report) being smaller than the experimental parameters causes an under-estimation of the loss of prestress. Part of this underestimation is due to the variation in the value of the modulus of elasticity at release (due to the use of Eq. 6) from the measured value. The scatter between the measured and computed loss of prestress along with the computed values of  $E_{ci}$  (using Eq. 6) is  $\pm 10\%$  for the experimental parameters and  $\pm 15\%$  for the general parameters. However, the use of the measured values of  $E_{ci}$  reduces the values of scatter for the general parameter results by  $\pm 5\%$  (Figure 22). This indicates that differences between the measured and computed values of the modulus of elasticity at release should not be overlooked.

2. The effect of the smaller general parameters is significantly felt on the values of camber. The scatter between the measured and computed values of camber along with the computed values of  $E_{ci}$  (using Eq. 6) is  $\pm 20\%$  for the experimental parameters and  $\pm 35\%$  for the general parameters. However, the use of the measured values of  $E_{ci}$  reduces the values of scatter for the general parameter results by  $\pm 10\%$  (Figure 23).

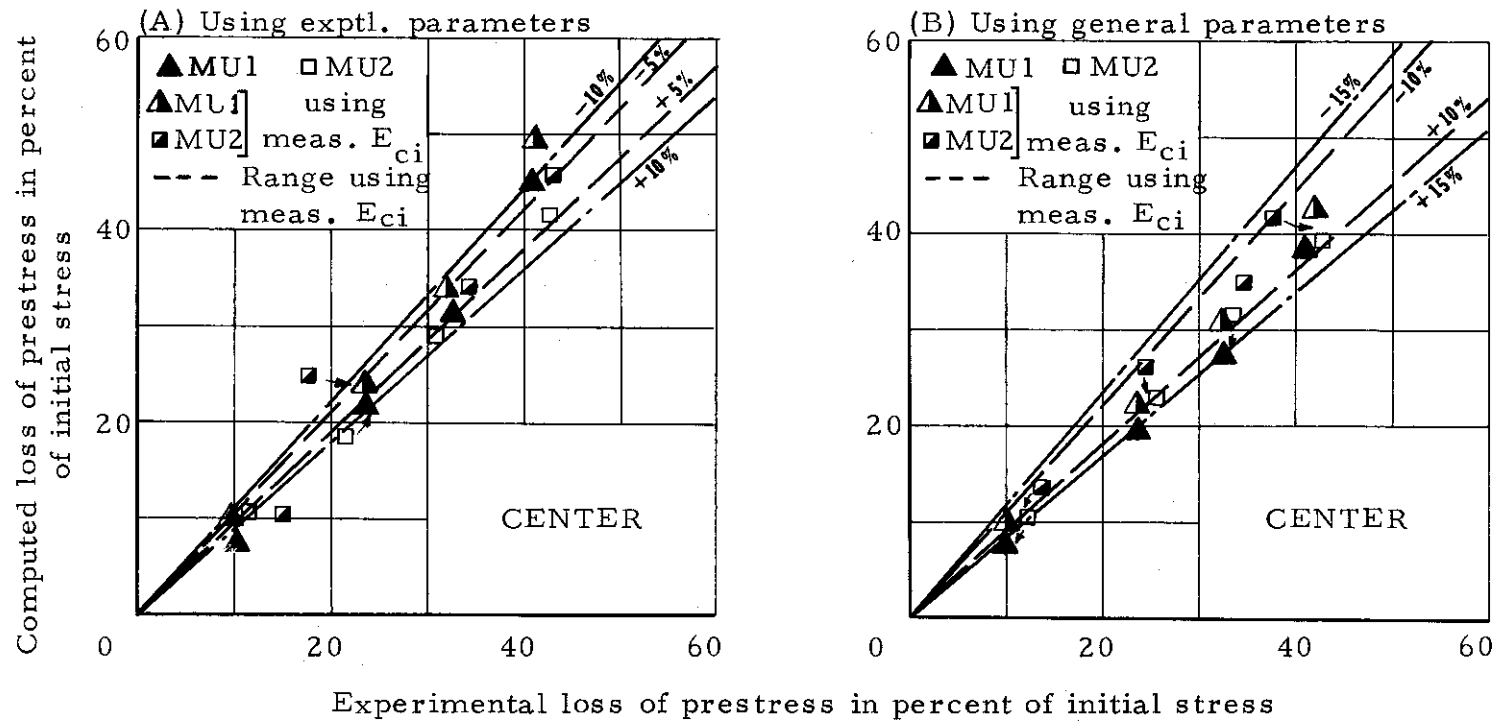


Figure 22 Computed and experimental loss of prestress at center of beams reported in Reference (24)

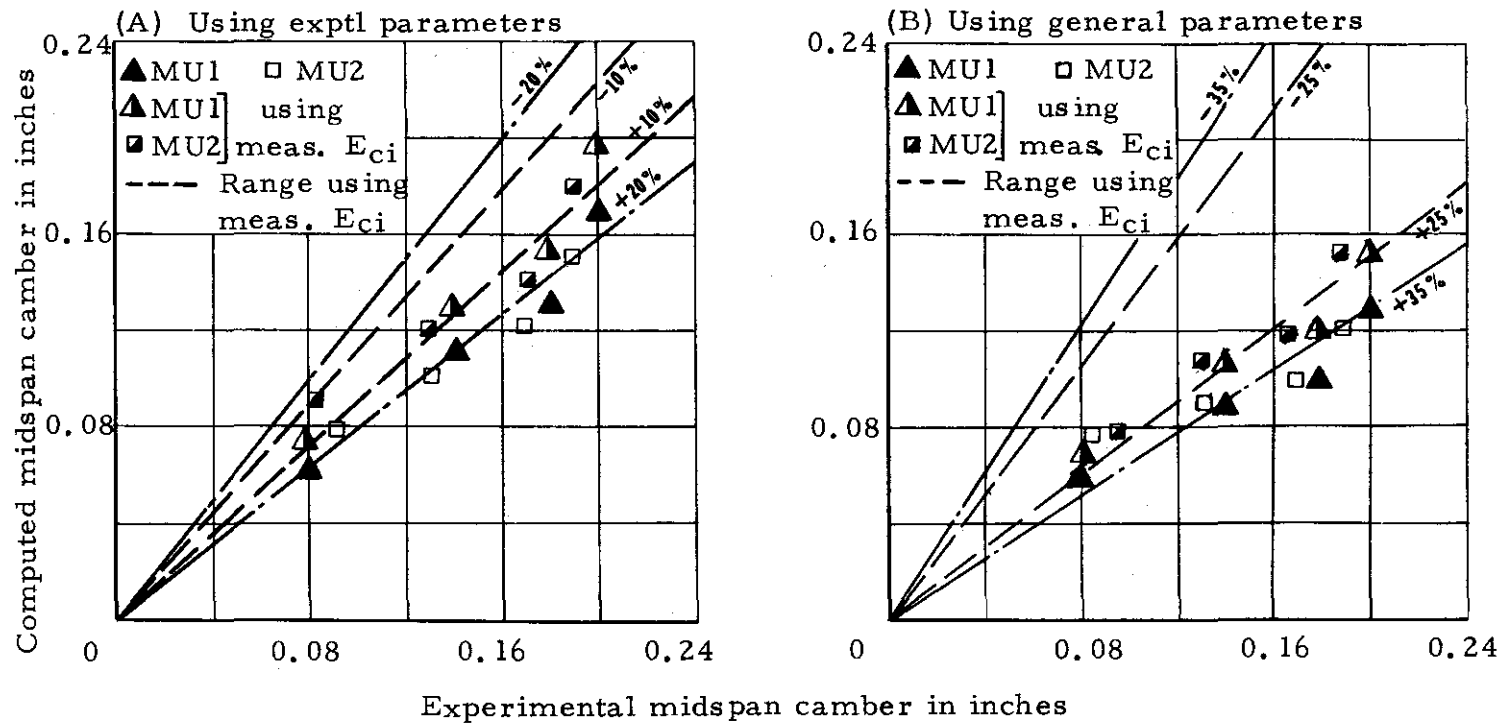


Figure 23 Computed and experimental midspan camber of beams reported in Reference (24)

3. The computed initial values of camber agree fairly well with the measured initial values of camber, though the magnitudes are very small. It is, however, noted that (due to the initial values of camber being very near zero) a small deviation from the measured value at the initial stage is reflected in a larger magnitude at a later stage. Even though the scatter between the measured and computed values of camber using general parameters along with the computed value of  $E_{ci}$  is  $\pm 35\%$ , the actual difference between the computed and measured camber is less than 0.06" (Figure 20).

#### Results of Tests at the Texas A & M University (27)

##### Description of Specimens:

Five non-composite pretensioned Type B bridge girders of the Texas Highway Department (4 lightweight and 1 normal weight) of spans 38'-45' were studied over a period of 1 year for both camber and loss of prestress. The girders were maintained in the field. The properties of the specimens used in this study are shown in Table C3. Standard 6" by 12" cylinders were cast and used to determine the strength of concrete. In addition to the five girders, 2 shrinkage specimens (of the same cross section as the girder) but 4' long were also cast.

This paper includes all the relevant information pertaining to elastic properties, creep, and shrinkage characteristics, that

are needed to perform the predictions presented in this study for the loss of prestress and camber. While using the general parameters, the correction factors were extrapolated for conditions other than the "standard" (see Chapter 2).

#### Discussion of Measured and Computed Results:

The results for the loss of prestress (at end and midspan) and the midspan camber are shown in Figures 24 - 26 for the five girders. From these comparisons, the following observations are made:

1. The general parameters (suggested in this report) being slightly greater than the experimental parameters overestimates slightly the loss of prestress and camber. The scatter between the computed and measured loss of prestress at the end of the beam using the experimental parameters and the general parameters are  $\pm 16\%$  and  $\pm 20\%$  respectively. The corresponding values at the center of the beam are  $\pm 15\%$  and  $\pm 20\%$  respectively. The difference between the experimental parameters and the general parameters is noticed in the slight increase of scatter for the latter case. This increase is, however, small and within the tolerances of design.
2. The computed values of initial camber agrees fairly well with the measured values.
3. The scatter between the measured and computed values

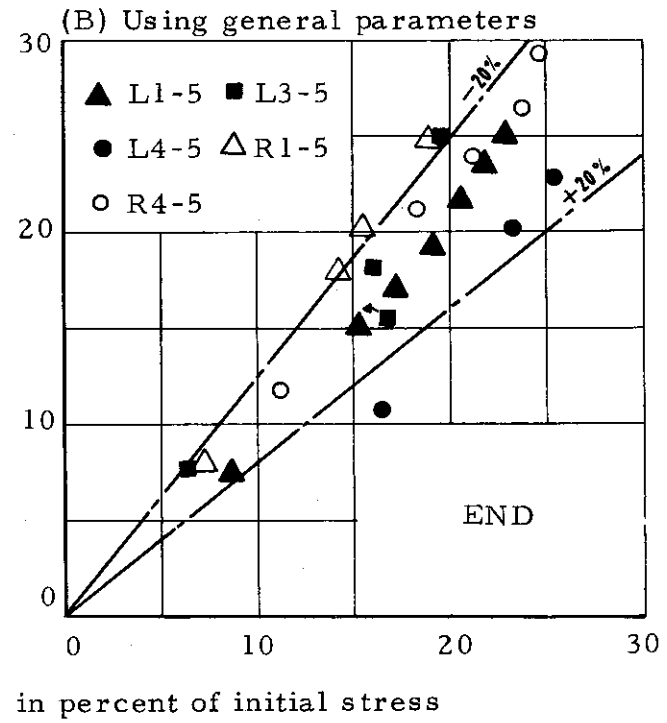
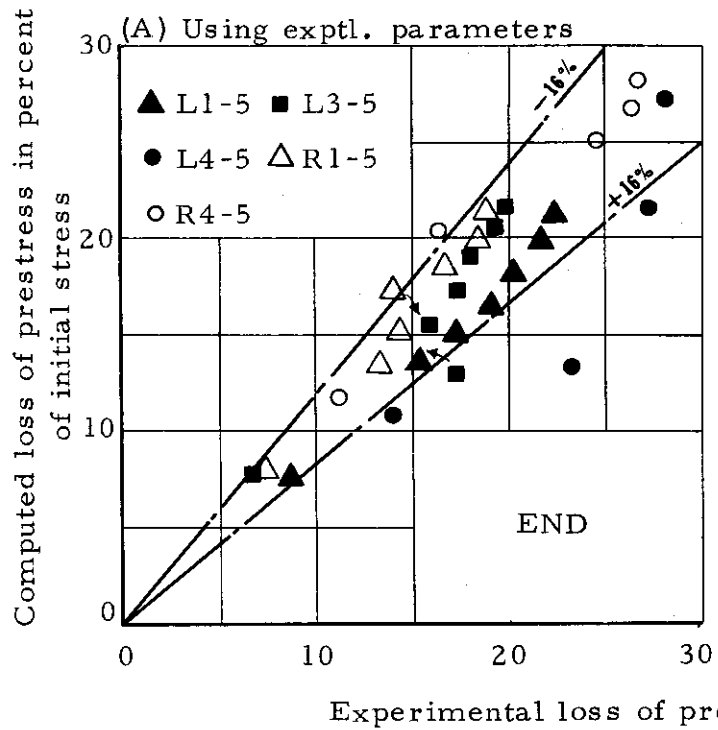


Figure 24 Computed and experimental loss of prestress at end of beams reported in Reference (27)

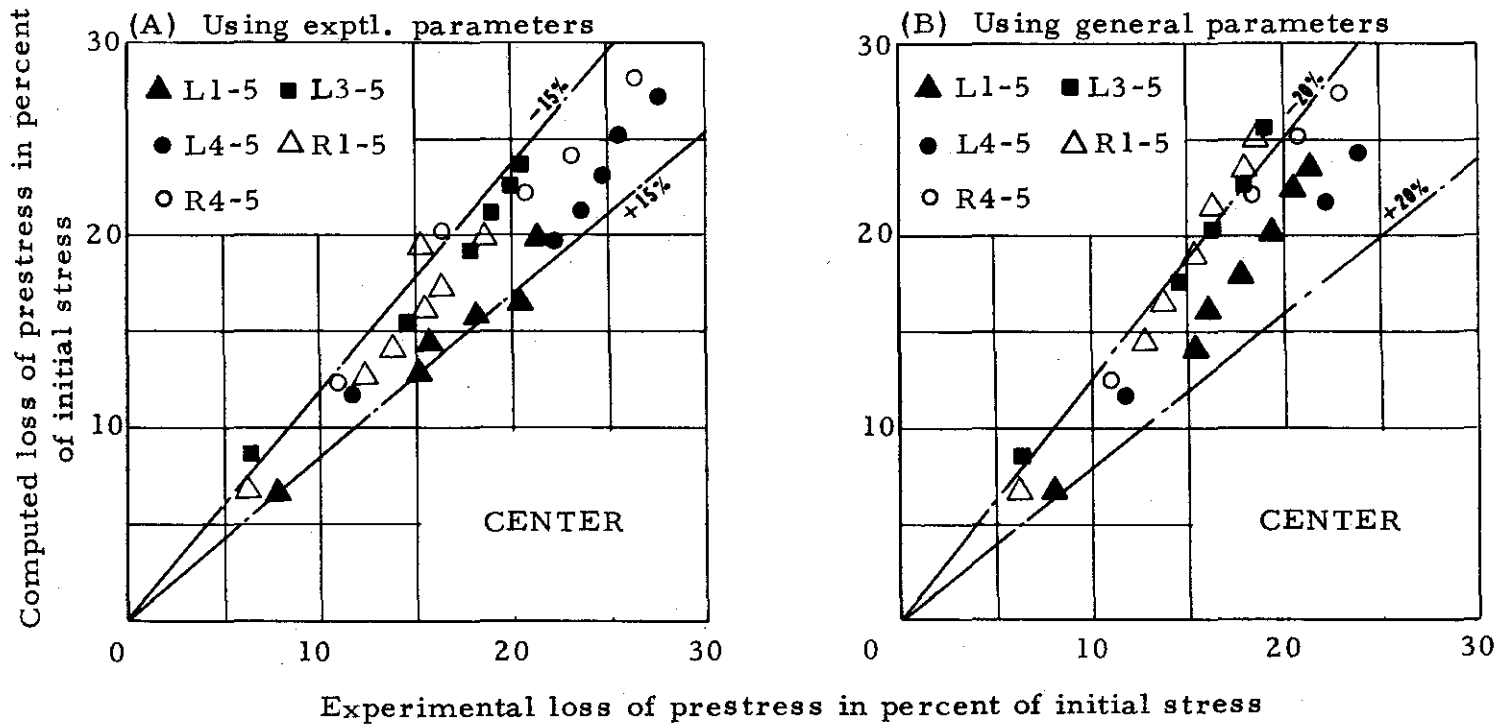


Figure 25 Computed and experimental loss of prestress at center of beams reported in Reference (27)

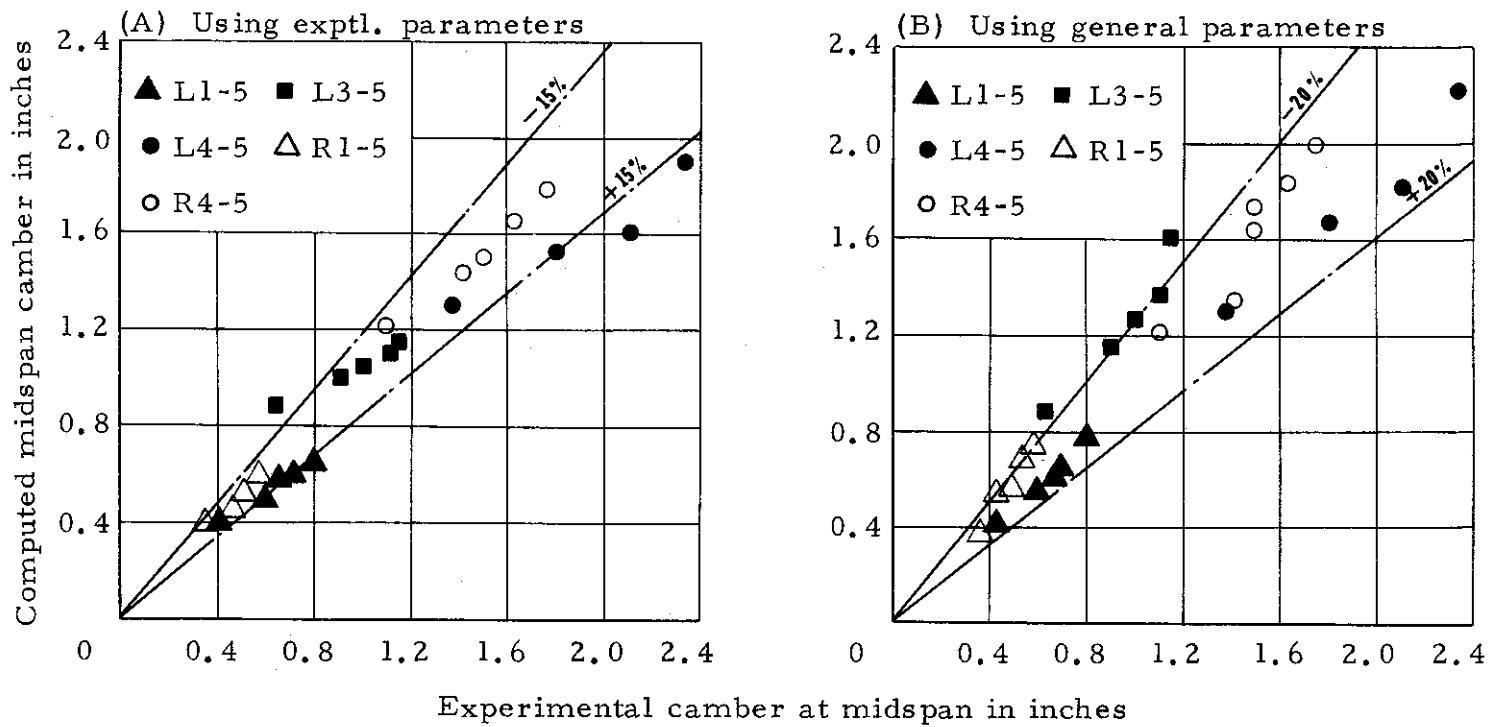


Figure 26 Computed and experimental midspan camber of beams reported in Reference (27)

of midspan camber using the experimental parameters and general parameters are  $\pm 15\%$  and  $\pm 20\%$  respectively. The sensitivity of camber computations to the choice of general parameters is noted. An increase of  $\pm 5\%$  in scatter for the use of general parameters is considered reasonable.

#### Results of Tests at the University of Missouri (31)

##### Description of Test Specimens:

Two post-tensioned prestressed composite beams of normal weight concrete and spans 99' were observed over a period of two years under field conditions for camber and loss of prestress. Concrete strains were measured at both end and midspan for both the beams. The properties of the test girders are shown in Table C4.

This paper does not include any information pertaining to the creep and shrinkage characteristics of the concrete. An arbitrary value of  $C_u = 3.00$  was used in this paper for the computation of camber. To obtain an idea of the range of behavior of this girder, the measured values of the loss of prestress (at end and midspan) are compared with the computed values of loss of prestress (using maximum and average general parameters). A similar comparison is made between the computed and the measured values of midspan camber (using maximum and average general parameters).

Slabs were cast on these girders at precast beam age = 200 days. However, the value of  $\beta_s$  as computed by Eq. 10 is based on data of specimens whose loading ages are not more than 50 days. As there is no available literature for later loading ages (200 days), an estimated value of  $\beta_s$  is used in all the computations for the loss of prestress and camber.

#### Discussion of Measured and Computed Results:

The results for the loss of prestress and camber are shown in Figures 27 - 29 for the east girder. The results for the west girder cannot be computed with the limited information available in the paper. In the computation of initial values of camber, numerical methods were used (to account for the variable moment of inertia). From these comparisons, the following observations are made:

1. The use of maximum general parameters overestimates the loss of prestress at both end and center by 20% and 25% respectively.
2. The use of average general parameters estimates reasonably well the loss of prestress at both end and midspan (scatter of + 10% for both).
3. The use of maximum general parameters estimates the midspan camber very well (scatter of  $\pm 10\%$ ).
4. The use of average general parameters results in a

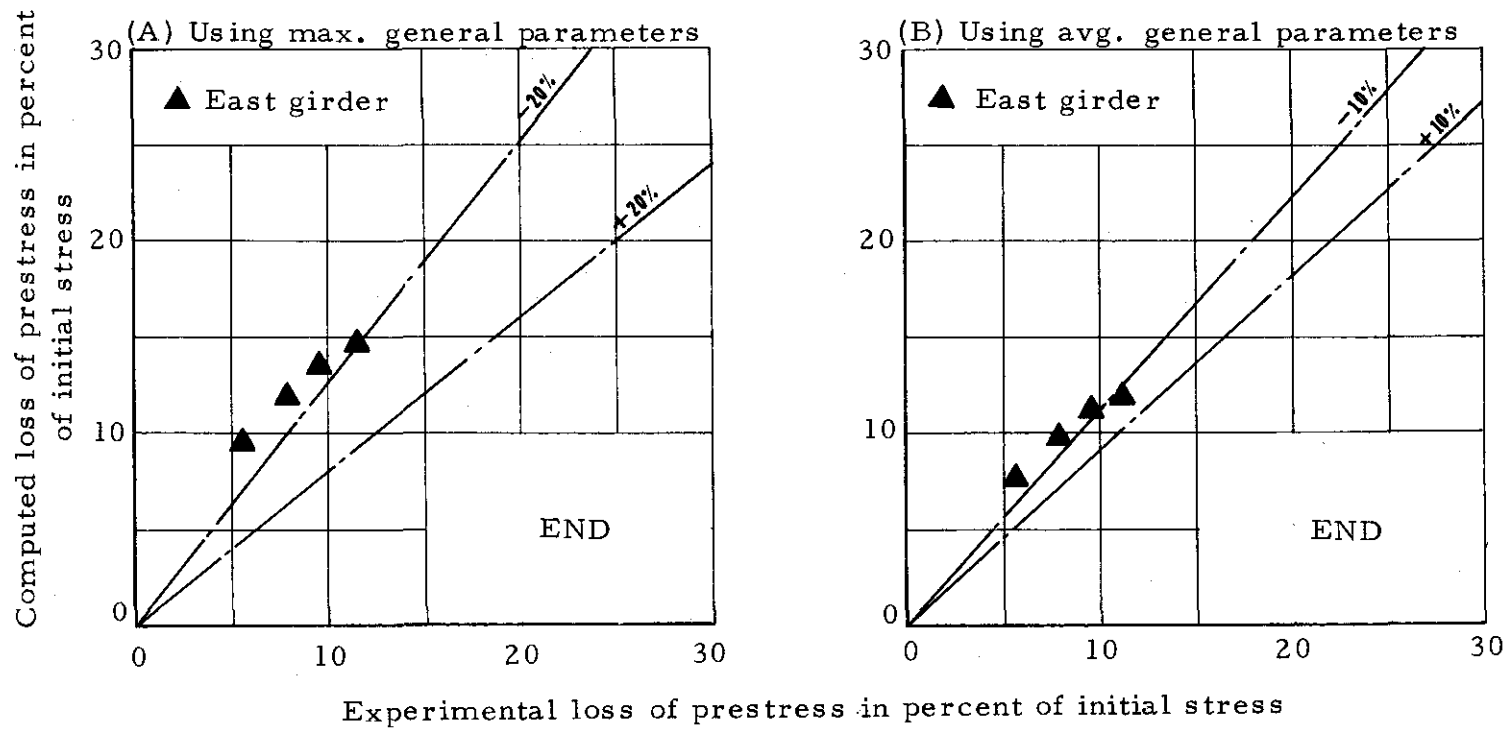


Figure 27 Computed and experimental loss of prestress at end of beam reported in Reference (31)

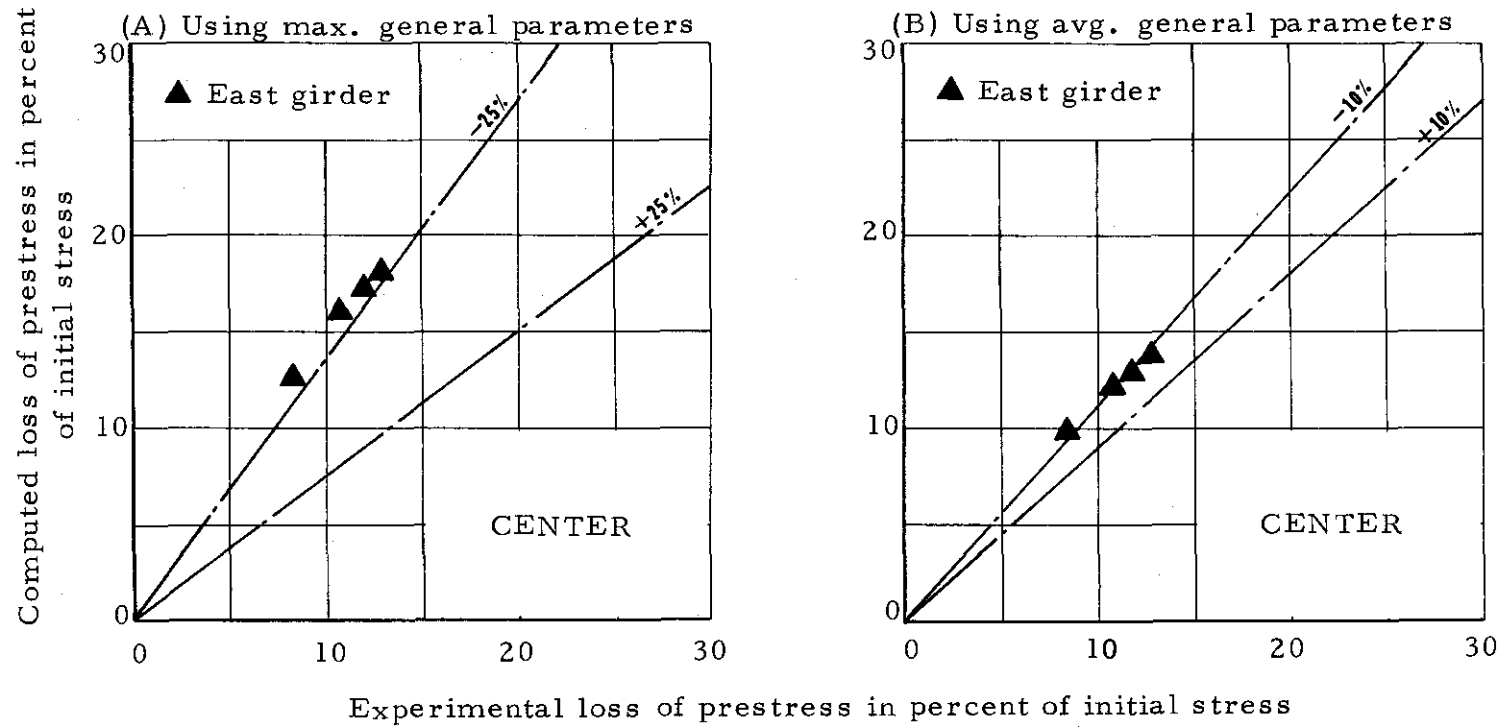


Figure 28 Computed and experimental loss of prestress at center of beam reported in Reference (31)

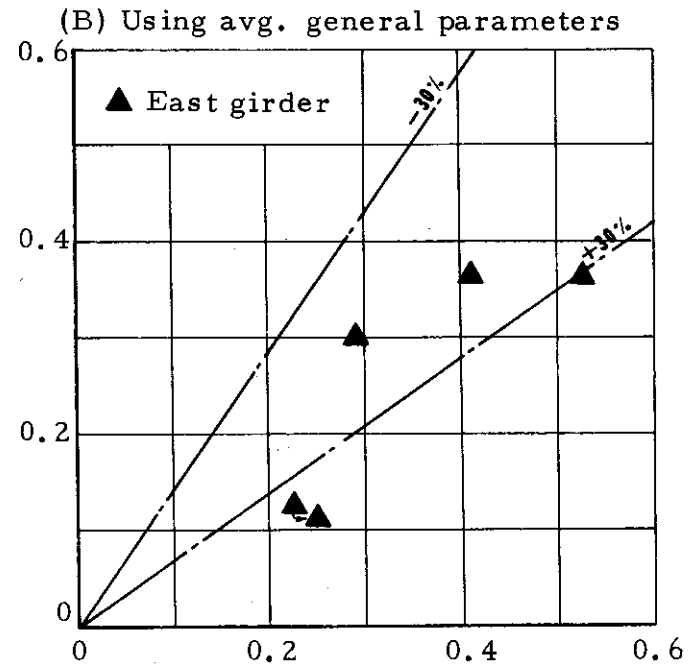
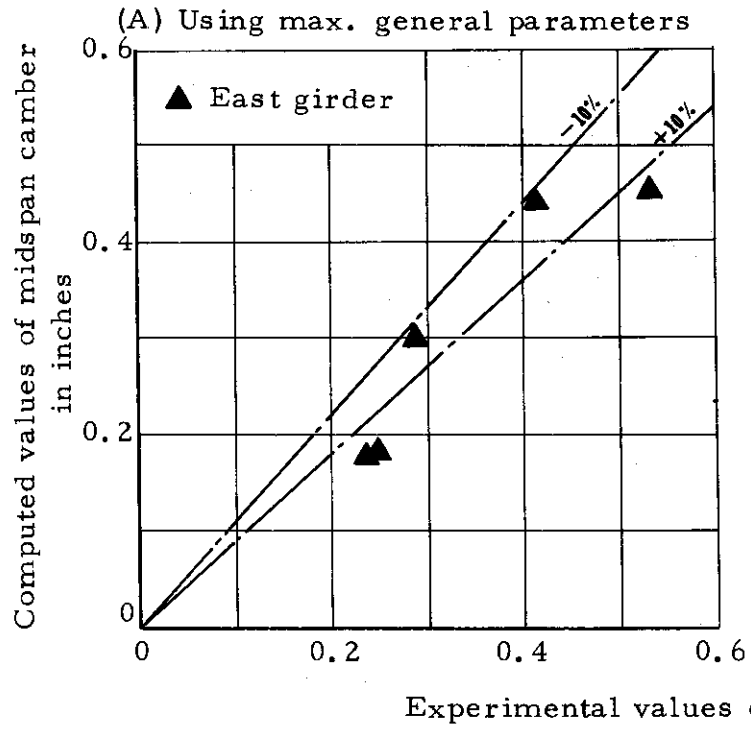


Figure 29 Computed and experimental midspan camber of beam reported in Reference (31)

difference between the computed and measured values of midspan camber of 30%. It should, however, be noted that in spite of the wide difference of 30%, the actual difference for the worst data point is less than 0.18". Realizing that this difference between the computed and measured values of camber is for a girder of about 100' span, the difference of 30% has only an academic significance.

#### 4.8 Summary of Results Reported by Others and Conclusion

On the basis of Figures 19 - 29, and the specific conclusions made in section 4.7, the following general observations are made concerning the design method suggested in this report and the experimental results of University of Florida (23), University of Illinois (24), Texas A & M University (27), and University of Missouri (31):

1. The use of the average general parameters and the general Eqs. (14) and (17) is a reasonable means of computing the loss of prestress for both composite and non-composite beams. Either an underestimation (Figures 19, 20, 22) or an overestimation (Figures 24, 25, 27, 28) may occur, depending on the difference between the experimental and general values of the creep and shrinkage parameters. However, the maximum scatter between the computed and the measured values of loss of prestress was  $\pm 20\%$  (using average general parameters) for these studies.

2. The use of the average general parameters and the general Eqs. (15) and (18) is a reasonable means of estimating midspan camber for both composite and non-composite beams. Either an underestimation (Figures 21, 23, 29) or an overestimation (Figure 26) may occur, depending on the difference between the experimental and general values of the creep and shrinkage parameters. The maximum scatter, however, between the computed and measured values of midspan camber is  $\pm 30\%$  (using average general parameters). This maximum value of scatter occurs only in 3 of the 18 beams studied (Figures 23, 29) and even in these cases, the difference between the computed and the measured value of camber is less than 0.18". The scatter between the computed and measured values of midspan camber for the remaining 15 beams is  $\pm 25\%$ .

3. The procedure suggested in this report for the prediction of initial camber is adequate.

4. Camber computations are more sensitive to the choice of creep and shrinkage parameters than loss computations for non-composite beams. The reverse is true for the composite beams because of the offsetting effects that may result in "near zero" camber or deflection values after slab casting. These offsetting effects are primarily due to the elastic and creep deflections due to the slab dead load, and increased stiffness of the section on the one hand as

opposed to the reduced prestress force and its creep deformation on the other.

5. The choice of the value of the initial modulus of elasticity can affect the loss of prestress and camber (see results of tests at the University of Illinois). In fact, the value of  $E_{ci}$  affects camber more than the loss of prestress.

6. It is reasonable to expect that the use of general parameters along with the approximate Eq. (31) (for ultimate loss of prestress) and Eqs. (30) and (32) (for ultimate midspan camber) will result in values slightly higher than those obtained by the use of the ultimate Eqs. (22) to (27).

## Chapter 5

LOAD-DEFLECTION STUDIES OF PRESTRESSED  
AND REINFORCED CONCRETE BEAMS5.1 General

Increasing interest is being shown in the design of prestressed concrete members that crack under working loads. Since substantial cracking occurs under working loads in ordinary reinforced concrete members, cracking at service load levels in prestressed concrete members should be acceptable provided appropriate safety and serviceability requirements are met.

This chapter is devoted to the study of prestressed concrete beam deflections under a single load cycle (a single cycle is defined herein as a continuously applied increasing load to failure at a static rate) and repeated load cycles, and reinforced concrete beam deflections under increasing loads and 24-hour sustained cracking loads. Both rectangular and composite T-beams are included.

The details of the test beams are shown in Tables A1 and A2. The concrete properties of the laboratory beams at the time of the load-deflection tests are shown in Table A6. The laboratory beams were tested as follows:

Groups A, B, and D:	Single-cycle load tests for prestressed beams
Group C:	Repeated load tests with constant load cycle for prestressed beams
Group E:	Repeated load tests with increasing load cycle for prestressed beams
Group F:	Increasing load and 24-hour sustained load tests for reinforced beams

Observed midspan deflections shown in Figures 32-34, 37-48 refer to the position of the beam just before the application of the transverse load. If the deflections from the positions of the beams before prestressing are desired, the initial camber under prestress and dead load and the time-dependent camber must be subtracted from the deflections in Figures 32-34, 37-48. A two-point loading system (Figure 30) symmetrical about the centerline of the beam was used in all of the tests.

## 5.2 Single Cycle Load Tests of Prestressed Members

### Deflection of uncracked members

The elastic theory can be accurately applied to concrete beams as long as the concrete is not cracked. Distinct changes occur in the behavior of concrete members after first cracking. After cracking, there is a change in the distribution of bond and shearing stresses and the load-deflection response changes sharply.

The determination of cracking loads can be based on the elastic theory, assuming that cracking starts when the tensile stress in the concrete reaches its modulus of rupture. The accuracy of the elastic

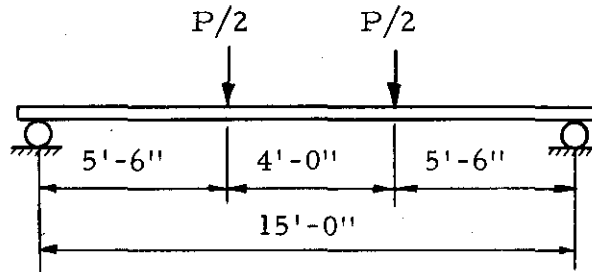


Figure 30. Two point loading for 'load-deflection' studies of laboratory beams

theory and also the modulus of rupture obtained from the usual bending tests as being representative of the tensile strength of concrete in bending has been questioned (48). However, most available test data indicates that the use of the elastic theory up to cracking (determined with the modulus of rupture) is sufficiently accurate.

For a prestressed concrete beam without non-tensioned steel, the cracking moment is given by:

$$M_{cr} = F_t e_x + \frac{F_t I_g}{A_g y_t} + \frac{f'_{cb} I_g}{y_t} \quad (35)$$

where  $F_t = F_i - \Delta F_t$ ;  $F_i$  is the initial prestressing force and  $\Delta F_t$  is total loss in prestressing force obtained by using Eq. (14) or (17).

- $A_g$  = gross area of section  
 $I_g$  = gross moment of inertia of section  
 $y_t$  = distance of tension fiber from cgc  
 $f'_{cb}$  = modulus of rupture of concrete.

Shaikh and Branson (49) indicated that the cracking moment of prestressed concrete beams is (for all practical purposes) not influenced by the addition of non-tensioned steel. It was concluded that Eq. (35) may be used to compute the cracking moment of prestressed concrete beams containing non-tensioned steel in addition to prestressing steel.

#### Deflection of cracked members

Under cracked conditions, the behavior of prestressed concrete members and ordinary reinforced concrete members is similar. Since ordinary reinforced concrete members are invariably cracked under working loads, most methods for computing these deflections do take into account the effect of flexural cracking in some form.

For this investigation, the method of Branson (4)(50)(51)(42) was used to compute the deflections of the test beams. The choice of this method (Eqs. (37) and (38)) is based on favorable comments from designers and on its indicated accuracy in the ACI Committee 435 report (4) on deflections of reinforced concrete flexural members. These have been proposed for the 1971 ACI Code (50)(51).

For an elastic homogeneous member subject to flexure:

$$\phi = \frac{M}{E I} \quad (36)$$

The curvature,  $\phi$ , at any section can be readily obtained using Eq. (36), with the appropriate bending moment,  $M$ , and flexural rigidity,  $EI$ , at that section. For uncracked sections either the gross, or, more precisely, the uncracked transformed moment of inertia may be used. Under cracked conditions, however, because of the varying amount and extent of cracking, the flexural rigidity,  $EI$ , is not a constant.

Theoretically one could evaluate zones for which the cracking moment is exceeded and thus calculate the corresponding transformed section moments of inertia along the length of the beams, based on appropriate cracked and uncracked sections. With the flexural rigidity known along the length of the beam, curvatures could be computed using Eq. (36) and deflections obtained by the usual procedures.

Due to the complexity involved in relating the height of cracks, spacing of cracks, etc. to the flexural rigidity of the member, mostly empirical or grossly approximate methods have appeared in the literature for computing flexural rigidity,  $EI$ , under cracked conditions.

Based on a sizable number of tests on rectangular beams (simple and continuous) and T-beams, Branson (50) has presented an empirical expression for the effective moment of inertia at a

given section,  $I_{\text{eff}}$ . The expression was given in a form that includes the effect of extent of cracking as:

$$I_{\text{eff}} = \left( \frac{M_{\text{cr}}}{M} \right)^4 I_g + \left( 1 - \left( \frac{M_{\text{cr}}}{M} \right)^4 \right) I_{\text{cr}} \quad (37)$$

where:  $M_{\text{cr}}$  = cracking moment as defined by Eq. (35)

$M$  = bending moment at the section where  $I_{\text{eff}}$  is desired

$I_g$  = moment of inertia of gross section

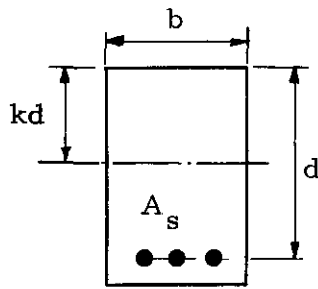
$I_{\text{cr}}$  = moment of inertia of the fully cracked section using Eq. (39). See Figure 31.

An expression for an average effective moment of inertia for the entire length of the simply supported beam under uniformly distributed load was also given by Branson (50) as:

$$I_{\text{eff}} = \left( \frac{M_{\text{cr}}}{M_{\text{max}}} \right)^3 I_g + \left( 1 - \left( \frac{M_{\text{cr}}}{M_{\text{max}}} \right)^3 \right) I_{\text{cr}} \quad (38)$$

where:  $M_{\text{max}}$  = maximum moment in the span.

It is to be noted that Eqs. (37) and (38) apply only when  $M$  or  $M_{\text{max}}$  is greater than or equal to  $M_{\text{cr}}$ ; otherwise  $I_{\text{eff}} = I_g$ . For continuous beams, the average of positive and negative moment region values in Eq. (38) is recommended (42)(50)(51).



$$I_{cr} = \frac{b(kd)^3}{3} + n A_s (d - kd)^2 \quad (39)$$

$$k = \frac{(np)^2 + 2np}{pn}$$

$$\text{where: } n = E_s / E_c$$

$$p = A_s / bd$$

Figure 31 Moment of inertia of cracked section ( $I_{cr}$ )

The concurrence of AASHO, ACI, and PCI codes on the methods of determination of ultimate strength of prestressed concrete beams establishes the reliability of the equations indicated in the codes. Therefore, in this investigation only a comparison of observed and computed (using equations from the ACI code) values of ultimate load was obtained.

Single cycle load tests were conducted on all the beams of Grps. A, B, and D. Midspan deflection of the test beams were obtained up to loads ranging from 76 to 88 percent of the ultimate loads. Eq. (38)

---

\*The same equations are also valid for composite beams (with transformed compression flange width to account for the different concretes) if the neutral axis falls within the flange. This was the case for the laboratory composite test beams studies herein.

was used to determine the effective moment of inertia in the computation of deflections. Eq. (35) was used for computing  $M_{Cr}$ , and Eq. (39) was used for the determination of  $I_{Cr}$ . The modulus of rupture,  $f'_{cb}$ , was obtained by bending tests on plain concrete specimens for the test beams. It is observed that Eq. (38) was originally established for use in the case of simply supported beams under uniformly distributed loads. Its use, however, is considered adequate for the two-point test loading.

The comparison of observed and computed midspan deflection curves are shown in Figures 32 to 34. Table 5 shows the computed and measured values of ultimate loads as well as the maximum discrepancies in the observed and computed deflection curves.

Based on Figures 32 to 34 and Table 5, the following observations are made:

1. There are three distinct stages of behavior in the load-deflection history of a prestressed concrete beam. In the first stage, the curve is virtually linear. This stage represents the behavior of the beam before cracking of the concrete. The extent of this stage depends on the geometrical and material properties of the section and the type of loading. In the second stage, the load-deflection curve is characterized by a constantly changing rate of deflection with applied load and represents the behavior of the beam after the

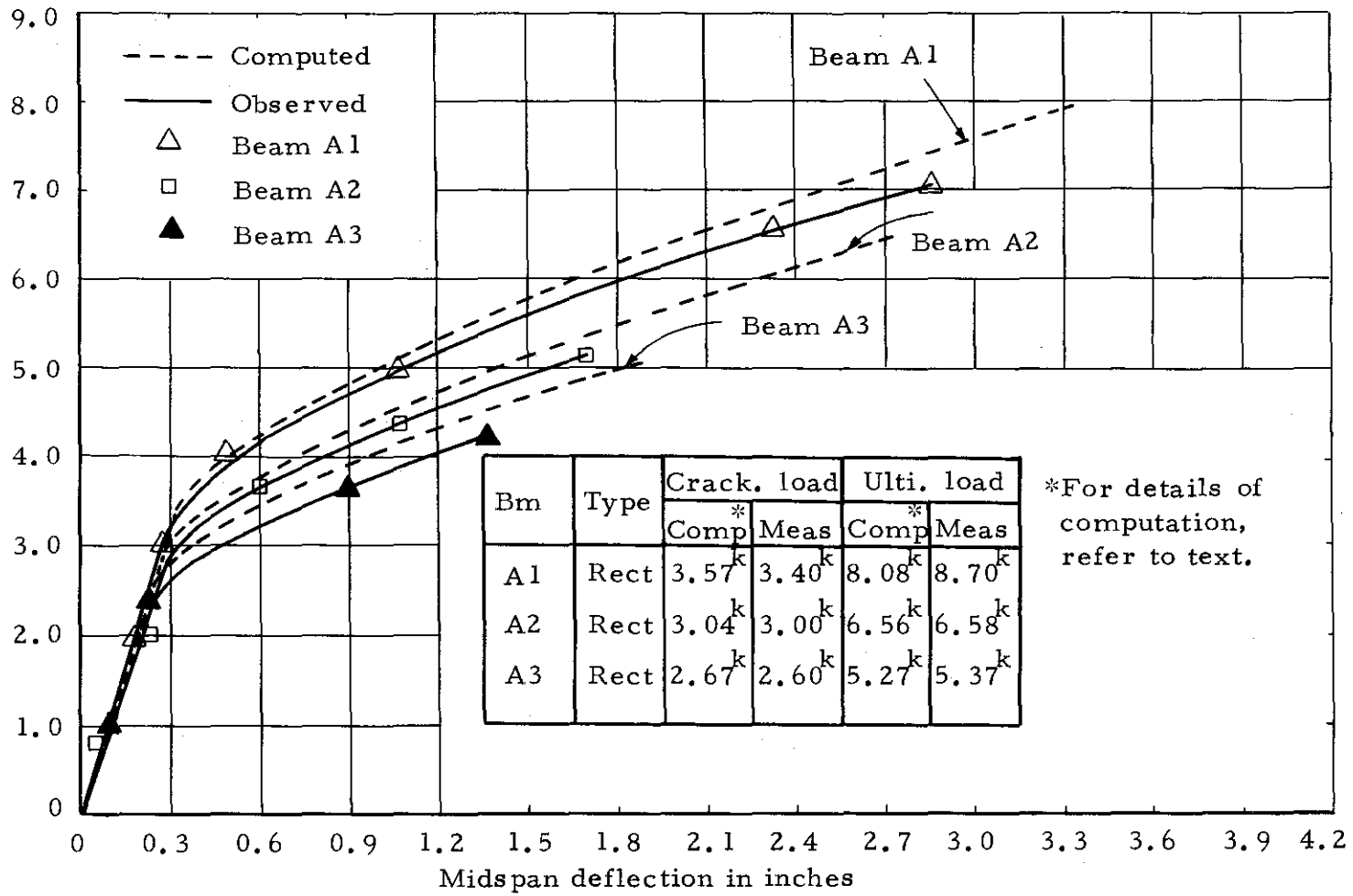


Figure 32 Observed and computed midspan deflection versus load curves for beams of Group A (three non-composite prestressed beams)

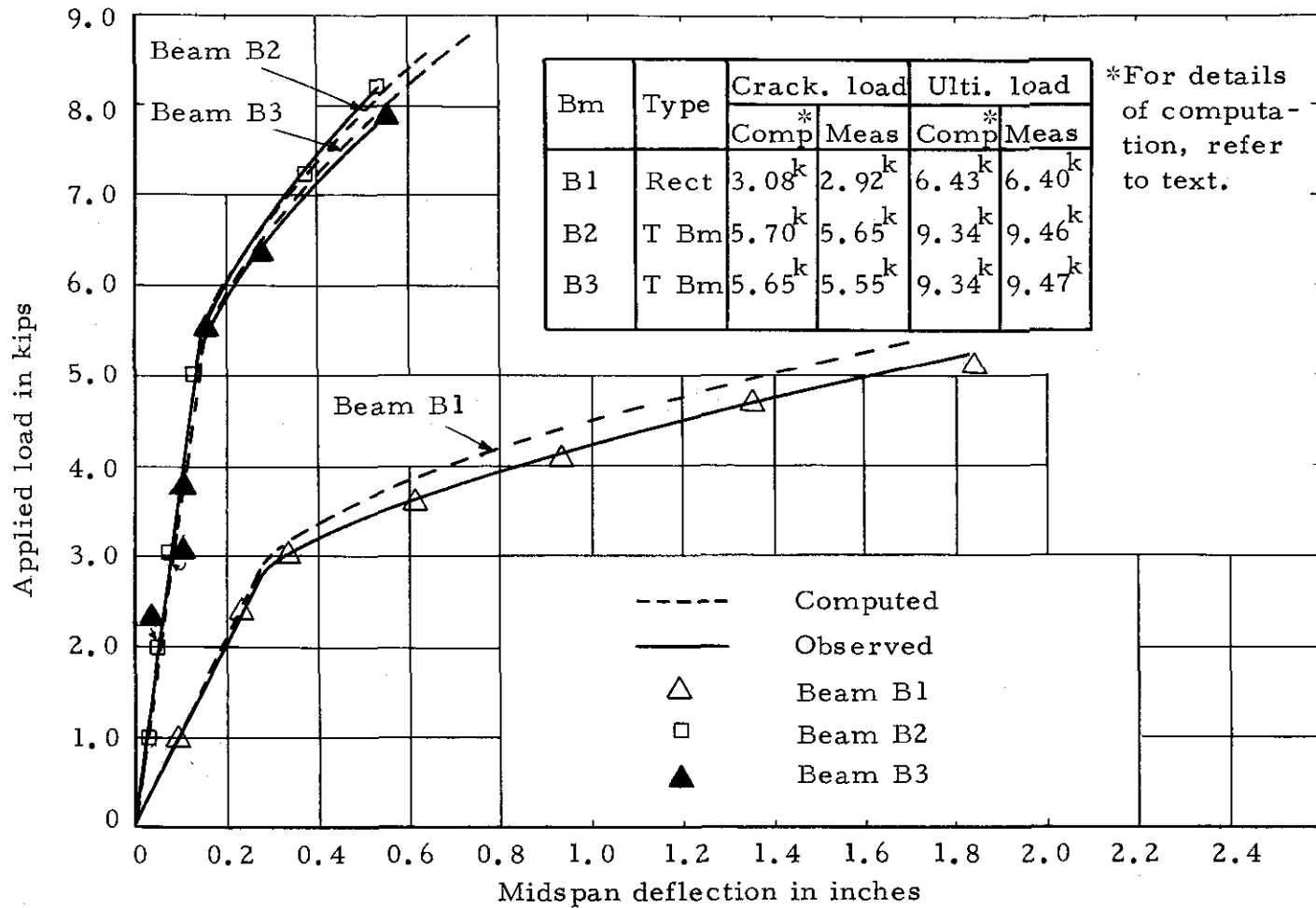


Figure 33 Observed and computed midspan deflection versus load curves for beams of Group B (one non-composite and two composite prestressed beams)

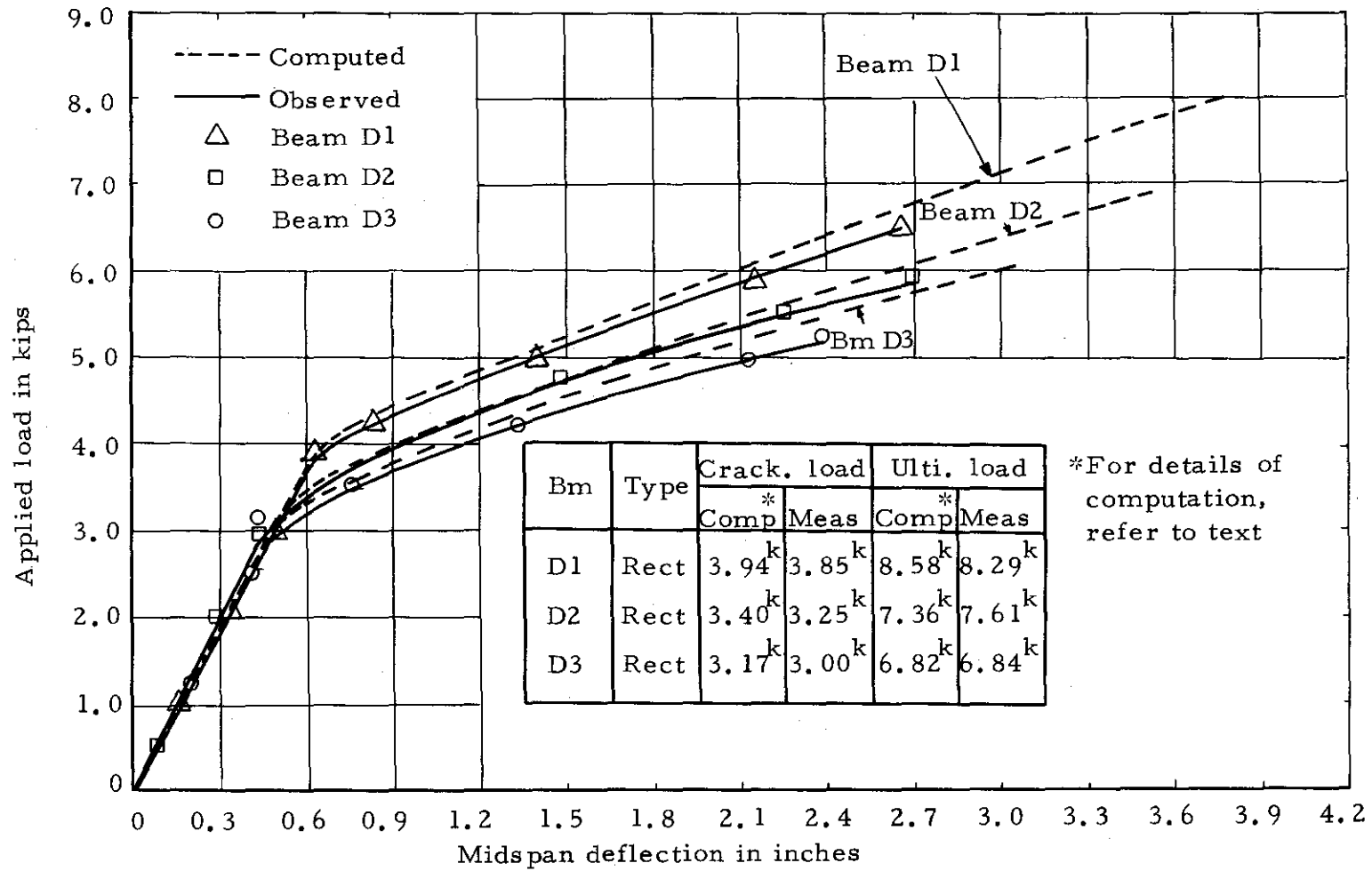


Figure 34 Observed and computed midspan deflection versus load curves for beams of Group D (three non-composite prestressed beams)

TABLE 5

WORKING LOAD, COMPUTED AND OBSERVED VALUES OF ULTIMATE LOAD  
AS WELL AS VALUES OF WORST DISCREPANCY BETWEEN  
COMPUTED AND OBSERVED DEFLECTION CURVES

Group No.	A			B			D		
Beam No.	A1	A2	A3	B1	B2	B3	D1	D2	D3
<sup>a</sup> Computed Ultimate load, $P_u$ kips	8.08	6.56	5.27	6.43	9.35	9.35	8.58	7.36	6.83
Measured Ultimate load, $P_{um}$ kips	8.70	6.58	5.37	6.40	9.46	9.47	8.29	7.61	6.84
<sup>b</sup> Working load, $P_w$ (kips)	3.57	3.04	2.67	3.08	5.71	5.66	3.94	3.40	3.17
Load factor, $P_u/P_w$	2.26	2.16	1.97	2.08	1.65	1.65	2.18	2.16	2.15
<sup>c</sup> $P_{max}$ (kips)	7.10	5.15	4.25	5.15	8.18	7.81	6.50	6.00	5.25
$(P_{max}/P_u)^{100}$	88%	80%	81%	80%	88%	84%	76%	82%	77%
<sup>d</sup> $P_\Delta$ (kips)	7.00	5.00	4.00	4.00	1.00	1.00	6.00	3.00	5.00
<sup>e</sup> Worst discrepancy in deflection curves	-12%	-12%	-21%	-24%	-14%	-13%	-5%	+8%	-10%

<sup>a</sup> The computation of ultimate loads is based on accepted procedures indicated in ACI 318-63 Code. The corresponding equations are not reproduced here. The test period varied between 45-60 min for each beam.

TABLE 5 (Cont'd)

<sup>b</sup> For the test beams, the working load was assumed to represent the condition that cracking would occur as soon as this load was exceeded. These values of  $P_w$  were the computed cracking loads.

<sup>c</sup> Represents the maximum load for which deflections were recorded.

<sup>d</sup> Represents the load at which the discrepancy between the observed and computed deflection is the greatest.

<sup>e</sup> Plus or minus indicate that computed deflection is greater than or smaller than the observed deflections.

concrete is cracked and while the reinforcement stress is still in the 'elastic' range of the stress-strain curve for the reinforcement. The third stage is marked by a very slow change in the slope of the load-deflection curve. In this stage, the reinforcement stress is in the 'inelastic' range of the stress-strain curve for the reinforcement and the load-deflection curve is nearly flat.

In addition, the presence of non-tensioned steel affects the deformational behavior of a prestressed concrete beam after the initial cracking (49). It was concluded by Shaikh and Branson (49), that the net deflection in a beam with non-tensioned steel as compared to the deflection of an identical beam without non-tensioned steel may be greater, comparable, or considerably smaller depending on whether the applied transverse load is approximately equal to, somewhat greater than or considerably greater than the cracking load.

Failure of the beam is usually the result of failure of the compressed concrete. However, a beam with a very small percentage of reinforcement may fail by fracture of the reinforcement. The third stage, however, is not exhibited by beams having a high value of steel percentage. The first two stages described above can be seen clearly for the laboratory beams in Figures 32 to 34 (the steel percentage varied from 0.93% to 0.38% for rectangular beams and was of the order of 0.1% for the composite beams).

2. The level of prestress affects the shape of the load-deflection curves. An increase in the level of prestress tends to increase the load required to produce the flexural cracking and thus extends the first stage. For example, Beam A1 (whose prestress level is greater than that of either Beam A2 or Beam A3) has a cracking load of  $3.57^k$  as compared to  $3.04^k$  for Beam A2 and  $2.67^k$  for Beam A3 (see Figure 32 and Table 5).

3. It is observed that for most of the beams (8 out of 9) studied under single load cycle (see Table 5), the computed values of deflection are smaller than the observed values of deflection. It is also observed that the discrepancy between the computed and measured deflection curves increases as the applied transverse load approaches the ultimate load capacity of the beam. Realizing that the tendency of concrete to creep under load exists even for very rapid rates of loading (52), it may reasonably be assumed that the discrepancy between the computed and observed deflection curves is due to the creep of concrete. Each load cycle required about 45-60 minutes to complete. This creep effect has not been accounted for in the development of Eq. (38). No attempt, however, is made to modify Eq. (38) for creep effects, because the use of Eq. (38) gives reasonable estimates of deflection (from a design point of view) up to 1.5 to 2.0 times the working load.

4. The use of Eq. (38) resulted in computed deflections being slightly greater than the observed deflections in most of the beams (8 out of 10) in Reference (49), while in the current study the use of the same equation results in the computed deflections being slightly smaller than the observed deflections. This effect appears to be due to the presence of non-tensioned steel in the beams reported in Reference (49) which tends to reduce the creep effect and to further distribute the cracks along the beam.

5. The composite Beams B2 and B3 exhibit greater resistance to applied loads than non-composite Beam B1 due to the inherent increased stiffness of the former (see Figure 33 and Table 5).

6. There does not seem to be any significant difference in the load-deflection response of composite beams for which slabs have been cast at different times. Both Beams B2 and B3 have almost identical load-deflection curves (see Figure 33). However, there could be a significant difference in the net deflections (when referred to the position before prestressing) due to the difference in the time-dependent contribution to camber (see discussion in Chapter 3).

### 5.3 Repeated Load Tests of Prestressed Members

Under single cycle loading, the load-deflection response of prestressed concrete members can be reasonably predicted in both the 'uncracked' and 'cracked' stage. This has been discussed in

Section 5.2. However, under repeated loading, the 'load-deflection' response is different.

To understand clearly the effect of repeated loads on prestressed concrete beams, it is necessary to know the effect of repeated loads on the two components of prestressed concrete, i. e., plain concrete and prestressing steel. Shah and Winter (53) studied the behavior of plain concrete prisms with flared ends under uniaxial compression, cycled at stress levels below the ultimate strength of the prism. They found that concrete possessed a shakedown limit at around 88 to 95 percent of the ultimate load. Below this level, concrete is relatively insensitive to several cycles of loading. Neither the strength nor the strain capacity is affected below the shakedown limit. Prestressing steel like reinforcing steel, behaves (for all practical purposes) like elasto-plastic material. Repeated loading at load levels below the yield strength of the material results in full recovery, while above the yield strength of the material results in an 'inelastic' set.

In this study of prestressed concrete beams, it is assumed that under repeated loading, the stress in concrete is below its 'shakedown limit' and the stress in steel is below the 'yield strength' of the steel. This implies that (1) if the concrete stress at the repeated load level is below the shakedown limit and (2) if the steel

The determination of deflections in the uncracked region (OA in Figure 35) and cracked region (ABC in Figure 35) has been discussed in Section 5.2. The use of Eq. (38) implies the determination of the point B on the assumption that the slope of OB is proportional to the effective moment of inertia,  $I_{\text{eff}}$ . The reliability of this equation has been accepted (50)(51). Unloading from the point B along BD (a line parallel to OA) indicates that there is only elastic recovery. This is true if the beam is severely cracked. If, however, the beam is not severely cracked a certain number of cracks will close on unloading (especially in regions of moments close to the cracking moment). This will result in a small amount of 'inelastic' recovery. This is indicated by FD in Figure 35. It follows, therefore, that the total recovery (FE in Figure 35) is a function of the cycling load -- the closer the cycling load is to the cracking load, the greater will be the total recovery. This is also a logical extension of the fact that when the beam is completely uncracked, the total recovery (indicated by EF in Figure 35) is equal to the total deflection.

On the basis of the above discussion, the following relationship is suggested for computing the average effective moment of inertia under repeated loads:

$$I_{\text{rep}} = \psi_1 I_{\text{eff}} + (1 - \psi_1) I_g \quad (40)$$

where:

stress (in the same concrete member at the same load) is below the yield strength of the steel, then the reloading curve after attaining the magnitude of the repeated load will follow the single cycle load-deflection curve as if nothing else had happened (see Figure 35). In Figure 35, this is indicated by the fact that if OAC is the single cycle load-deflection curve, and if cycling is done at a load corresponding to OB', the reloading curve (FB) will reach the point B and will follow BC as if nothing else had happened.

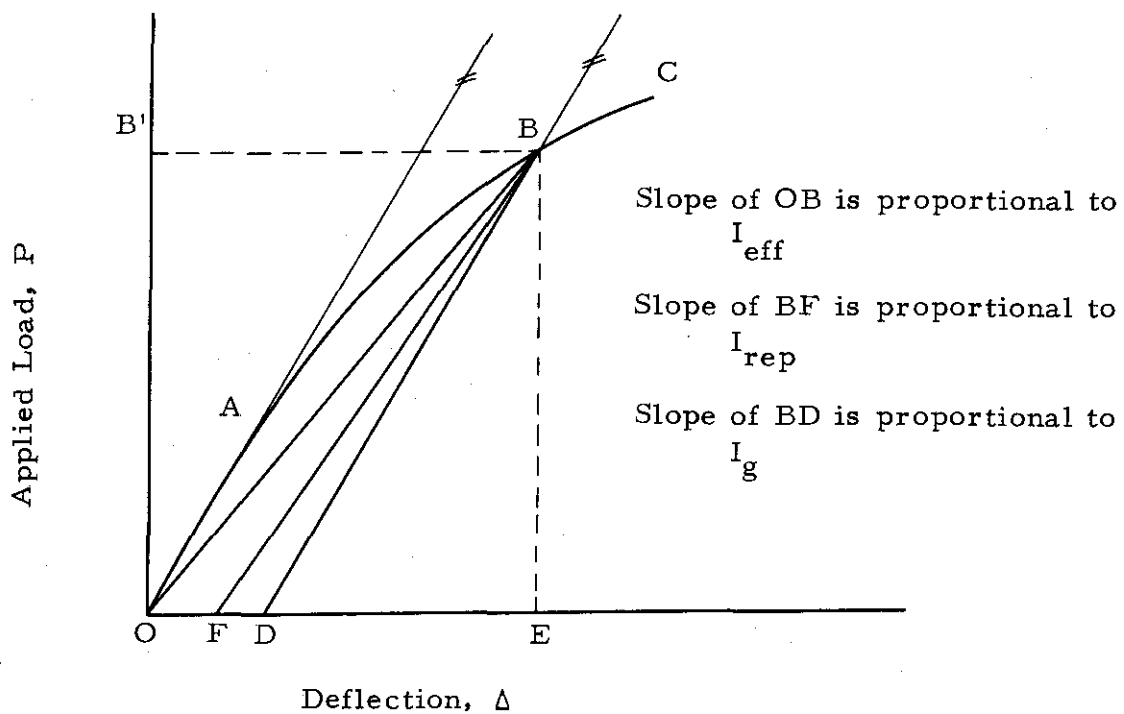


Figure 35 Details of deflections under repeated loadings

$I_{rep}$  is used to compute the recovery during the unloading part of the cycle. (Note that the slope of FB is proportional to  $I_{rep}$  in Figure 35.)

$$\psi_1 = (P_{ult} - P_{rep}) / (P_{ult} - P_{cr}) \quad (40-a)$$

$I_{eff}$  = effective moment of inertia as defined by Eq. (38)

$I_g$  = gross moment of inertia

$P_{ult}$  = estimated ultimate load based on current ACI procedures in the code

$P_{cr}$  = load at initial cracking corresponding to  $M_{cr}$  (using Eq. (35)).

$P_{rep}$  = cycling load or maximum load in a given cycle.

Eq. (40) is valid only if the loading cycle produces cracking, i.e.,  $P_{rep} > P_{cr}$ . The value of  $\psi_1$  requires some explanation. From Figure 35, it is clear that the slope of the line BF is greater than the slope of the line OB, but smaller than the slope of the line BD. Also, the slopes of lines OB and BD are proportional to  $I_{eff}$  and  $I_g$  respectively. For a severely cracked beam ( $P_{rep} \doteq P_{ult}$ ), the total recovery consists of only the elastic part of the deflection corresponding to the magnitude of the repeated load,  $P_{rep}$ . For an uncracked beam ( $P_{rep} \doteq P_{cr}$ ), the total recovery is equal to the deflection corresponding to the magnitude of the repeated load,  $P_{rep}$ . The value of  $\psi_1$  interpolates linearly between the two limits described above. For example:

- (a) when  $P_{rep} = P_{cr}$ ,  $\psi_1 = 1$ , and  $I_{rep} = I_{eff} = I_g$ . This is a condition of total recovery.
- (b) when  $P_{rep} > P_{cr}$ ,  $\psi_1$  varies between 1 and zero, and  $I_{rep}$  is between  $I_{eff}$  and  $I_g$ . This a condition of some inelastic recovery due to the cracks being closed.
- (c) when  $P_{rep} = P_{ult}$ ,  $\psi_1 = 0$ , and  $I_{rep} = I_g$ . This is a condition of no inelastic recovery due to the cracks being closed. This may also be considered as a condition of maximum residual deflection.

Thus, the use of Eq. (40) enables one to predict the effective moment of inertia under repeated cycles for any given range of loading.

Also, the use of Eq. (40) in determining the effective moment of inertia under repeated loading allows the slope of BF (see Figure 35) to become proportional to  $I_{rep}$ .

In the development of the relationship in Eq. (40), the following are implicitly assumed:

1. Absence of hysteresis loop in the unloading-reloading sequence.
2. Absence of time-dependent effects due to creep during the test.

The first assumption is justified on the basis that the stresses

due to repeated loading in concrete and steel are well below the shake-down limit and the yield strength of the concrete and steel respectively. This has also been observed in the study of reinforced concrete beams under repeated loading in similar loading regimes (54). The second assumption is probably justified on the basis of the small time involved in the tests (see Table 6).

In this work, repeated loads mean a small number of cycles at loads ranging from 1.05 to 1.43 times the working load (this corresponds to 55 to 72% of the ultimate load). The working load is defined herein as the load at which flexural cracking is initiated. The following sample calculations indicate the use of Eq. (40) in the determination of deflections of prestressed concrete members under repeated loading.

Sample calculations for the deflection of a prestressed concrete beam under three cycles of loading

To illustrate the procedure outlines above, the midspan deflection of beam E1 is computed under three cycles of repeated transverse loads of the following magnitude:

- (1)  $P_{rep} = 5.0$  kips in the first cycle
- (2)  $P_{rep} = 5.5$  kips in the second cycle
- (3)  $P_{rep} = 6.0$  kips in the third cycle. Note that  $P_{rep}$

corresponds to the maximum load in a specific load cycle.

The equations needed for the computations are Eqs. (35), (38), (40), and (41). The pertinent geometrical and material properties for the example beam are shown in Tables A1-A2 and A6.

For a simply supported beam under a two-point symmetrical loading system (see Figure 30), the midspan deflection,  $\Delta$ , is given as:

$$\Delta = \frac{P a}{48 E I} (8a^2 + 12ab + 3b^2) \quad (41)$$

where:  $b$  = distance between the loads

$a$  = distance of each load from the near support

$P$  = total load on the beam

$E$  = elasticity modulus of concrete

$I$  = moment of inertia.

Referring to Figure 30,  $a = 5.5$  ft; and  $b = 4.0$  ft. For purposes of illustration, the computed deflections will be referred to Figure 36.

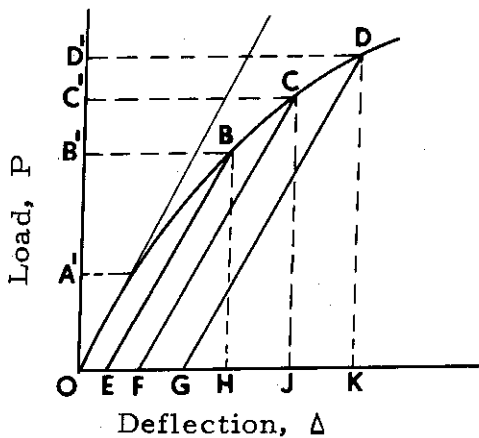


Figure 36 Sample Calculations

OABE, EBCF, and FCDG represent the first, second, and third cycle respectively. The values of  $P_{rep}$  correspond to  $OB'$ ,  $OC'$ , and  $OD'$  during the first, second, and third cycle respectively.  $OA'$  represents the 'cracking load' (also referred to as the working

load) and is defined as the load at which flexural cracking is initiated.

Parameters and terms for beam E1

Span = 15'; e (midspan) = e (end) = 1.75"; F = 38.7 kips (determined as  $F_i - \Delta F_t$ , where  $F_t$  is obtained using Eq. (17) in Chapter 4);  
 $A_s = 0.3196 \text{ in}^2$ ;  $A_g = 48.0 \text{ in}^2$ ;  $I_g = 256 \text{ in}^4$ ;  $I_{cr}$  (using Eq. (39))  
 $= 51.96 \text{ in}^4$ ;  $E_c$  (using Eq. (6)) =  $3.34 \times 10^6 \text{ psi}$ ;  $M_{cr}$  (Using Eq. (35))  
 $= 150.7 \text{ inkips}$ ;  $M_{DL} = 13.7 \text{ inkips}$ ;  $f'_{cb} = 490 \text{ psi}$  (see Table A6);  
 $f'_c = 5680 \text{ psi}$  (see Table A6).

Deflections during the first cycle corresponding to  $P_{rep} = 5.0 \text{ kips}$   
(OH in Figure 36)

$$M_{max} = M_{\text{transverse load}} + M_{\text{dead load}} = 5 \times 5.5 \times 12/2 + 13.7$$

$$= 178.7 \text{ inkips.}$$

$$I_{eff} \text{ (using Eq. (38))} = 174.29 \text{ in}^4$$

$$\Delta \text{ (using Eq. (41))} = 0.9422 \text{ in}$$

as compared to the observed value of 0.938 in (see Figure 40).

For the unloading stage of the first cycle:

$$P_{cr} \text{ (corresponding to } M_{cr} = 150.7 \text{ inkips)} = 4.15 \text{ kips}$$

$$P_{ult} \text{ (based on ultimate equations given in ACI 318-63 code)} = 8.54 \text{ kips}$$

$$\psi_1 \text{ (using Eq. (40a))} = 0.805$$

$$I_{rep} \text{ (using Eq. (40))} = 190.0 \text{ in}^4$$

Recovered deflection (using Eq. (41)) = 0.865 in  
(indicated by HE in Figure 36) with

$$I = I_{rep}$$

$$\begin{aligned} \text{Computed residual deflection} &= \text{Total deflection} - \text{Recovered deflection} \\ &= 0.0772 \text{ in} \end{aligned}$$

as compared to the observed value of 0.0710 in (see Table 6).

For loads less than  $P_{rep}$  during the unloading stage, the computed deflections are in a linear relationship with the applied transverse load (indicated by BE in Figure 36).

$$\begin{aligned} \text{Recovery ratio} &= \text{Recovered deflection} / \text{Total deflection} \\ &= 0.8650 / 0.9422 = 91.6\% \end{aligned}$$

The reloading curve for the second cycle is the same as the unloading curve for the first cycle (indicated by EB in Figure 36).

#### Deflections during the second and third cycles

The computation of recovered deflection in the second and third cycles is similar to that indicated for the first cycle. Only the computed results are indicated below:

<u>Cycle No</u>	<u><math>P_{rep}</math> (kips)</u>	<u>Deflection in inches</u>			
		<u>Total</u>	<u>Recovered</u>	<u>Residual</u>	<u>Recovery Ratio</u>
2	5.5	1.2388	1.005	0.2338	81%
3	6.0	1.5697	1.089	0.4807	70%

#### Comments:

1. The recovery ratio reduces with increasing load. This was the basic premise on which Eq. (40) was developed.
2. The residual deflection increases with increasing load.

This is a direct consequence of increased flexural cracks that remain open even after unloading is completed.

3. The loading and unloading curves for a given load level are linear, provided the stress in steel is below the yield strength of the steel and the stress in concrete is below the shakedown limit of the concrete. The linearity of the loading and unloading curves for a given load level has been observed for reinforced concrete beams also (54).

Repeated load tests (three cycles of loading) were conducted with a constant load cycle on beams of Group C and with an increasing load cycle on beams of Group E. Midspan deflections on all the test beams of these groups were obtained up to loads ranging from 76 to 87 percent of the ultimate loads. The range of the cycling loads varied from 55 to 72 percent of the ultimate load. Eq. (40) was used to determine the effective moment of inertia in the computation of deflections. Eq. (35) was used to determine  $M_{cr}$ , and Eq. (39) was used for the determination of  $I_{cr}$ . The modulus of rupture,  $f'_{cb}$ , was obtained by bending tests on plain concrete specimens for the test beams.

The comparison of observed and computed midspan deflection curves are shown in Figures 37 to 41. Figure 42 shows the variation between the total deflection (corresponding to the maximum value of

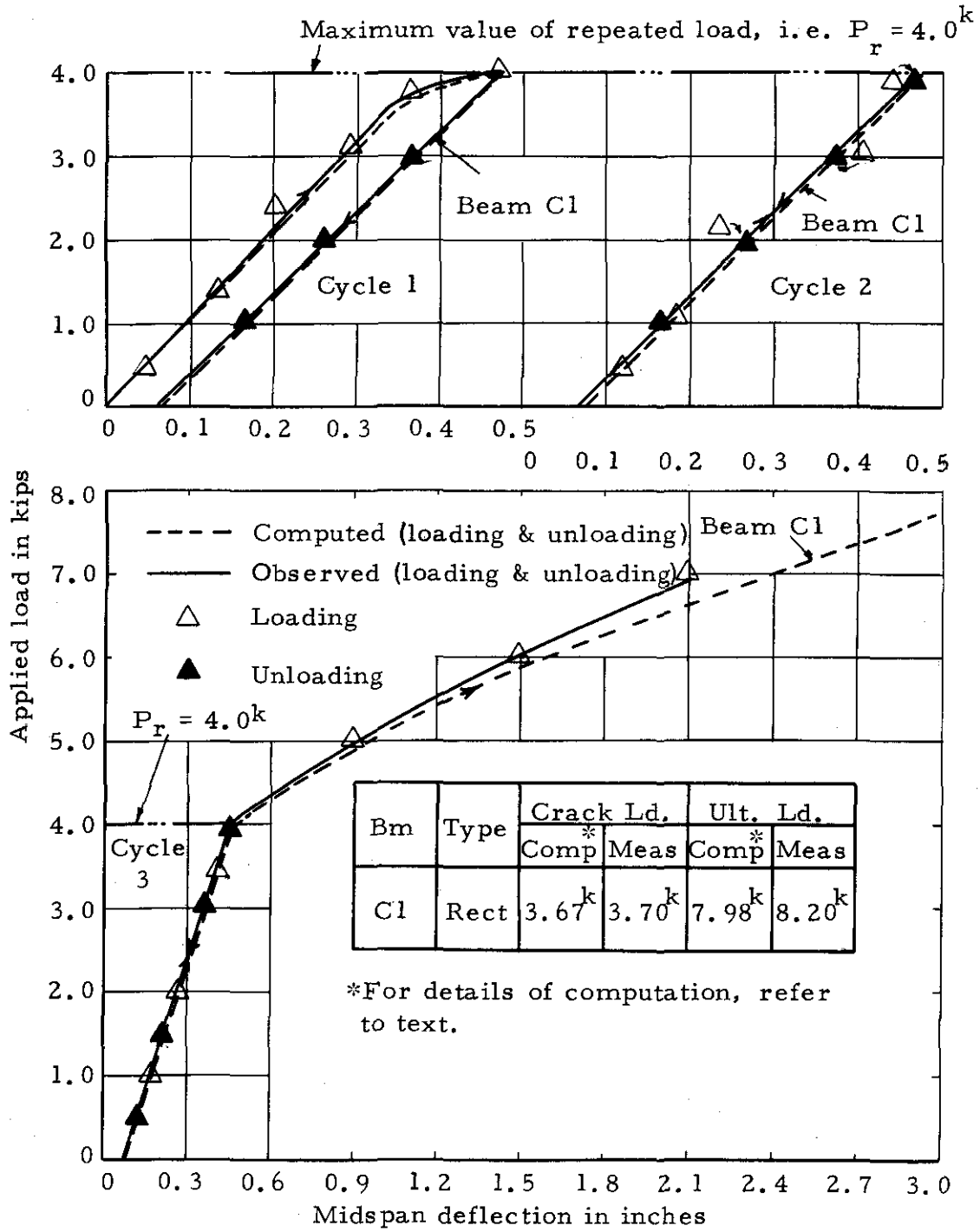


Figure 37 Observed and computed midspan deflection vs load curve of beam C1 under 3 cycles of repeated loading (one non-composite prestressed beam)

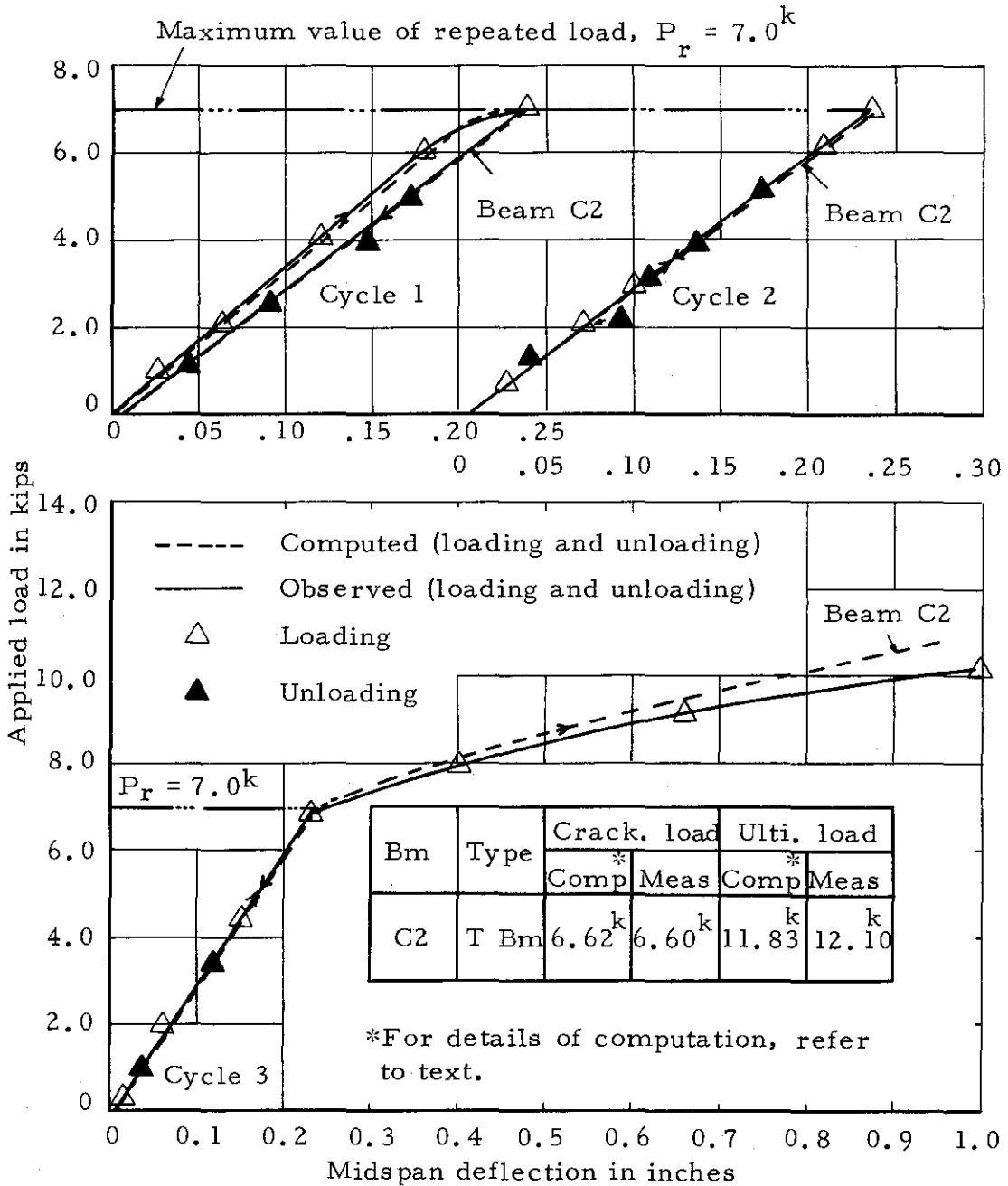


Figure 38 Observed and computed midspan deflection versus load curve of beam C2 under 3 cycles of repeated loading (one non-composite prestressed beam)

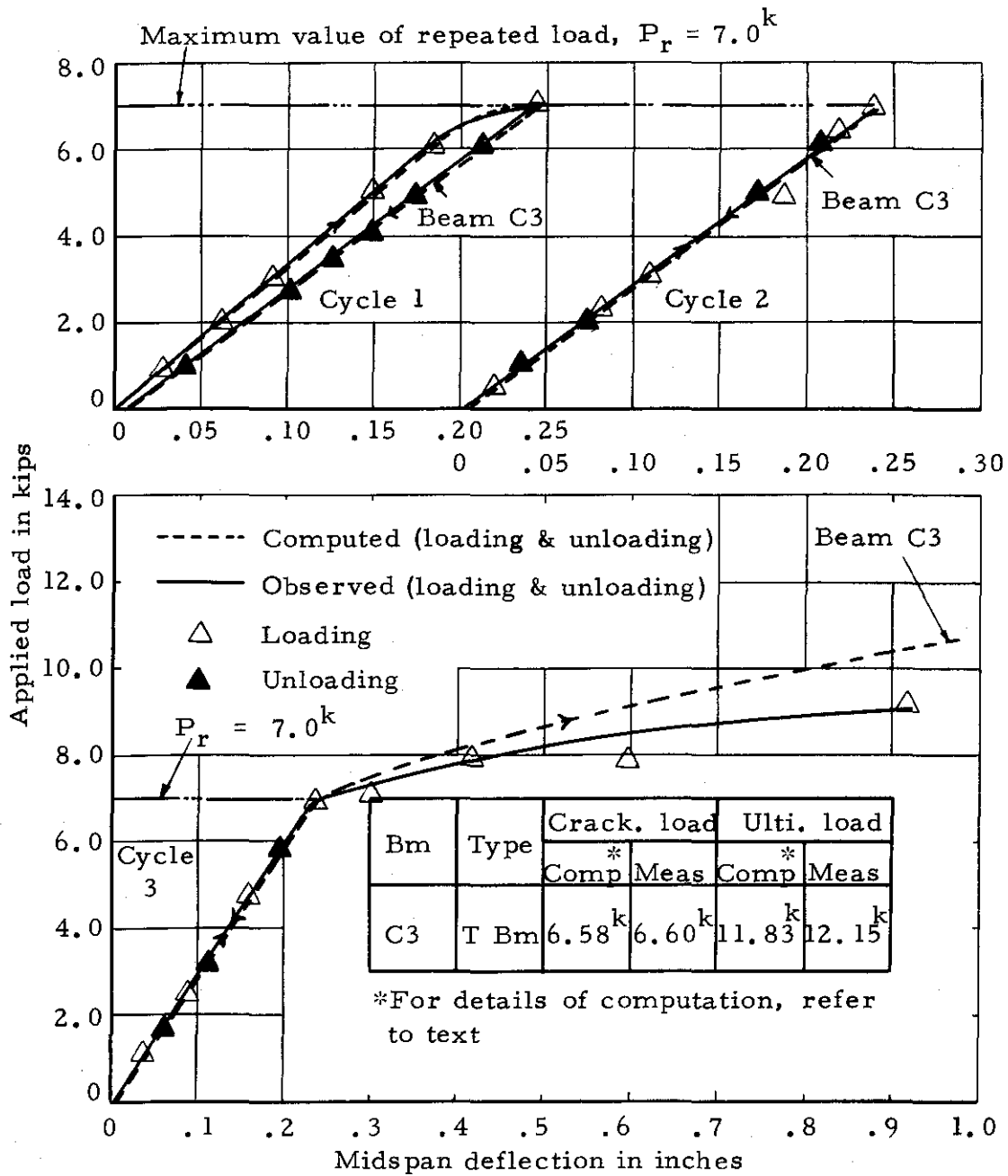


Figure 39 Observed and computed midspan deflection versus load curve of beam C3 under 3 cycles of repeated loading (one composite prestressed beam)

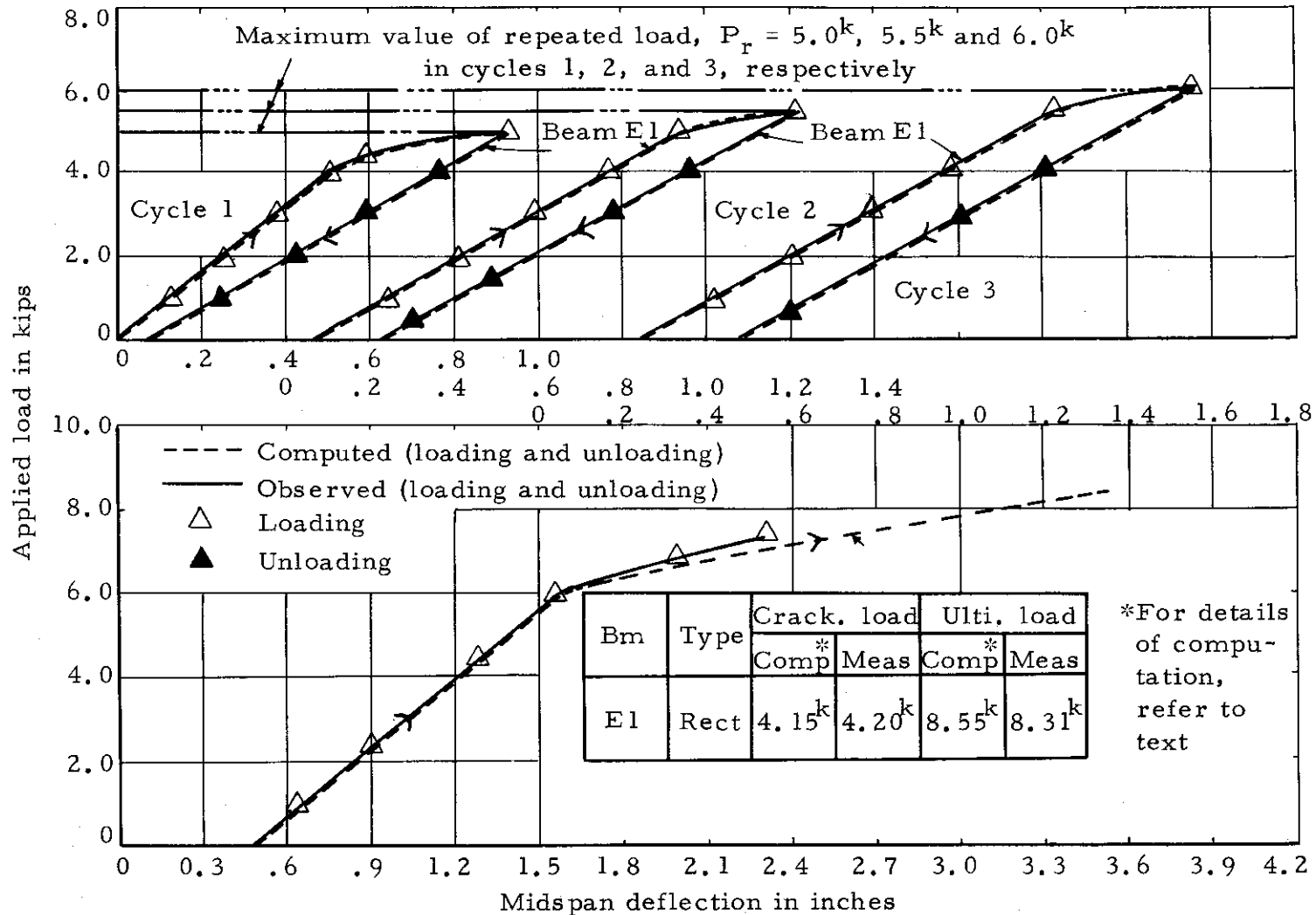


Figure 40 Observed and computed midspan deflection versus load curve of beam E1 under 3 cycles of repeated loading (one non-composite prestressed beam)

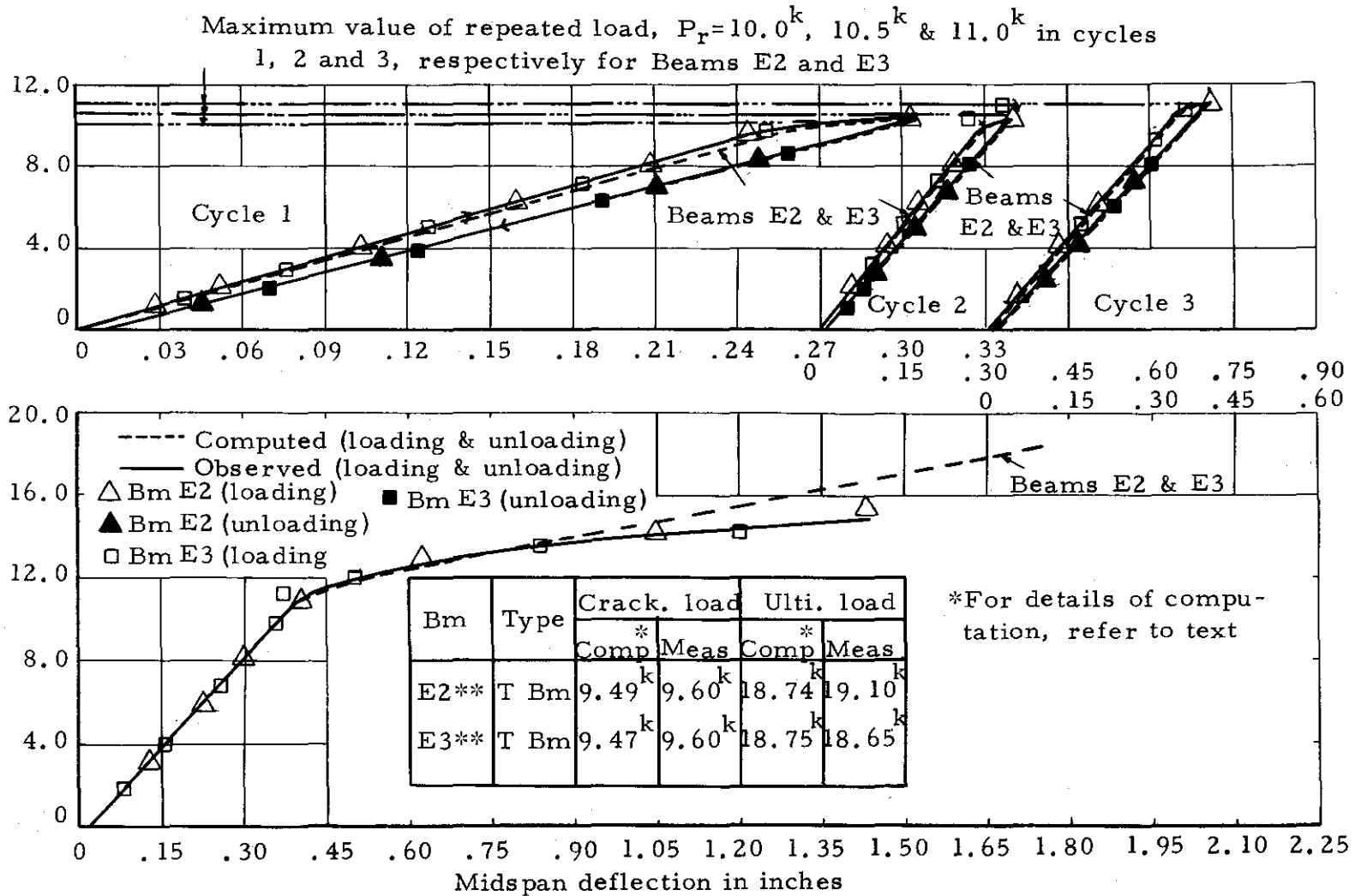


Figure 41 Observed and computed midspan deflection versus load curves for beams E2 and E3 under 3 cycles of repeated loading (two composite prestressed beams)

\*\*Only one curve is shown for the computed and measured values (for both beams E2 and E3) because only very small differences in deflection existed between the two beams.

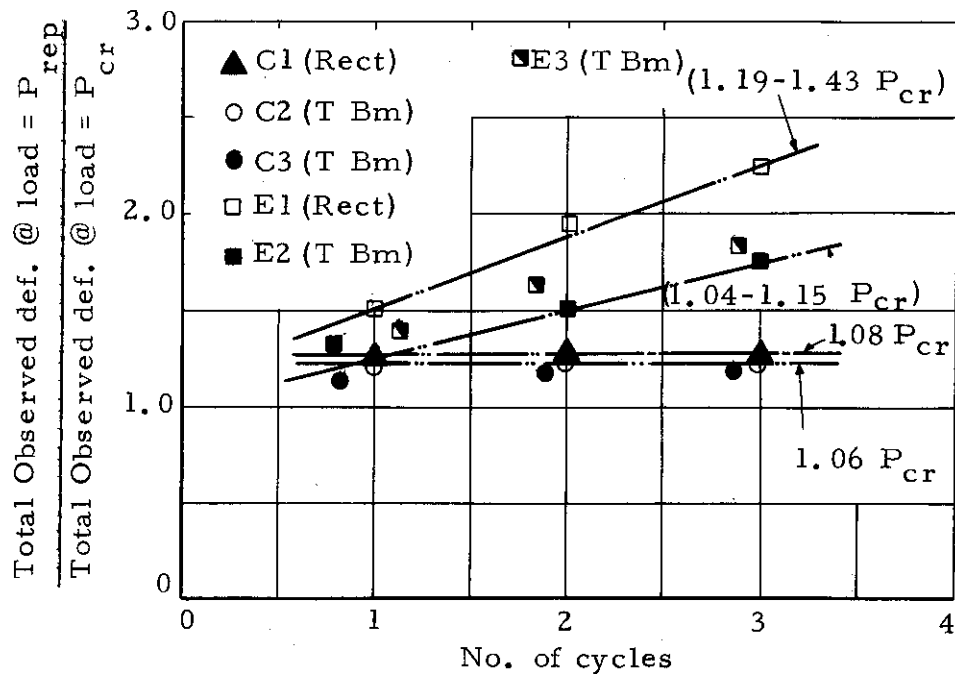


Figure 42 Effect of repeated loading (in the cracked range) on total deflections of laboratory beams of Groups C and E

TABLE 6

<sup>a</sup>DETAILS OF REPEATED LOAD CYCLES AND DISCREPANCY IN THE OBSERVED AND COMPUTED VALUES OF MIDSPAN DEFLECTION FOR BEAMS OF GRPS C & E

Detail	b Comp ult. ld, $P_u$	Meas ult. ld, $P_{um}$	c Work load, $P_w$	Load factor $P_u/P_w$	d $P_{max}$	Cycling Ld, $P_r$ for cycles			e Comp. res. def. (total)@ end of cycles			f Meas. res. def. (total)@ end of cycles			Worst discrep. in defl. curves	
						1	2	3	1	2	3	1	2	3		
Grp C	C1	7.98	8.20	3.67	2.18	7.00	4.5	4.5	4.5	.0683	.0683	.0683	.0600	.0610	.0610	+14%
	C2	11.83	12.10	6.62	1.79	10.25	7.0	7.0	7.0	.0046	.0046	.0046	.0040	.0040	.0040	-18%
	C3	11.83	12.15	6.58	1.81	9.20	7.0	7.0	7.0	.0043	.0043	.0043	.0040	.0040	.0040	-34%
Grp E	E1	8.55	8.31	4.15	2.06	7.20	5.0	5.5	6.0	.0772	.2338	.4807	.0710	.2310	.480	+10%
	E2	18.74	19.10	9.49	1.98	15.60	10.0	10.5	11.0	.0040	.0101	.0267	.0030	.0090	.025	-33%
	E3	18.76	18.65	9.47	1.98	14.80	10.0	10.5	11.0	.0040	.0101	.0267	.0030	.0080	.026	-33%

<sup>a</sup>All loads are expressed in kips and all deflections are expressed in inches.

<sup>b</sup>See Footnote 1, Table 5.

<sup>c</sup>See Footnote 2, Table 5.

<sup>d</sup>See Footnote 3, Table 5.

<sup>e</sup>The magnitudes of residual deflections being very small, any meaningful interpretation on the basis of a percentage of deflection at working load, (say  $P_w$ ) is difficult. See Sample Calculations also.

<sup>f</sup>The discrepancy in the deflection curves refers to the load-deflection curves after the cycling loads have been completed. The high values of discrepancy in this column corresponds to about 80-82% of the ultimate load. Also, see Footnote 5, Table 5.

the repeated load in a specific cycle,  $P_{rep}$ ) and the number of cycles at various load levels. Table 6 shows the computed and measured values of ultimate load as well as the computed and measured magnitudes of residual deflection.

Based on Figures 37 to 42, Table 6, and the sample calculation, the following observations are made:

1. The residual deflection at the completion of a cycle is a function of the load at which the cycling is done. At cycling loads close to the ultimate load, the residual deflection is larger than at cycling loads close to the cracking load (see Table 6 and Figures 37 to 41).

2. Repeated cycles (up to three cycles) of loading at a given load level does not increase the magnitude of the residual deflection.

Similar observations have been made on reinforced concrete beams (54) under load levels below the yield strength of the reinforcement.

3. The magnitude of the total recovery decreases with increasing load (see sample calculations). This was the basic premise on which Eq. (40) was developed, and is confirmed by observations (see Table 6).

4. The residual deflection at the end of a cycle is also a function of the geometric properties of the section. This, though obvious, is clearly seen in Figures 37 and 38, where the composite beams have less residual deflection than non-composite beams even at the same level of loading.

5. There does not seem to be any significant difference in the load-deflection response of composite beams under repeated loading for which slabs have been cast at different times. Both beams E2 and E3 have similar magnitudes of residual deflections and ultimate loads (see Figure 41 and Table 6).

6. It may safely be concluded, that the relationship suggested by Eq. (40) gives reasonable agreement between observed and computed values of deflections provided the stress under repeated loading in concrete and steel are below the shakedown limit of the concrete and the yield strength of the steel respectively. In the case of the laboratory beams, the range of the repeated load varied between 55 to 72% of the ultimate load. This corresponds to 1.05 to 1.43 times the working load. It is reasonable to expect that as the repeated load approaches the working load, the total recovery approaches the total deflection. This has been discussed in detail elsewhere. Also, comparison with data in the literature confirms the use of Eq. (40) as a reasonable means of estimating the effective moment of inertia under repeated loads for reinforced concrete beams under similar loading regimes (see Section 5.5).

7. It is reasonable to expect that at repeated loads close to the ultimate load (yield of steel reinforcement in the case of under-reinforced beams), there will be greater residual deflection (than when

steel has not yielded) as well as a hysteresis loop during the loading-unloading sequence. A detailed study of reinforced concrete beams in this loading regime has been reported by Ruiz (55).

#### 5.4 Increasing Load Plus 24-Hour Sustained Load Tests

Although much work has been reported on the effect of sustained load on reinforced concrete beams (4), (50) most of these works referred to beams at early loading ages. In this study, the beams were loaded (at beam age 6 months) into the 'cracked' or 'inelastic' range and left in that position for 24 hours.

Increasing load plus 24-hour sustained load tests in the cracked range were conducted on beams of Group F (one non-composite and two composite members). Midspan deflections on all the test beams were obtained up to loads ranging from 79 to 92 percent of the ultimate loads. The sustained loads ranged from 33 to 92 percent of the ultimate loads. Eq. (38) was used to determine the effective moment of inertia, Eq. (35) was used to determine the value of  $M_{cr}$  (with  $F_t = 0$ ). The modulus of rupture,  $f'_{cb}$ , was obtained by bending tests on plain concrete specimens of the test beams.

The creep coefficients for computational purposes were based on information and test results presented in Chapter 3. The following sample calculations indicate the use of Eqs. (7), (38) and the appropriate creep coefficients in the computation of deflections of reinforced

concrete members under increasing load plus 24-hour sustained loading.

Sample calculations for the deflection of a reinforced concrete beam under 24-hour sustained loads

Beam F1 is selected for illustrating the calculation of deflection under 24-hour sustained load in the 'inelastic' range of the load-deflection curve.

Parameters and terms for Beam F1:

Span = 15 ft;  $e$  (midspan) =  $e$  (end) = 2 in;  $A = 0.6 \text{ in}^2$ ;  $A_g = 48.0 \text{ in}^2$ ;  $I_g = 256 \text{ in}^4$ ;  $I_{cr}$  (using Eq. (39)) =  $102.6 \text{ in}^4$ ;  $E_c$  (using Eq. (6)) =  $2.98 \times 10^6 \text{ psi}$ ;  $M_{DL} = 13.7 \text{ inkips}$ ;  $M_{cr}$  (using Eq. (35)) =  $27.5 \text{ inkips}$ ;  $f'_{cb} = 430 \text{ psi}$  (see Table A6);  $f'_c = 4540 \text{ psi}$  (see Table A6);  $P_{ult}$  (based on ultimate equations given in ACI 318-63 Code) =  $3.56 \text{ k}$ ; age of beam at load deflection test = 201 days

Deflection under sustained load,  $P_{sust} = 1.2 \text{ kips}$

$$\begin{aligned} M_{max} = M_{DL} + M_{\text{transverse load}} &= 13.7 + 1.2 \times 5.5 \times 12 / 2 \\ &= 53.3 \text{ inkips} \end{aligned}$$

$$I_{eff} \text{ (using Eq. (38))} = 124.1 \text{ in}^4$$

$$\Delta_i \text{ (using Eq. (41))} = 0.356 \text{ in}$$

as compared to the observed value of 0.350 in (see Figure 43).

$$\text{Experimental } C_u \text{ (from 7 days at 40\% RH)} = 1.95$$

$$\text{Correction factor for 50\% RH (using Eq. (12))} = 0.94$$

Correction factor for age of loading (using Eq. (10))	=	0.684
Actual $C_u$	=	$1.95 \times 0.95 \times 0.684 = 1.26$
*Experimental value of $C_t/C_u$ at 1 day (based on loading at 9 days)	=	1/8
Actual $C_t$ for 24-hour loading	=	$1.26 \times 1/8 = 0.158$
**Deflection due to sustained loading (using Term (2) of Eq. (16))	=	$.158 \times .356 \times .85 = .048$ in

as compared to the observed value of 0.053 in (see Table 7)

\*The experimental value of  $C_t/C_u$  and not the computed value (based on Eq. (7)) is used in the calculations, because the validity of the latter for extremely short periods is questionable, although the equality of this ratio ( $C_t/C_u$ ) for various loading ages is implicitly assumed in the equations for creep (see Chapter 3).

\*\*The effect of shrinkage is very small (due to the very late age of loading as well as the short time period of the test) and is considered negligible.

The comparison of observed and computed midspan deflection curves are shown in Figure 43. Table 7 shows the computed and measured values of the ultimate load, as well as the computed and measured values of the deflections due to the 24-hour sustained load.

Based on Figure 43 and Table 7, the following observations are made:

1. The magnitude of the deflection due to sustained loading (24 hours) is a function of the level of the sustained load. Beam F2 has

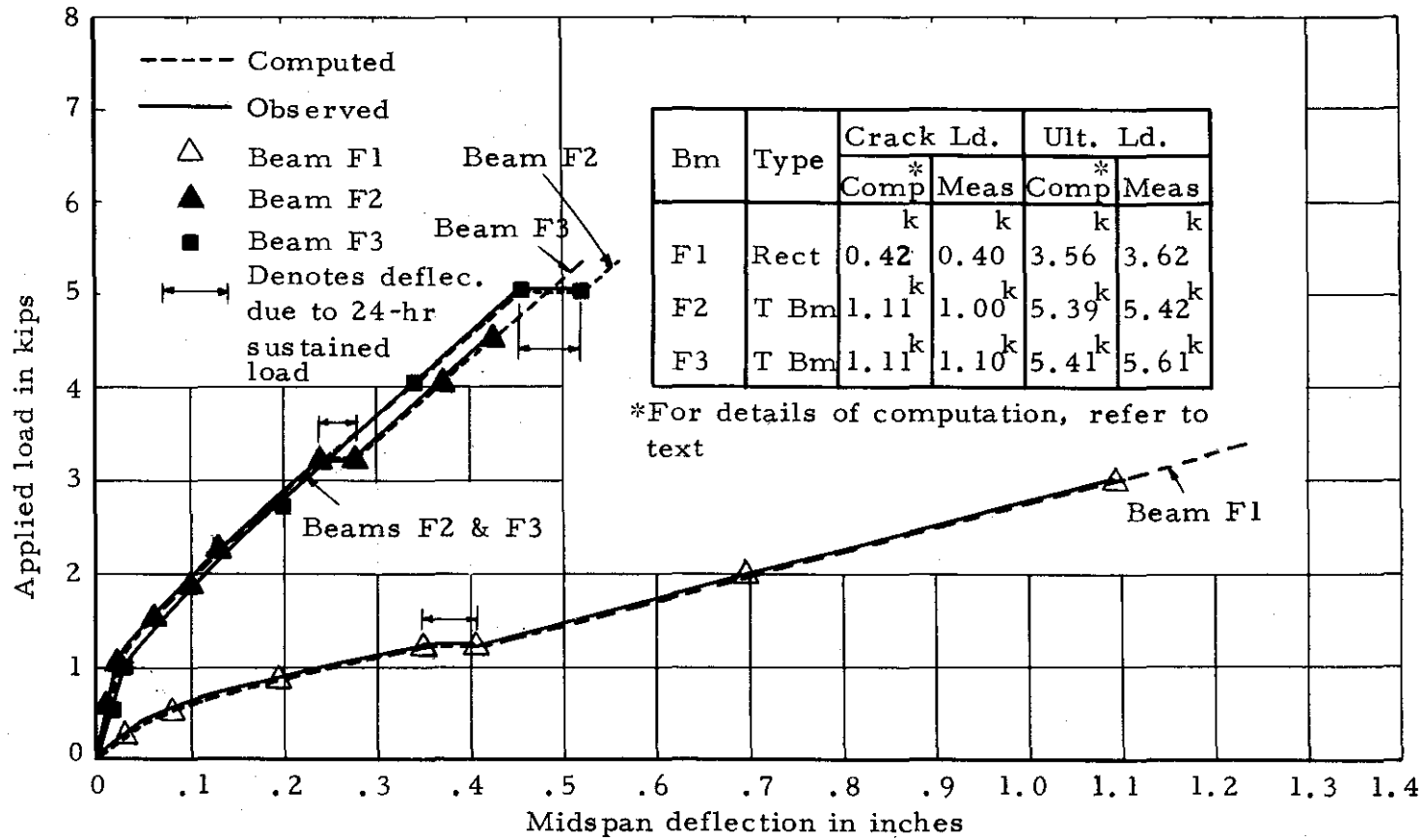


Figure 43 Observed and computed values of midspan deflection for beams of Group F under 24-hr sustained loading (one non-composite and two composite reinforced beams)

TABLE 7

<sup>a</sup>DETAILS OF INCREASING LOAD PLUS 24-HR SUSTAINED LOAD TESTS  
WITH REGARD TO WORKING LOADS, ULTIMATE LOADS AND  
DEFLECTIONS UNDER THESE LOADS

Detail		<sup>b</sup> Working load, $P_w$	Ult. Load		Load Factor $P_u/P_w$	Sustained Ld. factor $P_s/P_w$	Def. due to Sustained load		Worst <sup>e</sup> Discrepancy in def. curves
			<sup>c</sup> Comp	Meas			<sup>d</sup> Comp	Meas	
Grp F	F1	0.42	3.56	3.62	8.5	2.86	.048	.053	+10%
	F2	1.11	5.39	5.42	4.9	4.50	.062	.065	+5%
	F3	1.11	5.41	5.61	4.9	2.88	.032	.032	+5%

<sup>a</sup>All loads are expressed in kips and all deflections are expressed in inches. The period of the test varied between 15-25 min for each beam prior to the application of the sustained load and between 10-20 min after the end of the sustained load.

<sup>b</sup>See Footnote 2, Table 5.

<sup>c</sup>See Footnote 1, Table 5.

<sup>d</sup>The creep coefficient was the experimental value of  $C_t$  for the 24-hour sustained loading. See Sample Calculations.

<sup>e</sup>See Footnote 5, Table 5.

a higher deflection under sustained load than Beam F3 due to the higher level of loading due to the higher level of loading in the former (see Table 7 and Figure 43). The deflections due to creep is approximately proportional to the applied load.

2. For extremely short periods of sustained loading (24 hours), the use of Eq. (7) for the determination of creep coefficients in the computation of deflections due to sustained loads is, perhaps questionable. The experimental values of  $C_t/C_u$  is used in the computations. However, the experimental value of  $C_t/C_u$  ( $= 1/8$ ) does not differ very much from the computed value of  $C_t/C_u$  (using Eq. (7)  $= 1/11$ ).

3. The use of Eq. (38) for the determination of the effective moment of inertia of reinforced beams has been suggested for the 1971 ACI Code (4)(50)(51). It gives reasonable agreement at loads very close to the ultimate load also (see Figure 43).

### 5.5 Results Reported by Others

The observed load-deflection curves reported by Abeles (56), Warawaruk, Sozen, and Siess (41), Shaikh and Branson (49), and Burns and Siess (54) are compared with the computed values obtained by using the methods presented in Sections 5.1 to 5.4.

### Results Reported by Abeles (56)

In his investigation, Abeles reported the load-deflection response of three groups of rectangular prestressed beams (with different levels of prestress and steel percentage) under various conditions of single, repeated, and fatigue load cycles. His primary interest was in the fatigue loading of prestressed beams. Single and repeated load cycle tests were conducted on companion specimens to obtain a basis of reference. Beams of ordinary and lightweight concrete were included in the study. Of the 16 beams tested, only A01\* and AL1\* are used for purposes of this study. Table C5 shows the details of the beams used in this study. Beams A01\* and AL1\* were studied under three cycles of repeated loading. However, no measurements of residual deflections were reported. Hence no continuous load-deflection curves under repeated load cycles could be plotted and compared with the computed results.

Figure 44 shows the comparison between the computed and observed values of midspan deflection. On the basis of Figure 44, the following observations are made:

1. Within the working load (the working load being defined as the load at which flexural cracking is initiated), the use of the gross section properties along with the computed modulus of elasticity of concrete (using Eq. (6)) gives excellent agreement between the computed

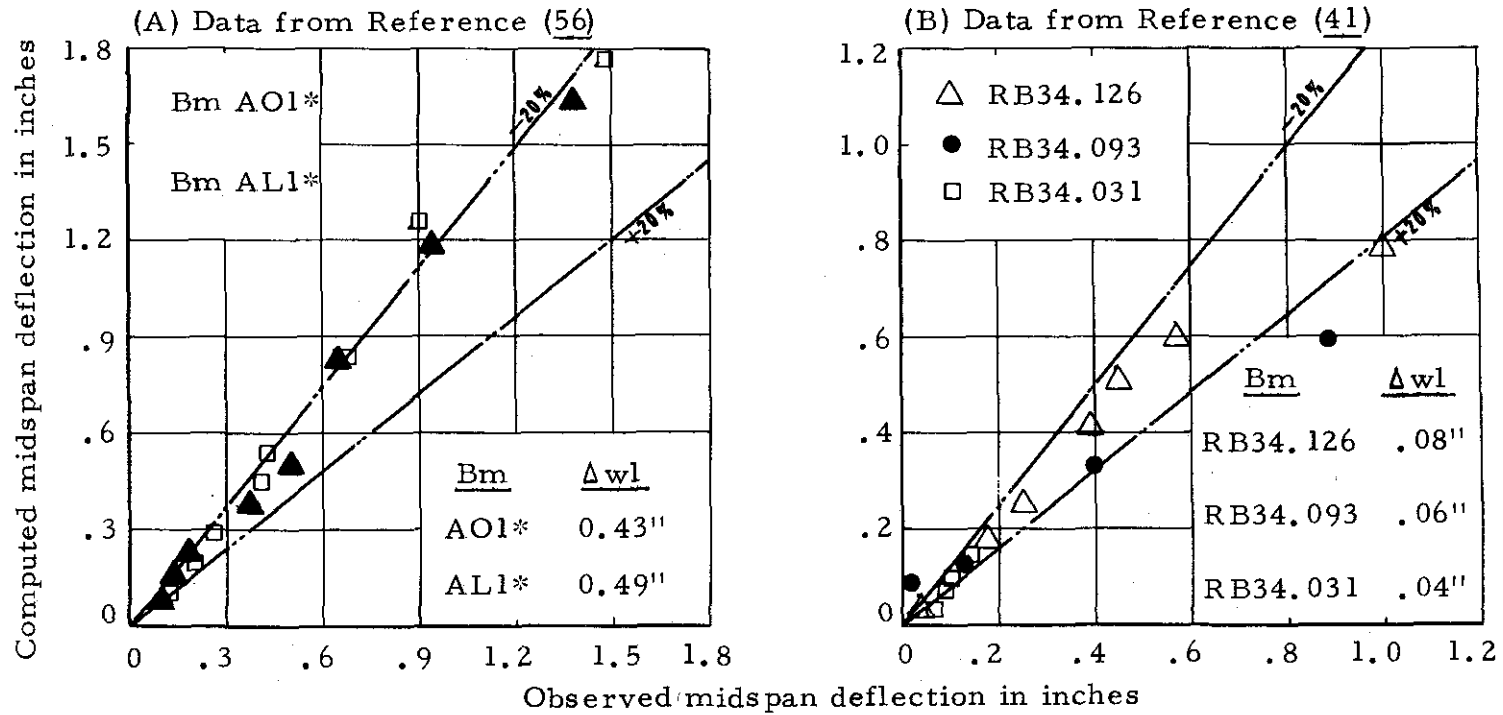


Figure 44 Observed and computed midspan deflection (using Eqs. (38) and (41) for beams under static loading as in (A) (Data from Reference 56) and as in (B) (Data from Reference 41)

and observed values of midspan deflection.

2. In the cracked stage, the scatter between the computed and measured deflections is noticeable. The magnitude of this scatter increases with an increase in the applied load. This is probably due to the omission of creep effects in the determination of the effective moment of inertia using Eq. (38) (see Section 5.2 for discussion). However, the magnitude of the scatter is within  $\pm 20\%$  for loads which are about 1.75 times the working load.

3. In the cracked stage, the computed values (using Eq. (38) for the determination of effective moment of inertia) of midspan deflection are greater than the observed values of midspan deflection. Similar results have been observed by the ACI Committee 435 (4) in the study of reinforced concrete beams containing 'compression' steel. This is probably due to the fact that the presence of compressive steel tends to lower the neutral axis and thereby retard the formation of cracks. (For a discussion of this phenomenon as related to other types of prestressed concrete beams, see Section 5.6).

Results Reported by Warawaruk, Sozen, and Siess (41)

In a comprehensive study of the strength and behavior in flexure of prestressed concrete beams, Warawaruk, et al. reported the load-deflection response of both post-tensioned and pretensioned beams. A large number of variables were studied, the most important

of which were the steel percentage, type of concrete, loading conditions, and type of bonding of reinforcement with the concrete. Of the 82 beams tested, only beams RB34.126, RB34.093, and RB34.031 (pretensioned) are used in this study. The details of these beams are shown in Table C6. The loading was done statically by a symmetrical two-point loading system.

Figure 44 shows the comparison between the computed and observed values of midspan deflection. On the basis of Figure 44, the following observations are made:

1. Within the working load, the use of the gross section properties along with the computed modulus of elasticity of concrete gives excellent agreement between the computed and observed values of midspan deflection.

2. In the cracked stage, the scatter between the computed and observed values of midspan deflection is noticeable and the magnitude of this scatter increases with an increase in the applied load. This is probably due to the omission of creep effects in the determination of the effective moment of inertia using Eq. (38) (see Section 5.2 for discussion). However, the magnitude of the scatter is within  $\pm 20\%$  for loads which are about 2.0 times the working load.

3. The beams studied in this report did not have 'compression' steel. Also, in the cracked stage, the computed values (using Eq.

(38) for the determination of effective moment of inertia) of midspan deflection were smaller than the observed values of midspan deflection. This is consistent with the results described in Section 5.1 for the laboratory beams and is probably due to creep effects that have been neglected in the development of Eq. (38). (For a discussion of this phenomenon as related to other types of prestressed concrete beams, see Section 5.6.)

#### Results Reported by Shaikh and Branson (49)

In a comprehensive study of the effects of non-tensioned steel on the behavior of prestressed concrete beams, Shaikh and Branson reported the load-deflection response of 12 pretensioned concrete beams containing various types and quantity of non-tensioned steel. The details of these beams are shown in Table C7. The loading was done statically by a symmetrical two-point loading system.

Figure 45 shows the comparison between the computed and observed values of midspan deflection. On the basis of Figure 45, the following observations are made:

1. Within the working load, the use of the gross section properties along with the reported modulus of elasticity results in excellent agreement between the computed and observed values of midspan deflection.

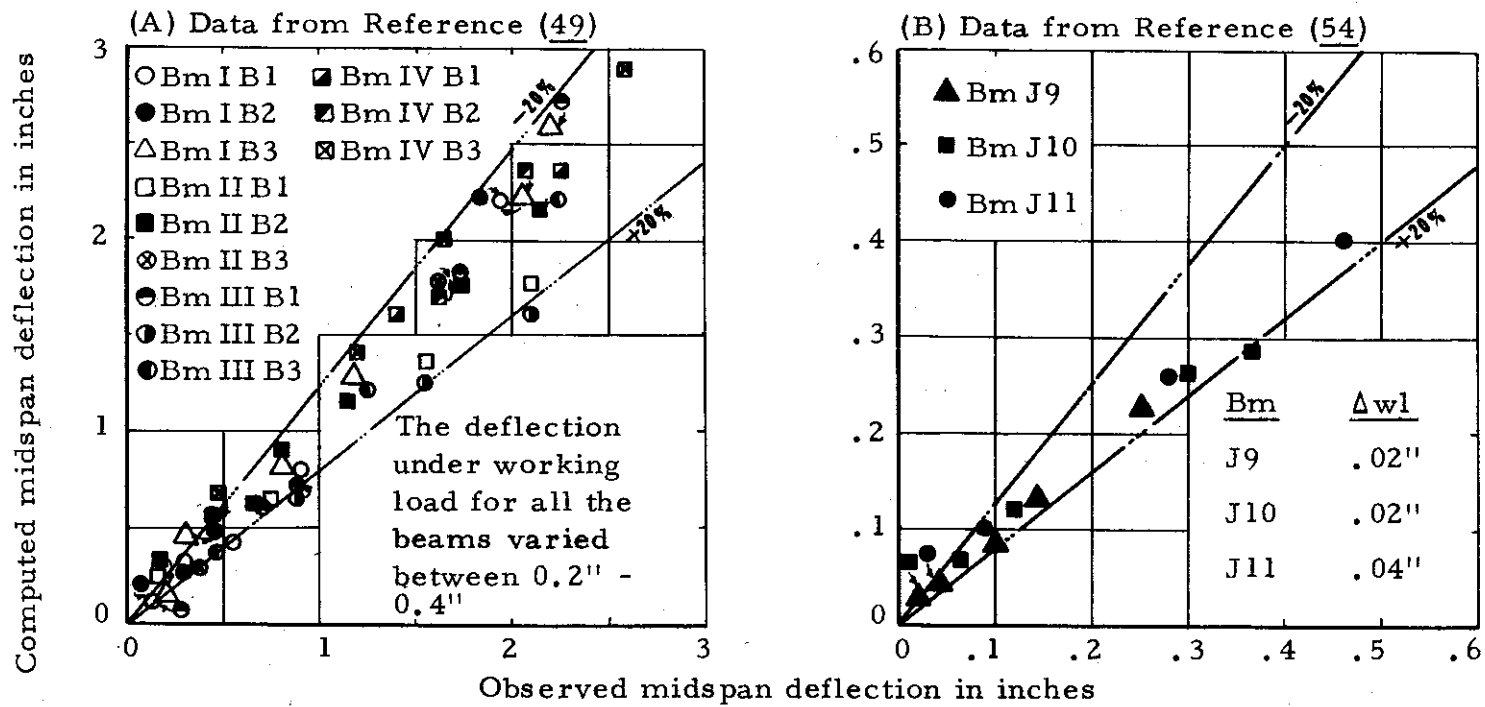


Figure 45 Observed and computed midspan deflection (using Eqs. (38), (40), and (41) for beams under static loading as in (A) (Data from Reference 49) and for beams under repeated loading as in (B) (Data from Reference 54)

2. In the cracked stage, the scatter between the computed and observed values of deflection is noticeable and the magnitude of the scatter increases with an increase in the applied load. The exclusion of creep effects in the determination of effective moment of inertia using Eq. (38) probably causes an underestimation of deflections. However, the magnitude of the scatter is within +20% for loads which are about 2.0 times the working load.

3. In the cracked stage, the computed values (using Eq. (38) for the determination of effective moment of inertia) of midspan deflection are slightly greater than the observed values of midspan deflection. This is probably due to the presence of non-tensioned steel which tends to reduce the creep effect and to further distribute the cracks along the beam. (For a discussion of this phenomenon as related to other types of prestressed concrete beams, see Section 5.6.)

#### Results Reported by Burns and Siess (54)

In a detailed study of the effects of repeated loading on the behavior of reinforced concrete beams, Burns and Siess reported the load-deflection response of 18 beams. A large number of variables were studied, the most important of which were the steel percentages, and the loading regimes. Of the 18 beams tested, only beams J9, J10 and J11 are included in this study. The beams were unloaded and reloaded at several stages before and after the yielding of the

tension reinforcement. The details of the beams are shown in Table C8. The loading was done by a symmetrical one-point loading system. This study indicates that the unloading and reloading from any point up to the ultimate did not affect the carrying capacity of the beam. The stiffness of the beam, as measured by the reloading slope of the load-deflection curve was found to depend on the amount of 'inelastic' deformation. This is consistent with the results described in Section 5.2 on the effects of repeated loading on prestressed concrete beams.

Figures 45 and 46 show the comparison between the computed values (using Eq. (40) for the determination of effective moment of inertia under repeated loading) and observed values of midspan deflection under two cycles of loading. The loading stage corresponded to a level prior to the yielding of the tension reinforcement. On the basis of Figures 45 and 46, the following observations are made:

1. Within the working load (the working load being defined as the load at which flexural cracking is initiated), the use of the gross section properties along with the reported modulus of elasticity of concrete gives excellent agreement between the computed and observed values of midspan deflection. The reported and not the computed (using Eq. (6)) modulus of elasticity of concrete because of the large difference that existed between these two values (a difference of about 20%).
2. At load levels in the cracking range of the beam, the scatter

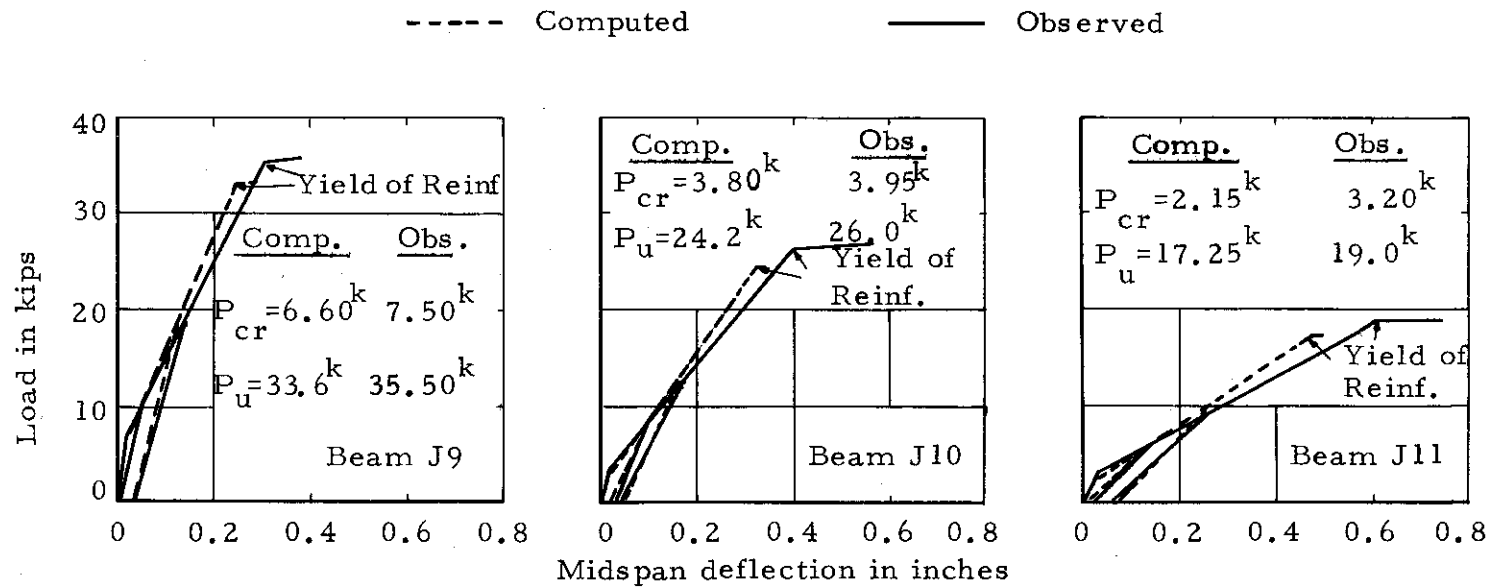


Figure 46 Comparison of computed and observed values of midspan deflection of beams in Reference (54), under two cycles of repeated loading (three non-composite reinforced beams)

begins to be appreciable, and the magnitude of the scatter increases as the applied load approaches the ultimate load (in this case, the yielding of the tension reinforcement). However, the scatter is within  $\pm 20\%$  for loads which are about 1.75 times the working load.

#### Summary of Results Reported by Others

A dimensionless plot (between load and deflection) is also shown in Figures 47 and 48 for prestressed rectangular and T-beams (composite or monolithic), respectively. The following observations are relevant to these figures: (Figures 47 and 48)

The allowance of 'severe cracking' in reinforced concrete beams as compared to 'no cracking' in fully prestressed beams and 'some cracking' (corresponding to the modulus of rupture of concrete) in partially prestressed beams at service loads, indicates the inconsistency of the current procedures in the design of reinforced and prestressed concrete members. One of the reasons for this inconsistency has been the unavailability of a reliable and simple method to predict the deflections under 'cracked' conditions for prestressed concrete members. Figures 47 and 48 show the load-deflection response (on a dimensionless plot) of 24 non-composite prestressed concrete beams (containing various amounts of tensile, compressive and non-tensioned reinforcement) and 6 composite prestressed concrete beams respectively. Both static and repeated loading results are included. Average curves for different steel percentages are

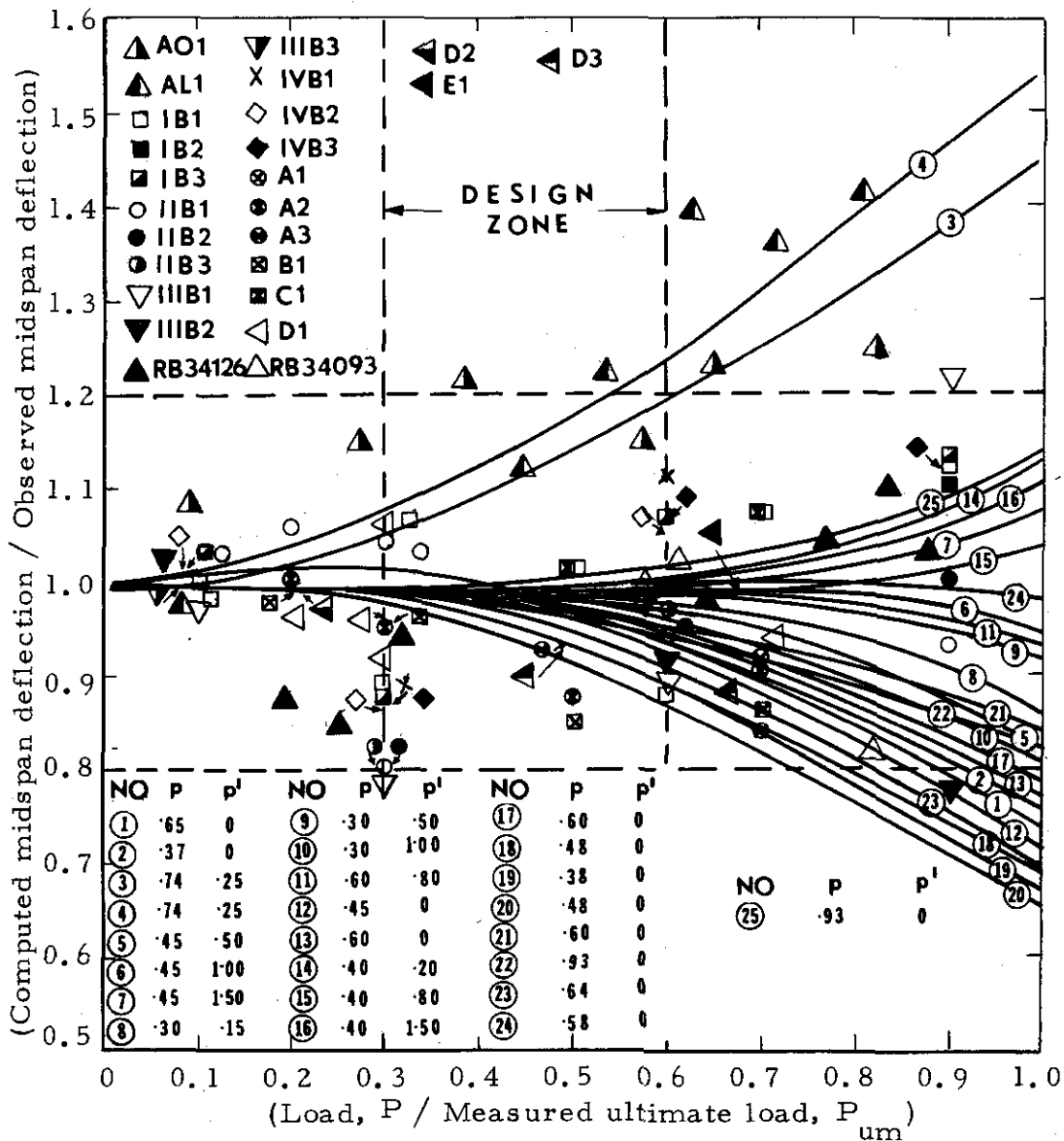


Figure 47 Range of validity of Eqs. (38)(40) and (41) for rectangular beams with different steel percentages\* -- included in this dimensionless plot are also the results from studies made on rectangular prestressed beams from References (41), (49), (54) and (56) as well as the current study.

\*The value of p' refers to compressive steel for curves ③ and ④ and to nontensioned steel for the other curves, and p refers to tensile steels for all curves.

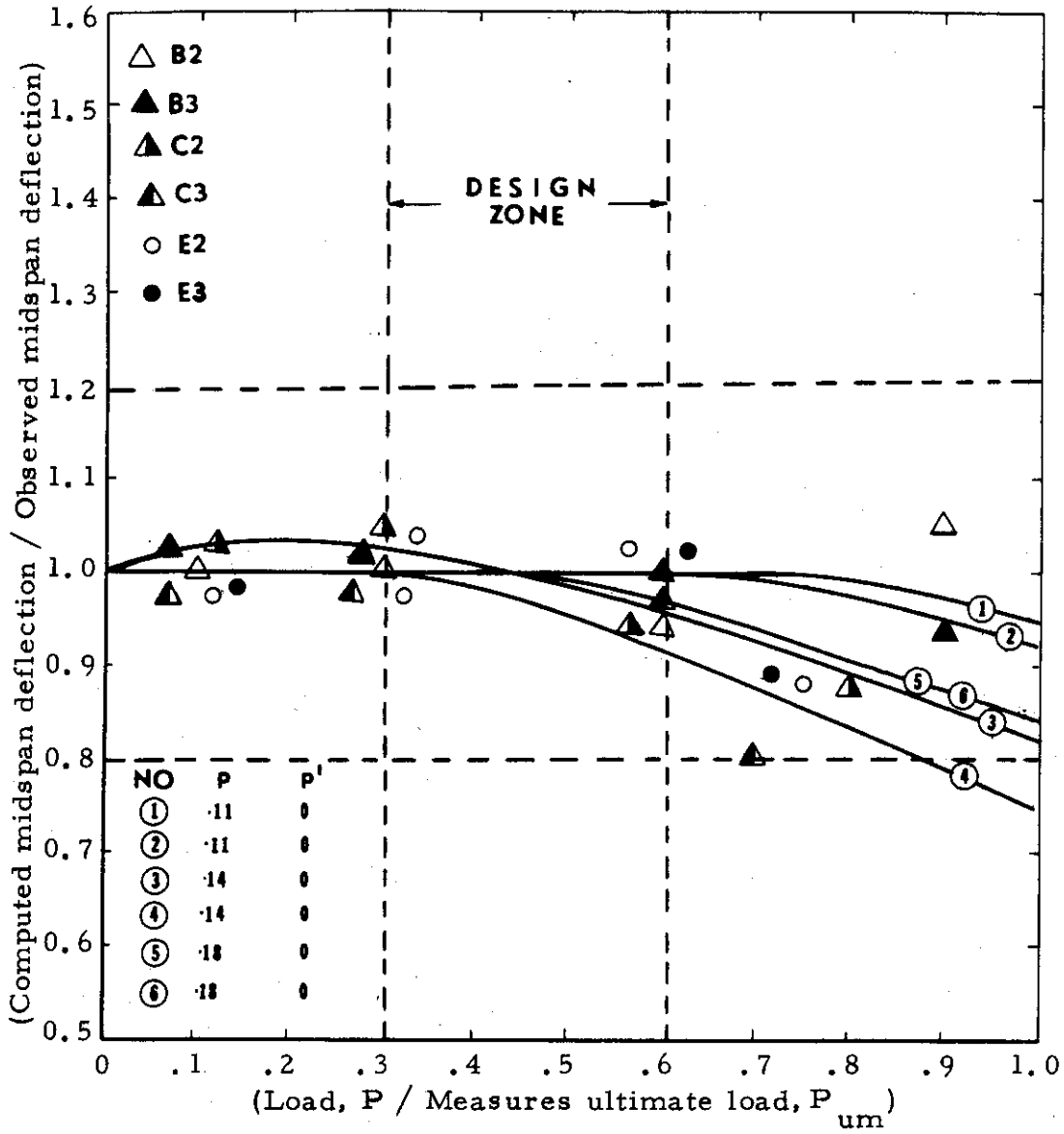


Figure 48 Range of validity of Eqs. (38), (40), and (41) for T beams with different steel percentages\* -- included in this dimensionless plot are the results from the current study only.

\*The values of p and p' in the figure refer to tensile and compressive steel percentages.

also indicated in the figures. The computed values of midspan deflection were based on the methods developed in Sections 5.1 to 5.4.

For purposes of discussion, the total load range is divided into three stages--(i) the 'uncracked stage (0 - 30% of the ultimate load), (ii) the 'cracked' stage or "design zone" (30 - 60% of the ultimate load) and (iii) the 'severely cracked' stage (60 - 100% of the ultimate load). The following observations refer directly to these figures.

1. In the 'uncracked' stage of non-composite and composite beams, the variation between the computed and observed values of midspan deflection is less than  $\pm 20\%$ . The working load of a fully prestressed beam usually falls within this stage. This confirms the use of the gross section properties in the determination of midspan deflections.

2. In the 'cracked' stage of non-composite and composite prestressed beams, the variation between the computed and observed values of midspan deflection is still less than  $\pm 20\%$ . However, the tendency for this scatter to increase is noticed in the shape of the average curves. The working load of a partially prestressed beam usually falls within this range. This suggests the use of the effective section properties (using Eq. (38) or (40)) as a reasonable method in the determination of midspan deflections.

3. In the 'severely cracked' stage of non-composite and composite prestressed beams, the variation between the computed and observed values of midspan deflection increases markedly as the applied load approaches the ultimate load. The working load of a prestressed beam is, of course, never within this stage. This suggests the invalidity of the use of Eq. (38) or (40) in the determination of the effective moment of inertia in this load range.

4. It is noticed that for prestressed beams (in the 'cracked' and 'severely cracked' stage) and containing only tensile reinforcement, the computed values of midspan deflection tend to be smaller than the observed values of midspan deflection. This appears to be due to the omission of 'creep effects' in the determination of deflections using the effective moment of inertia (for range of variation, see (7) below).

5. It is noticed that for prestressed beams (in the 'cracked' and 'severely cracked' stage) and containing both tensile and compressive reinforcement, the computed values of deflection tend to be greater than the observed values of midspan deflection. It is believed that this is due to the presence of compressive reinforcement which reduces creep and also lowers the neutral axis, thereby retarding the formation of cracks. Similar observations have been reported in the ACI Committee report (4) for reinforced concrete

beams containing both tensile and compressive reinforcement. (For range of variation, see (7) below.)

6. It is noticed that for prestressed beams (in the 'cracked' and 'severely cracked' stage) and containing tensioned and non-tensioned steel, the computed deflections differ slightly from the observed values of midspan deflection. However, the variation between the computed and observed values of midspan deflection for these beams are small when compared to the variation between the computed and observed values of midspan deflection for beams containing only tensioned steel. This is probably due to the presence of non-tensioned reinforcement that tends to reduce the creep effect and to further distribute the cracks along the beam.

7. One can safely conclude that 'cracking' (corresponding to concrete stresses greater than the modulus of rupture) can be allowed in prestressed concrete members provided the deflections under such loads satisfy the appropriate serviceability requirements. When compared to the measured deflections, the use of Eq. (38) for the effective moment of inertia of prestressed concrete members will result--(i) in smaller deflections (for prestressed beams containing only tensile steel), (ii) in larger deflections (for prestressed and reinforced beams containing both compressive and tensile steel), and (iii) in very slight deviation from the measured values (for prestressed

beams containing both tensioned and non-tensioned steel). However, the scatter between the computed and observed values of midspan deflection in all the cases studied herein is within +20% for loads that range up to 60-70% of the ultimate load. The corresponding load range for composite beams is of the order of 75-85% of the ultimate load.

### 5.6 Summary and Conclusions

In Sections 5.1 and 5.4 of this chapter, methods were presented for the computation of midspan deflections in both the 'uncracked' and the 'cracked' stages of prestressed and reinforced concrete beams under static or repeated loading. Comparisons with observed values of midspan deflection were made with laboratory beams of this study (Groups A, B, C, D, E, and F) in Section 5.1 to 5.4, and with other data from the literature in Section 5.5.

On the basis of Figures 32 to 48, and Tables 5, 6, and 7 as well as the specific conclusions in the earlier sections, the following general observations are made:

1. In the 'uncracked' or 'elastic' range, the use of the gross section properties along with the computed values of the elasticity modulus of concrete (using Eq. (6)) shows excellent agreement between the computed and observed values of midspan deflection for both reinforced and prestressed concrete beams under single or repeated

load cycles. (See Sections 5.1 to 5.3.)

2. The termination of the 'elastic' or 'uncracked' stage (herein defined as the cracking load or working load for prestressed members) can be predicted with confidence for both reinforced and prestressed concrete beams using the modulus of rupture,  $f'_{cb}$ . (See Figures 32-43.)

3. The allowance of 'severe cracking' in reinforced concrete beams as compared to 'no cracking' in fully prestressed beams and 'some cracking' (corresponding to the modulus of rupture of concrete) in partially prestressed beams at service loads, indicates the inconsistency of the current procedures in the design of reinforced and prestressed concrete members. One of the reasons for this inconsistency has been the unavailability of a reliable and simple method to predict the deflections under 'cracked' conditions for prestressed concrete members. Figures 47 and 48 show the load-deflection response (on a dimensionless plot) of 24 non-composite prestressed concrete beams (containing various amounts of tensile, compressive and non-tensioned reinforcement) and 6 composite prestressed concrete beams respectively. Both static and repeated loading results are included. Average curves for different steel percentages are also indicated in the figures. The computed values of midspan deflection were based on the methods developed in Section 5.1 to 5.4.

For purposes of discussion, the total load range is divided into three stages -- (i) the 'uncracked' stage (0 - 30% of the ultimate load), (ii) the 'cracked' stage or 'design zone' (30 - 60% of the ultimate load) and (iii) the 'severely cracked' stage (60 - 100% of the ultimate load). The following observations refer directly to these figures.

a. In the 'uncracked' stage of non-composite and composite beams, the variation between the computed and observed values of midspan deflection is less than  $\pm 20\%$ . The working load of a fully pre-stressed beam usually falls within this stage. This confirms the use of the gross section properties in the determination of midspan deflections.

b. In the 'cracked' stage of non-composite and composite prestressed beams, the variation between the computed and observed values of midspan deflection is still less than  $\pm 20\%$ . However, the tendency for this scatter to increase is noticed in the shape of the average curves. The working load of a partially prestressed beam usually falls within this range. This suggests the use of the effective section properties (using Eq. (38) or (40)) as a reasonable method in the determination of midspan deflections.

c. In the 'severely cracked' stage of non-composite and composite prestressed beams, the variation between the computed and observed values of midspan deflection increases markedly as the

applied load approaches the ultimate load. The working load of a prestressed beam is, of course, never within this stage. This suggests the invalidity of the use of Eq. (38) or (40) in the determination of the effective moment of inertia in this load range.

d. It is noticed that for prestressed beams (in the 'cracked' and 'severely cracked' stage) and containing only tensile reinforcement, the computed values of midspan deflection tend to be smaller than the observed values of midspan deflection. This appears to be due to the omission of 'creep effects' in the determination of deflections using the effective moment of inertia. (For range of variation see (g) below).

e. It is noticed that for prestressed beams (in the 'cracked' and 'severely cracked' stage) and containing both tensile and compressive reinforcement, the computed values of deflection tend to be greater than the observed values of midspan deflection. It is believed that this is due to the presence of compressive reinforcement which reduces creep and also lowers the neutral axis, thereby retarding the formation of cracks. Similar observations have been reported in the ACI Committee Report (4) for reinforced concrete beams containing both tensile and compressive reinforcement. (For range of variation, see (g) below.)

f. It is noticed that for prestressed beams (in the 'cracked' and 'severely cracked' stage) containing tensioned and

non-tensioned steel, the computed deflections differ slightly from the observed values of midspan deflection. However, the variation between the computed and observed values of midspan deflection for these beams are small when compared to the variation between the computed and observed values of midspan deflection for beams containing only tensioned steel. This is probably due to the presence of non-tensioned reinforcement that tends to reduce the creep effect and to further distribute the cracks along the beam.

g. One can safely conclude that 'cracking' (corresponding to concrete stresses greater than the modulus of rupture) can be allowed in prestressed concrete members provided the deflections under such loads satisfy the appropriate serviceability requirements. When compared to the measured deflections, the use of Eq. (38) for the effective moment of inertia of prestressed concrete members will result -- (i) in smaller deflections (for prestressed beams containing only tensile steel), (ii) in larger deflections (for prestressed and reinforced beams containing both compressive and tensile steel), and (iii) in very slight deviation from the measured values (for prestressed beams containing both tensioned and non-tensioned steel). However, the scatter between the computed and observed values of midspan deflection in all the cases studied herein is within +20% for loads that range up to 60-70% of the ultimate load. The corresponding load range for composite beams is of the order of 75-85% of the

ultimate load.

4. If the concrete and steel stress during a repeated cycle is below the shakedown limit of concrete (as defined in Section 5.2) and the yield strength of steel respectively, the following observations are valid:

a. The use of Eq. (40) is a reasonable and simple method of estimating the average effective moment of inertia of prestressed and reinforced concrete beams under repeated loading. (See Figures 37-41, 45, 46.) The use of Eq. (40) estimates the recovery during the unloading cycle. During the unloading cycle, there is no change in the slope of the load-deflection relationship.

b. Repeated cycles (up to 3 cycles) of loading at a given load level does not increase the magnitude of the residual deflection (see Figures 37-39). It is reasonable to expect that further increase in the number of cycles will not increase the residual deflection any more.

c. Repeated cycles (up to 3 cycles) of increasing load level increases the magnitude of residual deflection (see Figures 40-41).

d. The magnitude of the percentage of the total recovery decreases with increasing load (see sample calculations in Section 5.2).

5. For reinforced concrete beams under 24-hour sustained

cracking load, the following observations are valid:

a. The magnitude of the deflection due to sustained load is a function of the level of the sustained load -- the higher the magnitude of the sustained load, the greater will be the deflection under the sustained load. The use of experimentally determined creep coefficients predict satisfactorily the deflection under sustained loads (see Figure 43).

b. The use of Eq. (38) is a reasonable and simple means of estimating the effective moment of inertia of reinforced concrete beams. The reliability of this equation is confirmed by the fact that this has been suggested for the 1971 ACI Code (51).

6. For all the laboratory beams reported in this study, the use of the equivalent rectangular stress block for concrete gives reasonable agreement between the computed and observed values of ultimate strength.

7. There was no significant difference either in the strength or the load-deflection response between composite sections for which slabs have been cast at different times. This was true under both single and repeated loading (see Figures 33, 38, 39, 41, 43 and Tables 5, 6, and 7) cycles.

## Chapter 6

## SUMMARY AND CONCLUSIONS

Presented in this study are the results of a comprehensive investigation of non-composite and composite prestressed and reinforced structures using different weight concretes. Principal emphasis is placed on the initial plus time-dependent effects (prestress loss, camber, and deflection), and on the load-deflection response under single and repeated load cycles (with constant as well as increasing load levels) into the cracking range.

Systematic design procedures are described for predicting the material behavior and structural response. Continuous time functions are provided for all needed parameters, so that the general equations readily lend themselves to computer solution. Flow charts are explained and typical computer outputs are given for loss of prestress, camber, and load-deflection calculations in Appendix F. A summary of general parameters is also given in Chapter 4 for hand calculations.

These procedures are verified by comparisons between computed and experimental results for the data of this project, and for additional data in the literature. These data include normal weight, sand-lightweight, and all-lightweight concrete, non-composite and composite reinforced and prestressed members, and both laboratory specimens and actual

structures. Ranges of variation are shown and sample calculations are included for the procedures presented.

The problem, and the objectives and scope of the investigation are defined in Chapter 1. This chapter also includes a review of literature. A description of the experimental investigation of this project is given in Chapter 2.

Systematic procedures are described in Chapter 3 for predicting strength and elastic properties, creep and shrinkage characteristics of different weight concretes, types of curing, and types of cement (Eqs. 2 - 13). Standard equations and correction equations for significant conditions other than "standard" are outlined for design purposes. This chapter was developed in this project (33) and in Reference (18). Comparisons between experimental and computed results are shown to be quite satisfactory for the data of this project (Figures 2 - 7 and B3).

Procedures for predicting the initial plus time-dependent loss of prestress and camber of prestressed beams and deflection of reinforced beams are presented in Chapter 4 (Eqs. 14 - 34). Computed results by these equations, using both experimental material parameters and general or average parameters, are compared with experimental results for the laboratory beams and sand-lightweight composite bridge of this project; and with additional data in the literature (Figures 8 - 29 and Tables 1 - 4). Separate steel relaxation tests were conducted, and the contribution of steel relaxation to loss of prestress in beams (as distinguished from relaxation tests at constant length) is included in a

rational manner. It is concluded that the results in Chapter 4 serve to substantiate the prediction methods described. The approximate equations may be used for rough calculations only in some cases.

The ultimate loss of prestress for the sand-lightweight concrete (composite) prestressed bridge girders was 29% to 31% (see Figure 1, and Tables 1 and 3). It was determined that loss percentages for bridges under similar conditions using normal weight concrete will normally be of the order of 25%; and using all-lightweight concrete will normally be of the order of 35% or higher. Higher losses for the lighter concretes, for example, are due primarily to the lower modulus of elasticity (higher elastic strains for a given stress level), and not, necessarily, to greater creep and shrinkage behavior.

With respect to different slab casting schedules for composite prestressed and reinforced beams, an earlier slab tends to reduce the creep curvature by forming an earlier composite section, and also by reducing differential shrinkage. On the other hand, the creep effect for the precast beam concrete under the earlier slab loading tends to be greater. It appears from this study that the net result of these offsetting effects is beneficial in both prestressed and reinforced beams (earlier slab reduces prestress loss, camber, and deflection). It was found in this study that the beneficial effect of an earlier slab (3 to 4 weeks versus 9 to 10 weeks herein) is relatively small for prestressed beams and relatively significant in reinforced beams. The decrease in computed ultimate prestress loss and camber for the laboratory beams and bridge girders herein (see Figures 1, 11, 12, 15, 16, 18, and Tables 1, 2) was negligible for the laboratory beams; and 2% less prestress loss,

and 0.10" less midspan camber, for the bridge girders. Only the numerical camber, and not the percentage, is meaningful for the bridge girders, because the total camber is near zero due to the heavy deck slab. The decrease in the ultimate deflection of the laboratory composite beams was 0.13" or 30% (see Figures 1, 17, and Table 2). The reason for the difference in the relative effects between prestressed and reinforced beams has to do with the offsetting effects of prestress and dead load (including slab dead load) in the one case, and only additive dead load effects in the case of reinforced beams.

A detailed discussion of the experimental results and conclusions is also given in Chapter 4.

From the results in Chapter 4, it is concluded that the procedures presented will normally agree with actual results within  $\pm 15\%$  when using experimentally determined material parameters. The use of the general or average material parameters herein predicted results that agreed with actual results in the range of  $\pm 30\%$ . With some knowledge of the time-dependent behavior of concretes using local aggregates and under local conditions, it is concluded that one should normally be able to predict initial plus time-dependent loss of prestress, camber, and deflection within about  $\pm 20\%$ , using these procedures. Some 41 laboratory specimens and actual structures were included in Chapter 4. In the cases compared, it is noted that most of the results are considerably better than these limits.

This project is thought to be the first such comprehensive study of the initial plus time-dependent material behavior and related

structural response of both non-composite and composite structures using different weight concretes.

Developed in Chapter 5 for the first time is a simple and efficient design method for predicting the entire short-time load-deflection curve (or a single point, such as at maximum load) under repeated load cycles into the cracking range for both prestressed and reinforced members. This method is based on a procedure developed by Branson (50), (4), (30), (42) for predicting the deflection of reinforced beams under single-cycle loading and adopted for the 1971 ACI Building Code (51), and applied to prestressed beams under single-cycle loading by Shaikh and Branson (49). The effects of increasing load levels in subsequent cycles, and of 24-hour sustained loading are also included. Eqs. (35) - (41), the accompanying descriptions, Figures 32 - 43, Tables 5 - 7, and the corresponding sample calculations serve to illustrate these procedures.

The reliability of the procedures described are indicated by comparisons between computed results and the experimental data of this project, and with data in the literature (Figures 31 - 34, 37 - 48, and Tables 5 - 7).

It was found (Figures 37 - 42, and Table 6) that repeated load cycles (up to 3 cycles in this project) of short duration did not increase the deflection at a given load level nor the residual deflection after unloading. However, repeated cycles to increasing load levels did increase the residual deflection after unloading, and also increased the magnitude of the deflection at a given load level when reloaded (Figures

40 - 42 and Table 6). Similar results have been shown in Reference (54). This is attributed to the effect of greater crack development at the higher loads, and correspondingly greater residual crack effects.

A detailed discussion of the experimental results and conclusions is also given in Chapter 5.

From the results in Chapter 5, it is concluded that the procedures presented for predicting load-deflection behavior of reinforced and prestressed members will normally agree with actual results within  $\pm 20\%$  for loads as high as 60% to 70% of the ultimate load for non-composite beams and as high as 75% to 85% for composite beams under both single and repeated load cycles. This included partially prestressed beams loaded well into the cracking range. The accuracy is generally better than  $\pm 20\%$  for normal working load levels. Some 38 non-composite and composite specimens were included in Chapter 5 (Figures 31 - 34, 37 - 48, and Tables 5 - 7).

With the aid of the material parameter equations presented in Chapter 3, and the procedures developed in Chapters 4 and 5, the structural designer can more reliably than in the past predict the initial plus time-dependent prestress loss, camber, and deflection (including effects of repeated load cycles) of non-composite and composite reinforced and prestressed structures of different weight concretes. As a result of this study, he can also make a better judgement as to the reliability of his computational procedures and the range of variation to be expected between computed and actual results, depending primarily on the degree of care with which the material properties and parameters (mainly creep and shrinkage) are determined for a given design.

## LIST OF REFERENCES

1. Davis, R., "A Summary of Investigation of Volume Changes in Cement Mortars and Concrete Produced by Causes Other Than Stress," ASTM, Proceedings, V. 30, Part I, 1930, pp. 668-685.
2. Carlson, R. W., "Drying Shrinkage of Concrete as Affected by Many Factors," ASTM, Proceedings, V. 38, Part II, 1938, pp. 419-440.
3. Hveem, F. N., and Tremper, B., "Some Factors Influencing the Shrinkage of Concrete," ACI Journal, Proceedings, V. 53, No. 8, Feb. 1957, pp. 781-802.
4. ACI Committee 435, "Deflections of Reinforced Concrete Flexural Members," ACI Journal, Proceedings, V. 63, No. 6, June 1966, pp. 637-674.
5. Lorman, W. R., "The Theory of Concrete Creep," ASTM, Proceedings, V. 40, 1940, pp. 1082-1102.
6. McHenry, Douglas, "A New Aspect of Creep in Concrete and Its Application to Design," ASTM, Proceedings, V. 43, 1943, pp. 1969-1984.
7. Neville, A. M., "Theories of Creep in Concrete," ACI Journal, Proceedings, V. 52, No. 1, Sept. 1955, pp. 47-60.
8. Ross, A. D., "Creep of Concrete Under Variable Stress," ACI Journal, Proceedings, V. 54, No. 9, Mar. 1958, pp. 739-758.
9. Troxell, G. E.; Raphael, J. M.; and Davis, R. E., "Long Time Creep and Shrinkage Tests of Plain and Reinforced Concrete," ASTM, Proceedings, V. 58, 1958, pp. 1-20.

10. Kesler, C. E., and Ali, I., "Mechanisms of Creep," Symposium on Creep of Concrete, "ACI Special Publication No. 9, 1964, pp. 35-63.
11. Meyers, B. L.; Slate, F. O.; and Winter, G., "Time-Dependent Deformation and Microcracking of Plain Concrete," ACI Journal, Proceedings, V. 66, No. 1, Jan. 1969, pp.
12. Meyers, B. L., and Neville, A. M., "Creep of Concrete: Influencing Factors and Prediction," Symposium on Creep of Concrete, ACI Special Publication No. 9, 1964, pp. 1-33.
13. Pauw, A., and Chai, J. W., "Creep and Creep Recovery for Plain Concrete," Missouri Cooperative Highway Research Programme, Report No. 67-8.
14. Hansen, T. C., and Mattock, A. H., "Influence of Size and Shape of Member on Shrinkage and Creep of Concrete," ACI Journal, Proceedings, V. 63, No. 2, Feb. 1966, pp. 267-290.
15. Jones, T. R.; Hirsch, T. J.; and Stephenson, H. K., "The Physical Properties of Structural Quality Lightweight Aggregate Concrete," Texas Transportation Institute, Texas A & M University, College Station, Texas, August 1959, pp. 1-46.
16. ACI Committee 213, "Guide for Structural Lightweight Aggregate Concrete," ACI Journal, Proceedings, V. 64, No. 8, Aug. 1967, pp. 433-470.
17. Pfeifer, D. W., "Sand Replacement in Structural Lightweight Concrete--Creep and Shrinkage Studies," ACI Journal, Proceedings, V. 65, No. 2, Feb. 1968, pp. 131-142.
18. Christiason, M. L., "Time-Dependent Concrete Properties Related to Design--Strength and Elastic Properties, Creep and Shrinkage," MS Thesis, University of Iowa, Iowa City, Feb. 1970.

19. Schumann, C. G., "Creep and Shrinkage Properties of Lightweight Aggregate Concrete Used in the State of Iowa," MS Thesis, University of Iowa, Iowa City, Jan. 1970.
20. Finsterwalder, Ulrick, "Ergebnisse von Kriech und Schwindmessungen an Spannbetonbauwerken," Beton und Stahlbetonbau (Berlin), V. 53, No. 5, May 1958, pp. 136-144.
21. Lofroos, W. N., and Ozell, A. M., "The Apparent Modulus of Elasticity of Prestressed Concrete Beams Under Different Stress Levels," Prestressed Concrete Institute Journal, V. 4, No. 2, Sept. 1959, pp. 23-47.
22. Mattock, Alan H., "Precast-Prestressed Concrete Bridges; 5. Creep and Shrinkage Studies," Journal, Research and Development Laboratories, Portland Cement Association, V. 3, No. 2, May 1961, pp. 32-66.
23. Branson, D. E., and Ozell, A. M., "Camber in Prestressed Concrete Beams," ACI Journal, Proceedings, V. 57, No. 12, June 1961, pp. 1549-1574.
24. Corley, W. G.; Sozen, M. A.; and Siess, C. P., "Time-Dependent Deflections of Prestressed Concrete Beams," Bulletin No. 307, Highway Research Board, 1961, pp. 1-25.
25. Branson, D. E., "Time-Dependent Effects in Composite Concrete Beams," ACI Journal, Proceedings, V. 61, No. 2, Feb. 1964, pp. 213-230.
26. Zia, P., and Stevenson, J. F., "Creep of Concrete Under Non-Uniform Stress Distribution and Its Effect on Camber of Prestressed Concrete Beams," Report of Highway Research Programme No. ERD-110-R, June 1964, pp. 1-110.
27. Sinno, R., "The Time-Dependent Deflections of Prestressed Concrete Bridge Girders," Dissertation, Texas A & M University, 1968.
28. Yang, D. D., "Creep in Prestressed Lightweight Aggregate Concrete," Dissertation, Texas A & M University, 1966.

29. Scordelis, A. C., Subcommittee Chairman, Branson, D. E., and Sozen, M. A., "Deflections of Prestressed Concrete Members," ACI Committee 435, Subcommittee 5 Report, ACI Journal, Proceedings, V. 60, No. 12, Dec. 1963, pp. 1697-1728.
30. Branson, D. E., "Design Procedures for Computing Deflections," ACI Journal, Proceedings, V. 65, No. 9, Sept. 1968, pp. 730-742.
31. Pauw, Adrian, and Breen, J. E., "Field Testing of Two Prestressed Concrete Girders," Highway Research Board Bulletin 307, pp. 42-63, 1961.
32. Young, J. A., "Field Observation of Five Lightweight Aggregate Pretensioned Prestressed Concrete Bridge Beams," Final Report, Iowa Highway Research Board Project No. HR-104, pp. 1-39, 1969.
33. Branson, D. E.; Meyers, B. L.; and Kripanarayanan, K. M., "Time-Dependent Deformation of Non-Composite and Composite Prestressed Concrete Structures," Iowa Highway Commission Research Report 69-1, Feb. 1969, pp. 1-80. Also condensed papers presented at the 49th Annual Meeting, Highway Research Board, Washington, D. C., Jan. 1970, pp. 1-42; and at the 6th Congress, Federation Internationale de la Precontrainte, Prague, Czechoslovakia, June 1970, pp. 1-28.
34. Delarue, J., "Fluage et Beton Precontraint," RILEM Colloquim, Munich, Nov. 1958.
35. Abeles, P. W., "Static and Fatigue Tests on Partially Prestressed Concrete Constructions," ACI Journal, Proceedings, V. 50, No. 7, Dec. 1954, pp. 361-376.
36. Abeles, P. W., "Partial Prestressing and Possibilities for Its Practical Application," Prestressed Concrete Institute Journal, V. 4, No. 1, June 1959, pp. 35-51.
37. Abeles, P. W., "Partial Prestressing in England," Prestressed Concrete Institute Journal, V. 8, No. 1, Feb. 1963, pp. 51-72.

38. Abeles, P. W., "Studies of Crack Widths and Deformation Under Sustained and Fatigue Loading," Prestressed Concrete Institute Journal, V. 10, No. 6, Dec. 1965.
39. Burns, N. H., "Moment Curvature Relationships for Partially Prestressed Concrete Beams," Prestressed Concrete Institute Journal, V. 9, No. 1, 1964, pp. 52-63.
40. Hutton, S. G., and Loov, R. E., "Flexural Behavior of Prestressed, Partially Prestressed and Reinforced Concrete Beams," ACI Journal, Proceedings, V. 63, No. 12, Dec. 1966, pp. 1401-1408.
41. Warawaruk, J., Sozen, M. A., and Siess, C. P., "Strength and Behavior in Flexure of Prestressed Concrete Beams," Engineering Experiment Station Bulletin No. 464, University of Illinois, August 1962, pp. 1-105.
42. Branson, D. E., Subcommittee Chairman, "Prediction of Creep, Shrinkage and Temperature Effects in Concrete Structures," Subcommittee II, ACI Committee 209, Draft Report, April 1970, pp. 1-32.
43. Keeton, J. R., "Study of Creep in Concrete, Phases 1-5," Technical Reports Nos. R333-I, II, III, U.S. Naval C. E. Lab., Port Hueneme, Calif., 1965.
44. The California Producers Committee on Volume Change and Affiliated Technical Organizations, "Drying Shrinkage of Concrete," p. 1-40, Mar. 1966.
45. Magura, D. D.; Sozen, M. A.; and Siess, C. P., "A Study of Relaxation in Prestressing Reinforcement," Prestressed Concrete Institute Journal, V. 9, No. 2, Apr. 1964, pp. 13-58.
46. Antill, J. M., "Relaxation Characteristics of Prestressing Tendons," Civil Engineering Transactions, Inst. of Engr., Australia, V. CE 7, No. 2, 1965.
47. Evans, R. H., and Bennet, E. W., Prestressed Concrete, Wiley, New York, 1958.

48. Rogers, G. L., "Validity of Certain Assumptions in the Mechanics of Prestressed Concrete," ACI Journal, Proceedings, V. 49, No. 7, Dec. 1953, pp. 317-330.
49. Shaikh, A. F., and Branson, D. E., "Non-Tensioned Steel in Prestressed Concrete Beams," Prestressed Concrete Institute Journal, V. 15, No. 1, Feb. 1970.
50. Branson, Dan E., "Instantaneous and Time-Dependent Deflections of Simple and Continuous Reinforced Concrete Beams," Part I, Report No. 7, Alabama Highway Research Report, Bureau of Public Roads, Aug. 1963, (1965), pp. 1-78.
51. ACI Committee 318, "Proposed Revisions to the ACI-318-63 Code," ACI Journal, Proceedings, V. 67, No. 2, Feb. 1970, pp. 77-186.
52. Noble, P. M., "The Effect of Aggregate and Other Variables on the Elastic Properties of Concrete," Proceedings, ASTM, V. 31, Part I, 1931, pp. 399-426.
53. Shah, S. P., and Winter, G., "Response of Concrete to Repeated Loads," RILEM International Symposium on the Effects of Repeated Loading on Materials and Structural Elements, Sept. 1966, Mexico.
54. Burns, N. H., and Siess, C. P., "Repeated and Reversed Loading in Reinforced Concrete," ASCE Journal (Structural Division), V. 92, Paper No. 4932, Oct. 1966.
55. Ruiz, M. W., "Effect of Repeated Loads on the Rotation Capacity of Reinforced Concrete Beams," Dissertation, Cornell University, Sept. 1968.
56. Abeles, P. W., Brown, E. I., and Woods, J. O., "Report on Static and Sustained Loading Test," Prestressed Concrete Institute Journal, V. 13, No. 4, Aug. 1968, pp. 12-32.
57. Reichart, T. W., "Creep and Drying Shrinkage of Lightweight and Normal-Weight Concretes," NBS Nomograph 74, National Bureau of Standards, Mar. 1964.
58. Shideler, J. J., "Lightweight Aggregate Concrete for Structural Use," ACI Journal, Proceedings, V. 54, No. 4, pp. 299-328, Oct. 1957.

APPENDIX A

Appendix A includes the details of the laboratory specimens and the bridge girders as well as the different types of concretes used in this project. This also includes details of the creep and shrinkage specimens such as the age of loading, ambient relative humidity, etc.

TABLE A1  
DETAILS OF LABORATORY BEAMS (GRPS. A, B, C) AND BRIDGE GIRDERS

Beam Group	<sup>a</sup> All Beams are 6" x 8", d=6", Span=15", <sup>b</sup> Slabs are 20" x 2"									L=86', 7" slab
	Group A			Group B			Group C			Bridge
Beam No.	A1	A2	A3	B1	B2	B3	C1	C2	C3	152-156
Beam			<sup>c</sup> 							<sup>f</sup> 
Eccentricity in	2.00	2.00	2.00	2.00	2.00	2.00	2.00	2.00	2.00	14.50 6.20
Prestressing Strand dia in	2-3/8 1-5/16	3-5/16	1-3/8 1-5/16	3-5/16	3-5/16	3-5/16	2-3/8 1-5/16	2-3/8 1-5/16	2-3/8 1-5/16	30-1/2
<sup>e</sup> A <sub>s</sub> in <sup>2</sup>	0.2176	0.1734	0.1377	0.1734	0.1734	0.1734	0.2176	0.2176	0.2176	4.56
p = A <sub>s</sub> /A <sub>g</sub>	0.00453	0.00361	0.00287	0.00361	0.00361	0.00361	0.00453	0.00453	0.00453	0.00883
Des. Pre. For. F <sub>i</sub> , k	38.0	30.0	24.0	30.0	30.0	30.0	38.0	38.0	38.0	867.0
Meas. Pre. F <sub>i</sub> , kip	37.0	29.6	23.4	30.0	29.9	29.9	38.0	37.9	37.9	867.0
<sup>d</sup> Concrete Stresses at release of prestress, psi	t=+340 b=-1840	t=+307 b=-1511	t=+241 b=-1201	t=+310 b=-1530	t=+309 b=-1527	t=+309 b=-1527	t=+390 b=-1527	t=+390 b=-1930	t=+390 b=-1930	t=-429 t=-107 b=-2623 t=-2955

For footnotes see following page.

TABLE A1 (Cont'd)

- a •3/8" Strand, •5/16" Strand, Measured stress in all strands of lab beams =  $(172 \pm 4)$  ksi. Measured stress in all strands of bridge girders = 190 ksi. All beams are made of Idealite - Sand Lt. Wt. concrete.
- b Six gage WWF, 6" x 6", ( $A_g = 0.058 \text{ in}^2/\text{ft width}$ ), slab steel placed in center of slab. No. 3 U-Stirrups in form of ties for composite slab are spaced at 6" c/c in end quarter span and at 22-1/2" cc in middle half of beam.
- c Strands placed so that lateral eccentricity is eliminated.
- d These stresses are computed using the Measured  $F_i$ , t= top fiber stress, b= bottom fiber stress. These initial stresses refer to prestressed section in all cases. The stresses in the case of laboratory beams refer to the end section only. The rectangular (6" x 8") beam dead load, extreme fiber stress at midspan = 218 psi.
- e The ultimate strength and yield strength (0.1% offset) were: for the laboratory beam steel 250 ksi and 235 ksi, respectively, and for the bridge girder steel 270 ksi and 250 ksi, respectively.
- f The lower values in this column refer to the center of the girder.

TABLE A2

DETAILS OF LABORATORY BEAMS (GRPS. D, E AND F)

Beam Group	<sup>a</sup> All Beams are 6" x 8", d=6", Span=15', <sup>b</sup> Slabs are 20" x 3"								
	Group D			Group E			<sup>c</sup> Group F		
Beam No.	D1	D2	D3	E1	E2	E3	F1	F2	F3
Beam									
Eccentricity in	1.75	2.00	2.00	1.75	1.75	1.75	2.00	2.00	2.00
Prestressing Strand dia in	4-3/8	4-5/16	1-1/4 3-5/16	4-3/8	4-3/8	4-3/8	3-1/2	3-1/2	3-1/2
<sup>e</sup> A <sub>s</sub> in <sup>2</sup>	0.3196	0.2312	0.2090	0.3196	0.3196	0.3196	0.6000	0.6000	0.6000
p = A <sub>s</sub> /A <sub>g</sub> <sup>c</sup>	0.00666	0.00482	0.00435	0.00666	0.00666	0.00666	0.01667	0.01667	0.01667
Des. Pre. For. F <sub>i</sub> , k	56.00	40.60	36.75	56.0	56.0	56.0	Reinforced Concrete Beams		
Meas. Pre. F <sub>i</sub> , kip	56.50	41.00	36.75	56.0	56.2	56.3			
<sup>d</sup> Concrete Stresses at release of prestress, psi	t=+385 b=-2585	t=+421 B=-2049	t=+369 b=-1831	t=+375 b=-2585	t=+370 b=-2591	t=+370 b=-2600			

For footnotes see following page.

Ap 4

TABLE A2 (Cont'd)

- <sup>a</sup> ● 3/8" Strand, ○ 5/16" Strand, □ 1/4" Strand, × 1/2" bar, Measured stress in all strands of lab beams =  $(175 \pm 2)$  ksi.
- <sup>b</sup> See Footnote b, Table A1
- <sup>c</sup> The value of  $p$  for reinforced beams is  $A_s/bd$ .
- <sup>d</sup> These stresses are computed using the Measured  $F_1$  :  $t$  = top fiber stress,  $b$  = bottom fiber stress. These initial stresses refer to the prestressed section in all cases. The stress in the case of laboratory beams refer to the end section only. The rectangular (6" x 8") beam dead load, extreme fiber stress at midspan are 178 psi, 208 psi, 208 psi for the beams of Group D, E, and F, respectively.
- <sup>e</sup> See Footnote e, Table A1

TABLE A3

## DETAILS OF CONCRETE MIXES AND MIXING PROCEDURE FOR LT-WT CONCRETES

Description	Concrete for			
	Grps A, B, C & Bridge Girders	Group D	Group E	Group F
Mix design objectives				
Conc. Qty.	1 cu yd	1 cu yd	1 cu yd	1 cu yd
Conc. str. @ 28d	5000 psi	5000 psi	5000 psi	4000 psi
Mix ingredients				
Cement (Type I)	705 lbs	752 lbs	705 lbs	611 lbs
F. aggregate	Sand - 1395 lbs	Haydite agg. (3/16" to dust) - 950 lbs	Sand - 1150 lbs	Sand - 1250 lbs
C. aggregate	Idealite Agg. (60% of 3/4 to 5/16 & 40% of 5/16 to #8) 822 lbs	Haydite Agg. (3/4" to #4) - 700 lbs	Haydite Agg. (3/4" to #4) - 825 lbs	Haydite Agg. (3/4" to #4) - 825 lbs
Water	35.0 gal	42.0 gal	42.0 gal	40.0 gal
Darex	6.5 oz	7.0 oz	6.5 oz	5.7 oz
WRDA	50 oz	53.5 oz	50 oz	43.5 oz

- Mixing procedure:
1. Proportion and batch fine aggregate and coarse aggregate.
  2. Add 50% of total water requirement.
  3. Mix for approximately 2 min.
  4. Proportion and batch cement.
  5. Add 12.5% of water requirement.
  6. Add Darex (in solution with 3 gallons of water), WRDA and the remaining water while adjusting to 2-1/2" slump.

TABLE A4

<sup>a-g</sup> CONCRETE PROPERTIES (GRPS A, B, C AND BRIDGE GIRDERS),  
TEMPERATURE AND HUMIDITY DATA

Property	Concrete Batch								
	Gp. A SLt. Wt	Gp. B SLt. Wt	Gp. C SLt. Wt	Slab B2 N. Wt	Slab C2 N. Wt	Slab B3 N. Wt	Slab C3 N. Wt	<sup>f</sup> Bridge Lt. Wt	<sup>g</sup> Bridge Slab N. Wt
$f'_c$ (7 days)    psi	6700	5500	6150	--	--	--	--	5600	
$f'_c$ (28 days)    psi	9350	8150	8750	4800	4140	5100	4300	6100	3500
Unit Wt (Wet)    pcf	124.0	124.0	125.0	--	--	--	--	--	--
U. Wt (Dry-7d)    pcf	123.0	123.5	123.5	153	152	152	153	122.0	145
Meas. Air Ent.    %	4.0	6.0	6.0	--	--	--	--	--	--
Slump             in	2.0	2.5	2.5	2.5	2.5	3.0	2.5	--	--
<sup>c</sup> Modulus of Elasticity        psi at 7 days        x 10 <sup>6</sup>	-- -- <u>3.68</u>	-- -- <u>3.35</u>	a. 3.20 b. 3.33 c. <u>3.55</u>	-- -- --	-- -- --	-- -- --	-- -- --	a. 3.04 b. 3.10 c. <u>3.32</u>	-- -- --
<sup>c</sup> Modulus of Elasticity        psi at 28 days        x 10 <sup>6</sup>	-- -- <u>4.35</u>	-- -- <u>4.09</u>	a. 3.28 b. 3.58 c. <u>4.23</u>	-- -- <u>4.33</u>	-- -- <u>3.97</u>	-- -- <u>4.41</u>	-- -- <u>4.05</u>	-- -- <u>3.47</u>	-- -- <u>3.41</u>

For footnotes, see following page.

TABLE A4 (Cont'd)

<sup>a</sup> Lab. temp: 61-85 deg. F., avg. temp. 78 deg. F. Lab. relative humidity: 25-61%, avg. rel. hum. 40%. Avg. rel. hum. for central Iowa (from U.S. Weather Bur.): Jan. -79%, July-66%, Mean Annual 71%. For Spr-Sum-Fall, use 70%.

<sup>b</sup> Stress levels for creep tests were approx. design stresses for lab. beams:

Mix	Strength, $f_c$ , at 7 days	Stress Level for Creep Tests	% of 7d - $f'_c$
Gp. A	6700 psi	2010 psi	30%
Gp. B	5500	1375	25
Gp. C	6150	1845	30

<sup>c</sup> The modulus of elasticity values are as follows: a. Measured secant (to  $0.5 f'_c$ ) mod. of el., b. Measured initial tangent mod. of el., c. All values underlined are computed using  $E_c = 33 \sqrt{w^3} f'_c$ , psi.

<sup>d</sup> Computed values of modulus of elasticity at release for bridge girders:

<u>Girder No.</u>	<u>Age at Release</u>	<u>Strength at Rel.</u>	<sup>c</sup> <u>Mod. of El. at Rel.</u>
152	2 days	5160 psi	<u><math>3.19 \times 10^6</math></u> psi
153	2	4670	<u>3.04</u>
154	2	4685	<u>3.05</u>
155	3	5130	<u>3.19</u>
156	3	4440	<u>2.96</u>

<sup>e</sup> Computed mod. of el. of pres. units at time of slab casting,  $E_c \times 10^6$  psi: Gp. B--4.09, 4.30; Gp. C--4.23, 4.44; Girders 152, 153, 154--3.50; Girders 155, 156--3.40.

<sup>f</sup> Concrete specimens for data in this column obtained from casting yard for Bridge Girders 155 and 156. Measurements made in laboratory.

<sup>g</sup> "Design" values were used for bridge slab concrete.

TABLE A5

<sup>a</sup> CONCRETE PROPERTIES (GRPS D, E, & F),  
TEMPERATURE AND HUMIDITY DATA

Property	Concrete Batch						
	Gp D A. Lt. Wt	Gp E S. Lt. Wt.	Gp F S. Lt. Wt	Slab E2 N. Wt	Slab F2 N. Wt	Slab E3 N. Wt	Slab F3 N. Wt
<sup>b</sup> $f'_c$ (Release) psi	4150	4250	3650	--	--	--	--
$f'_c$ (28 days) psi	4925	4950	3950	4200	4250	4300	4200
Unit Wt (Wet) pcf	105.5	122.2	122.5	153.1	153.2	154.3	153.5
U. Wt (Dry-7d) pcf	105.0	122.0	122.0	153.0	153.0	154.0	153.0
Meas. Air Ent. %	5.5	6.0	5.0	--	--	--	--
Slump in	2.5	3.0	3.0	--	--	--	--
<sup>c</sup> Modulus of Elasticity at Release psi $\times 10^6$	<u>2.33</u>	<u>2.90</u>	<u>2.70</u>	--	--	--	--
<sup>c</sup> Modulus of Elasticity at 28 Days psi $\times 10^6$	<u>2.52</u>	<u>3.13</u>	<u>2.80</u>	<u>4.04</u>	<u>4.06</u>	<u>4.12</u>	<u>4.04</u>

For footnotes, see following page.

TABLE A5 (Cont'd)

<sup>a</sup> Lab. Temp: 60-88 deg. F., avg. temp. 75 deg. F. Lab. relative humidity: 20-65%, avg. rel. hum. 50%.

<sup>b</sup> Stress levels for creep tests were approximate design stresses for lab. beams:

<u>Mix</u>	<u>Age @ release</u>	<u>Strength @ release</u>	<u>Stress level for creep tests</u>	<u>% initial stress</u>
Gp D	7 days	4150 psi	2000 psi	48%
Gp E	9 days	4250 psi	2000 psi	47%
Gp F	21 days	3650 psi	1000 psi	27%

The age at release for Gps D and E refer to the age at release of prestress and for Gp F this refers to the age at which the reinforced beams were in position.

<sup>c</sup> All values are computed using  $E_c = 33 \sqrt{w^3 f'_c}$ , psi.

TABLE A6

## CONCRETE PROPERTIES OF LAB BEAMS AT "LOAD-DEF" STUDIES

Description	dGrp A	dGrp B	Grp C	Grp D	dGrp E	dGrp F
<sup>a</sup> Computed, $f'_c$ psi	10850	9350	10050	5650	5680	4540
Measured, $f'_c$ psi	10560	9420	9995	5600	5725	4600
<sup>b</sup> Computed modulus of rupture, $f'_{cb}$ psi	625	580	600	450	452	405
<sup>c</sup> Measured modulus of rupture, $f'_{cb}$ psi	650	608	628	480	490	430

<sup>a</sup> Computed using Eq. (2). The beams of Group A, B, C, D, E and F were aged 367, 187, 187, 187, 189 and 189 days respectively at the time of the load deflection studies.

<sup>b</sup> For lightweight concrete in a drying condition, the modulus of rupture ranges from  $5\sqrt{f'_c}$  to  $11\sqrt{f'_c}$ . The observed values of the modulus of rupture correspond to approximately  $6\sqrt{f'_c}$ .

<sup>c</sup> Obtained by bending tests on plain concrete members.

<sup>d</sup> The concrete strength of slab concretes of B2, B3, C2, C3, E2, E3, F2, and F3 were 5500, 5760, 4720, 4860, 4200, 4860, 4860 and 4750 psi, respectively.

APPENDIX B

Appendix B includes a discussion of the variables that affect creep and shrinkage of concretes as well as a discussion of the correction factors for these variables with relation to the method developed in the text.

## APPENDIX B

Discussion of variables affecting creep and shrinkage (4)(13)(18)(42)(58)

Concrete undergoes time-dependent deformations under the action of sustained loads that are substantially greater than those of a corresponding unstressed specimen. These additional strains due to the effect of sustained stress are attributed to creep of the concrete. Current nomenclature regarding creep of concrete is summarized in Figure B1.

When specimens are subjected to uniform axial stress, only normal strains (both elastic and inelastic) are usually considered. The elastic strains are stress dependent and recoverable. These strains include both time-independent and time-dependent strains. The time-independent elastic strain is also referred to as initial or instantaneous strain.

The stress independent component of the inelastic strain is normally called shrinkage. This strain is partially reversible. The stress dependent irrecoverable strains include microcracking effects as well as shrinkage or drying creep resulting from moisture migration due to applied stress. The drying creep cannot be separated from the irreversible shrinkage.

The total creep strain consists of (a) Basic creep--delayed strain due to the interaction between solid and fluid phase, (b) Drying

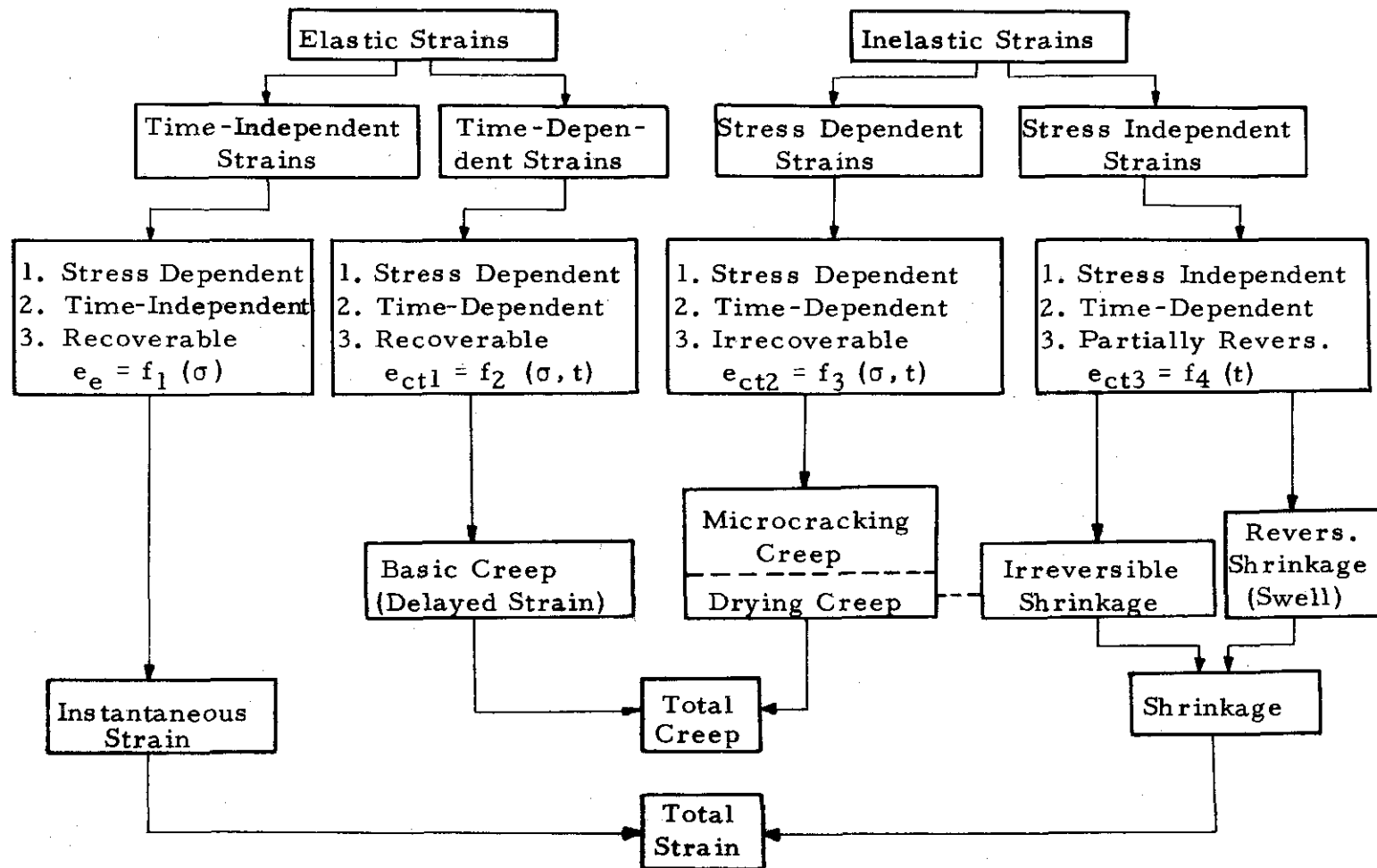


Fig. B1 Strain Components

creep--consolidation due to seepage of internal moisture, and (c) Microcracking creep--creep due to irrecoverable creep strains accompanying microcracking.

The recoverable strains may be time-independent (instantaneous recovery), time-dependent (delayed strain), or stress independent strain recovery (swelling). The independence of creep and shrinkage of concrete has yet to be established. However, creep and shrinkage occur simultaneously in concrete structures and, from a practical standpoint, these may be considered additive in nature. This independence is assumed through the use of companion stressed and unstressed specimens, so that the total time-dependent strain minus the free shrinkage strain is attributed to creep.

The prediction of time-dependent concrete strains is further complicated by the fact that strains and internal stresses are affected by the properties of the material as well as by curing and environmental conditions. A comprehensive study of time-dependent concrete strains includes a large number of variables. These variables are summarized in Figure B2. A detailed study of all these variables is beyond the scope of this report. However, with reference to the principal factors that effect time-dependent concrete strains, the following are considered in this report in the development of procedures for predicting creep and shrinkage:

### Parameters affecting Creep and Shrinkage Concrete Strains

- |                       |                     |                             |                        |
|-----------------------|---------------------|-----------------------------|------------------------|
| 1. Min. Memb. Thk.    | 5. Length of curing | 9. Environment temp.        | 12. No. of load cycles |
| 2. Water-Cement ratio | 6. Curing temp.     | 10. Time of init. load      | 13. Unloading period   |
| 3. Mix proportions    | 7. Curing humidity  | and time init. shrink-      | 14. Stress Distr.      |
| 4. Type of aggregate  | 8. Environment hum. | age considered              | 15. Stress magnitude   |
|                       |                     | 11. Duration of load period | 16. Stress rate        |

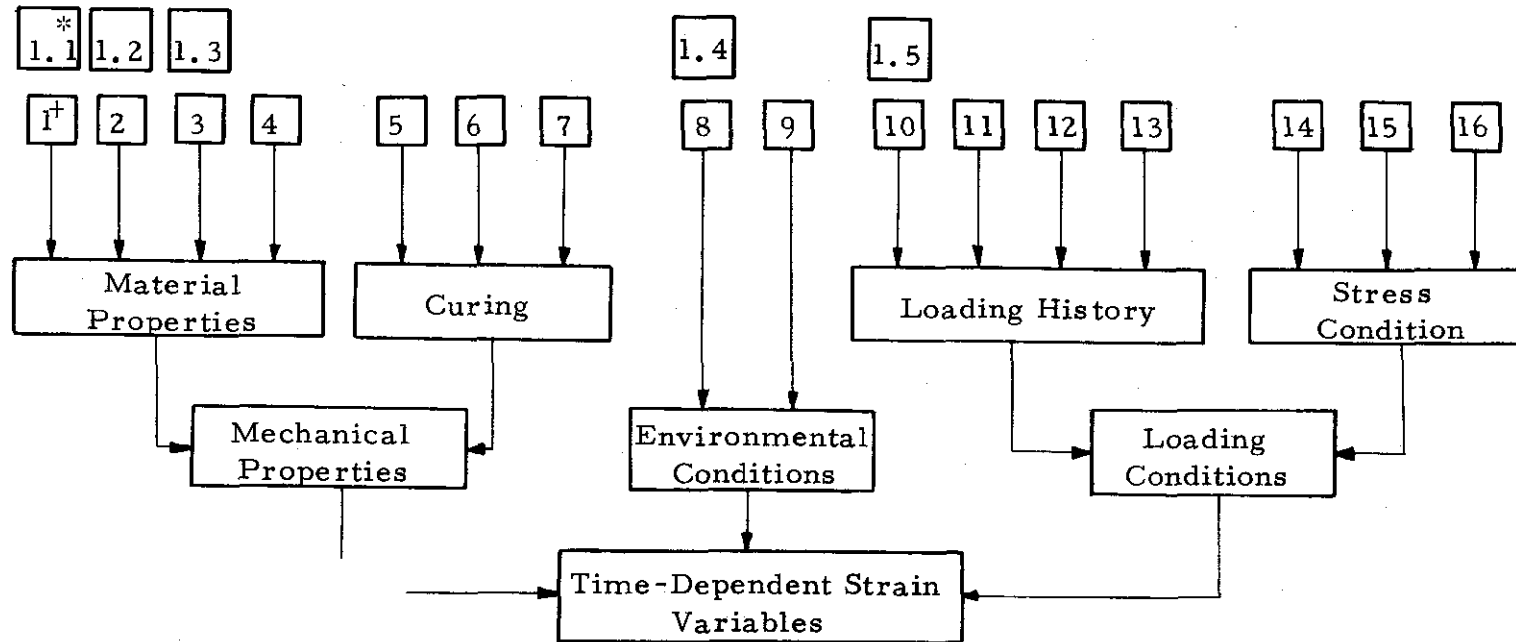


Figure B2. Time-Dependent Strain Variables

\* Parameters studied by Jones (15), and used in this report  
 † These numbers refer to the parameters listed above

- 1.1 Minimum thickness of member
- 1.2 Water-cement ratio in the form of slump and cement content
- 1.3 Mix proportions in the form of percent fines and air content
- 1.4 Environmental humidity
- 1.5 Time of initial loading and time initial shrinkage considered

Presented here is a summary of the principal variables that affect creep and shrinkage (10), (12), (13), (15), (18) in most cases. The corresponding nominal correction factors, based on the standard conditions herein, are given in the text and in Figure B3 (13), (15), (18). The results in Figure B3, and equations for these curves, were developed in Reference (18).

The following comments refer to the nominal correction factors for creep and shrinkage (from Figure B3), which are normally not excessive and tend to offset each other. For design purposes in most cases, these (except possibly for the effect of member size as discussed in the text) may normally be neglected:

Creep correction factors

Slump: C.F. = 0.95 for 2", 1.00 for 2.7", 1.02 for 3", 1.09 for 4", 1.16 for 5". Comment--Tends to be offset by effect of member thickness. May be marginal but normally can be neglected.  
Cement content (sacks/cu.yd.): C.F. = 1.00. No correction factor required for concrete of say 5 to 8 sacks per cu. yd. at least.  
Percent fines (by wt.): C.F. = 0.95 for 30%, 1.00 for 50%, 1.05 for 70%. Comment--Normally negligible.

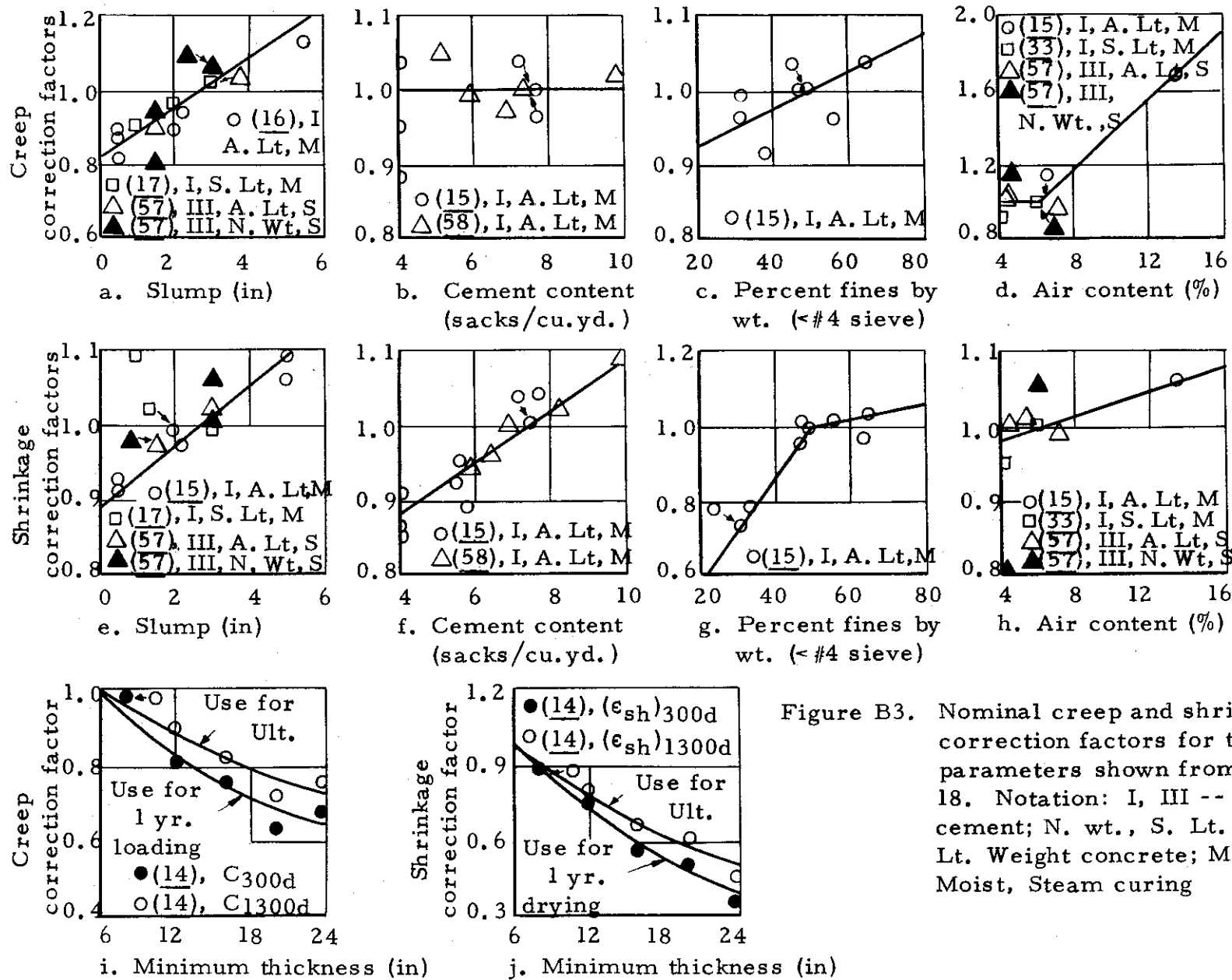


Figure B3. Nominal creep and shrinkage correction factors for the parameters shown from Ref. 18. Notation: I, III -- type cement; N. wt., S. Lt., A. Lt. Weight concrete; M, S -- Moist, Steam curing

Air content (in%): C.F. = 1.00 up to 6%, 1.09 for 7%, 1.17 for 8%.

Comment--Tends to be offset by effect of member thickness.  
May be neglected for say up to 7% air.

Minimum thickness of member: C.F. = 1.00 for 6" or less, 0.82 for 12". Comment--Tends to be offset by effect of slumps greater than 3" and air contents greater than 6%. Can normally be neglected for members up to about 10" to 12".

#### Shrinkage correction factors

Slump: C.F. = 0.97 for 2", 1.00 for 2.7", 1.01 for 3", 1.05 for 4", 1.09 for 5". Comment--Tends to be offset by effect of member thickness. Normally can be neglected.

Cement content (sacks/cu.yd.): C.F. = 0.87 for 4 sacks, 0.95 for 6 sacks, 1.00 for 7.5 sacks, 1.09 for 10 sacks. Comment--Normally negligible for say 5 to 8 sacks per cu. yd. at least.

Percent fines (by wet.): C.F. = 0.86 for 40%, 1.00 for 50%, 1.04 for 70%. Comment--May be marginal but normally can be neglected.

Air content (in %): C.F. = 0.98 for 4%, 1.00 for 6%, 1.03 for 10%.  
Comment--Normally negligible.

Minimum thickness of member: C.F. = 1.00 for 6" or less, 0.84 for 9". Comment--Tends to be offset by effect of slumps greater than 3". Can normally be neglected for members up to about 8" to 9" minimum thickness.

### APPENDIX C

Appendix C includes the details of the test beams from References (23), (24), (27), and (31). The loss of prestress and camber of these beams have been discussed in the text on the basis of the methods developed therein. Also included are the details of the test beams from References (41), (49), (54), and (56). The load-deflection response of these beams have been discussed in the text on the basis of the methods developed therein.

TABLE C1 PROPERTIES OF TEST BEAMS AT UNIVERSITY OF FLORIDA (23)

Beam	Cable Profile	Eccentricity <sup>a</sup>		Concrete Type	Curing Cond.	Loading Age	A <sub>s</sub> in <sup>2</sup>	F <sub>o</sub> (kip)	f' <sub>c</sub> rel (psi)	Conc. Stress <sup>b</sup>	
		End	Center							End (psi)	Center (psi)
1	STRT	2.16	2.31	Nr wt	MC	28d	1.32	57.9	5030	902	805
2	STRT	2.02	2.16	Nr wt	MC	28d	1.32	65.1	5030	982	891
3	STRT	2.20	2.44	Nr wt	MC	28d	1.32	101.5	5030	1602	1568
4	STRT	1.91	2.26	Nr wt	MC	28d	1.32	99.9	5030	1457	1460
5	STRT	2.00	2.35	Nr wt	MC	28d	1.32	142.1	5030	2115	2196
6	STRT	2.03	2.41	Nr wt	MC	28d	1.32	139.5	5030	2108	2184
7	STRT	1.97	2.22	Nr wt	MC	28d	1.32	93.6	3760	1383	1352
8	STRT	2.30	2.55	Nr wt	MC	28d	1.32	87.4	3760	1407	1365
9	STRT	2.33	2.41	Nr wt	MC	28d	1.32	90.0	3760	1461	1354
10	STRT	2.41	2.51	Nr wt	MC	28d	1.32	91.6	3760	1520	1416

<sup>a</sup> The eccentricities are measured values.

<sup>b</sup> These stresses refer to the steel cgs. and uses the measured values of F<sub>o</sub> and the net section properties (+) compression; (-) tension.

Remarks: All beams have a span= 19.5'; all bars are 3/4"  $\phi$  steel bars; composite slabs (26" x 3") were cast on beams 1, 4, 6, 8 & 10 at 101, 101, 101, 37 & 93 days after stressing. The steel bars (of E<sub>s</sub> = 26380 ksi) were not grouted. Beams 1-8 were stored in the lab at 75% humidity & 9-10 were stored in the field at 90% R.H. The mix had a cement content of 6-6.5 sacks/cu yd of Type I cement.

TABLE C2 PROPERTIES OF TEST BEAMS AT UNIVERSITY OF ILLINOIS (24)

Beam <sup>c</sup>	Cable Profile	Eccentricity <sup>a</sup>		Concrete Type	Curing Cond.	Loading Age	A <sub>s</sub> in <sup>2</sup>	F <sub>i</sub> (kips)	f' <sub>c</sub> rel (psi)	Conc. Stress <sup>b</sup>	
		End	Center							End (psi)	Center (psi)
MU-1	STR	1.03"	1.03"	Nr wt	MC	5 d	.18	26.9	3760	1285	1266
MU-2	STR	1.03"	1.03"	Nr wt	MC	5d	.18	26.9	3930	1230	1271

<sup>a</sup>All eccentricities are measured values.

<sup>b</sup>These stresses refer to the steel cgs and uses the stress diagram indicated in Reference (24)  
(+) Compression; (-) Tension.

<sup>c</sup>All beams were cast of Type III cement with a water-cement ratio of 0.74-0.76 and a ratio of (1:2.98:3.35) of cement, sand and gravel by wt.

Remarks: All beams have a span = 6', all wires are .196"  $\phi$  ( $E_s = 30 \times 10^3$  ksi). All beams were stored at 50% RH.

TABLE C3 PROPERTIES OF TEST BEAMS AT TEXAS A & M UNIVERSITY (27)

b Beam	Length	Span	Cable Profile	Eccentricity		Conc. Type	Curing Cond.	Load. Age	A <sub>s</sub> in <sup>2</sup>	F <sub>i</sub> (k)	f' <sub>c</sub> rel psi	Conc. Stress <sup>a</sup>	
				End	Center							End (psi)	Center (psi)
L1-5	40'	38.16'	STRT	9.19"	9.19"	Lt wt	SC	2d	1.75	304	4650	1387	1252
L4-5	56'	54.29'	HRPED	7.20"	9.60"	Lt wt	SC	1d	3.28	564	5540	2116	2322
R1-5	40'	38.16'	STRT	9.19"	9.19"	Lt wt	MC	2d	1.75	293	4820	1343	1207
R4-5	56'	54.29'	HRPED	5.82"	7.82"	Lt wt	MC	7d	3.93	670	5540	2223	2390
L3-5	56'	54.29'	HRPED	5.55"	9.05"	Nr wt	MC	2d	3.50	605	5260	2021	2366

<sup>a</sup> All concrete stresses are computed using F<sub>i</sub> and the transferred section properties. (+ compression), (- tension) and are at the steel cgs.

<sup>b</sup> All girders have the section designated as Type B by the Texas Highway Department.

Remarks: All strands are 7/16"  $\phi$  (E<sub>s</sub> = 28500 ksi) at an average humidity of 88%. The mix had a cement content of 7 - 7-1/2 sc/cu yd of Type III cement. All harping was at 5' from  $\phi$  of the girder.

TABLE C4 PROPERTIES OF TEST BEAMS AT UNIVERSITY OF MISSOURI (31)

Beam	Cable Profile	Eccentricity		Concrete Type	Curing Cond.	Load Age	$A_s$ in <sup>2</sup>	<sup>b</sup> $F_o$ k	$f'_c$ rel psi	Conc. Stress	
		End	Center							End (psi)	Center (psi)
East Girder	Parabolic	.83"	27.55"	Nr wt	MC	61d	2.65	452.4	5160	682	1440
<sup>a</sup> West Girder	Parabolic	.83"	27.55"	Nr wt	MC	37d	2.65	450.3	5190	--	--

<sup>a</sup> Data from West Girder not available in this reference.

<sup>b</sup> This force  $F_o$  is after el. losses and is the measured value of the force at the end. The value of  $F_o$  at the center has been estimated from the strain measurements. The steel had an ( $E_s = 28.8 \times 10^3$  ksi).

Remarks: Both girders had a span = 88'; slab cast at age of concrete of 146d, 54 no of 1/4"  $\phi$  strands; 3 diaphragms at 24'-10", 49'-6", 74'-2" from end; these are shared at 1/4, 1/2, 3/4 points and stored at 70%.

TABLE C5

<sup>a</sup> DETAILS OF BEAMS REPORTED BY ABELES (56)

Beam	Type of conc.	Area of steel $A_s$ (in <sup>2</sup> )	<sup>b</sup> Eff. prest. force $F_t'$ (kips)	Ecc. of prest. steel (in)	<sup>c</sup> Modulus of rupture $f_{cb}'$ (psi)	Meas. conc. strength $f_c'$ (psi)
AO1*	Nr wt	.2848	37.2	1.25	570	5725
AL1*	Lt wt	.2848	32.5	1.25	486	6600

<sup>a</sup> The beams were 4" x 9" in section and simply supported on a span of 13'-9". A two point loading symmetrical about the center line of beam (i.e., at a distance of 5' from either support) was used for the test.

<sup>b</sup> The value of the effective prestressing force is based on the reported magnitude of the effective prestress.

<sup>c</sup> The modulus of rupture was based on a value of  $6\sqrt{f_c'}$  for lightweight concrete and  $7.5\sqrt{f_c'}$  for normal weight concrete.

Remarks: .0712 in<sup>2</sup> of steel area was provided as compressive reinforcement for both beams. The measured steel stress at ultimate was 240 ksi.

TABLE C6

<sup>a</sup> DETAILS OF BEAMS REPORTED BY  
WARAWARUK, SOZEN & SIESS (41)

Beam	Area of steel, $A_s$ (in <sup>2</sup> )	Eff. Prestress force, $F_t$ (kips)	Ecc. of Prestress steel (in)	Modulus of rupture $f_{cb}$ , psi	Meas. conc. strength $f_c$ , psi
RB34.126	.362	40.6	3.08	543	5230
RB34.093	.211	24.1	3.06	472	3970
RB34.031	.091	10.8	3.00	544	5280

<sup>a</sup> The beams were 6" x 12" in section and simply supported on a span of 9'-0". A two point loading symmetrical about the center line of the beam (i. e., at a distance of 3'-0" from either support) was used for the test.

TABLE C7

DETAILS OF BEAMS REPORTED BY SHAIKH AND BRANSON (49)

All beams 6" by 8", All d = 6.5", All span = 15' simply supported												
Series No.	I			II			III			IV		
Beam No.	1	2	3	1	2	3	1	2	3	1	2	3
<sup>a</sup> Actual, $F_i$ (kips)	29.8	29.0	30.1	20.2	20.0	19.7	30.5	29.8	29.8	25.2	25.8	24.4
<sup>b</sup> $A_s$ (in <sup>2</sup> )	.173	.173	.173	.116	.116	.116	.173	.240	.240	.160	.160	.160
<sup>c</sup> $A'_s$ (in <sup>2</sup> )	.200	.400	.600	.058	.200	.400	0	0	.310	.080	.310	.600
<sup>d</sup> $f'_c$ in psi	5400			5890			6570			5880		
<sup>e</sup> Modulus of rupture, $f'_{cb}$ (psi)	806			855			894			830		

<sup>a</sup> The value of the effective prestress force,  $F_t$  was determined as  $F_i - \Delta F_t$  was determined using relationships developed in Reference (49).

<sup>b</sup> Refers to total tensile reinforcement (tensioned only).

<sup>c</sup> Refers to total non-tensioned tensile reinforcement.

<sup>d</sup> Refers to concrete strength at 28 days.

<sup>e</sup> Refers to modulus of rupture of concrete as measured from laboratory tests on plain concrete specimens.

TABLE C8

<sup>a</sup> DETAILS OF BEAMS REPORTED BY BURNS & SIESS (54)

Beam	<sup>b</sup> $A_s$ (in <sup>2</sup> )	Eccentricity	<sup>c</sup> $f'_{cb}$ (psi)	<sup>d</sup> $f'_c$ (psi)	<sup>e</sup> $f_y$ (psi)	Remarks
J9	1.58	8.00	510	4190	47.0	All beams had a span of 12'-0"; The reinforcing steel had an elasticity modulus of $30 \times 10^6$ psi.
J10	1.58	6.00	474	3590	45.1	
J11	1.58	4.00	505	4110	46.9	

<sup>a</sup> All beams had a width of 8". The total depth for beams J9, J10, and J11 was 20", 16" and 12" respectively. All beams were centrally loaded.

<sup>b</sup> Refers to the total tensile reinforcement.

<sup>c</sup> Refers to the modulus of rupture of concrete at the time of the test.

<sup>d</sup> Refers to the concrete strength at the time of the test.

<sup>e</sup> Refers to the yield strength of the reinforcement.

## APPENDIX D

Appendix D includes the details of the common cases of prestress moment profiles along with the formulas for computing camber.

APPENDIX D

COMMON CASES OF PRESTRESS MOMENT DIAGRAMS  
WITH FORMULAS FOR COMPUTING CAMBER

Prestressed Beam	$F_0 e$ Moment Diagram	Midspan Camber Due to $F_0 e$ Moments
		$(\Delta_1)_{F_0} = F_0 e L^2 / 8 E_{ci} I_g$
		$(\Delta_1)_{F_0} = F_0 e_c L^2 / 12 E_{ci} I_g$ $(\Delta_1)_{F_0} = \frac{F_0 (e_c - e_0) L^2}{12 E_{ci} I_g} + \frac{F_0 e_0 L^2}{8 E_{ci} I_g}$ $(\Delta_1)_{F_0} = \frac{F_0 (e_c + e_0) L^2}{12 E_{ci} I_g} - \frac{F_0 e_0 L^2}{8 E_{ci} I_g}$
		$(\Delta_1)_{F_0} = 5 F_0 e_c L^2 / 48 E_{ci} I_g$ $(\Delta_1)_{F_0} = \frac{5 F_0 (e_c - e_0) L^2}{48 E_{ci} I_g} + \frac{F_0 e_0 L^2}{8 E_{ci} I_g}$ $(\Delta_1)_{F_0} = \frac{5 F_0 (e_c + e_0) L^2}{48 E_{ci} I_g} - \frac{F_0 e_0 L^2}{8 E_{ci} I_g}$
		$(\Delta_1)_{F_0} = \frac{F_0 e_c}{E_{ci} I_g} \left[ \frac{L^2}{8} - \frac{a^2}{6} \right]$ $(\Delta_1)_{F_0} = \frac{F_0 (e_c - e_0)}{E_{ci} I_g} \left[ \frac{L^2}{8} - \frac{a^2}{6} \right] + \frac{F_0 e_0 L^2}{8 E_{ci} I_g}$ $(\Delta_1)_{F_0} = \frac{F_0 (e_c + e_0)}{E_{ci} I_g} \left[ \frac{L^2}{8} - \frac{a^2}{6} \right] - \frac{F_0 e_0 L^2}{8 E_{ci} I_g}$

APPENDIX E

Appendix E includes photographs of the laboratory specimens during the various stages of the experimental program.

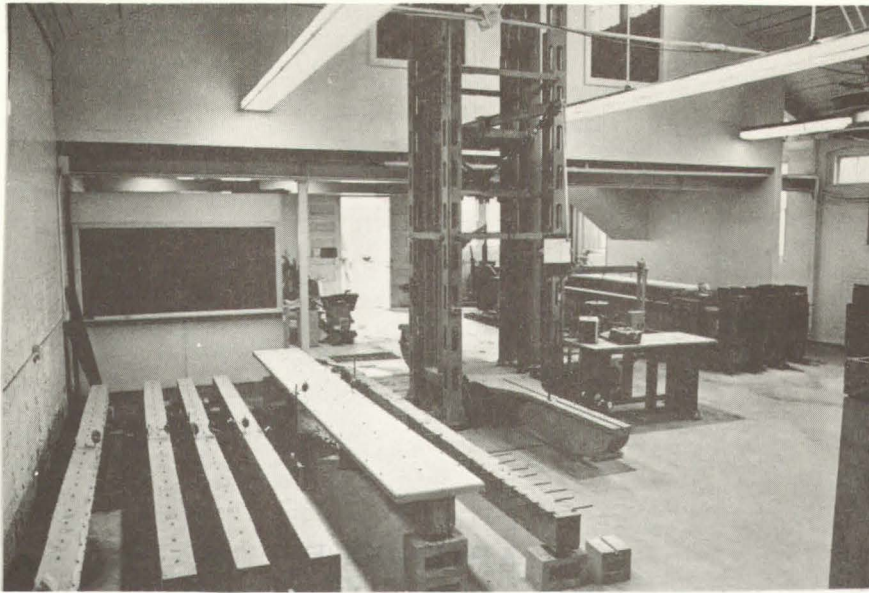


Figure E1 View of laboratory showing beams in foreground and prestressing bed containing additional beams at right.

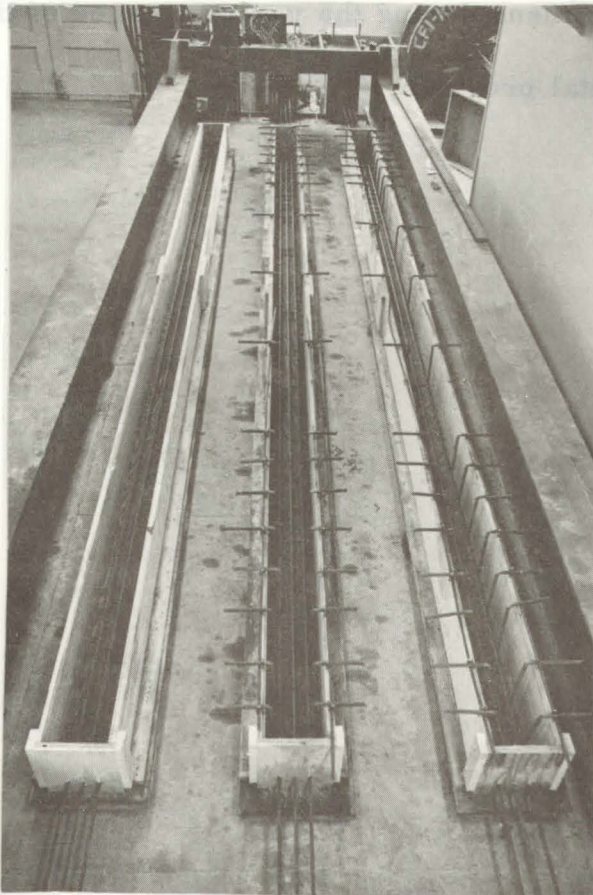


Figure E2 Forms for beams in prestressing bed

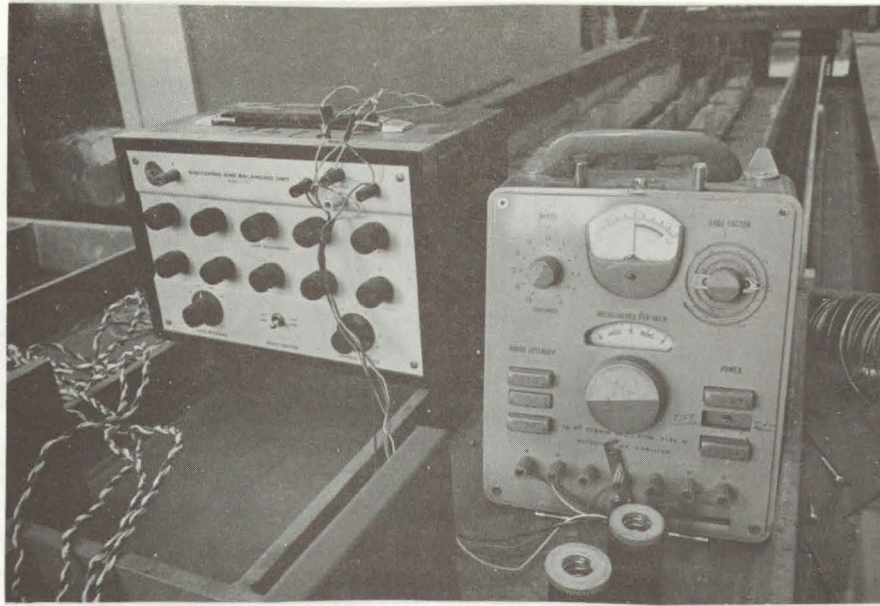


Figure E3 Strain gage indicator and switching and balancing unit used with load cells to measure prestress force

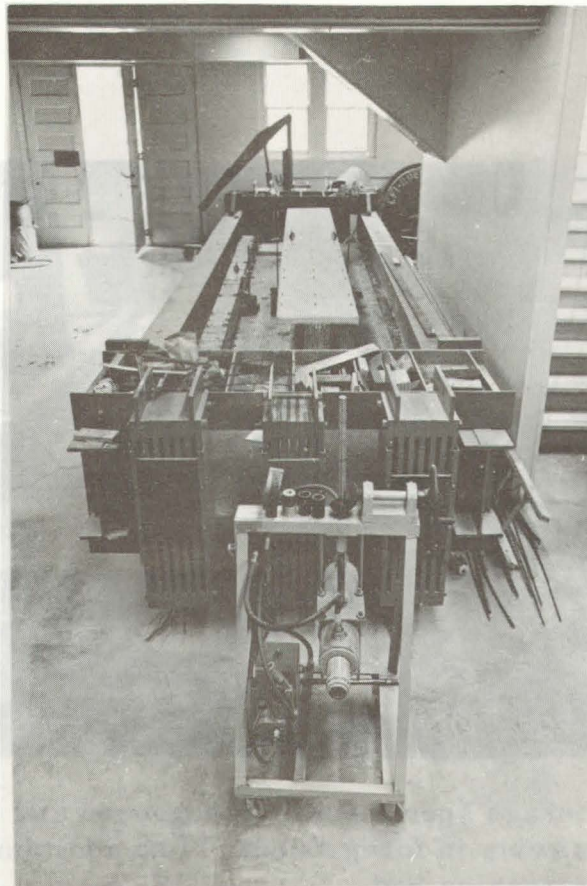


Figure E4 Prestressing bed, jacking equipment and beams stored in bed

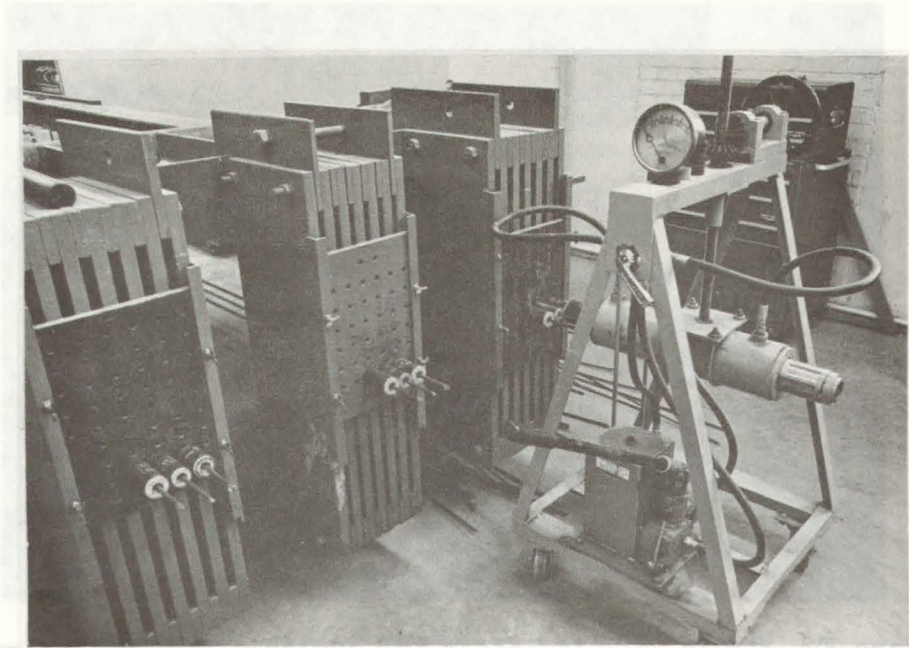


Figure E5 Close-up of jacking equipment, bulkheads, and grips

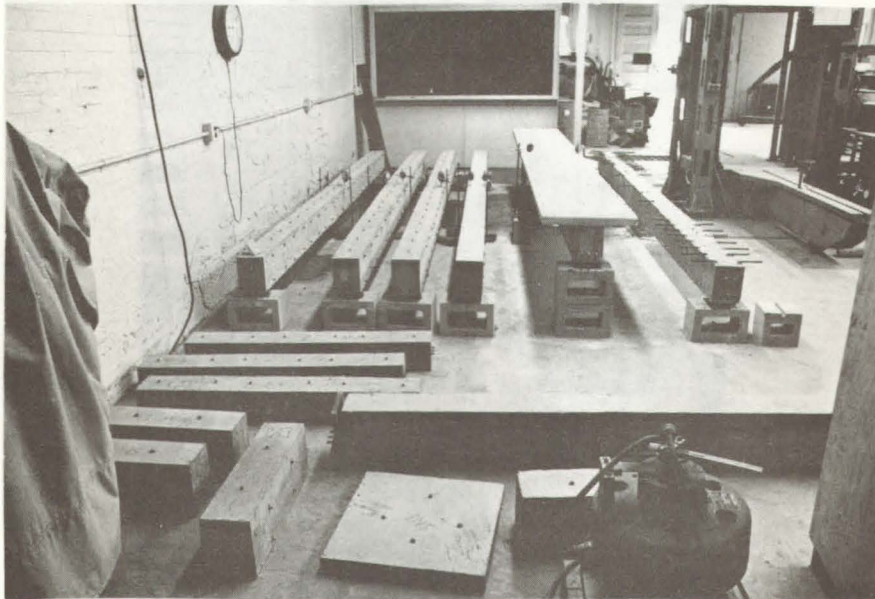


Figure E6 Shrinkage specimens in foreground and 7 beams (1 beam crosswise in foreground). Two additional beams in prestressing bed

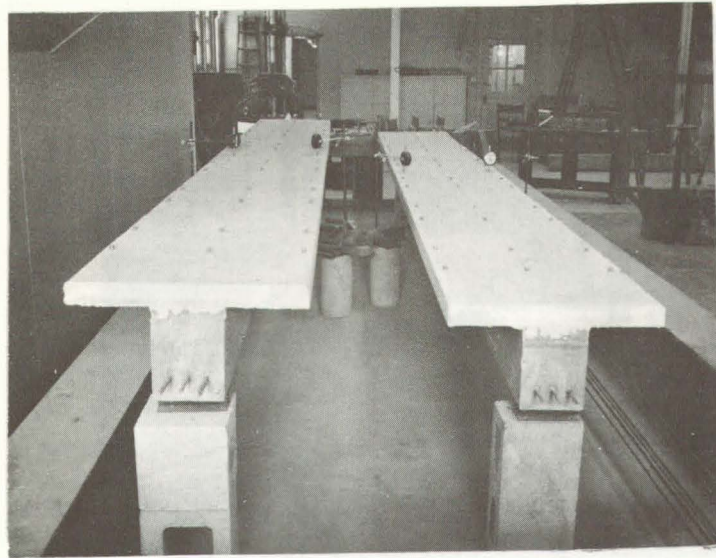


Figure E7 Two of 4 composite beams. Strain gage points and dial gages can be seen. Strands used in relaxation tests are seen at right

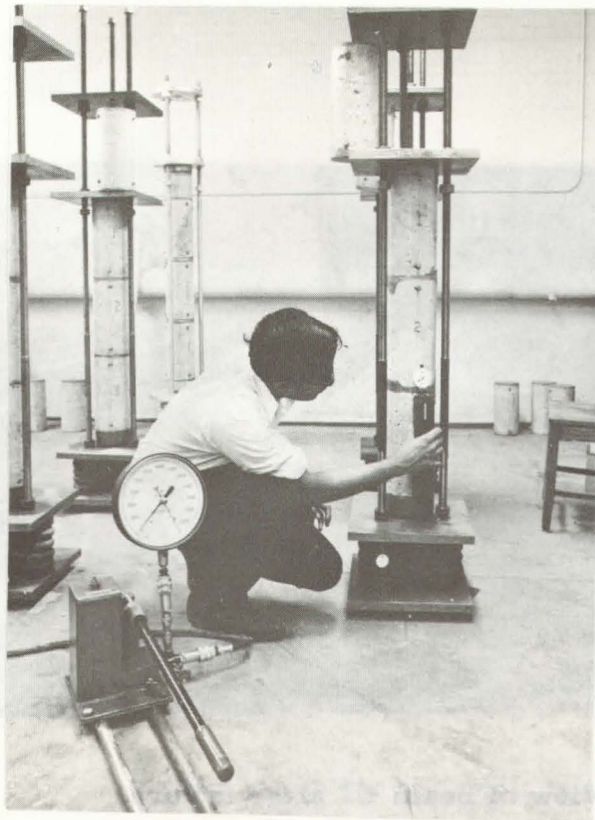


Figure E8 Cylinders loaded in creep racks and Whittemore gage used to measure strains of beams and shrinkage and creep specimens

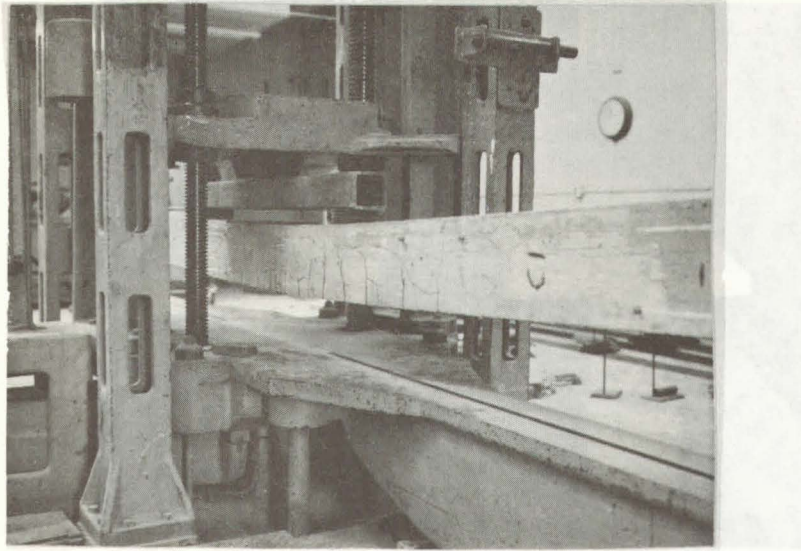


Figure E9 View of beam C1 showing the crack pattern prior to failure

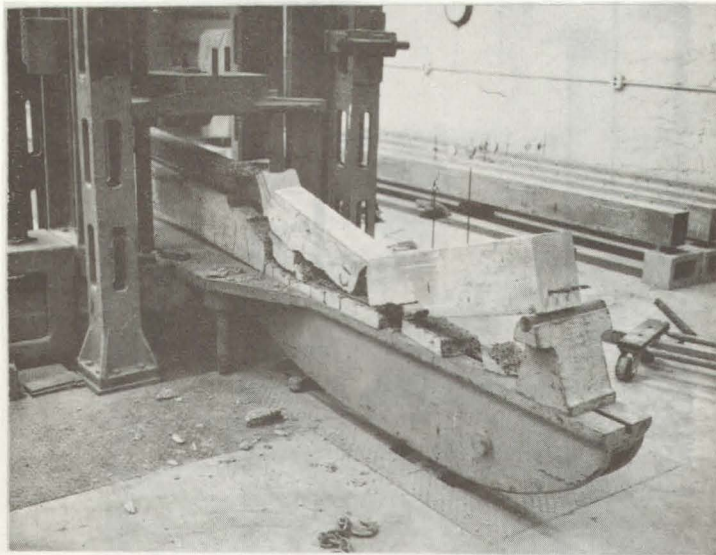
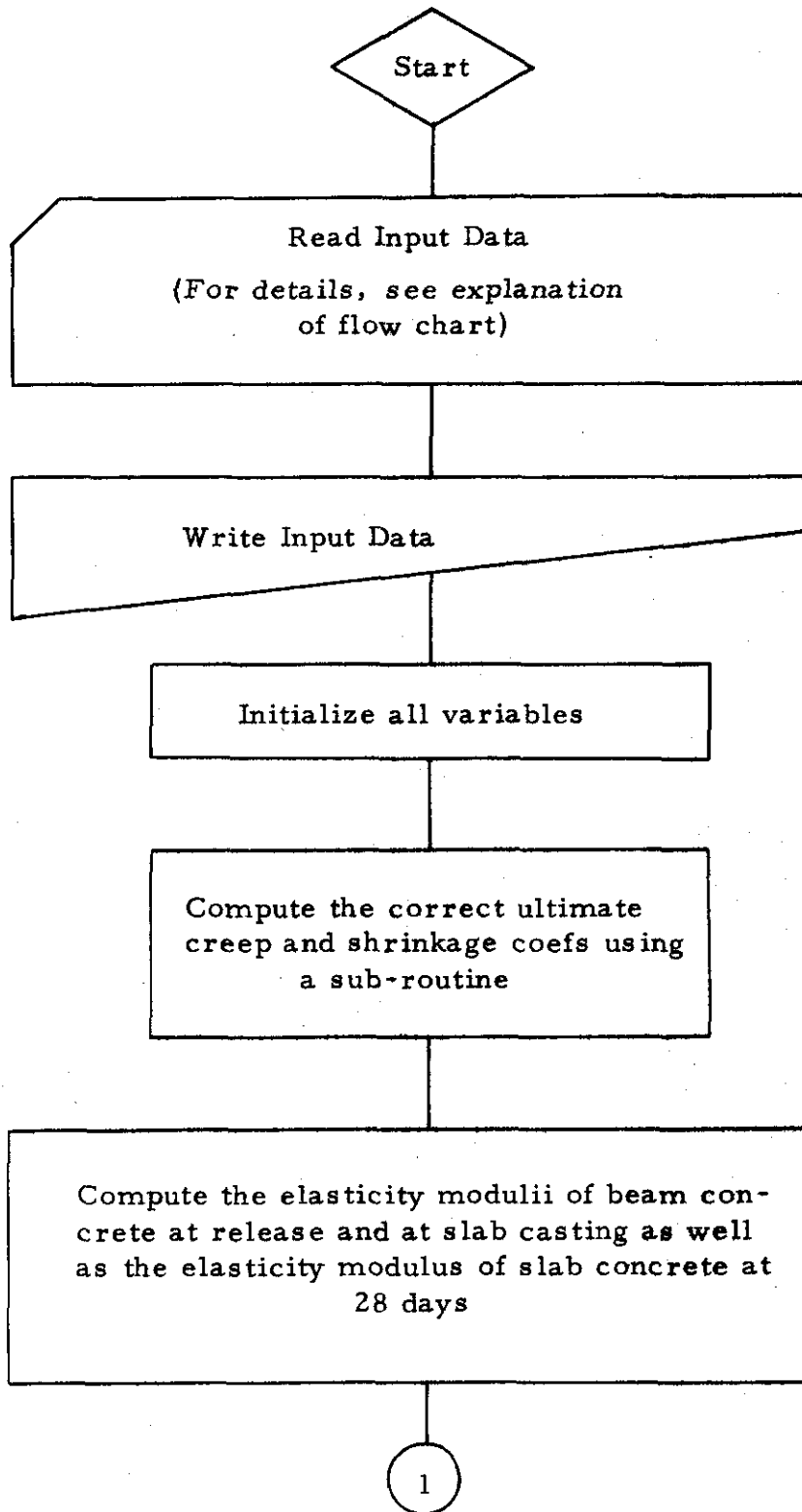


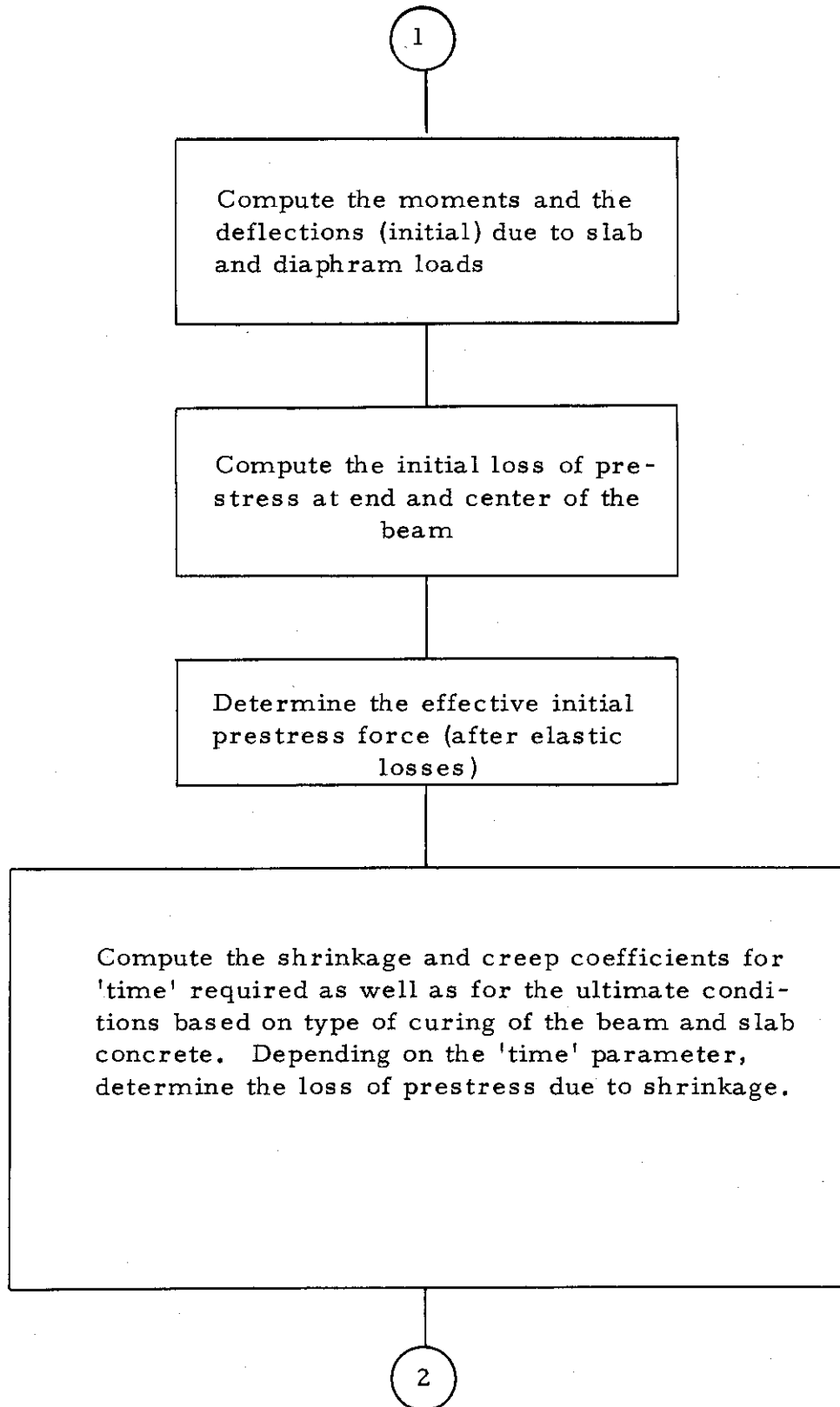
Figure E10 View of beam C1 after failure

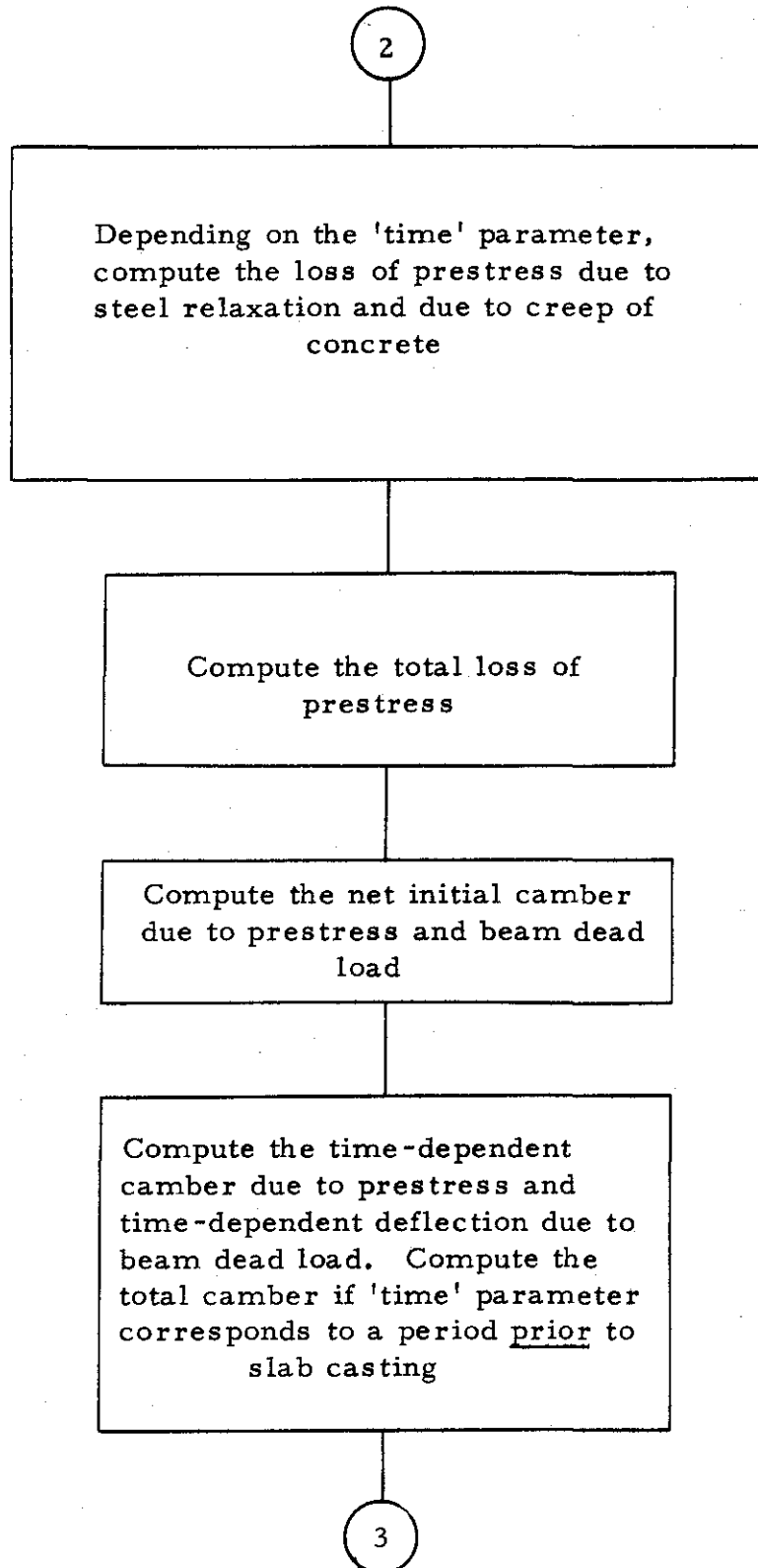
APPENDIX F

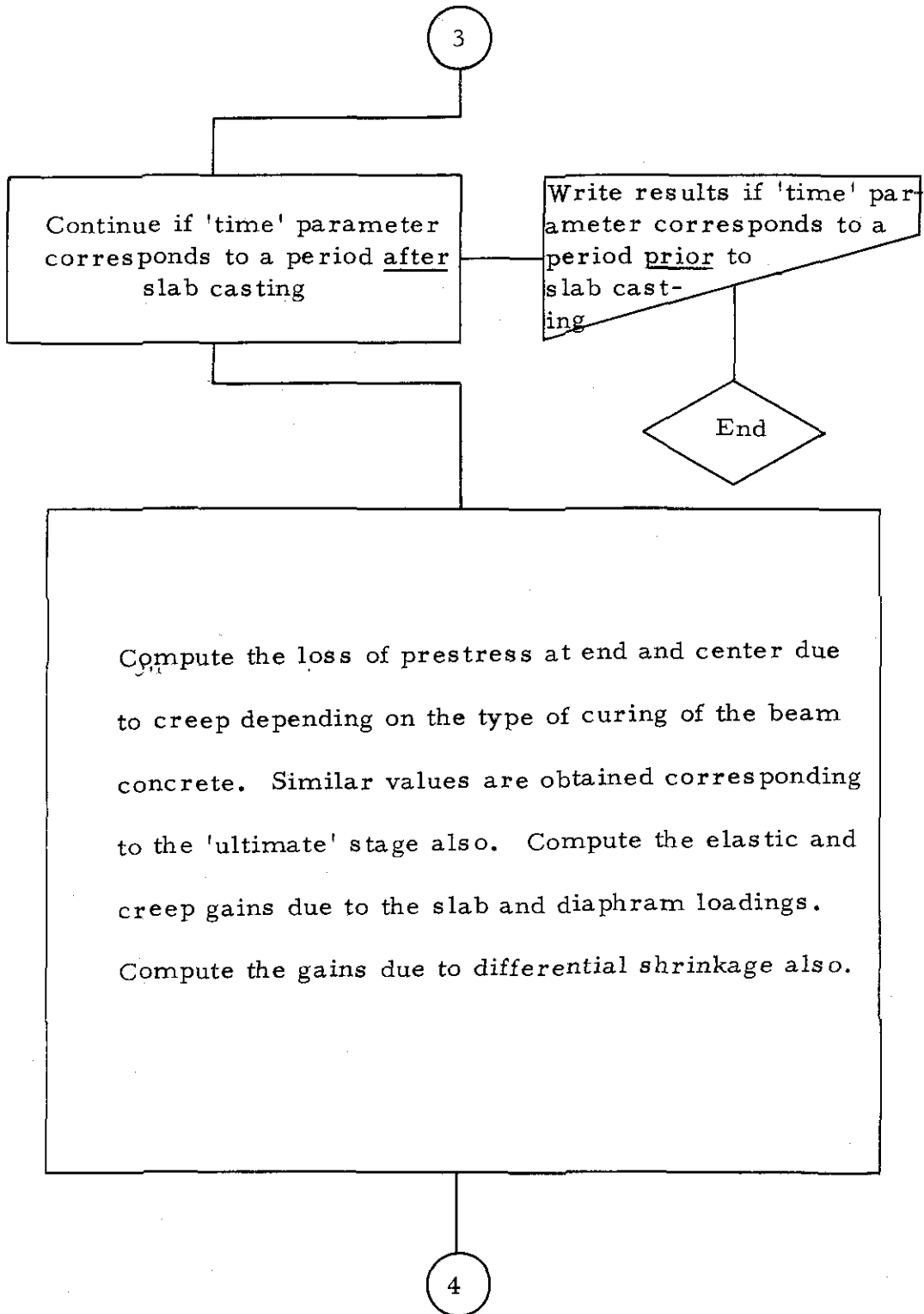
Appendix F includes the following:

- (i) A 'loss of prestress and camber' flow chart, its explanation and a typical computer output for interior girder No. 153.
- (ii) A 'load-deflection' flow chart, its explanation and a typical computer output for laboratory beam A1.









4

Compute the total loss of prestress corresponding to the 'time' parameter and the 'ultimate' stage

Compute the initial camber due to prestress, the initial deflection due to beam dead load and time-dependent camber and deflection prior to and after slab casting due to prestress and beam dead load respectively. Also compute the time-dependent deflection due to slab plus diaphragm loading. Determine the deflection due to differential shrinkage and then the total camber corresponding to the 'time' parameter and the 'ultimate' stage.

Write results of analysis

End

## EXPLANATION OF FLOW CHART FOR LOSS AND CAMBER

<u>SL No.</u>	<u>Explanation</u>
1-21	The read-in data includes the unit weight of beam concrete, unit weight of slab concrete, beam concrete strength at release, beam concrete strength at 28 days, slump of beam concrete, slab concrete strength at 28 days, ultimate shrinkage coefficient of slab concrete, elasticity modulus of prestressing steel, gross properties of the beam section, initial prestressing force, ultimate creep and shrinkage coefficients of beam concrete (referred to standard conditions), thickness and gross area of slab section, relative humidity, age of beam concrete at release of prestress and at slab casting, identifiers for type of curing and type of cement for beam concrete, diaphragm loading and diaphragm deflection, composite section properties, time parameter, and the correction factors for creep and shrinkage coefficients for the 'ultimate' stage.
22-50	Write input data.
51-96	Initialize all variables.
97-98	Compute the correct ultimate creep and shrinkage coefficients using a sub-routine.
99-115	Compute the elasticity moduli of beam concrete at release and at slab casting as well as the elasticity modulus of slab concrete at 28 days.
116-120	Compute the moments and the deflections (initial) due to slab and diaphragm loads.
121-134	Compute the initial loss of prestress at end and center of the beam.
135-139	Determine the effective initial prestress force (after elastic losses).
140-190	Compute the shrinkage and creep coefficients for 'time' required as well as for the ultimate conditions based on type of curing of the beam and slab concrete. Depending

on the 'time' parameter, determine the loss of prestress due to shrinkage.

- 191-209 Depending on the 'time' parameter, compute the loss of prestress due to steel relaxation and due to creep of concrete.
- 210-213 Compute the total loss of prestress.
- 214-225 Compute the net initial camber due to prestress and beam dead load.
- 226-237 Compute the time-dependent camber due to prestress and time-dependent deflection due to beam dead load. Compute the total camber if 'time' parameter corresponds to a period prior to slab casting.
- 238-307 Compute the loss of prestress at end and center due to creep depending on the type of curing of the beam concrete. Similar values are obtained corresponding to the 'ultimate' stage also. Compute the elastic and creep gains due to the slab and diaphragm loadings. Compute the gains due to differential shrinkage also.
- 308-352 Compute the initial camber due to prestress, the initial deflection due to beam dead load and time-dependent camber and deflection prior to and after slab casting due to prestress and beam dead load respectively. Also compute the time-dependent deflection due to slab plus diaphragm loading. Determine the deflection due to differential shrinkage and then the total camber corresponding to the 'time' parameter and the 'ultimate' stage.
- 353-386 Write results of analysis.
- 389-467 This is a sub-routine to apply correction factors for the ultimate values of creep and shrinkage coefficients.

```

$JOB 'KRIPA'
1  COMMON/CNE/CU,ESHU,CUM,CUS,CUMS,CUSS,ESHUS,TESHU,TI,TS,TK1,H,
  *ESHUM,10,S1,CGR4,SCR4,CORIT,CORT
2  READ(5,110)TIME,COPT,CCRTT
3  READ(5,100)W1,FCR,FC128,S1
4  READ(5,110)W2,FC228,TESHU
5  READ(5,102)ESI
6  READ(5,103)AG,G1,EE,EC,SP,AS,TK1,HP,R,DCGC
7  READ(5,102)FI
8  READ(5,105)CU,ESHU
9  READ(5,105)TK2,AG2
10 READ(5,102)H
11 READ(5,105)TI,TS
12 READ(5,109)ID,I10
13 READ(5,105)CLDM,DEFCM
14 READ(5,103)CII,YCCS,ECC,ECE,RATIO
15 102 FORMAT(F15.2)
16 103 FORMAT(5F15.5)
17 105 FORMAT(2F10.2)
18 109 FORMAT(2I3)
19 100 FORMAT(4F10.2)
20 101 FORMAT(6F10.2)
21 110 FORMAT(3F10.2)
22 WRITE(6,22555)
23 22555 FORMAT(1H1)
24 WRITE(6,33333)
25 33333 FORMAT(1H,14X,'INPUT DATA '///)
26 WRITE(6,2200)
27 2200 FORMAT(1H,10X,'BEAM CONCRETE '///)
28 WRITE(6,201)W1,FCR,FC128,S1
29 201 FORMAT(1H,3X,'UNIT WT. (PCF) *F25.2//
  *4X,'CONC. STR. AT REL. (PSI) *F14.2//
  *4X,'CONC. STR. AT 28-DAY (PSI) *F14.2//
  *4X,'CONC. SLUMP (INCHES) *F14.2//)
30 WRITE(6,2201)
31 2201 FORMAT(1H,10X,'SLAB CONCRETE '///)
32 WRITE(6,203)W2,FC228
33 203 FORMAT(1H,3X,'UNIT WT (PCF) *F25.2//
  *4X,'CONC. STRN. (PSI) *F14.2//)
34 WRITE(6,204)
35 204 FORMAT(1H,10X,'BEAM SECTION '///)
36 WRITE(6,205)AG,G1,EE,EC,SP,AS,TK1,HP,FI,ESI,CORT,CCRTT
37 205 FORMAT(1H,3X,'GROSS AREA (IN**2)*F25.2//
  *4X,'GROSS MI (IN**4) *F14.2//
  *4X,'ECC. AT END (IN) *F14.2//
  *4X,'ECC. AT CTR (IN) *F14.2//
  *4X,'SPAN (FT) *F14.2//
  *4X,'STEEL AREA (IN**2) *F14.2//
  *4X,'LEAST DIM OF MEMB. (IN) *F14.2//
  *4X,'HAPPING DIST. (FT) *F14.2//
  *4X,'INITIAL PREST. FORCE (KIPS) *F14.2//
  *4X,'ELASTICITY MODULUS (KSI) *F14.2//
  *4X,'ULT. THK. CORR. FACTOR FOR CRP *F14.2//
  *4X,'ULT. THK. CORR. FACTOR FOR SHRK *F14.2//)
38 WRITE(6,206)
39 206 FORMAT(1H,1X,'SLAB SECTION '///)
40 WRITE(6,207)TK2,AG2,CLDM,DEFCM
41 207 FORMAT(1H,3X,'SLAB THK. (IN) *F25.2//
  *4X,'SLAB AREA (IN**2) *F14.2//
  *4X,'CLM DUE TO DIAPH. (IN-KIPS) *F14.2//

```

```

      *4X,'DEF. DUE TO DIA. (IN)          'F14.2//)
42      WRITE(6,208)
43      208 FORMAT(1H ,10X,'T I M E - D E P E N D E N T F A C T O R S'////)
44      WRITE(6,209)T1,TS,H
45      209 FORMAT(1H ,3X,'OM AGE AT REL (DAY)'F24.2//
      *4X,'AGE OF BM AT SLAB CAST(DAYS)'F14.2//
      *4X,'AVERAGE REL. HUM. (0/0)      'F14.2//)
46      WRITE(6,400)
47      400 FGMAT(1H ,10X,'C O M P .   S E C T .   D E T A I L S'////)
48      WRITE(6,401)C11,YCCS,ECC,ECE,RATIC
49      401 FORMAT(1H ,3X,'COMP. MI (IN**4) 'F25.2//
      *4X,'ECC. OF DIFF. FORCE (IN)      'F14.2//
      *4X,'CGS DIST AT END (IN)         'F14.2//
      *4X,'CGS DIST AT CTR (IN)        'F14.2//
      *4X,'RATIO I2/IC                  'F14.2//)
50      66667 FOPMAT(1H1)
51      CZE=0.
52      ESLE1=0.
53      ESHENT=0.
54      CLEBS1=0.
55      CLEAS1=0.
56      CSEULT=0.
57      DFR1=0.
58      DFRULT=0.
59      EGE=0.
60      CGSE1=0.
61      GLELLT=0.
62      PGCE1=0.
63      PRAY2=0.
64      TL1=0.
65      TLEULT=0.
66      C3C=0.
67      ESHLC1=0.
68      ESHCNT=0.
69      CLCBS1=0.
70      CLCAS1=0.
71      CSCLLT=0.
72      EGCI=0.
73      GLCCLT=0.
74      CGSCI=0.
75      PRAY1=0.
76      PGCC1=0.
77      TLCULT=0.
78      TL2=0.
79      DELTA1=0.
80      DELTA2=0.
81      TERM31=0.
82      ULTA2=0.
83      TERM41=0.
84      ULTSP=0.
85      TERM51=0.
86      ULTA4=0.
87      TERM61=0.
88      ULTA9=0.
89      TERM71=0.
90      ULTA6=0.
91      TERM81=0.
92      ULTA3=0.
93      TERM91=0.
94      ULTA1=0.

```

```

95      D1=0.
96      ULT=0.
97      T=TIME
98      CALL CRCEP
99      ECI=33.*W1**1.5*FCR**0.5/1000.
100     ESLAR=33.*W2**1.5*FC223**0.5/1000.
101     IF(110-1)1,2,2
102     1 IF(110-1)4,5,5
103     4 FCS=FC126*TS/(1.+0.95*TS)
104     ECS=33.*W1**1.5*FCS**0.5/1000.
105     GC TO 3
106     5 FCS=FC126*TS/(0.70+0.98*TS)
107     ECS=33.*W1**1.5*FCS**0.5/1000.
108     GC TO 3
109     2 IF(110-1)6,7,7
110     6 FCS=FC128*TS/(4.0+0.95*TS)
111     ECS=33.*W1**1.5*FCS**0.5/1000.
112     GC TO 3
113     7 FCS=FC128*TS/(2.3+0.92*TS)
114     ECS=33.*W1**1.5*FCS**0.5/1000.
115     3 CONTINUE
116     W2=W2*AG2/144.
117     DLSM=W2*SP*SP*1.5/1000.
118     DELTAS=15.*PLS**SP*SP/(GI*ECS)
119     DELL=DELTAS+DEFDM
120     DELM=DLSM+ELDM
121     TN=ESI/ECI
122     FSI=F1/AS
123     AT=AG+(TN-1.)*AS
124     GIE=GI+(TN-1.)*AS*EE*EE
125     GIC=GI+(TN-1.)*AS*EC*EC
126     C=F1/AT
127     C1E=F1*EE*EE/GIE
128     C2E=TN*(C+C1E)*100./FSI
129     C1C=F1*EC*EC/GIC
130     W1=W1*AG/144.
131     C2C=W1*SP*SP*12.*EC/(1800.*GIC)
132     C3C=TN*(C+C1C-C2C)*100./FSI
133     FCC=F1-(C3C*AS*FSI/100.)
134     FCE=F1-(C2E*AS*FSI/100.)
135     IF(HP-0.)700,700,701
136     700 FC=0.5*(FCE+FCC)
137     GC TO 702
138     701 FQ=FCC
139     702 CONTINUE
140     WRITE(6,66667)
141     WRITE(6,66669)
142     66669 FORMAT(1H ,10X,' I N I T I A L S T A T E ' //)
143     IF(TS-30.)750,750,751
144     750 TSK=TS*0.1/30.
145     GC TO 760
146     751 IF(TS-180.)752,752,753
147     752 TSK=0.1+(TS-30.)*0.1/150.
148     GC TO 760
149     753 IF(TS-(5.*360.))754,754,755
150     754 TSK=0.2+(TS-180.)*0.05/1620.
151     GC TO 760
152     755 TSK=0.25
153     760 CONTINUE
154     IF(10-1)703,704,704

```

```

155 703 CT=CUS*(T**0.6)/(10.+(T**0.6))
156 PRY=(TS-TI)**0.6
157 CTIT=CUS*PRY/(10.+PRY)
158 TCCT1=(T+TI-2.5)/(55.+T+TI-2.5)
159 TCCT2=(TI-2.5)/(55.+TI-2.5)
160 TCCT=(TCCT1-TCCT2)*10.**(-6.0)
161 ESHI=ESHUM*TCCT
162 TCCT3=(TS-2.9)/(55.+TS-2.5)
163 TCCT4=(TCCT3-TCCT2)*10.**(-6.0)
164 ESHISS=TCCT4*ESHUM
165 TCCTS=(1.-TCCT2)*10.**(-6.0)
166 GC TC 705
167 704 PRY=T**0.6
168 CT=CUM*PRY/(10.+PRY)
169 PRY1=(TS-TI)**0.6
170 CTI1=CUM*PRY1/(10.+PRY1)
171 TCCT1=(T+TI-7.)/(35.+T+TI-7.)
172 TCCT2=(TI-7.)/(35.+TI-7.)
173 TCCT=(TCCT1-TCCT2)*10.**(-6.0)
174 ESHI=ESHUM*TCCT
175 TCCT3=(TS-7.)/(35.+TS-7.)
176 TCCT4=(TCCT3-TCCT2)*10.**(-6.0)
177 ESHISS=TCCT4*ESHUM
178 TCCTS=(1.-TCCT2)*10.**(-6.0)
179 705 CONTINUE
180 P=AS/AG
181 TKS1=1.+AG*EE*EE/GI
182 TKS2=1.+AG*EC*EC/GI
183 T11=TN*P*TKS1
184 T12=TN*P*TKS2
185 ESHLE1 =ESH*ESI*100./(FSI*(1.+T11))
186 ESHLC1 =ESH*ESI*100./(FSI*(1.+T12))
187 ESSTSC=ESHISS*100.*ESI/(FSI*(1.+T12))
188 ESSTSE=ESHISS*100.*ESI/(FSI*(1.+T11))
189 ESHCMT=ESHUM*TCCTS*ESI*100./(FSI*(1.+T11))*CORIT/SCR4
190 ESHCMT=ESHUM*TCCTS*ESI*100./(FSI*(1.+T12))*CORIT/SCR4
191 TI=T*24.
192 CFR1 =1.5*ALOG10(TI)
193 T212=TS*24.
194 CFR2=1.5*ALOG10(T212)
195 CFRULL=7.5
196 IF(T-(TS-TI))706,706,707
197 706 IF(T-30.)708,708,709
198 708 TKK=T*0.1/30.
199 GC TC 710
200 709 IF(T-150.)711,711,712
201 711 TKK=0.1+(T-30.)*0.1/150.
202 GC TC 710
203 712 IF(T-(5.*300.))713,713,714
204 713 TKK=0.2+(T-150.)*0.05/1620.
205 GC TC 710
206 714 TKK=0.25
207 710 CONTINUE
208 CLC1=CCT*CT*(1.-(TKK/2.0))
209 CLC1=C3C*CT*(1.-(TKK/2.0))
210 CLCPSI=CLC1
211 CLCPS1=CLC1
212 TL1=C2C+CLC1+ESHLE1+CFR1
213 TL2=C3C+CLC1+ESHLC1+CFR1
214 IF(TP)715,715,716

```

```

215 715 DELTA=FC*EC*SP*SP*144./(R.*ECI*GI)
216 GC TO 725
217 716 CONTINUE
218 CRY1=EC*SP*SP/R.
219 CRY2=(EC-EE)*HP*HP/6.
220 CRY=CRY1-CRY2
221 DELTA1=F0*144.*CRY/(ECI*GI)
222 725 CONTINUE
223 DLN=W1*SP*SP*1.5/1000.
224 DELTA2=15.*DLN*SP*SP/(GI*ECI)
225 DELTA=DELTA1-DELTA2
226 F01=F1/F0
227 IF(HP-0.)726,726,727
228 726 DFI=(TL1+TL2-C2E-C3C)*0.5
229 GC TO 728
230 727 DFI=TL2-C3C
231 728 CONTINUE
232 DFI=DFI*F01/100.
233 TERM11 =(-DFI+(1.-(DFI/2.0))*CT)*DELTA1
234 TERM22 =-CT*DELTA2
235 DI=DELTA+TERM11+TERM22
236 TERM31=TERM11
237 TERM31=TERM22
238 GC TO 9999
239 707 CONTINUE
240 IF(T-30.)730,730,731
241 730 TKK=T*0.1/30.
242 GC TO 740
243 731 IF(T-180.)732,732,733
244 732 TKK=0.1+(T-30.)*0.1/150.
245 GC TO 740
246 733 IF(T-(5.*360.))734,734,735
247 734 TKK=0.2+(T-180.)*0.05/1620.
248 GC TO 740
249 735 TKK=0.25
250 740 CONTINUE
251 COMP=CUM*CRT/CCR4
252 CCSP=CUS*CRT/CCR4
253 CLCBS1 =C2E*CTTT*(1.-(TSK/2.))
254 CLCAS1 =C3C*CTTT*(1.-(TSK/2.))
255 CLCAS1 =C2E*(CT-CTTT)*(1.-(TSK+TKK)/2.)*RATIO
256 CLCAS1 =C3C*(CT-CTTT)*(1.-(TSK+TKK)/2.)*RATIO
257 CLELLT=C2E*(COMP-CTTT)*(1.-(0.25+TSK)/2.)*RATIO
258 CLCULT=C3C*(CCSP-CTTT)*(1.-(0.25+TSK)/2.)*RATIO
259 CSEULT=C2E*(COSP-CTTT)*(1.-(0.25+TSK)/2.)*RATIO
260 CSCULT=C3C*(CCSP-CTTT)*(1.-(0.25+TSK)/2.)*RATIO
261 EGE=0.
262 FGC1 =-ESI*DELM*EC*100./(ECS*GI*FS1)
263 IF(ID-1)770,771,771
264 770 CT5=CUS*(1-(TS-TI))*0.6/(10.+(T-TS+TI))*0.6)
265 GC TO 775
266 771 CT5=CUSS*(T-TS+TI))*0.6/(10.+(T-TS+TI))*0.6)
267 775 CONTINUE
268 CGSE1 =EGE*CT5*RATIO
269 CGSC1=EGC1*CT5*RATIO
270 CGELLT=EGE*CUSS*RATIO*CRT/CCR4
271 CGCULT=EGC1*CUMS*RATIO*CRT/CCR4
272 GLELLT=EGE*CUMS*RATIO*CRT/CCR4
273 GLCULT=EGC1*CUMS*RATIO*CRT/CCR4
274 IF(ID-0)780,780,781

```

```

275 780 TRY1=(T-TS+TI)/(35.+T-TS+TI)
276 TRY2=(TS-2.5)/(55.+TS-2.5)
277 TRY22=(T+TI-2.5)/(55.+T+TI-2.5)
278 DIFF1=ESHUS*TRY1-ESHUM*(TRY22-TRY2)*CORTT/SCR4
279 PRI=ESHUS-ESHUM*(1.-TRY2)*CORTT/SCR4
280 GO TO 790
281 781 CONTINUE
282 TRY1=(T-TS+TI)/(35.+T-TS+TI)
283 TRY3=(TS-7.)/(35.+TS-7.)
284 TRY32=(T+TI-7.)/(35.+T+TI-7.)
285 DIFF1=ESHUS*TRY1-ESHUM*(TRY32-TRY3)*CORTT/SCR4
286 PRI=ESHUS-ESHUM*(1.-TRY3)*CORTT/SCR4
287 790 CONTINUE
288 PRII=ABS(PRI)*(10.**(-6.0))
289 DIFF=ABS(DIFF1)*(10.**(-6.0))
290 CULT=ESLAB*PRII*AG2*ESLAB/(3.*ECS)
291 Q=ESLAB*DIFF*AG2*ESLAB/(3.*ECS)
292 PGDC1 =-ESI*Q*YCCS*ECC*100./(ECS*CII*FSI)
293 PGCE1 =-ESI*Q*YCCS*ECE*100./(ECS*CII*FSI)
294 PRAY2=-ESI*QULT*YCCS*ECE*100./(ECS*CII*FSI)
295 PRAY1=-ESI*QULT*YCCS*ECC*100./(ECS*CII*FSI)
296 TL1=C2E+CLEBS1+CLEAS1+ESHLE1+DFR1+EGE+CGSE1+PGDE1
297 TL2=C3C+CLCHS1+CLCAS1+ESHLC1+DFR1+EGC1+CGSC1+PGDC1
298 IF(JD-1)7788,7789,7789
299 7788 TLEULT=C2E+CLEBS1 +CSEULT+ESHENT+DFRULT+EGE+GLEULT+PRAY2
300 TLCULT=C3C+CLCHS1 +CSCULT+ESHENT+DFRULT+EGC1 +GLCULT+PRAY1
301 GO TO 7790
302 7789 CSEULT=CLEULT
303 CSCLLT=CLCULT
304 GLEULT=CSEULT
305 GLCULT=CSCLLT
306 GO TO 7788
307 7790 CONTINUE
308 IF(HP-0.)#00,800,801
309 800 DELTA1=FO*EC*SP*SP*144./(8.*ECI*GI)
310 DFT=(TL1+TL2-C2E-C3C)*0.5
311 DFTULT=(TL=ULT+TLCULT)*0.5-(C2E+C3C)*0.5
312 GO TO 802
313 801 CONTINUE
314 DRY1=EC*SP*SP/8.
315 DRU=(EC-EE)*HP*HP/6.
316 DRY=DRY1-DRU
317 DELTA1=FO*144.*DRY/(ECI*GI)
318 DFT=TL2-C3C
319 DFTULT=TLCULT-C3C
320 802 CONTINUE
321 DLM=W1*SP*SP*1.5/1000.
322 DELTA2=15.*DLM*SP*SP/(GI*ECI)
323 DELTA=DELTA1-DELTA2
324 F01=FI/FO
325 DFTULT=DFTULT*F01/100.
326 DFI=DFT*F01/100.
327 RE=SSSTSE+DFRS+C2E+C2E*(1.-(TSK/2.0))*CITT
328 RC=SSSTSC+DFRS+C3C+C3C*(1.-(TSK/2.0))*CITT
329 IF(HP-0.)#40,840,841
330 840 RAVC=(RC+RC)*0.5-(C2E+C3C)*0.5
331 GO TO 850
332 841 RAVC=RC-C3C
333 850 CONTINUE
334 RAVC1=RAVC*F01/100.

```

```

335      TERM91  =-Q*YCCS*SP*SP*144./(8.*ECS*CII)
336      TERM31  =(-RAVG1+(1.-0.5*RAVG1)*CTTT)*DELTA1
337      TERM41  =(-(DF1-RAVG1)+(1.-(DF1+RAVG1)*0.5))*(CT-CITT)
          **DELTA1*RATIO
338      TERM51  =-CTTT*DELTA2
339      TERM61  =-(CF-CITT)*DELTA2*RATIO
340      TERM71  =-DELL
341      TERM81  =-CT5*DELL*RATIO
342      C1=DELTA+TERM31+TERM41+TERM51+TERM61+TERM71+TERM81
          **TERM21
343      ULTA1=-QULT*YCCS*SP*SP*144./(8.*ECS*CII)
344      ULTA2=TERM31
345      ULTSR=(-(DF1ULT-RAVG1)+(1.-(DF1ULT+RAVG1)*0.5))*(CCSP-CITT)
          **DELTA1*RATIO
346      ULTA3=(-(DF1ULT-RAVG1)+(1.-(DF1ULT+RAVG1)*0.5))*(CCMP-CITT)
          **DELTA1*RATIO
347      ULTA4=TERM51
348      ULTA5=- (COMP-CITT)*DELTA2*RATIO
349      ULTA6=TERM71
350      ULTA7=-CUSS*DELL*RATIO*CORT/CCR4
351      ULTA8=-CUMS*DELL*RATIO*CORT/CCR4
352      ULTA9=- (COSP-CITT)*DELTA2*RATIO
353      WRITE(6,210)C2E,C3C,FO,DELTA
354      210  FORMAT(1H ,3X,'EL. LOSS (END)      'F25.2//
          *4X,'EL. LOSS (CTR)                'F14.2//
          *4X,'PRES. FORCE FO (KIPS)          'F14.2//
          *4X,'INITIAL CAMPER (IN)           'F14.2//
          IF(10-1)5533,5534,5534
355      5533  ULT=DELTA+ULTA2+ULTSR+ULTA4+ULTA9+ULTA6+ULTA1+ULTA8
356      GC TO 5535
357      5534  CONTINUE
358      ULTA8=ULTA7
359      ULTA9=ULTA5
360      ULTSR=ULTA3
361      GC TO 5533
362      5535  CONTINUE
363      9999  CONTINUE
364      WRITE(6,11111)T
365      11111  FORMAT(1H ,6X,'LOSS AT BEAM END AT TIME = ',F6.1,2X,'DAYS'//)
366      WRITE(6,9501) C2E,ESHLE1,CLCBS1,CLEAS1,DFR1,EGE,CGSE1,PGDEL1,TL1
367      9501  FORMAT(1H ,3X,'EL. LOSS
          *4X,'SHRK LOSS                        'F14.2//
          *4X,'CREEP BEFORE SLAB CAST          'F14.2//
          *4X,'CREEP AFTER SLAB CAST          'F14.2//
          *4X,'STEEL RELAX.                   'F14.2//
          *4X,'EL. GAIN                         'F14.2//
          *4X,'CREEP GAIN                       'F14.2//
          *4X,'GAIN DUE TO DIFF SHRINK         'F14.2//
          *4X,'TOTAL LOSS                       'F14.2//)
368      WRITE(6,11112)
369      11112  FORMAT(1H ,6X,'LOSS AT BEAM END AT ULTIMATE'//)
370      WRITE(6,9501) C2E,ESHMT,CLCBS1,CSEULT,DFRULT,EGE,GLEULT,
371      *PRAY2,TLULT
372      WRITE(6,11113)T
373      11113  FORMAT(1H ,6X,'LOSS AT BEAM CTR. AT TIME = ',F6.1,2X,'DAYS'//)
374      WRITE(6,9501) C3C,ESHLC1,CLCBS1,CLCAS1,DFR1,EGC1,CGSC1,
          *PGUC1,TL2
375      WRITE(6,11114)
376      11114  FORMAT(1H ,6X,'LOSS AT BEAM CTR. AT ULTIMATE'//)
377      WRITE(6,9501) C3C,ESHMT,CLCBS1,CSCULT,DFRULT,EGC1,GLCULT,

```

```

*PRAY1,TLCULT
378 WRITE(4,11115) T
379 11115 FORMAT(1H,6X,'MIDSPAN CAMBER AT TIME = ' F6.1, 2X,'DAYS'//)
380 DELTA2=-DELTA2
381 WRITE(6,9502)DELTA1,DELTA2,TERM31,TERM41,TERM51,TERM61,
*TERM71,TERM81,TERM91,C1
382 9502 FORMAT(1H,3X,'CGR DUE TO PRES. ' F25.2//
*4X,'DM. DEAD LOAD DEFL. ' F14.2//
*4X,'CRP. CMBR BEFORE SLR CAST ' F14.2//
*4X,'CRP CMBR. AFTER SLAB CAST ' F14.2//
*4X,'CRP DEFL BEFORE SLAB CAST ' F14.2//
*4X,'CRP DEFL AFTER SLAB CAST ' F14.2//
*4X,'EL. SLAB DEFL ' F14.2//
*4X,'CRP DEFL. DUE TO SLAB ' F14.2//
*4X,'DEFL. DUE TO DIFF. SHRK ' F14.2//
*4X,'TOTAL DEFLECTION OR CAMBER ' F14.2//)
383 WRITE(6,11117)
384 11117 FORMAT(1H,6X,'MIDSPAN CAMBER AT ULTIMATE '//)
385 WRITE(6,9502) DELTA1,DELTA2,ULTA2,ULTSR,ULTA4,ULTA9,
*ULTA6,ULTA8,ULTA1,ULT
386 WRITE(6,22555)
387 CALL EXIT
388 END

SUBROUTINE CREEP
389 COMMON/CNE/CU,ESHU,CUM,CUS,CUMS,CUSS,ESHUS,TESHU,TI,TS,TK1,H,
390 *ESHUM,IO,S1,COR4,SCR4,CORTT,CORT
391 IF(TS-0.)1,1,2
392 1 CGR1=0.
393 GO TO 3
394 2 IF(10-1)4,5,5
395 4 CGR1=1.13*TS**(-0.095)
396 GO TO 3
397 5 CGR1=1.25*TS**(-0.118)
398 3 CONTINUE
399 IF(10-1)6,7,7
400 6 IF(11-3.)9,9,8
401 9 CGR2=1.
402 GO TO 10
403 8 CGR2=1.13*TI**(-0.095)
404 GO TO 10
405 7 IF(11-7)11,12,11
406 12 CGR2=1.
407 GO TO 10
408 11 CGR2=1.25*TI**(-0.118)
409 10 CONTINUE
410 IF(S1-3.)13,13,14
411 13 CGR3=1.
412 SCR3=1.
413 GO TO 15
414 14 CGR3=0.82+0.067*S1
415 SCR3=0.89+0.0407*S1
416 15 CONTINUE
417 IF(TK1-6.)16,16,17
418 16 CGR4=1.
419 SCR4=1.
420 GO TO 18
421 17 CGR4=1.12-0.02*TK1
422 SCR4=1.193-0.032*TK1
423 18 CONTINUE

```

```

424      IF(I-40.)19,19,20
425      19 COR5=1.
426      SCR5=1.
427      GC TO 21
428      20 IF(I-80.)22,22,23
429      22 COR5=1.27-0.0067*H
430      SCR5=1.40-0.01*H
431      GC TO 21
432      23 IF(I-100.)24,25,25
433      24 COR5=1.27-0.0067*H
434      SCR5=3.0-0.03*H
435      GC TO 21
436      25 CONTINUE
437      WRITE(6,201)
438      201 FORMAT(1H , 'INVALID DATA CONCERNING HUMIDITY ')
439      GC TO 8988E
440      21 CONTINUE
441      CUM=CU*COR2*COR3*COR4*COR5
442      CUS=CU*COR2*COR3*COR4*COR5
443      CUMS=CU*COR1*COR3*COR4*COR5
444      CUSS=CU*COR1*COR3*COR4*COR5
445      ESHUM=ESHU*SOR3*SOR4*SOR5
446      ESHUS=ESHU
447      IF(I0-1)26,27,27
448      26 CUM=0.
449      CUSS=0.
450      GC TO 30
451      27 CUS=0.
452      CUMS=0.
453      30 CONTINUE
454      WRITE(6,1200)
455      1200 FORMAT(1H ,10X,'COMPUTED RESULTS'///)
456      B1=CUM*COR1/COR4
457      B2=CUS*COR1/COR4
458      B3=CUMS*COR1/COR4
459      B4=CUSS*COR1/COR4
460      B5=ESHUM*COR1/SOR4
461      WRITE(6,200)
462      200 FORMAT(1H , 3X,'CREEP AND SHRINKAGE COEFFS INCLUDING CORR FACTORS'
///)
463      WRITE(6,2000)B1,B2,B3,B4,B5,ESHUS
464      2000 FORMAT(1H ,3X,'ULT.CRP COEFF--M.C. 'F23.2//
*4X,'ULT.CRP COEFF--S.C. 'F14.2//
*4X,'ULT. CRP COEFF-- SLB ON S.C. 'F14.2//
*4X,'ULT. CRP COEFF-- SLB ON M.C. 'F14.2//
*4X,'ULT.SHRK COEFF--PRECAST PM 'F14.2//
*4X,'ULT. SHRK COEFF--SLB FROM DAY1 'F12.2//)
465      8988E CONTINUE
466      RETURN
467      END

```

1ENTRY

## INPUT DATA

## BEAM CONCRETE

UNIT WT. (PCF)	122.00
CONC. STR. AT REL. (PSI)	4670.00
CONC. STR. AT 28-DAY (PSI)	5980.00
CONC. SLUMP (INCHES)	3.00

## SLAB CONCRETE

UNIT WT (PCF)	150.00
CONC. STRN. (PSI)	3500.00

## BEAM SECTION

GROSS AREA (IN**2)	519.50
GROSS MI (IN**4)	108512.00
ECC. AT END (IN)	6.20
ECC. AT CTR (IN)	14.30
SPAN (FT)	86.00
STEEL AREA (IN**2)	4.56
LEAST DIM OF MEMB. (IN)	8.00
HARPING DIST. (FT)	34.40
INITIAL PREST. FORCE (KIPS)	867.00
ELASTICITY MODULUS (KSI)	29000.00
ULT. THK. CORR. FACTOR FOR CRP	0.94
ULT. THK. CORR. FACTOR FOR SHRK	0.90

## SLAB SECTION

SLAB THK. (IN)	7.00
----------------	------

SLAB AREA (IN**2)	588.00
OLM CLE TO DIAPH. (IN-KIPS)	776.00
DEF. CLE TO DIA. (IN)	0.23

## T I M E - D E P E N D E N T F A C T O R S

RM AGE AT REL (DAY)	2.00
AGE OF RM AT SLAB CAST(DAYS)	67.00
AVERAGE REL. HUM. (%)	70.00

## C O M P . S E C T . D E T A I L S

COMP. MI (IN**4)	331167.00
ECC. OF DIFF. FORCE (IN)	13.56
CGS DIST AT END (IN)	29.20
CGS DIST AT CTR (IN)	21.20
RATIO I2/IC	0.23

## C O M P U T E D R E S U L T S

## CREEP AND SHRINKAGE COEFFS INCLUDING CORR FACTORS

ULT.CRP.COEFF--M.C.	0.00
ULT.CRP.COEFF--S.C.	1.62
ULT. CRP COEFF-- SLD ON S.C.	1.23
ULT. CRP COEFF-- SLP ON M.C.	0.00
ULT.SHRK COEFF--PRECAST BM	352.80
ULT. SHRK COEFF--SLD FROM DAY1	330.00

## I N I T I A L S T A T E

EL. LCSS (END)	9.01
EL. LCSS (CTR)	12.03
PRES. FORCE PO (KIPS)	762.73
INITIAL CAMBER (IN)	2.23

LCSS AT BEAM END AT TIME = 560.0 DAYS

EL. LOSS	9.01
SHRK LCSS	4.54
CREEP BEFORE SLAB CAST	7.69
CREEP AFTER SLAB CAST	1.08
STEEL RELAX.	6.19
EL. GAIN	0.00
CREEP GAIN	0.00
GAIN DUE TO DIFF SHRINK	-0.47
TOTAL LCSS	28.05

LCSS AT BEAM END AT ULTIMATE

FL. LCSS	9.01
SHRK LCSS	4.78
CREEP BEFORE SLAB CAST	7.69
CREEP AFTER SLAB CAST	1.70
STEEL RELAX.	7.50
EL. GAIN	0.00
CREEP GAIN	0.00
GAIN DUE TO DIFF SHRINK	-0.44
TOTAL LCSS	30.24

LCSS AT BEAM CTR. AT TIME = 560.0 DAYS

EL. LCSS	12.03
SHRK LCSS	4.29
CREEP BEFORE SLAB CAST	10.26
CREEP AFTER SLAB CAST	1.44
STEEL RELAX.	6.19
EL. GAIN	-4.20
CREEP GAIN	-1.38
GAIN DUE TO DIFF SHRINK	-0.64
TOTAL LCSS	27.98

## LCSS AT BEAM CTR. AT ULTIMATE

EL. LCSS	12.03
SHRK LCSS	4.52
CREEP BEFORE SLAB CAST	10.26
CREEP AFTER SLAB CAST	2.27
STEEL RELAX.	7.50
EL. GAIN	-4.20
CREEP GAIN	-1.68
GAIN DUE TO DIFF SHRINK	-0.61
TOTAL LCSS	30.03

## MIDSPAN CAMBER AT TIME = 560.0 DAYS

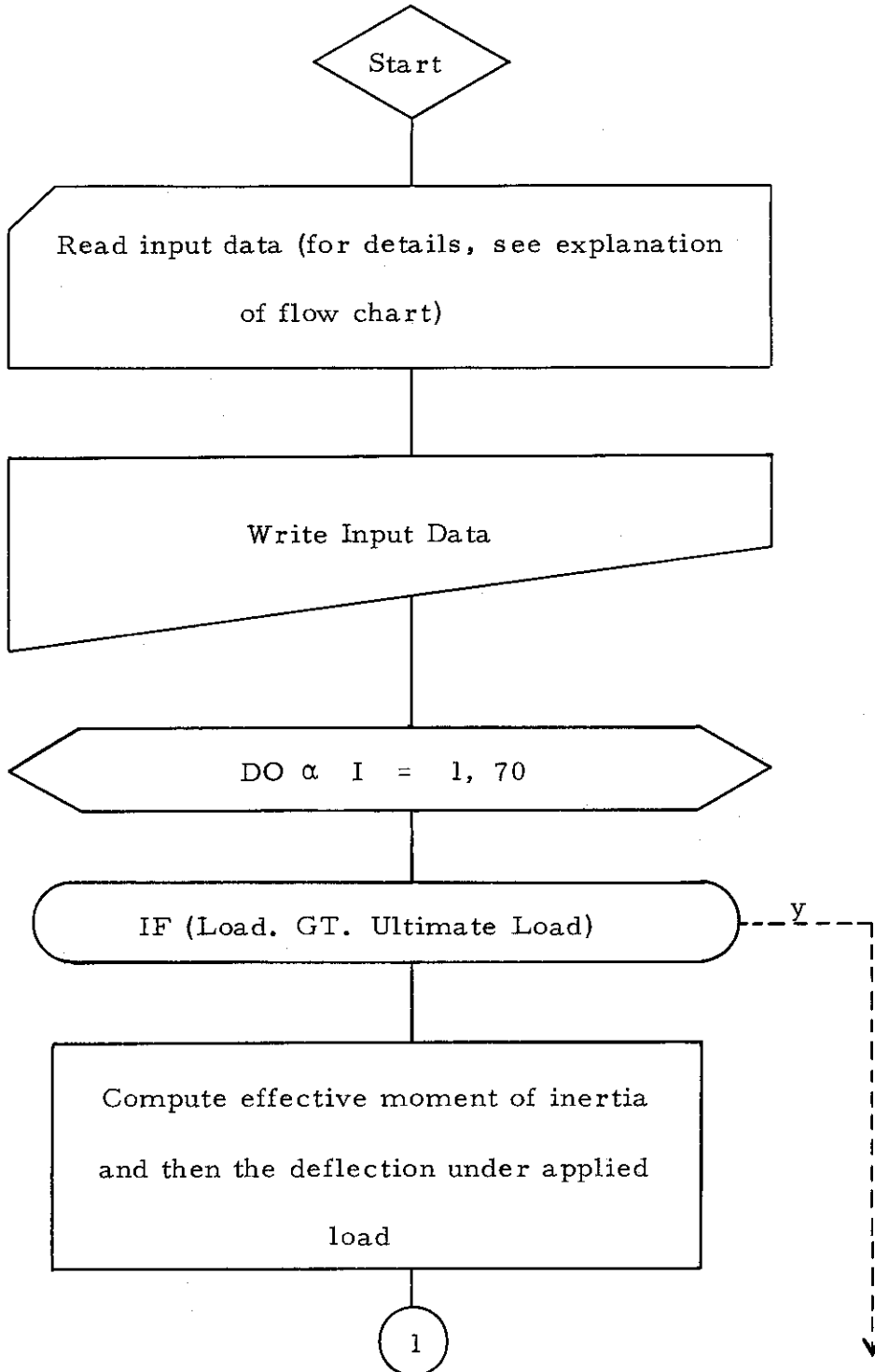
CBR DUE TO PRES.	3.87
RM. DEAD LOAD DEFL.	-1.64
CRP. CMBR BEFORE SLB CAST	2.39
CRP CMBR. AFTER SLAB CAST	0.46
CRP DEFL BEFORE SLAB CAST	-1.49
CRP DEFL AFTER SLAB CAST	-0.24
EL. SLAB DEFL	-2.21
CRP DEFL. DUE TO SLAB	-0.73

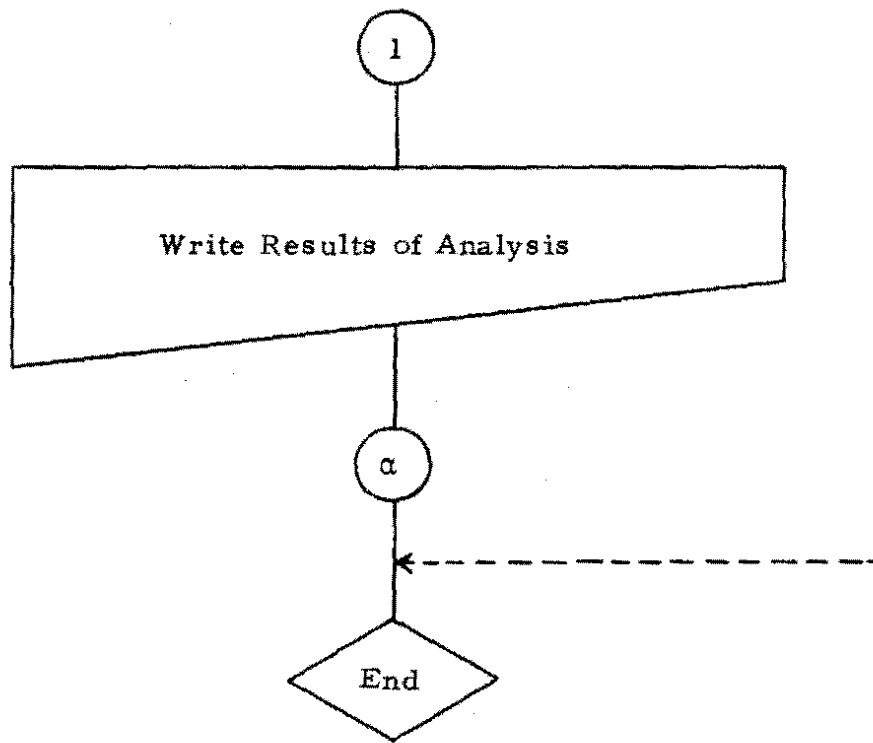
DEFL. DUE TO DIFF. SHRK	-0.20
TOTAL DEFLECTION OR CAMBER	0.21

## MIDSPAN CAMBER AT ULTIMATE

CBR DUE TO PRES.	3.87
BM. DEAD LOAD DEFL.	-1.64
CRP. CMBR BEFORE SLAB CAST	2.39
CRP CMBR. AFTER SLAB CAST	0.71
CRP DEFL BEFORE SLAB CAST	-1.49
CRP DEFL AFTER SLAB CAST	-0.38
EL. SLAB DEFL	-2.21
CRP DEFL. DUE TO SLAB	-0.89
DEFL. DUE TO DIFF. SHRK	-0.19
TOTAL DEFLECTION OR CAMBER	0.17

FLOW CHART FOR LOAD-DEFLECTION STUDIES





EXPLANATION OF FLOW CHART FOR LOAD DEFLECTION STUDIES

<u>SL No.</u>	<u>Explanation</u>
1-5	The read-in data includes the beam dead load, effective prestress force at the time of test, concrete modulus of rupture, gross sectional properties of the beam, the concrete strength at the time of test, the ultimate load of the beam, the cracking load of the beam and the cracked moment of inertia.
5-7	Compute the maximum dead load moment of the beam and the cracking moment of the beam.
8-13	Write pertinent information from the read-in data.
14-31	Compute the deflection under applied load and print the results.

```

$JOB 'KRIPA'
1  DIMENSION D(100)
2  READ(5,444)W,FT,FCB,AG,TI,ET,YT,EC,AS,B,D1,A1,B1,SP,FC
3  444  FORMAT(5F15.5)
4  READ(5,445)PULT,PCR,TCR
5  445  FORMAT(3F10.2)
6  DMCL=1.5*Y*SP*SP
7  CRM=FT*ET+(TI*FT/(AG*YT))+FCR*TI/YT
8  WRITE(6,101)
9  101  FORMAT(1H1)
10 WRITE(6,102)PULT,PCR,TCR
11 102  FORMAT(1H ,15X,'ULTIMATE LOAD IN KIPS' ,F26.5//
    *16X,'CRACKING LOAD IN KIPS' ,F15.5//
    *16X,'CRACKED MOMENT OF INERTIA IN INCHES**4' ,F15.5//
    *)
12 WRITE(6,106)
13 106  FORMAT(1H ,5X,'LOAD (KIPS)',10X,'EFF MI (IN**4)',10X,'DEFLECTION (
    *INCHES)')
14 DO999I=1,70
15 TY=I
16 P=TY/3.
17 IF(P.GT.PULT)GO TO 9999
18 TMCL=33.*P+DMCL
19 IF(TMCL-CRM)10,10,11
20 10 TEF=TI
21 GO TO 12
22 11 RAT=CRM/TMCL
23 TEF=TI*(RAT**3)+TCR*(1.-(RAT**3))
24 12 CONTINUE
25 D(I)=P*A1*1728.*(8.*A1*A1+12.*A1*B1+3.*B1*B1)/(48.*EC*TEF)
26 WRITE(6,88)P,TEF,D(I)
27 88  FORMAT(1H ,/,7X,F6.2,15X,F8.2,16X,F8.4)
28 999  CONTINUE
29 9999 CONTINUE
30 CALL EXIT
31 END

```

\$ENTRY

ULTIMATE LOAD IN KIPS	8.07900
CRACKING LOAD IN KIPS	3.56900
CRACKED MOMENT OF INERTIA IN INCHES**4	33.11200

LOAD (KIPS)	EFF MI (IN**4)	DEFLECTION (INCHES)
0.33	256.00	0.0317
0.67	256.00	0.0635
1.00	256.00	0.0952
1.33	256.00	0.1270
1.67	256.00	0.1587
2.00	256.00	0.1904
2.33	256.00	0.2222
2.67	256.00	0.2539
3.00	256.00	0.2857
3.33	256.00	0.3174
3.67	240.49	0.3717
4.00	197.01	0.4949
4.33	164.89	0.6406
4.67	140.64	0.8088
5.00	121.99	0.9991
5.33	107.42	1.2102
5.67	95.87	1.4409
6.00	86.59	1.6891
6.33	79.05	1.9528
6.67	72.87	2.2300
7.00	67.75	2.5186
7.33	63.47	2.8163
7.67	59.87	3.1215
8.00	56.82	3.4323